EARTHQUAKE ENGINEERING TO EXTREME EVENTS

ISSN 1520-295X

Behavior of Steel Plate Shear Walls Subjected to Long Duration Earthquakes

by
Ramla Qureshi and Michel Bruneau

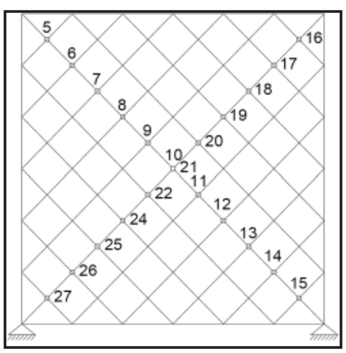

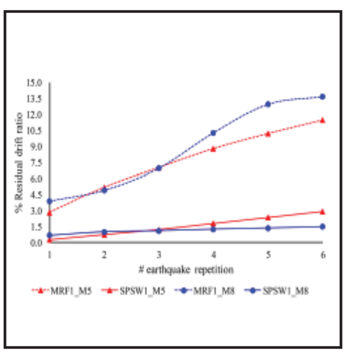

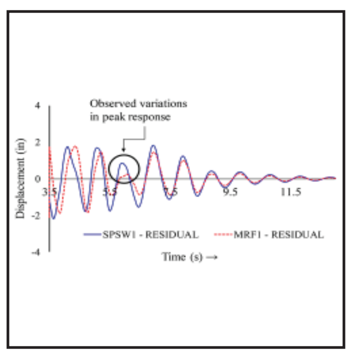

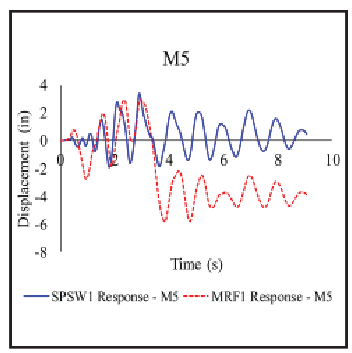

Technical Report MCEER-17-0002

September 1, 2017

This research was conducted at the University at Buffalo, State University of New York, and was supported primarily by MCEER.

Behavior of Steel Plate Shear Walls Subjected to Long Duration Earthquakes

by

Ramla Qureshi[1] and Michel Bruneau[2]

Publication Date: September 1, 2017
Submittal Date: May 4, 2017

Technical Report MCEER-17-0002

1 Graduate Student, Department of Civil, Structural and Environmental Engineering, University at Buffalo, State University of New York
2 Professor, Department of Civil, Structural and Environmental Engineering, University at Buffalo, State University of New York

MCEER
University at Buffalo, State University of New York
212 Ketter Hall, Buffalo, NY 14260
E-mail: *mceer@buffalo.edu*; Website: *http://mceer.buffalo.edu*

Preface

MCEER is a national center of excellence dedicated to the discovery and development of new knowledge, tools and technologies that equip communities to become more disaster resilient in the face of earthquakes and other extreme events. MCEER accomplishes this through a system of multidisciplinary, multi-hazard research, in tandem with complimentary education and outreach initiatives.

Headquartered at the University at Buffalo, The State University of New York, MCEER was originally established by the National Science Foundation in 1986, as the first National Center for Earthquake Engineering Research (NCEER). In 1998, it became known as the Multidisciplinary Center for Earthquake Engineering Research (MCEER), from which the current name, MCEER, evolved.

Comprising a consortium of researchers and industry partners from numerous disciplines and institutions throughout the United States, MCEER's mission has expanded from its original focus on earthquake engineering to one which addresses the technical and socio-economic impacts of a variety of hazards, both natural and man-made, on critical infrastructure, facilities, and society.

The Center derives support from several Federal agencies, including the National Science Foundation, Federal Highway Administration, Department of Energy, Nuclear Regulatory Commission, and the State of New York, foreign governments and private industry.

This research was conducted to provide a deeper understanding of the seismic response of steel plate shear walls (SPSW) when subjected to long duration earthquakes. A parametric study was conducted for various configurations of SPSWs, which were analyzed using nonlinear inelastic dynamic analyses. The presence of the steel plate infill was found to delay yielding of the boundary frame, limit the overall accumulation of residual drifts, and significantly restrict the boundary frame from drifting freely. It continued to provide strength and stability even after extensive exposure to seismic loading. In addition, it was found that the presence of substantial boundary frame members is important for achieving appropriate performance of the SPSW structural system as a whole, as the horizontal boundary element members accounted for a significant part of the system's energy dissipation, even when the steel plate yielded beyond its preceding maximum elongation. Moment connections within the boundary frame were found to be instrumental in limiting drifts and preventing collapse. Overall, the effects of increasing earthquake duration for the SPSWs were found to be not as detrimental as those for the bare frame.

ABSTRACT

Steel plate shear walls (SPSW) have been shown to display relatively high energy dissipating capabilities and have been often used to provide seismic resistance in buildings. Previous research has shown SPSW to be capable of maintaining stability during earthquakes by exhibiting satisfactory hysteretic behavior. However, the infill plates of these walls typically only yield in tension and have no compressive resistance, leading to the question of whether long-duration seismic excitation could detrimentally affect their behavior. This report presents the results of nonlinear inelastic dynamic analyses of various SPSWs for which earthquake magnitude, response modification factor, and duration of earthquake excitation were varied. SPSWs in this parametric study have been modeled with the commonly used diagonal strip model. Single story SPSWs with panel aspect ratios of 1:1 and 2:1 have been considered. A 3-story SPSW has also been analyzed for comparison purposes. Spectra compatible synthetically generated ground motions were used in the analyses. Response of SPSW have been compared with that of their respective boundary frames. Inelastic and residual drifts were used as indicators of the performance of SPSW over the duration of the earthquake. The objective of this research is to provide an understanding of the expected ductile performance of SPSW when subjected to prolonged seismic excitation, and hopefully, an improved confidence in their seismic behavior under such conditions.

TABLE OF CONTENTS

TABLE OF CONTENTS (CONT'D)

LIST OF FIGURES

LIST OF FIGURES (CONT'D)

LIST OF TABLES

SECTION 1
INTRODUCTION

1.1 Overview

A Steel Plate Shear Wall (SPSW) is a lateral load resisting structural system often used in the United States, Canada, and other regions of high seismicity. SPSW systems typically consist of thin, unstiffened vertical steel web panels bounded by a steel boundary frame of horizontal and vertical structural members, respectively called Horizontal Boundary Elements (HBEs) and Vertical Boundary Elements (VBEs). These steel paneled walls are typically multi-story, and have been found to be an economic and efficient system for resisting lateral forces in tall buildings (Sabelli and Bruneau 2007) as they increase usable floor space and decrease wall dead loads. SPSWs also save up substantially on construction time, as they are easy to install and quick to replace, making them suitable not only for new buildings but also for the upgrading and retrofit of existing damaged or vulnerable structures (Berman and Bruneau 2003b).

Based on the type of beam-to-column connections used, the boundary frame can be either simple or moment resisting frames, however, AISC 341 allows only moment-resisting connections for seismic applications. It has been found through large-scale experiments carried out by various researchers (e.g., Timler and Kulak in 1983; Driver, et al. in 1998; and B. Qu, M. Bruneau, et al. in 2008) that SPSWs possess qualities of ductility, high initial stiffness, strength and robustness under cyclic loading, and can therefore be used to provide seismic resistance as they offer an effective energy dissipation system for buildings when using moment-resisting boundary frames.

The steel plate web is characteristically relatively thin, (generally ranging from 3/16” to ½” in midrise buildings), and, as a consequence of this slenderness, buckle under compression during earthquake loading. An inclined tension field action is activated and the thin steel web panel is subjected to pure shear with diagonal tension stresses oriented at 45 degrees to the direction of shear loading. Even though the post-buckling strength and ductility of the panel is substantial (Elgaaly, Caccese and Du 1993), this tension field action mechanism increases the capacity demands on the boundary frame quite significantly. However, this only makes it possible to dissipate energy in tension, and presumably only at tensile strains larger than previously reached (much like the braces would in a tension-only braced frame). This tension-only behavior raises a legitimate question as to what would be the expected behavior of SPSWs during long duration earthquakes – a questions for which there is currently no answer. For these reasons, this report investigates the effects of prolonged earthquake loading on the behavior of SPSW systems designed and analyzed with different characteristics.

1.2 Scope of Research

The objective of this research was to better understand, and improve confidence in the overall ductile performance of the SPSW structural system under the influence of long duration seismic loading, such as what would be expected, for example, during a subduction zone earthquake. It is imperative to understand the contribution of the steel plate web and the boundary frame towards seismic response under such conditions. To investigate this, several analyses were performed, considering various specific conditions and wall geometries; parameters varied included earthquake magnitude and duration (as related parameters in this study), the value of structural damping ratio used in the analyses, the steel web panel aspect ratio, and the value of the response modification factor considered for design. In addition to this, a 3-story SPSW model was also analyzed. For the purpose of controlling duration of the earthquake loading, spectra compatible synthetic ground motions were generated, with moment magnitudes ranging from 5 to 9. These ground motions were used as input for nonlinear time history analyses performed for each individual case. The data obtained from all these analyses was used to compare the seismic response behavior observed for variation of values for each parameter.

It is important to note here that the purpose of this study was to investigate the behavior of SPSWs to determine if there might be a time during the earthquake, when the steel plate ceases to participate towards response, leaving the system to behave only as a bare frame, with possible major consequences in seismic performance. Here, research focused on identifying fundamental behavior and response on the basis of idealized ductile behavior alone, to provide an understanding of the factors that would affect ductile response alone (i.e., in the best conditions when all other limit states could be prevented). Therefore, the material models used for analyses and modelling within this study consider infinitely ductile elasto-perfectly-plastic material. Also, all other limit states that could potentially affect the behavior of SPSWs and lead to their collapse (Purba and Bruneau 2014, 2015), such as the effects of strain hardening, progressive fracture of the steel web panel from the boundary frame, local buckling of the boundary frame members, P-Δ effects, and other failure modes leading to strength degradation and possible collapse, have been ignored. In actuality, strength degradation caused by lateral drifts, and strain hardening within the boundary frame have large influence on the effectiveness of the SPSW system as a whole during cyclic inelastic response at large and increasing drifts. However, the results discussed in this report look only into the efficacy of the SPSWs with reference to the tension-only behavior of the steel plate when subjected to prolonged earthquake ground motions.

1.3 Organization of Report

Organization of this report is as follows. Section 2 presents a review of selected previously literature relevant to this report, starting from the historical development of steel plate shear walls, to current research being conducted to better understand the influence of long duration earthquakes over various structural systems. Section 3 describes the methodology followed for the development of the analytical model. Calculation of considered seismic parameters, modeling considerations, and generation of synthetic ground motions that match with the targeted spectrum are also summarized. Using these analytical models, a series of nonlinear time history analyses are performed in Section 4. A matrix of the analyses conducted is included, listing the cases considered for the purpose of cross-comparison of results. It outlines the various parameters involved for this study, and describes the basis of comparison for each analysis considered. Some of the early steps taken as part of this research project are also described, to show a road-map of the progression of the research thought process, starting from the Fast Fourier Transform method attempted to the decision to repeat the same magnitude earthquakes multiple times to investigate the effect of duration. Section 5 then condenses results obtained from these analyses in an attempt to understand trends in seismic behavior of the structural system, and to outline sensitivity to the changing parameters. Finally, Section 6 presents findings and conclusions, and points out avenues for future research.

SECTION 2
LITERATURE REVIEW

2.1 Introduction

The use of Steel Plate Shear Walls (SPSWs) in buildings has lately seen a significant increase in areas of high seismicity, particularly in the United States, Canada and Japan. The introduction of SPSWs in design specifications like the CSA (1994, 2001, 2009), the 2003 NEHRP recommendations (FEMA 2004), and the AISC (2005, 2010, and the upcoming AISC 341-16 version in 2016) has been supported by many research projects that have studied this structural system to understand its many behavioral trends. This section provides a review of the previously published research in this domain, with focus towards the chronological development of knowledge of the SPSW behavior in Section 2.2, and the current research being carried out for various other structural systems in order to better understand the many effects of long duration earthquakes towards seismic response in Section 2.3.2.

2.2 General Behavior of SPSW

The incorporation of a steel plate shear wall within a building holds many advantages as a lateral force resistant structure. The boundary frame for this system consists of horizontal and vertical boundary elements with connections that can either be shear only, or can have a moment resisting configuration. When subjected to cyclic loading, these walls have been shown to exhibit ductile behavior, with high initial stiffness, enabling these structures to dissipate large amounts of energy. Initially, SPSW systems were designed to prevent out-of-plane buckling of their infill plate, with recommendations to stiffen the steel infill plate to restrict inelastic buckling locally between the stiffening elements (Takahashi, et al. 1973). Later, it was seen that the thin web panels, although buckling at low shear, could still resist sizable loads. It was found that the post-buckling strength of the web was substantial (Thorburn, Kulak and Montgomery 1983), and that stiffening did not have a substantial effect on the overall strength (Guo, Hao and Liu). When strength does control in the design, the behavior was seen to rely on a tension field action mechanism caused by buckling due to shear. Thorburn, et al. utilized a diagonal “strip model” based on the theory of pure diagonal tension (Wagner 1931) to represent this diagonal tension field. In this model, the steel plate web panel corresponded to diagonal, pin-ended strips within the SPSW, which were oriented in the direction characteristic of the tension field. The resulting strip model was shown to be an adequate representation of the tension field by comparing predictions from the model with experimental results, as was verified and later, refined, by the tests conducted by Timler and Kulak (1983), Driver et al (1998), Qu et al (2008) and other researchers.

2.2.1 Tension-Only Behavior of Steel Plate

The principal tension field action mechanism can be understood by the example of a panel bounded by rigid elements on its contour and subjected to pure shear; an idealization of the manner in which the lateral forces due to ground motion interact with an SPSW. Given the small thickness of the web plate, the buckling strength is low, and does not contribute significantly to the ultimate capacity of the system (corresponding to very high depth-to-thickness and width-to-thickness ratios for thin walls). Also, these plates are not perfectly straight, and will have undulations and a degree of curvature. When subjected to lateral load, the combination of these factors makes the plate buckle readily under diagonal compressive stresses, producing folds perpendicular to the compressive stresses and parallel to the tensile stresses, and therefore creating a tension field. With the assumption that the bounding beams have infinte stiffness, and that the compressive stresses perpendicular to the strips are negligible, Thorburn, et al. (1983) represented this tension field with discrete diagonal strips, each having an area equal to the plate thickness times the width of the strip. For practical purposes, it was established that a minimum of 10 numbers of strips were found to be sufficient to model the behavior of SPSW, and orienting them at an angle of inclination α corresponding to the inclination of the tension field, an accurate analytical tool can be obtained. Figure 2-1 shows a schematic of the tension field action developed in a typical SPSW, having tensile and compressive principal stresses oriented at a 45° angle to the direction of the load.

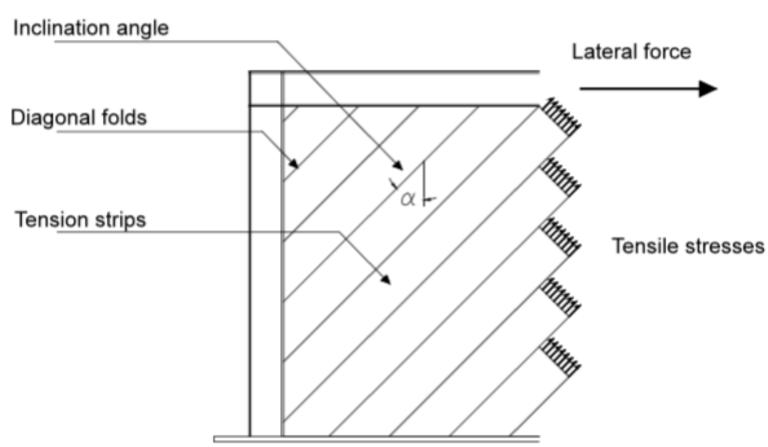

Figure 2-1 Schematic idealization of Tension-field action (Bruneau, Sabelli and Uang, 2011, Cou rtesy of *Diego Lopez-Garcia, Pontificia Universidad Catolica de Chile, Chile*)

To verify this analytical approach, Timler and Kulak (1983) tested a pair of single story SPSWs. The inclination angle corresponding to the direction of the tension field was derived from elastic strain energy principles by Timler and Kulak (1983) as:

$$tan^4\alpha = \frac{1 + \frac{t_w L}{2A_c}}{1 + t_w h\left(\frac{1}{A_b} + \frac{h^3}{360 I_c L}\right)}$$

Where, t_w = Thickness of web plate, h = story height, L = bay width, I_c = moment of inertia of the VBE, A_c = cross-sectional area of the VBE, and A_b = cross-sectional area of the HBE. The resulting angle of inclination typically ranges between 38° and 45° in well-designed SPSWs; knowledge of this angle is important for calculating corresponding demands on the boundary frame elements. Elgaaly, Caccese and Du (1993) established that even though the post-buckling strength and ductility of the steel panel is substantial, from capacity design, so are the demands on the boundary frame.

2.2.2 Connection Type

For seismic applications, AISC 341 only allows for the use of moment-resisting type of connections for SPSWs. Elgaaly and Caccese, in 1993, conducted a series of experiments on SPSW systems, and concluded that the boundary frame could be either simple or moment resisting, and that there was not much difference between the behaviors of the two. Earlier, Tromposch and Kulak (1987) had conducted analyses using moment-resisting connections and reported a substantial increase in the SPSW's ability to dissipate energy. Later, Kulak, Kennedy and Driver (1994) obtained hysteris curves for 30 inelastic analytical cycles and re-established that using moment-resisting connections for SPSWs not only increases amount of energy dissipated (as was observed by the wide area enclosed by the hysteresis curves), but also improves seismic performance by providing inherent redundancy.

Following the Northridge earthquake of January 17, 1994, it was found that a large number of steel moment-frame buildings had experienced brittle fractures within beam-to-column connections, calling for extensive research to understand the implications of the choice of connection used. For the case of the SPSW, the connections of the horizontal and vertical bounding elements are expected to form plastic hinges, but the majority of the seismic energy is dissipitated by the steel plate web, rather than the connection. The drifts enountered by a SPSW are expected be much less than those experienced by a simple-moment frame, and, on that basis, design requirements for SPSWs have permitted the use of ordinary moment frame connections (Ericksen and Sabelli 2008).

2.3 Effects of Prolonged Seismic Loading

It has been found through numerous studies that the duration of seismic loading has a significant effect on structural reliability. Housner (1965), Trifunac and Brady (1975), Vanmarcke and Lai (1980), and Kawashima et al. (1985) determined that earthquake duration was critical when quantitatively measuring the damaging effect caused by seismic loading. Xie and Zhang (1988) also established that severity of ground motion, and how it influences damage on structures, can be represented as a function of the length of earthquake duration. This was later refined by Novikona and Trifunac (1994) and Trifunac and Novikona (1995) by redefining strong ground motion duration in terms of the earthquake magnitude, distance from site to the epicenter, site conditions and site geometry. Jeong and Iwan (1988) found that when damage accumulates, structural failure can occur under cyclic loading conditions, and is highly dependent on ductility of the response as well as the duration of the excitation. Rahnama and Manuel (1996) found that strong motion duration does not affect strength demands heavily, but it does affect cumulative damage measures significantly. Van de Lindt and Goh (2004) determined, through the use of an oscillator, a procedure for quantifying the effect of earthquake duration on structural reliability indices using a low-cycle damage based limit state. The effect of duration becomes especially influential when a specific reliability index is being targeted for performance based seismic design, but also becomes influential when calibrating LRFD Codes (Van de Lindt and Goh 2004). It was concluded that earthquake duration has a considerable effect on structural reliability.

2.3.1 On SPSW

In 1991, Sabouri-Ghomi and Roberts (1991) conducted analyses which demonstrated that the onset of yielding for the SPSW prevented resonance throughout the course of loading, and resulted in a lesser vibration amplitudes, even when the frequencies of the SPSW in its elastic state and that of the forcing function were closely similar. However, the performance of SPSW when subjected to prolonged seismic loading was not addressed. Considering these factors and placing value on the importance that earthquake duration can play in seismic design, it is worthwhile to investigate, in a preliminary manner, some of the effects of duration on SPSW design and performance. This research has been conducted in order to understand some aspects of the seismic response of the SPSW under the influence of long duration earthquakes, and to assess the adequacy of relevant design procedures in that perspective.

2.3.2 On Other Structural Systems

The influence of earthquake duration on various structural systems has been studied and contested over the past few decades. When comparing results between structures made of different materials, such as steel and reinforced concrete, the level of damage that the structure is subjected to can be found to be a strong function of ductility of the response as well as the duration of the excitation. The specifics of how duration affects structural response, however, depend on the nature of the structure and the materials used. Extensive research has been conducted to understand the performance of structural systems, but for sake of brevity, only some is summarized as follows.

a) Reinforced Concrete Frame Buildings

Studies have shown that for concrete frame buildings, the dynamic characteristics of the building and the seismic excitation levels both have a significant influence on the effects of strong motion duration on seismic structural response. Marsh and Gianotti (1994), analyzed single degree of freedom for high magnitude artificial earthquake record having long duration The results observed for reinforced concrete models (with a degrading stiffness approach) depicted that the maximum inelastic displacements increase when any of the following three factors occurred: earthquake magnitude is increased, the yield strength of the structure is decreased, or the epicentral distance is reduced. However, it was found that the displacement is not strongly affected by duration. Energy demand is increased slightly by increase in earthquake magnitude but shows a great increase when earthquake duration is lengthened or when structural yield strength is reduced.

Thompson (2004) modeled two existing concrete highway bridges using WSU-NEABS to analyze their behavior during long duration earthquakes. The results obtained showed that the earthquakes would not cause major damage to the bridges, but the bridge structure would experience pounding and possible failure of bearing pads. Research conducted to study the effects of multiple sequential earthquakes (fore-, main- and after-shocks), on reinforced concrete structures depicted that existing damage to the structure could help better subsequent seismic performance as compared to initially undamaged structures. (Abdelnaby 2012)

While the effects of strong-motion duration on the seismic response of reinforced concrete structures depend strongly on the period of the structure, they do not as strongly depend on the response parameter considered in the analysis. For reinforced concrete frame structures with short-periods, larger responses were found to be linked to long strong motion duration. The reverse was true for intermediate and long-period structures, having larger responses in shorter strong motion duration. It was also determined that the effects of strong-motion duration on the seismic response were not dependent on the nature of the excitation records used. For both, the case of synthetically generated records, as well as real records, the structural performance remained grossly the same (Sarieddine 2013).

b) Steel Frames

Duration influences were also explored by Suidan and Eubanks (1973) by investigating the cumulative fatigue damage in seismic steel structures, while considering two failure mechanisms; the maximum single excursion mechanism when a preset displacement is exceeded, and the fatigue failure mechanism when the cumulative effect of a number of excursions exceeds a preset damage accumulation level. It was concluded from this that with structural periods on the lower end of the medium period range, the cumulative fatigue damage is significant; and also that the damage may be estimated from absorbed hysteretic energy.

The analyses conducted by Marsh and Gianotti (1994) for high magnitude, prolonged, synthetic time histories showed that a bi-linear steel model resulted in lesser demands placed on the steel structure as compared to the degrading stiffness approach used for the reinforced concrete structure. Lignos, et al. (2011) conducted numerous analyses and tests for high-rise steel buildings to evaluate their sesimic performance and capacity under the influence of long duration earthquakes by simulating fracture of beam-to-column connections due to low cycle fatigue of steel. It was shown that the story drift ratios were initally increased owing to the continued accumulation of damage within the connections, until fracture of connections, after which moment-redistribution caused further inter-story drifts. Krishnan and Muto (2013) conducted parametric analyses of two 18-story steel moment frame buildings, and found that the increase in inter-story drift and overall degradation was swifter with increasing duration parameters.

SECTION 3
DEVELOPMENT OF ANALYTICAL MODELS

3.1 Introduction

A Steel Plate Shear Wall comprises of steel plate webs which are connected as infills to a moment resisting boundary frame to form a cantilever wall structure. As depicted in Figure 3-1 below, the beams and columns are named as Horizontal Boundary Elements (HBEs) and Vertical Boundary Elements (VBEs) respectively. Section 3.2 outlines the analytical design of these walls using the Equivalent Lateral Force Method prescribed by ASCE 7 (2010) with input from USGS Seismic Design Maps Tool. Design of these SPSWs was varied based on changes in aspect ratio, response modification factors, and number of stories. Capacity design of the boundary frame elements is also discussed. Section 3.3 presents development of the dual strip model for analysis in SAP2000. To capture nonlinear behavior of SPSWs and corresponding boundary frame archetypes, plastic hinges were also assigned to the analytical models. A series of non-linear time history analyses were performed for all SPSW archetypes considered, using synthetic ground motions. These synthetic acceleration time histories were varied for duration of earthquake loading that the SPSW models were subjected to, and are detailed in Section 3.4.

3.2 Archetype Steel Plate Shear Wall Design

The steel plate webs buckle under diagonal compression and therefore transmit lateral loads only by principal tensile stresses. Tension field action developing in the web plates, together with plastic hinging in the HBEs are the mechanisms by which hysteretic energy is dissipated during earthquakes. In order to investigate the seismic performance of SPSW under long duration earthquakes, two basic single story models were developed having aspect ratio of 1:1 and 2:1 respectfully. These walls were assumed to be in industrial buildings situated on site class B soils in San Francisco. A 3-story wall was also taken into consideration for comparison purposes. The archetype walls considered are shown in Figure 3-1. For reference, the SPSW archetypes considered are labelled SPSW1, SPSW2 and SPSW3. The bare boundary frame is labelled as MRF.

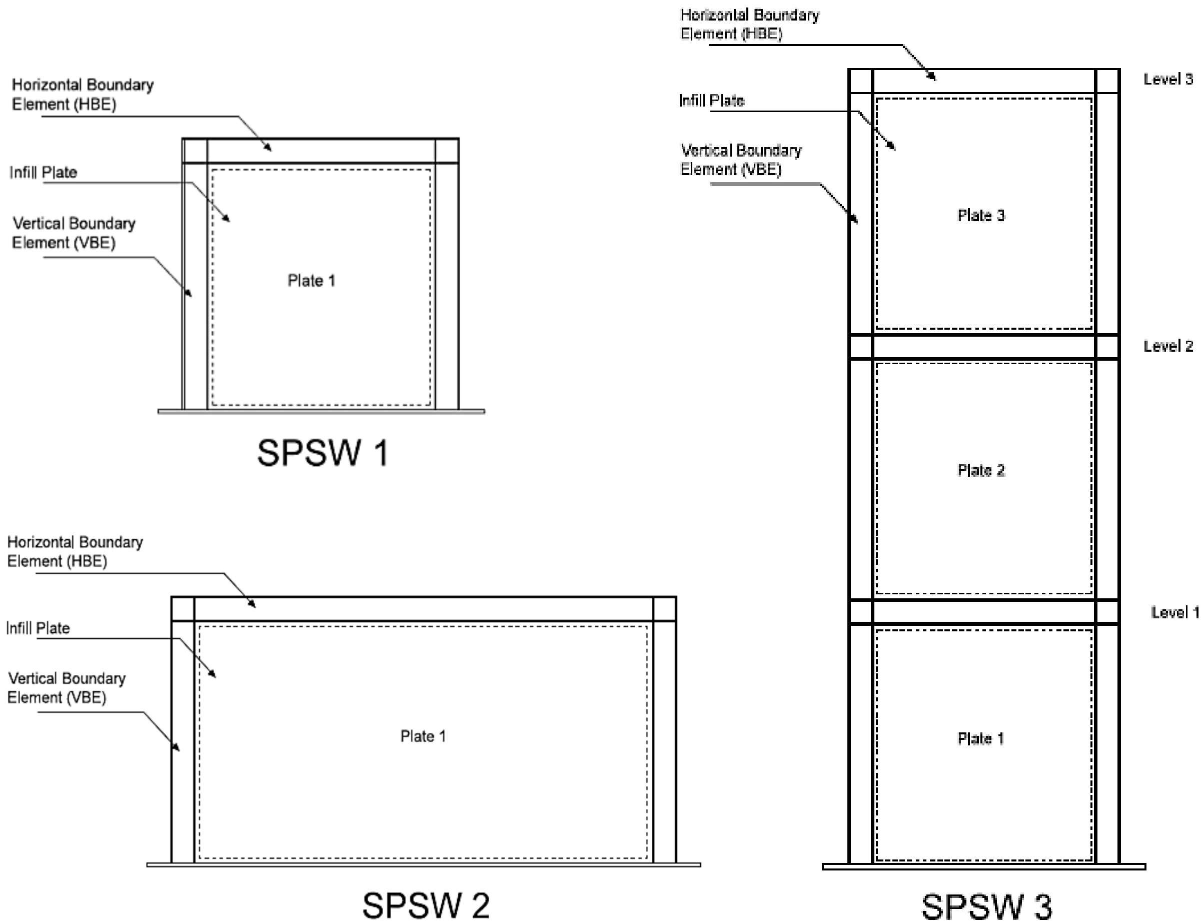

Figure 3-1 Schematic of SPSW archetypes

3.2.1 Seismic Parameters

The USGS Seismic Design Maps Tool was used to generate the design parameter values required by ASCE/SEI 7 Standard 2010 for the location under consideration. The 5% damped short period, S_{MS} and 1 second period, S_{M1} spectral acceleration obtained for the site considered were 0.649 g and 1.50g respectively, for site class B soil (for which soil factors are all 1.0). For the Design Basis Earthquake, the Design Spectral Acceleration parameters S_{DS} and S_{D1} are 2/3 of the above values, and therefore 0.432g and 1.0g, respectively. A target response spectrum was generated using those parameters to provide a target for generating the synthetic ground motions needed for this study and described in Section 3.4.

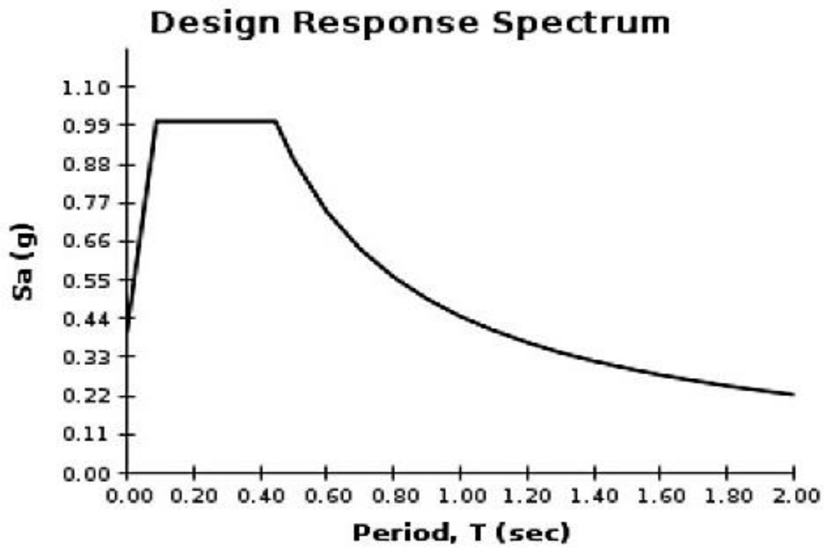

Figure 3-2 Design Response Spectrum generated by USGS output

3.2.2 Equivalent Lateral Force Method and Capacity Design

Lateral seismic forces obtained for design have been calculated according to the equivalent lateral force procedure from ASCE 7-10 Section 12.8. Calculations are detailed in Appendix A. As per ASCE 7-10 Table 12.2-1, the response modification coefficient R, overstrength factor Ω_0, importance factor I, and deflection amplification factor, C_d for the SPSW were defined as 7, 2, 1, and 6 respectively. The approximate fundamental period of the structure, T_0, calculated based on ASCE 7-10 provisions, was 0.13s for the single story archetypes with SPSWs having 1:1 and 2:1 aspect ratios, and 0.35s for the multistory SPSW archetype considered. Note that both of these periods fell on the constant acceleration zone of the design spectra.

The design base shear for each SPSW archetype was calculated varied as per values of R-factor. Note that for SPSW design, per AISC 341-16, the web plates designed resist 100% of the specified base shear. For preliminary design the angle of tension stress action, α was assumed to be 45°, and the design strength of the steel plate web panels was calculated per AISC 341 Equation F5-1:

$$\phi V_n = 0.90(0.42)F_y t_w L_{cf} \sin(2\alpha)$$

where, L_{cf} is the clear distance between column flanges, and t_w is the thickness of steel plate web (both in inches).

The basis of this design was the expectation that plastic hinges form at the ends of the HBE near the face of columns, and that the web plates yield under tension. Capacity Design was used to ensure that yielding remained confined to the deformation controlled elements and that the VBEs and connections have sufficient strength to remain elastic. Loads transferred from the web-plates to the face of the HBEs and VBEs were determined based on the expected capacity of the web plates. The HBE and VBE were then designed based on expected demands from the web-plate and the moment due to the plastic hinging in the HBE. The VBEs were not expected to yield in flexure except at the base. The resulting web plate thicknesses, member sizes for HBEs and VBEs for the archetypes are presented in **Table 3-1**. The designed HBEs and VBEs were checked for compliance with shear, combined axial and flexure requirements and seismic compactness limits. Appendix A details the calculations performed for these designs.

Table 3-1 SPSW Web thickness, HBE and VBE sizes

	Single Story				**Multi Story**		
	SPSW1		SPSW2		SPSW3		
Aspect Ratio	1:1		2:1		1:3		
***R* value**	R5	R7	R5	R7	R7		
Story					1st	2nd	3rd
Plate thk.	3/16”	3/16”	3/16”	1/8”	½”	7/16”	½”
HBE	W40x327	W30x116	W40x431	W36x330	W40x199	W40x199	W40x149
VBE	W40x593	W14x398	W36x652	W40x431	W40x431	W40x431	W40x324

3.3 Modeling in SAP2000

The CSi SAP2000 v17 structural analysis and design program was used for modeling and analysis of the SPSWs under consideration subjected to multiple strong ground motions. Multiple SAP2000 models were prepared to observe changes in behavior as a function of response modification factor used for their design, their aspect ratio and number of stories, and the number of earthquake repetitions to which they are subjected. Key aspects related to the modeling of SPSW analyzed with this software are presented in this section.

3.3.1 Dual Strip Model for Nonlinear Dynamic Analyses

The design and analysis of slender-web SPSWs recognizes that yielding of thin web-plates develops by diagonal tension field action. As a result, a correspondingly simplified analysis method, referred to as the dual strip model and presented in Figure 3-3, is commonly used to model SPSWs and obtain their lateral load carrying capacity. The dual strip model, first proposed by Thorburn et al. in 1983, transforms the solid steel panel into parallel pin ended tension-only diagonal strips that serve as an equivalent for the tension field action, yielding only in tension and buckling under compression. The angle of inclination of these strips, α is the angle measured from the vertical at which the tension field occurs and is taken as 45 degrees in the present study for modeling simplicity. The minimum number of strips should not be less than 10 in order to obtain reliable moment values for the boundary frame elements. Strips were modeled as beam elements (referred to as “frame sections” in the software), and were provided in two directions (as shown in Figure 3-3) to accurately capture behavior under earthquake loading in both directions (Qu and Bruneau 2007). The area of each strip, A_s, was set equal to infill plate web thickness t_w, times the perpendicular distance between any two strips.

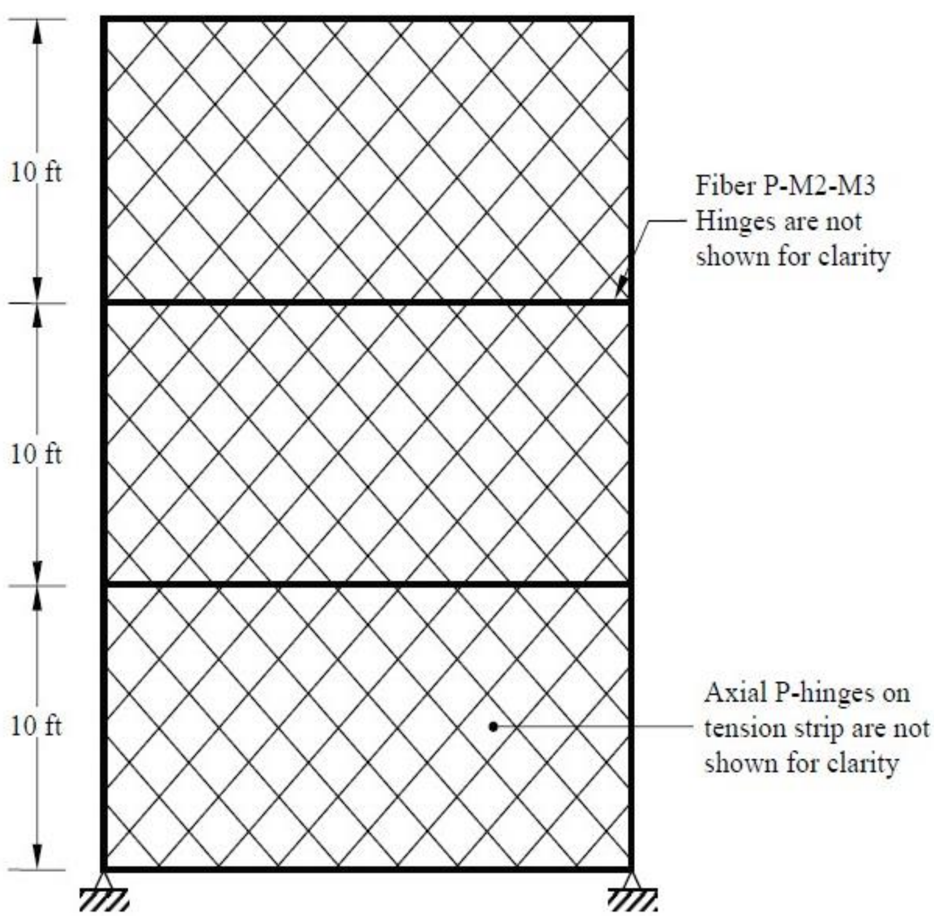

Figure 3-3 Dual Strip Model for Time History analysis (Purba and Bruneau 2010)

3.3.2 Material Properties and Plastic Hinge Models

ASTM A36 material with F_y = 36 ksi was used for steel plate webs, whereas ASTM A992 Gr. 50 steel with F_y = 50 ksi was used for the boundary frame elements. A simplified bilinear elasto-perfectly plastic stress-strain model was used to model the non-linear material behavior of both materials. In order to observe plastic behavior of the SPSWs under the effect of a long duration earthquake, while not knowing ahead of time the drift demand that this could require, the plastic plateau for each material model was assumed constant up to large strains.

It was expected of the strips to load up to yield strength under tension, follow the plastic plateau during the course of continued tension loading, unload until tension was reduced to zero as the seismic loading reversed direction and exhibit no strength as soon as the plate underwent compression. In SAP2000, “Axial P” hinges were assigned at the center of each of the strips to model this non-linear hysteretic behavior (Purba and Bruneau 2010). As is evident from its name, this hinge only allows to develop yielding caused by axial loads. For the strips to mimic actual behavior of the web panels, these axial hinges were required to yield only in tension without any compression strength, and therefore were assigned compression limits set to zero. The assignment of tension/compression limits in SAP2000 is a nonlinear analysis property, and these compression limits were only activated for the non-linear time history analysis procedure described in Section 3.4.

However, because the strips are typically slender and have no significant compression strength, assigning zero compression limits to these very slender strips caused them to buckle very early in the earthquake loading. Errors were introduced in intended behavior as these failed strips did not start re-dissipating hysteretic energy right from the values of deformation corresponding to the onset of last buckling. Purba and Bruneau (2010) recommended assigning an arbitrary near-zero compression limit value while activating a “No Compression Strength” feature in SAP2000, which caused the strips to buckle elastically, enabling the program to remember last deformation values before compression loading and the strips to recover all elastic buckling deformation before entering the tension regime. However, it was noticed for SAP2000 v17 that assigning compression limits set to near-zero and correspondingly setting material model as explained above, the Axial P hinge was effectively able to eliminate the development of compression strength in the stress-strain curve for steel plate webs and follow intended hysteretic behavior as is depicted in Figure 3-4. A simple check was performed for verification of intended behavior in SAP2000, which is explained in Appendix B.

HBEs and VBEs were modeled as two-noded frame elements with six-degrees of freedom at each node. Plastic hinge properties in these boundary frame elements were modeled using Fiber P-M2-M3 hinges. In such hinges, the cross-sections for the HBEs and VBEs were divided into layers (i.e. “fibers”) in both strong and weak directions, with each fiber associated with its own stress-strain relationship depending on the properties of the material at the corresponding location in the cross-section. During seismic response, the development of plastic hinging can be detected by the observation of the resulting moment-rotation plots for overall hinge response, or of the stress-strain curves for each individual fiber. Here, each of the HBE flexural hinges was assigned multiple layers of fibers (e.g. 38 fibers for SPSW1 designed for R = 7) to provide more accurate results with relatively lesser computational effort. Relative length of each flexural plastic fiber hinge was kept as 0.90 times the HBE member depth. This length corresponds to a spread of plasticity that might happen on the onset of inelastic deterioration.

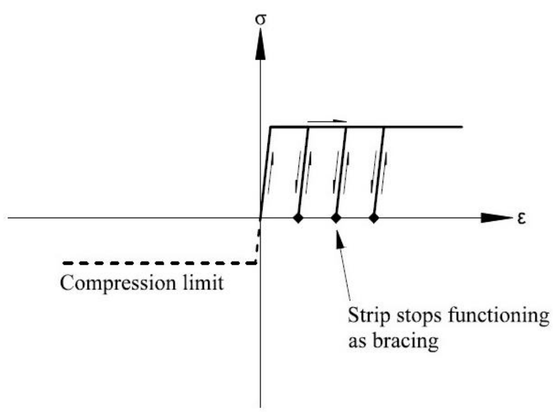

Figure 3-4 Generic Strip Hysteretic Behavior (Purba and Bruneau 2010)

3.3.3 Boundary Frame Model

For comparison purposes, SAP2000 models consisting only of the boundary elements from the above mentioned SPSWs were prepared as moment resisting frames for each respective SPSW archetype. These frames were assigned the same Rayleigh damping mass and stiffness coefficients (obtained from period of 1st mode and 99 percent mass participation mode) as those used for their respective SPSW, such as to give same damping at specific periods to both the models. Fiber P-M2-M3 hinges were assigned to beams in the boundary frame models (same members as HBEs for SPSWs) to compare flexural behavior of both archetypes under seismic loading.

3.4 Non-Linear Time History Analysis using Synthetic Ground Motions

Nonlinear Time History analysis was conducted in detail to investigate performance of SPSWs during long duration earthquakes. SPSWs and Boundary Frame models were both analyzed using the Nonlinear Direct Integration History option in SAP2000. For the archetypes to replicate actual behavior, Rayleigh coefficients for 2% damping were input. As the considered SPSWs have a high lateral stiffness, P-delta effects were ignored for the intent of this research. Analyses were performed for the three SPSWs archetypes described earlier, designed per different response modification factors and subjected to earthquakes of different moment magnitudes. Analyses were also conducted for series of earthquake repetitions to observe the incremental plastic deformations and residual drifts of SPSWs under prolonged seismic loading. Details for these analyses are presented in Section 4.

Spectra compatible synthetic ground accelerations for site class B soils were generated from RSCTH or "Response Spectrum Compatible Time Histories" (Papageorgiou and Halldorsson 2004). The 5% damped target elastic response spectrum presented in Section 3.2.1 was used as an input file for a successful run of the RSCTH code to generate synthetic time histories. Other inputs include required moment magnitude of the seismic source, M_w, and epicentral distance of the source to site, based on which the duration of the synthetic time history can be calculated using the Specific Barrier source model (Papageorgiou and Aki 1983).

The RSCTH program has a parameter called "Duration switch," *"idurpm,"* that allows for increasing the duration of the desired acceleration time history by increasing the number of input time steps and number of data points. Five ground motions, representative of earthquakes of magnitude M5, M6, M7, M8 and M9, were therefore generated with durations of 9, 12, 19, 42, and 116 seconds respectively. As the ground velocity and displacement traces of those artificial ground motions were observed to drift, baseline corrections of those records was performed using the open-source software SeismoSpect. The output accelerations obtained from the RSCTH were in units of cm/s^2 and were scaled by a factor of 0.3937 to convert into units of in/s^2 for input in SAP2000 for the nonlinear direct integration time history analyses. Figure 3-5 shows the time histories obtained.

Compatibly of these ground motions with specified target spectra was rechecked. Figure 3-6 displays spectra matching with required target spectrum for ground motions for magnitudes M5 and 6 respectively. Detailed spectral matching is shown in Appendix C for all earthquake magnitudes.

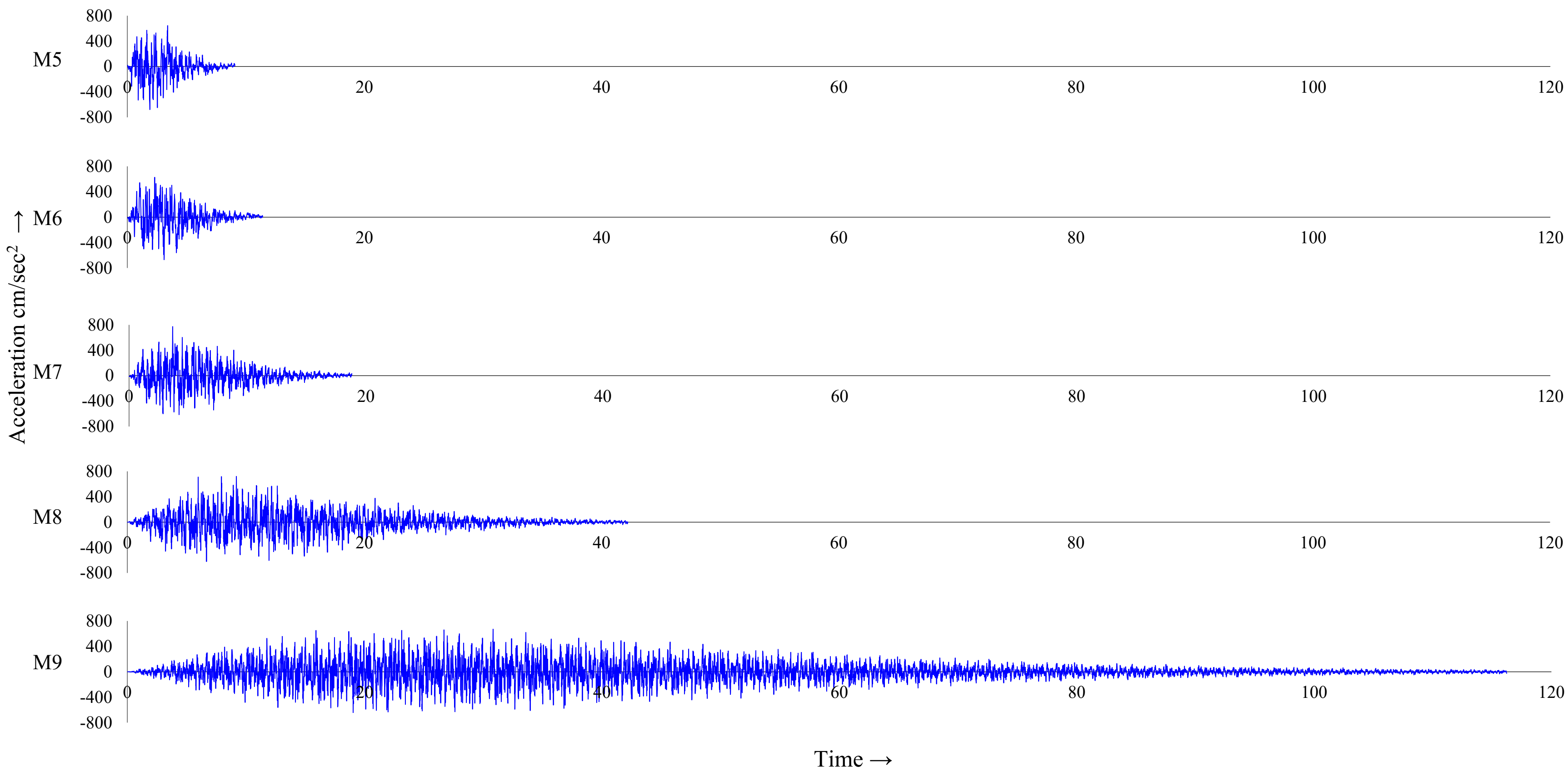

Figure 3-5 RSCTH generated Time Histories

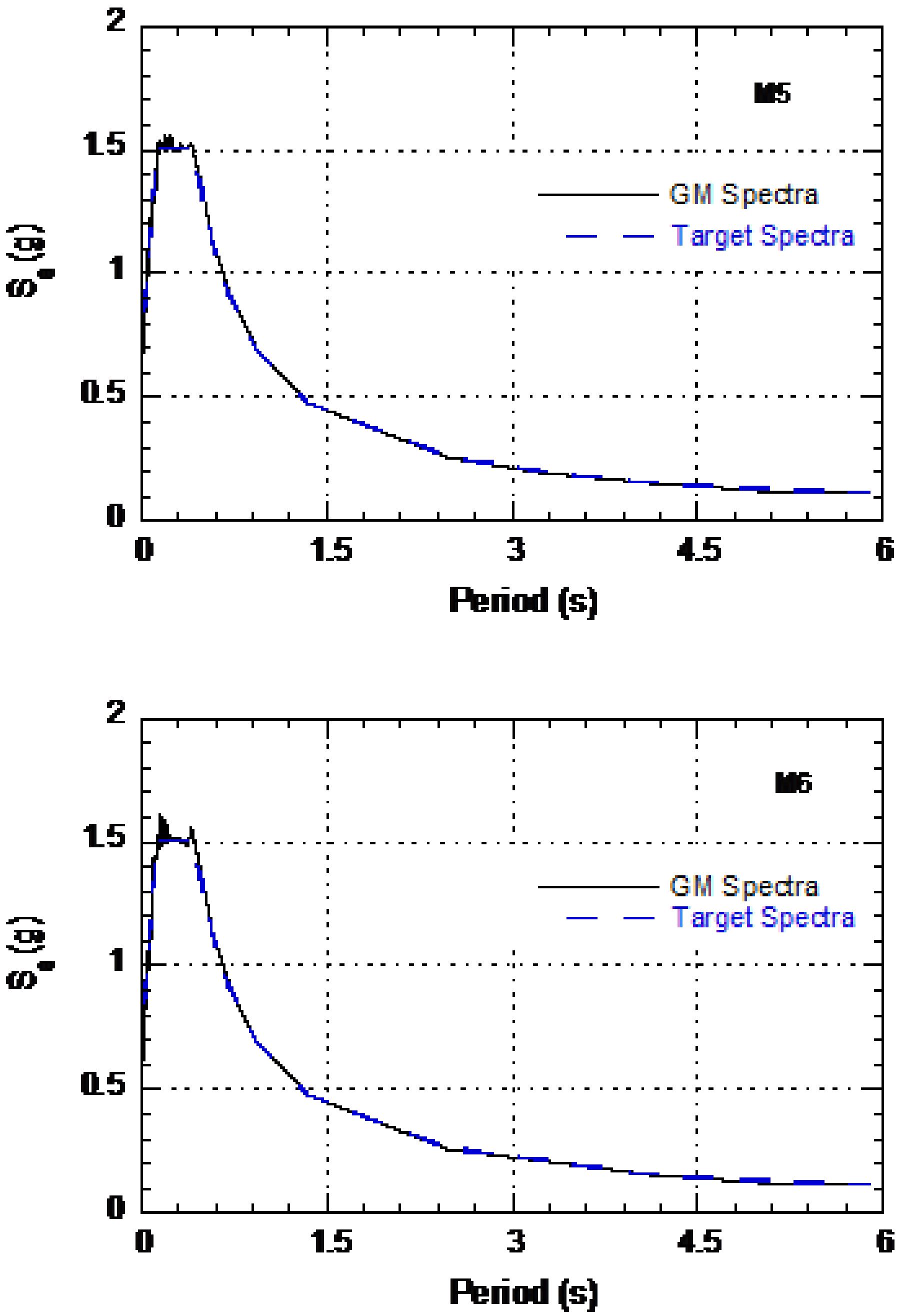

Figure 3-6 Response Spectra matching with specified target spectra, M5 and M6

SECTION 4
COMPARATIVE ANALYSES

4.1 Basis of Comparison

For this parametric study, a number of analyses were performed considering variations in the following parameters:

- *R*-factor: ASCE-7 specifies the value of response modification factor, *R* that should be used for the design of SPSW. However, because *R* is related to the level of inelastic demand to be developed in a structural system, structural systems designed for two different values of the *R* factor are considered, namely 7 and 5.
- Damping ratio, ζ: Different values of structural damping used in the analyses allowed for comparison. Here, for the case of $R = 7$, damping values of 2% and 5% of critical damping ratio have been considered.
- Panel aspect ratios: Considering the range of values used in practice, SPSWs having panel aspect ratios of 1:1 and 2:1 have been analyzed.
- Number of stories: Single story and three story frames have been considered.
- Duration of earthquake: As discussed in the Section 3.4 synthetic ground motions were related to Magnitude. Five different Magnitudes ranging from 5 to 9 were taken for this purpose.
- Repetition of earthquakes: In addition to analyses for individual earthquakes, sequences in which the Magnitude 5 and 8 earthquakes were repeated twice, thrice, or six times, were also considered.

Figure 4-1 displays a flowchart of the various analyses that were performed on the considered archetypes. Note that the list of cases in Figure 4-1 is not an exhaustive list of all possible combinations, but the cases analyzed allow to compare the relative influence of individual factors. Then, Section 4.2 first presents results and observations of the different analyses done for the case $R = 7$, $\zeta = 2\%$, and panel aspect ratio = 1:1, (highlighted by a box in Figure 4-1) for SPSW1. For the ensemble of all other cases considered, the effect of varying individual factors on the response of SPSWs is investigated and detailed in Section 5. Similar comparative analyses for single-story SPSW2 and multi-story SPSW3 were also performed, but because similar findings were obtained, for brevity in presentation, only results obtained for the analyses performed on SPSW1 are presented in this section. All other results obtained are presented in Section 5 in detail.

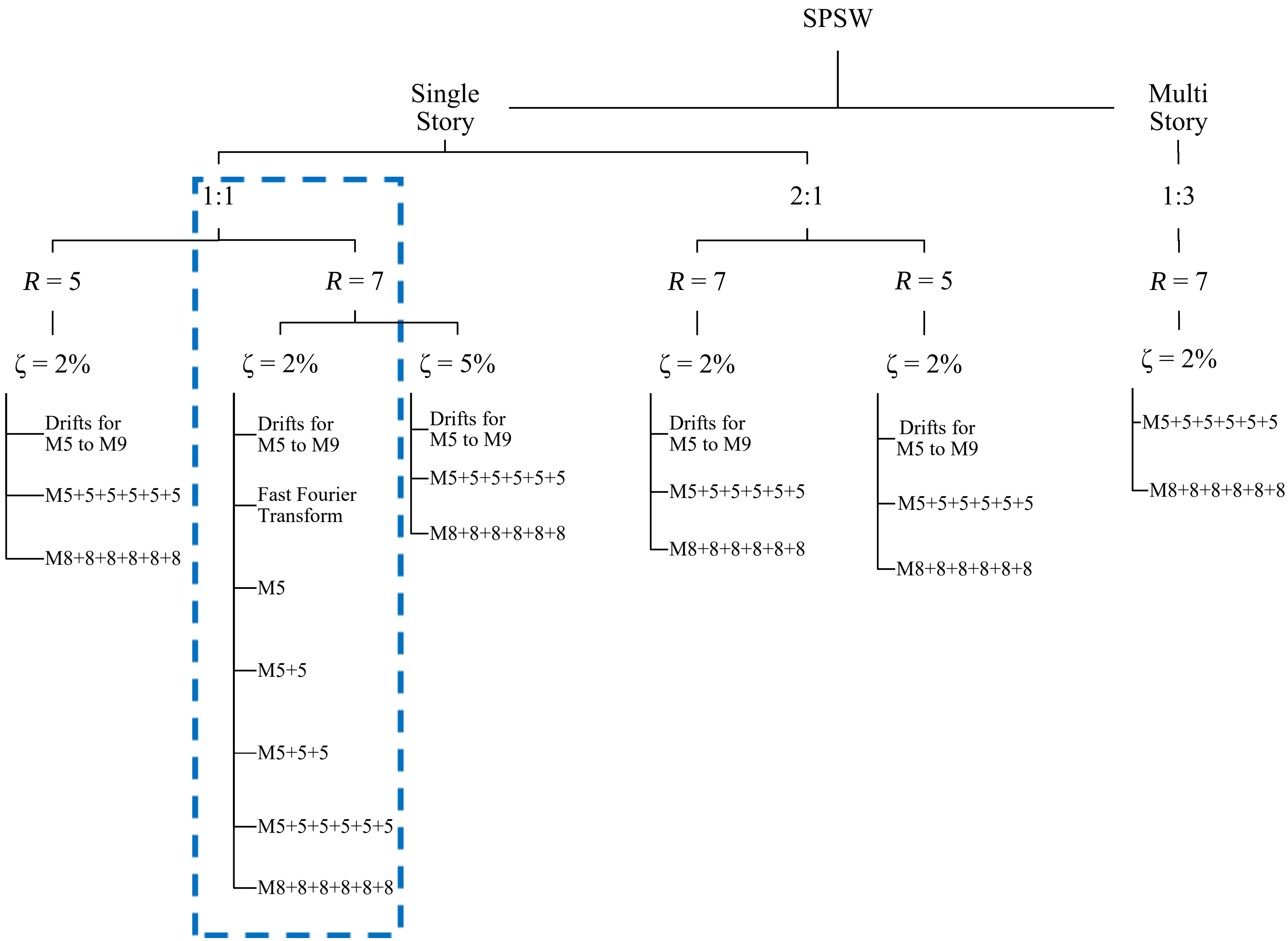

Figure 4-1 Sequence for performed comparative analyses

4.2 SPSW1 – Single-story SPSW with 1:1 aspect ratio

Results obtained for analyses performed for SPSW1 designed for $R = 7$ are discussed in the following sub-sections. A first approach to quantify changes in behavior was attempted using Fast Fourier Transform on segments of the response. This is described in Section 4.2.1. However, as this approach was found to be too sensitive to selection of segment size and consequently not as accurate as originally expected, it was discarded. Sections 4.2.2 and 4.2.3 present results obtained by comparing the time history response of SPSWs and their respective boundary frames (without the infills, and therefore acting as moment resisting frames, and referred to as MRF hereafter). Sections 4.2.4 to 4.2.6 then build on those findings, considering earthquakes repeated twice, thrice, and then six times, with a particular emphasis on identifying the instances of yielding over time to better understand the effect of duration.

4.2.1 Fast Fourier Transform

In order to understand the effect of earthquake duration on behavior of the structure, the first step taken was to consider variations in period of vibration with respect to time, for which a Fast Fourier transform (or FFT) was performed on SPSW1 for value of $R = 7$. The idea was to convert SPSW top HBE lateral drift data from time domain to frequency domain so that changes in time period of SPSW archetypes with respect to time could be noted throughout the duration of the earthquake. As the FFT requires periodic functions, the displacement response was divided into smaller segments of 1.28 second durations; where this duration was selected such that it exceeded the period of the observed response for the SPSW considered. The FFT was performed for responses obtained when the SPSW1 and MRF1 archetypes were subjected to ground motions of moment magnitudes of 5 and 6. It was expected that the initial time period of the SPSW would be smaller than that of the boundary frame alone acting as a MRF, due to its larger stiffness. The initial expectation here was that the period obtained from the FFT per above approach, for both the MRF and the SPSW, would converge due to a gradual decrease in stiffness of the SPSW after the steel plate web has yielded plastically, as shown in Figure 4-2. This would have enabled to quantitatively determine when the SPSWs would start to behave exactly like a moment resisting frame.

Figure 4-3a and b show actual behavior obtained for the response of archetypes subjected to ground motions of moment magnitudes M5 and M6 respectively. As can be seen from the figure, the FFT results did not align with initial expectations. Firstly, the FFT results did not accurately match the fundamental period of vibration for both, the SPSW1 (0.32 s instead of 0.24 s obtained from SAP2000) and the MRF1 (1.28 s instead of 0.9 s). Also, abrupt reductions in time period were observed over a duration of 1.5 s (from 5 s to 6.5 s) within the response history. An identical reduction in the period of MRF1 was observed. These reductions could not be physically explained. It was suspected that this reduction in time period might have been an undesirable numerical artifact occurred due to the small period of time over which the FFT was conducted.

For a better assessment of the obtained results, it was therefore decided to repeat the FFT method for drift response of archetypes subjected to ground motion of M5, but this time by dividing the response into relatively larger segments of 2.56 second durations. Figure 4-4 shows the obtained results, which are observed to be very different from those achieved earlier using 1.28 s segments. It was also seen that the FFT repeatedly gave inaccurate fundamental periods of vibration for both SPSW1 and MRF1, regardless of segment duration size. Given that the FFT method for obtaining time period of vibration was sensitive to duration of the segment chosen, it was determined that this was not a reliable method for getting variations in time period of the structure with regard to time.

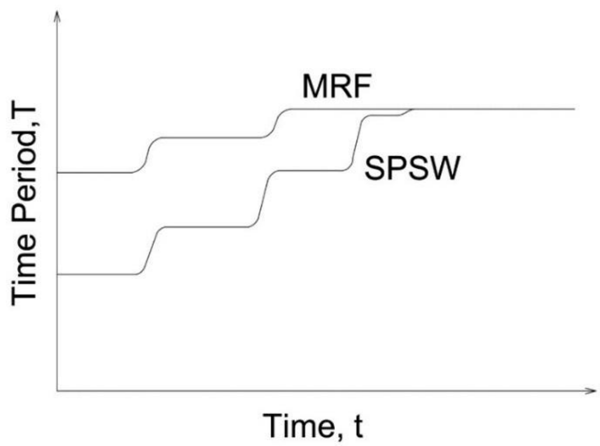

Figure 4-2 Expected Behavior - Time Period Gradation w.r.t. time

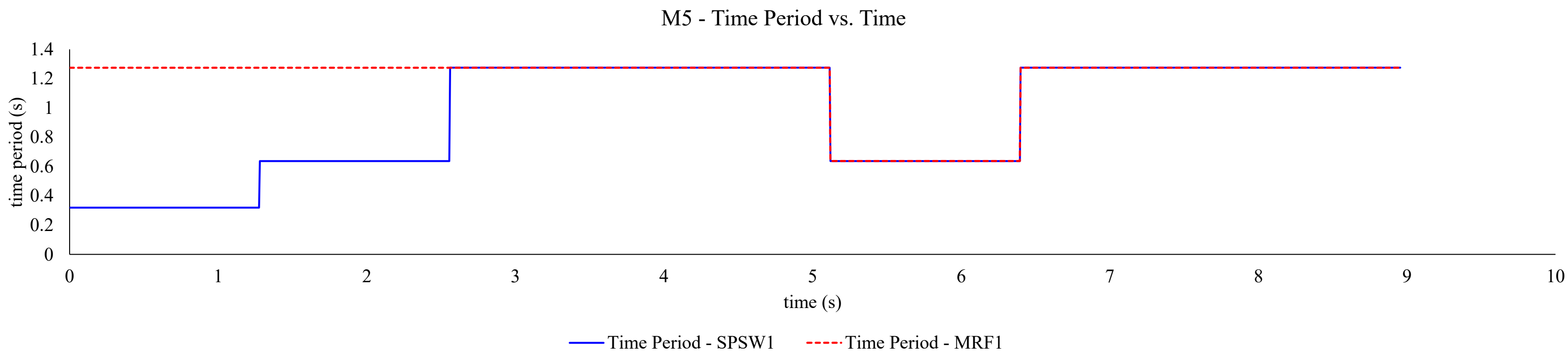

(a)

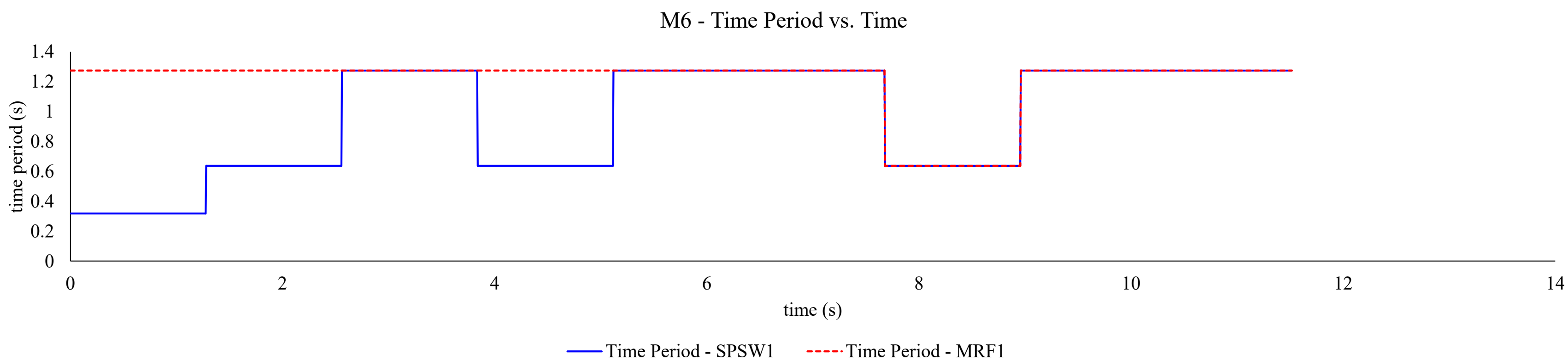

(b)

Figure 4-3 Obtained Time Period gradation w.r.t. time for response to ground motions of a) M5 and, b) M6, for 1.28 s segments FFT

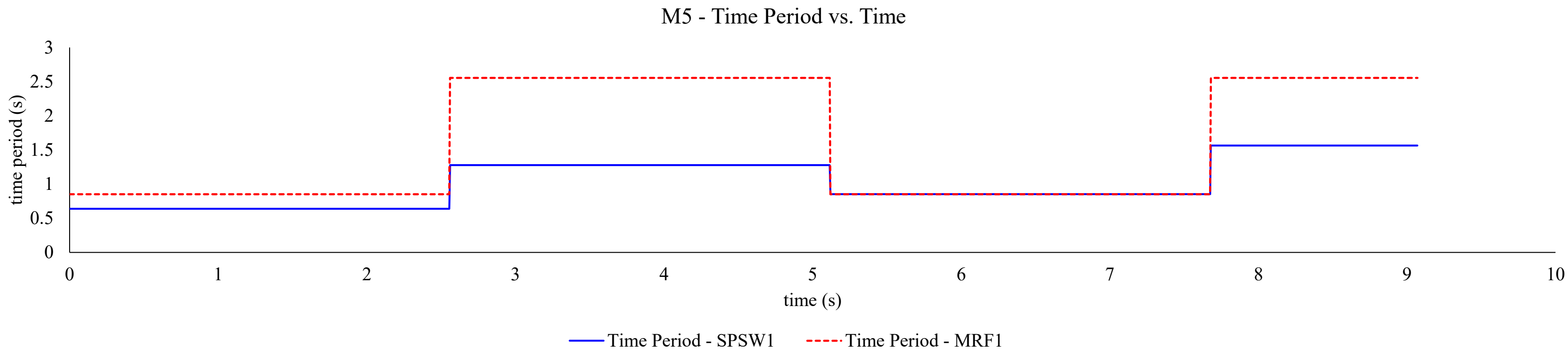

Figure 4-4 Obtained Time Period gradation w.r.t. time for response to ground motion of M5 for 2.56 s segments FFT

4.2.2 Drift response

Since the FFT approach above did not achieve reasonable results, it was decided, as a different approach, to compare the nonlinear response time histories of the SPSW and MRF. The objective here was to detect if there is a point in time where the SPSW behavior matches that of the MRF, which would indicate that the web plates no longer contribute to response. Figure 4-5 a, and 4-5 b show top HBE lateral displacement response of SPSW1 compared to that of MRF1 for moment magnitudes of M5 and M6. As expected, the MRF showed more relative displacement for the top joint than that for the SPSW. Note that similar behavior was observed for archetypes subjected to ground motions of M7, M8, and M9, as shown in Appendix D. Note that while synthetically generating ground motions using the RSCTH program, selecting a greater moment magnitude translates into a longer duration of the earthquake. As a result, the synthetic ground motion time histories for lesser durations had to match the same target spectra as those for longer durations (9 seconds for M5 compared to 116 seconds for M9), resulting in lower peak ground acceleration for higher magnitude earthquakes. This was also evident in maximum displacement response observed for each moment magnitude, i.e., the maximum drift observed for smaller magnitude earthquakes was greater than that for larger ones, as shown in **Table 4-1**. As the ground accelerations were larger for the smaller magnitude earthquakes, more severe yielding occurred due to those smaller earthquakes. This was illogical for the purpose of this research, as these smaller magnitude earthquakes also had smaller duration. From the perspective of studying the effects of duration, these results confirmed that the comparison should be made on earthquakes of various durations, but with similar peak ground acceleration. It was decided that a simple solution to study effects of prolonged earthquake loading on SPSW archetypes would be to repeat the same earthquake a number of times.

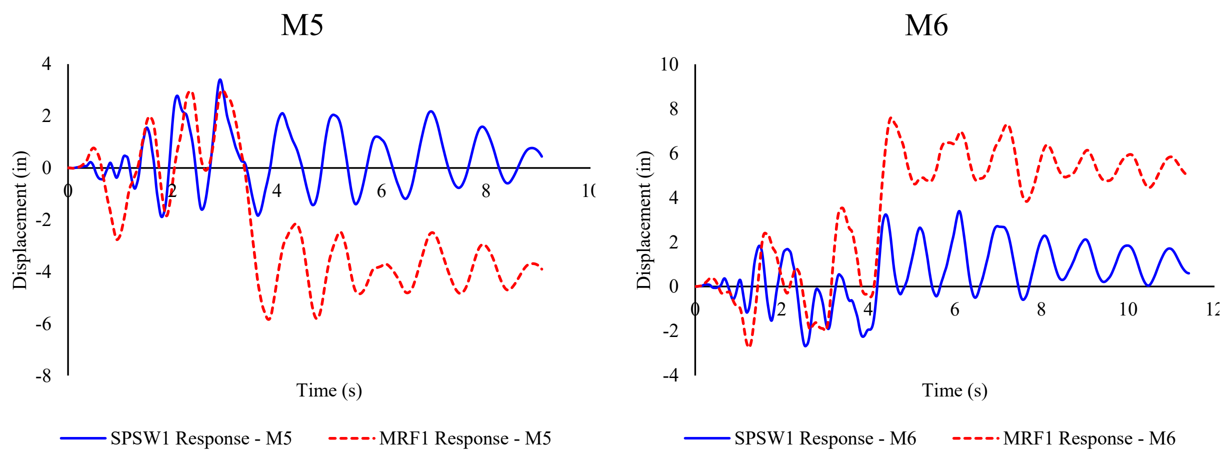

(a) **(b)**

Figure 4-5 Drift response for SPSW1 compared with that of MRF1 for a) M5, and b) M6

4.2.3 Residual Drifts

Even though response histories for individual moment magnitudes did not adequately explain the different effects of earthquake duration, it was noted that during the course of displacement histories, certain sequence of peaks for SPSW1 response appeared similar to those observed for MRF1, but with a visibly evident offset caused by plastic drift. It was suspected that if the value of this residual displacement could be calculated and subtracted from the MRF response, the resulting curves obtained for both SPSW and MRF could be almost identical when superimposed. This approach could effectively indicate if there were parts of response during which identical behavior between both the archetypes would be obtained, thereby helping to identify of the duration after which the steel web is no longer serving its purpose.

The methodology adopted to extract residual drifts consisted of adding a tail of zeros (i.e., “zero-padding”) at the end of the input file of the acceleration time history, enabling the archetypes to first undergo their seismic displacement response, and then damp out in free-vibration over the time of zero ground acceleration, giving a constant value of plastic displacement at the end of response. Figure 4-6a depicts the SPSW1 response obtained for the M5 ground motion time history with 20 seconds duration of null-accelerations added at the end, which gave a value of residual displacement equal to 0.35 inches. The same procedure was followed for MRF1 response, which resulted in a residual displacement value of 3.95 inches. Both these response histories are shown in Figure 4-6b. Residual displacements obtained from this procedure are tabulated in **Table 4-1** along with maximum displacements for each moment magnitude. These residual displacements were then subtracted from the total response histories for both SPSW1 and MRF1, and the resulting curves were superimposed together to observe if the expected similarities in behavior existed.

As shown in Figure 4-6c, peaks obtained as a result of this superimposition did not completely match with each other, showing variations in both amplitude and shape in the overlay of response histories for both archetypes. This observed variations in behavior of the SPSW and the MRF was presumably (and expectedly) caused by the presence of the steel infill plate within the SPSW. These results also pointed towards a requirement for a deeper understanding of how plastic yielding developed over time in the archetypes under consideration. Therefore, a more thorough examination of time-dependent behavior of axial and flexural fiber hinges, incorporated in the models as per Section 3.3.2 was performed to understand and identify their respective contributions to the instances of yielding throughout the duration of earthquake; this is described in the next section.

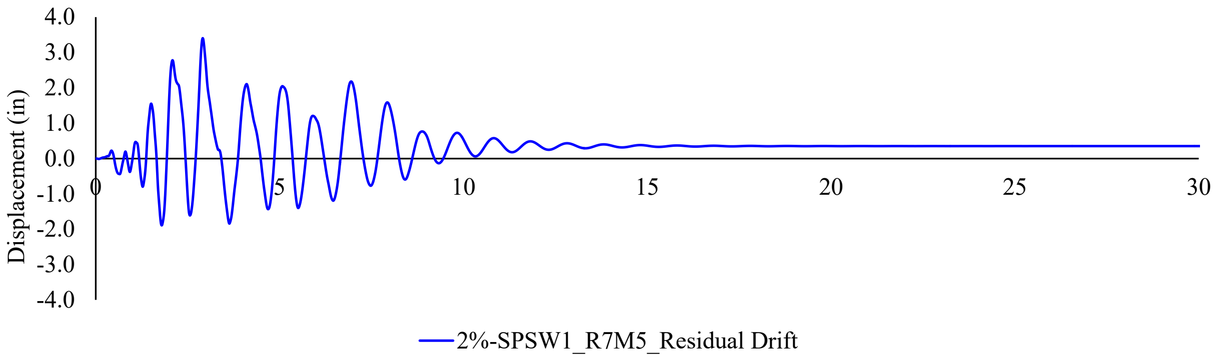

(a)

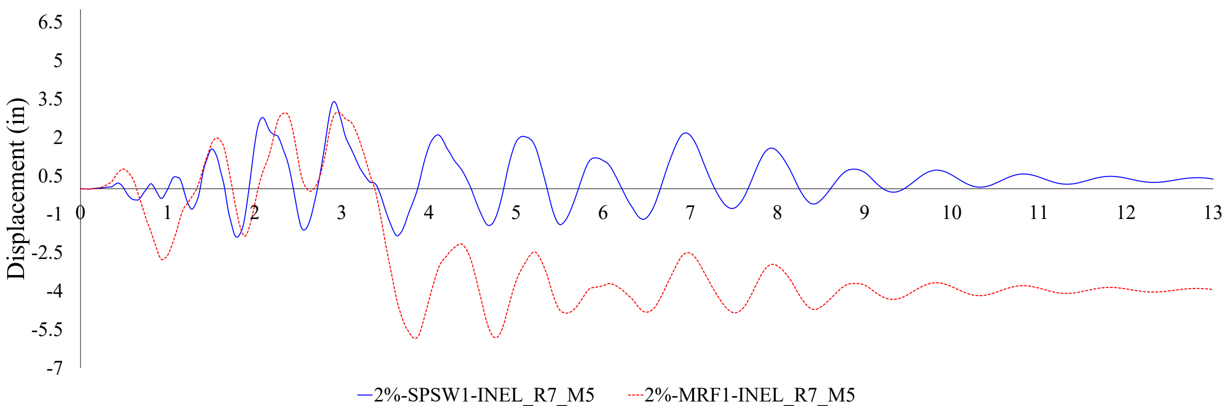

(b)

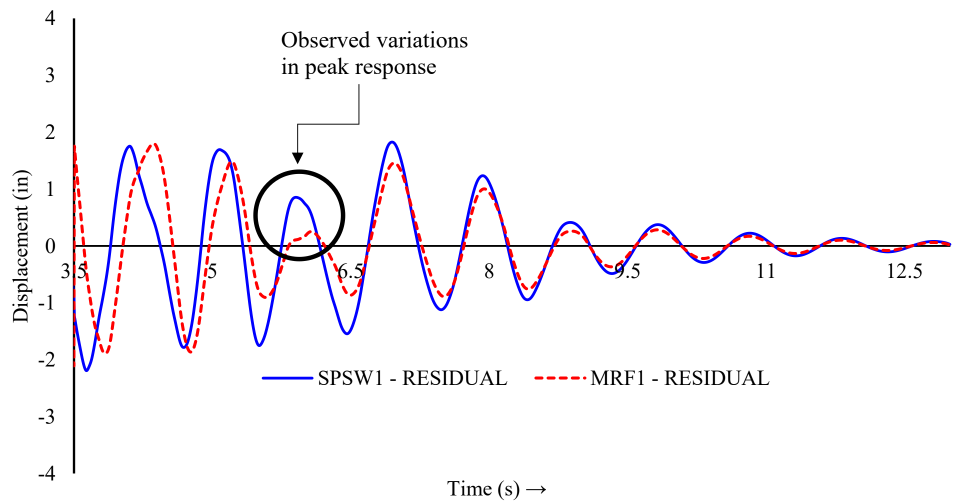

(c)

Figure 4-6 For *R* = 7, M5 Displacement response a) SPSW1 with 20 second zero-padding, b) SPSW1 and MRF1, and c) Residual displacement subtracted from both responses.

Table 4-1 Maximum Roof and Residual Displacements with respective % Drifts

	Max. Roof Disp. (in)		Residual Roof Disp. (in)		Max. Drift % Δ_{max}		Residual Drift % Δ_{res}	
	MRF1	**SPSW1**	**MRF1**	**SPSW1**	**MRF1**	**SPSW1**	**MRF1**	**SPSW1**
5	5.84	3.40	3.95	0.35	4.1	2.4	2.7	0.2
6	7.59	3.39	5.41	1.18	5.3	2.4	3.8	0.8
7	4.64	4.78	1.93	2.31	3.2	3.3	1.3	1.6
8	4.16	3.77	0.79	0.97	2.9	2.6	0.5	0.7
9	7.01	3.70	5.10	0.36	4.9	2.6	3.5	0.2

4.2.4 Points of First and Last Yield with respect to Time

As mentioned in the previous section, the observed differences in peaks, noticed from superimposing response curves obtained after subtracting residual plastic displacements, implied that a deeper understanding of the plastic yield behavior of the considered archetypes was required. It was expected that the drift response of these models, as noted in Section 4.2.2, would be driven by the boundary frame after extensive yielding of the infill plates, which could possibly be an explanation for the similarities observed in response history. To get a better insight into the SPSW response and the specific contribution of the boundary frame to this response, it was decided to investigate, with respect to time, the hysteretic behavior of the flexural fiber hinges assigned to the HBEs in both archetypes. SAP2000 provides fiber hinge output as moment-rotation hysteresis curves; giving out the exact stress in each individual fiber at every time step. From this information, it is also possible to determine the points in time during which yielding of each individual fiber of the cross-section occurred. Instances of fiber yielding were extracted for the hinges defined in the HBE as described in Section 3.3.2. The instances when the first and last fibers in these hinges undergo yielding, for the very first and the very last time, were used to define a bracket of time that limits the occurrence of inelastic response during the entire response history. This method was expected to illustrate the plastic flexural behavior of the HBEs in an effective manner.

The same approach was adopted for the axial hinges, assigned to the tension-only strips, which model the steel plate web panel. All intervals during which the strips undergo plastic yielding for the first and last time were obtained by extracting the force-displacement output data for these axial hinges, and plotting the results with respect to time. In this way, the internal yield behavior of the SPSW and MRF archetypes could be “mapped” over time. It was expected that such a graph showing the individual contribution of both the steel plate and the boundary frame during the seismic response could provide insights as to what causes the difference in response behavior, and how duration of the earthquake affects it. The above mentioned method was carried out for response obtained from the following three input ground motions, namely:

- *M5*: Acceleration time history for moment magnitude of 5 (i.e. M5) with 9 seconds duration.
- *M5+5*: Duration of loading increased by using twice the above input acceleration with 4 seconds worth of intermittent zero-padding before and after the second consecutive M5 earthquake, increasing the total duration under consideration to 26 seconds.
- *M5+5+5*: Similarly increased ground motion, but this time by sequencing three times the original M5 time history, for a total duration of 39 seconds (when including the zero-padding after each M5 earthquake).

For each of these analyses, Figure 4-7 to Figure 4-9 show displacement response with the points of observed yielding for the axial and fiber hinges marked with respect to time for each consecutive earthquake repetition, where; for the axial hinges:

$AHFF_i$ = *First* yield point for the *first* axial hinge that experienced yielding
$AHFL_i$ = *Last* yield point for the *first* axial hinge that experienced yielding
$AHLF_i$ = *First* yield point for the *last* axial hinge that experienced yielding
$AHLL_i$ = *Last* yield point for the *last* axial hinge that experienced yielding

For the fiber hinges in both, the SPSW and the MRF, the following annotations were used:

$FHFF_i$ = *First* yield point for the *first* fiber in a fiber hinge that experienced yielding
$FHFL_i$ = *Last* yield point for the *first* fiber in a fiber hinge that experienced yielding
$FHLF_i$ = *First* yield point for the *last* fiber in a fiber hinge that experienced yielding
$FHLL_i$ = *Last* yield point for the *last* fiber in a fiber hinge that experienced yielding

The subscript "*i*" refers to the number of times the input time history was repeated to increase duration of loading. For this section, so far, i = 1 to 3.

From these figures it can be observed that there was a visible delay for the first fiber within the SPSW1 flexural fiber hinges to initiate plastic behavior, as compared to those in the MRF1 archetype. As expected in SPSWs, the axial hinges, owing to the higher lateral stiffness of the steel web panel compared to that of its boundary frame, underwent plastic yielding first, limiting drift and delaying involvement of the flexural hinges; for example, the first fiber to experience yielding for the SPSW1 hinge engaged at value of $FHFF_1$ = 1.715s compared to 0.81s for that of the MRF.

When comparing the behavior of the last fiber to initiate yielding, an inconsistency was observed in the MRF response for the three input cases; i.e. the value of $FHLF_1$ was found equal to 3.6s for the case of *M5*, as compared to that of 16.485s for both $FHLF_2$ (for *M5+5*) and $FHLF_3$ (for *M5+5+5*). It was found upon investigation that this inconsistency corresponded to the fact that not all fibers had reached yield stress for the case of *M5*, and hence the last fiber to engage in this case was not at the same depth within the HBE cross-section as that in the other two cases. Therefore, the values of $FHLF_1$ and $FHLL_1$ marked in Figure 4-7 do not represent the same fiber as the values of $FHLF_{2,3}$ and $FHLL_{2,3}$. For the SPSW response, it was observed that the last fiber to yield was engaged at a much earlier time as compared to the last fiber for the MRF. It was therefore concluded that within the SPSW archetype, the entire HBE cross-section fully yielded earlier than the MRF cross-section. It was possible that this was a direct result of the axial force interaction within the SPSW system, and therefore required a better understanding of the contribution of the steel plate towards response.

It was also noted that the values of $AHLF_i$ and $AHLL_i$ were found to be zero for the repetitions. The reason for this behavior was expected to be a shift in the direction of strips engaged, as the direction of accumulation of residual drift was observed to shift direction, but validation for this expectation was required in detail. Although this method gave an insight towards the progression of plastic yielding for both the SPSW1 and MRF1 archetypes, it did not fully articulate the contribution of the infill plate, and a more comprehensive approach was required in order to map the yielding of the modeled strips with respect to time. Following Section 4.2.5 further elaborates on this aspect.

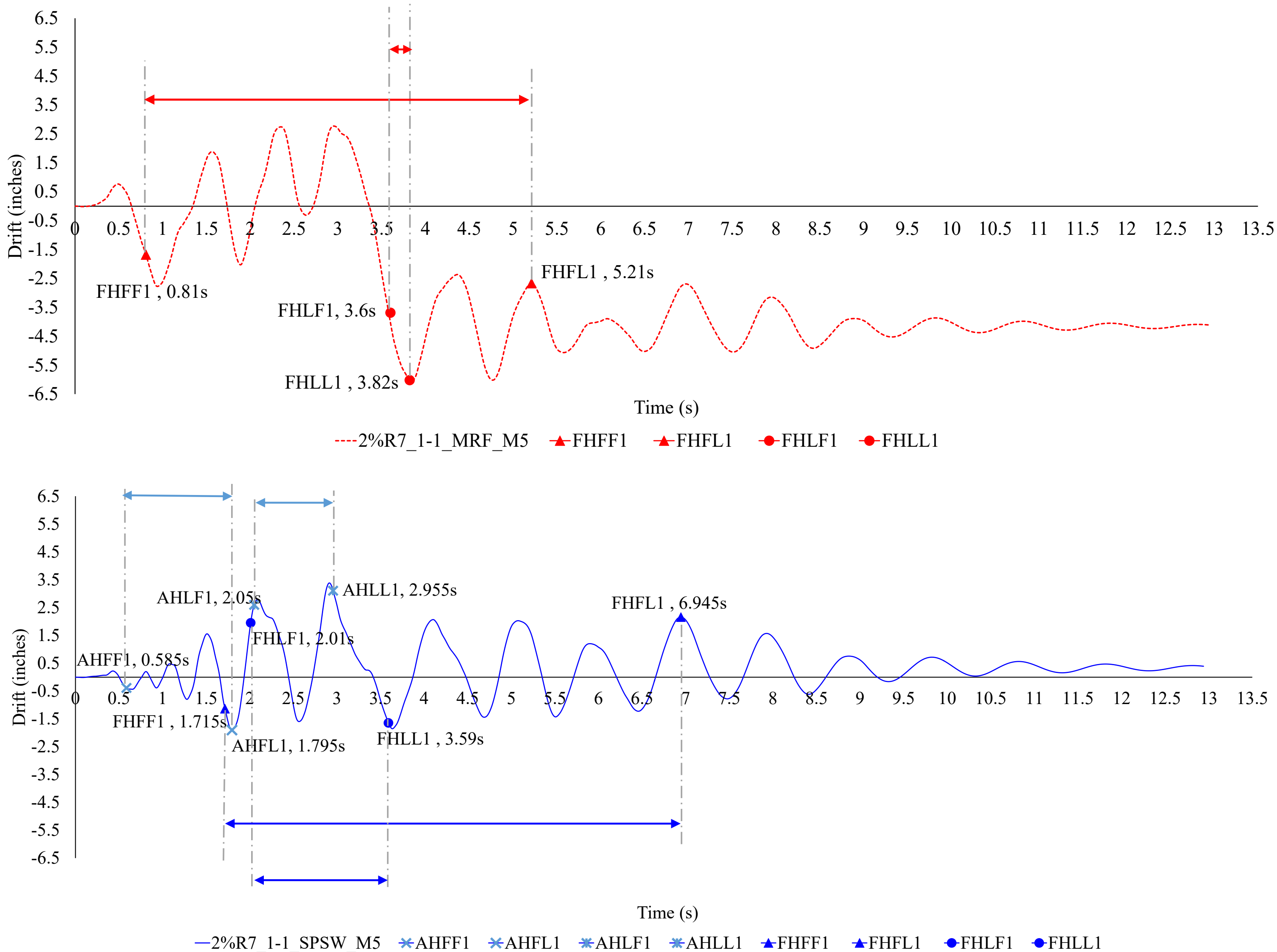

Figure 4-7 MRF1 and SPSW1 Response History for case M5 with yield points

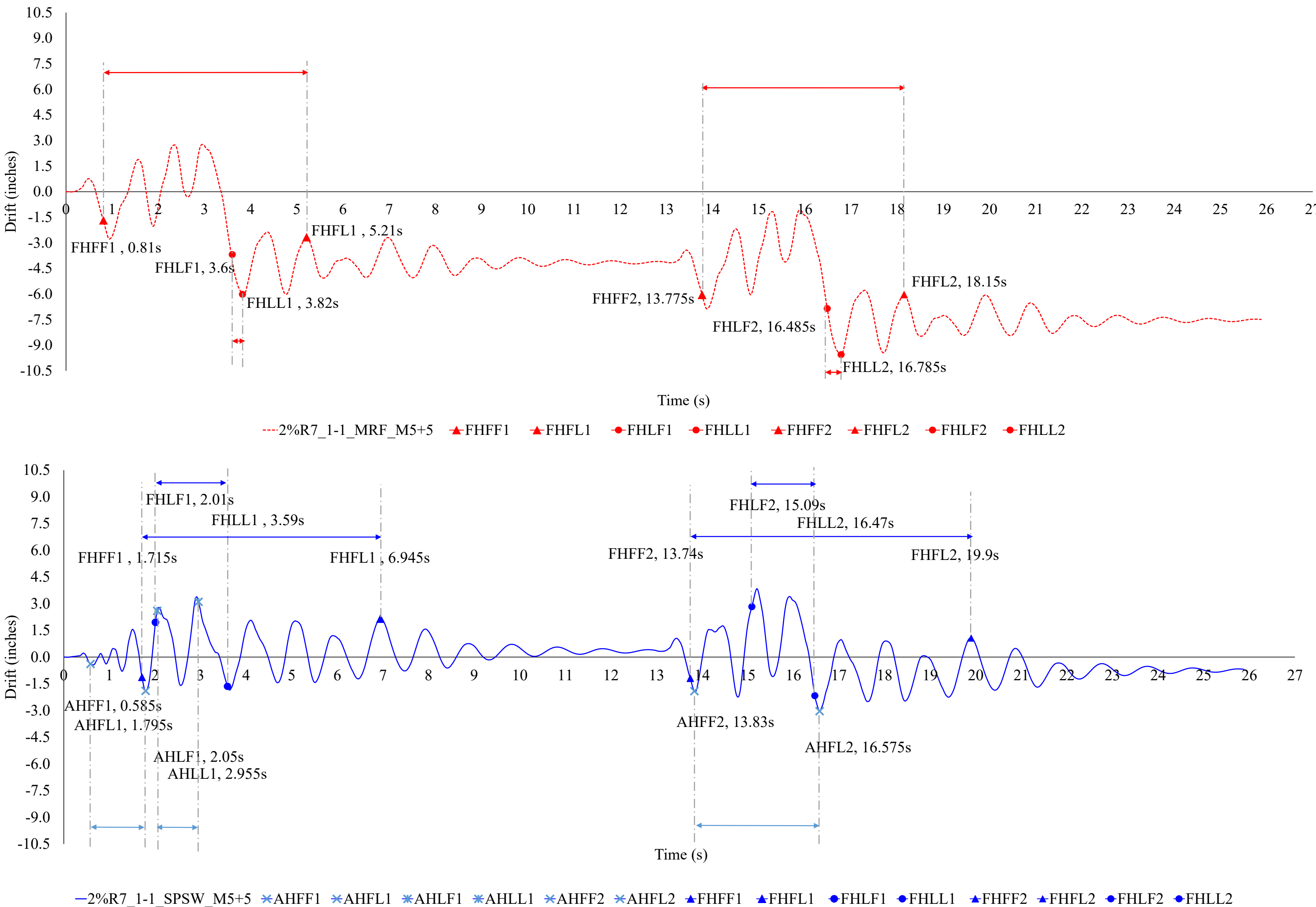

Figure 4-8 MRF1 and SPSW1 Response History for case M5+5 with yield points

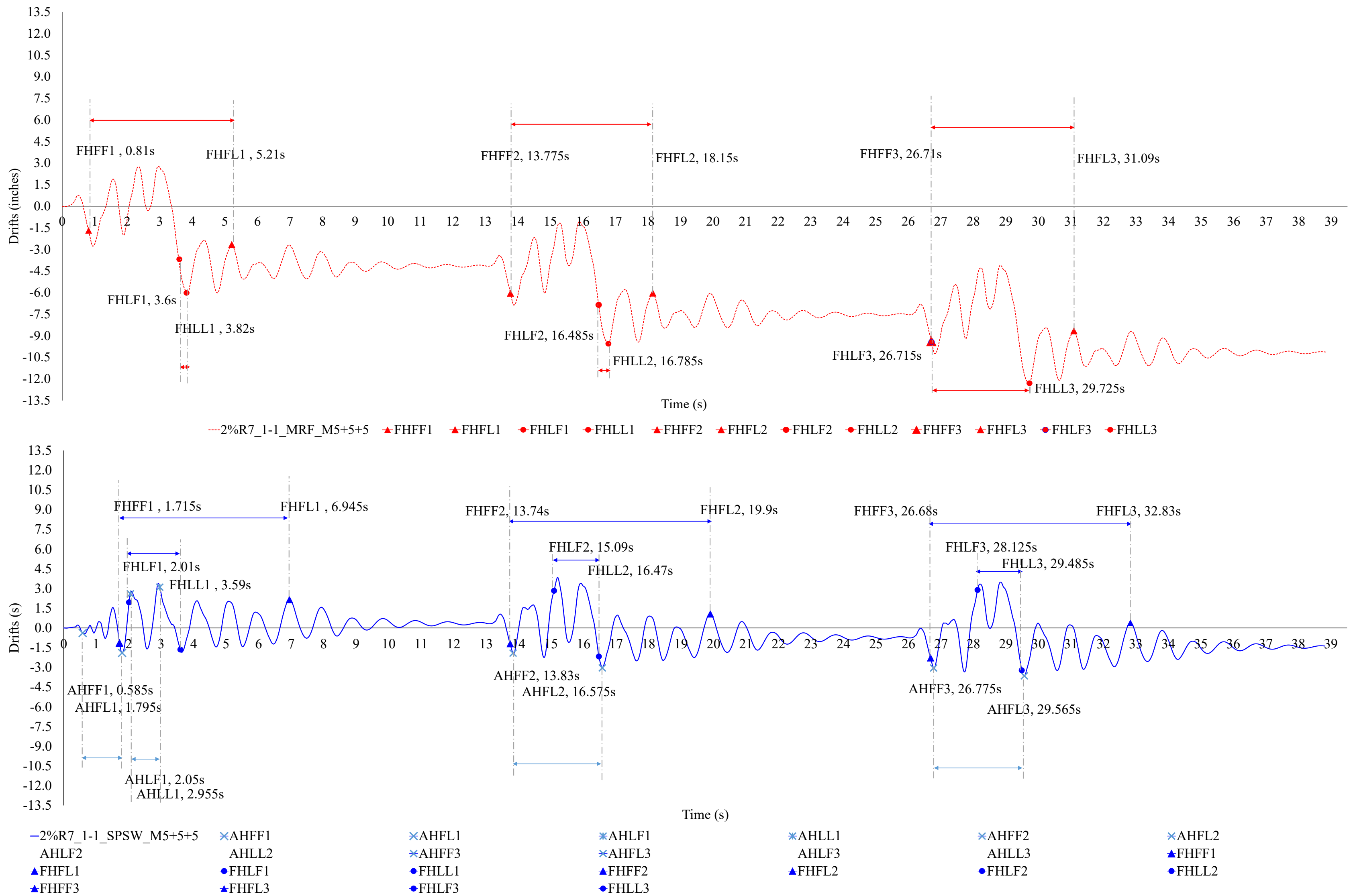

Figure 4-9 MRF1 and SPSW1 Response History for case M5+5+5 with yield points

4.2.5 Contribution of the Steel Infill Plate

In the previous section, it was noted that the presence of the steel plate infill within the boundary frame not only led to a delay in overall structural yielding, but also appeared to "catch" the boundary frame and prevent it from drifting excessively, as was evident from the lesser values of residual displacements obtained for the SPSW compared to those for the MRF, both of which were noted previously in Table 4 1. The work presented in this section further investigates, in more details, the contribution of how yielding of the infill plate affects response over increasing duration of earthquake loading.

Similar to preceding sections, the displacement response history was plotted for the top HBEs of SPSW1 models for the cases of *M5*, *M5+5*, and *M5+5+5*. Then, instances of plastic yielding for all the axial hinges were extracted from the program for each of these cases in a manner similar to Section 4.2.4. However, here, three states were noted for each axial hinge, namely; the onset of yielding, the onset of unloading, and the duration between both these points during which the hinge follows the constant plastic backbone for the pre-defined material model. All three states were plotted with respect to time in the form of a bar chart, where the length of the bar indicated the duration for which the considered hinge underwent plastic yielding. These "yield bars" were overlaid with the response histories for each of the three input cases to get a better visual correlation between seismic behavior and time.

Figure 4-10a, b and c show plots where the bar charts correspond to each axial hinge with a "hinge number". Note that axial hinge numbers are marked on the primary vertical axes, whereas the secondary vertical axes depict top HBE lateral displacement in inches. There were a total of 21 strips modeling the steel plate in the SPSW1 archetype (having R = 7), and the corresponding 21 Axial-P hinges were labelled 5H to 27H. Axial hinge 23H did not exist, and was not plotted. It can be observed from these figures that most of the axial hinges were engaged readily in the first few cycles when the SPSW experienced higher values of drift. For every subsequent yielding to occur, the structure had to undergo drift of higher value than the previous one. For the cases of *M5+5* and *M5+5+5*, it was seen that the response peaks that continued to engage the strips plastically, during repetitions of the earthquake, corresponded to movements that were in the same direction as the residual drift for the entire system. This caused instances of increase in the value of maximum drift, leading the axial hinges to repeat yielding for all such instances. Peaks in the direction opposite to that of the residual drift eventually cease to cause the corresponding strips to yield. This procedure helped show progression of plastic behavior of the steel plate, and accumulation of plastic strains, with the passage of time. To understand how these strips limited the increase in residual drifts, it was decided to extensively plot these "yield bars" simultaneously with the response from all other elements of the system. This is done in Section 4.2.6.

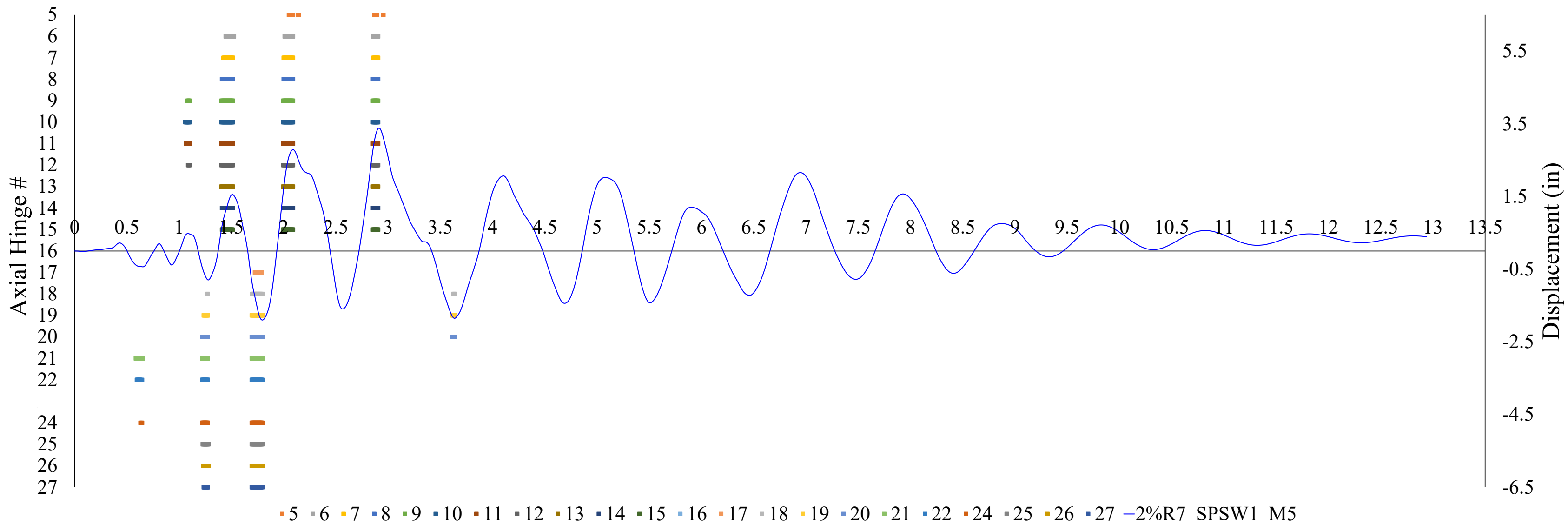
Axial Hinge #
Displacement (in)
5 6 7 8 9 10 11 12 13 14 15 16 17 18 19 20 21 22 24 25 26 27
5.5 3.5 1.5 -0.5 -2.5 -4.5 -6.5
0 0.5 1 1.5 2 2.5 3 3.5 4 4.5 5 5.5 6 6.5 7 7.5 8 8.5 9 9.5 10 10.5 11 11.5 12 12.5 13 13.5
5 6 7 8 9 10 11 12 13 14 15 16 17 18 19 20 21 22 24 25 26 27 2%R7_SPSW1_M5

a)

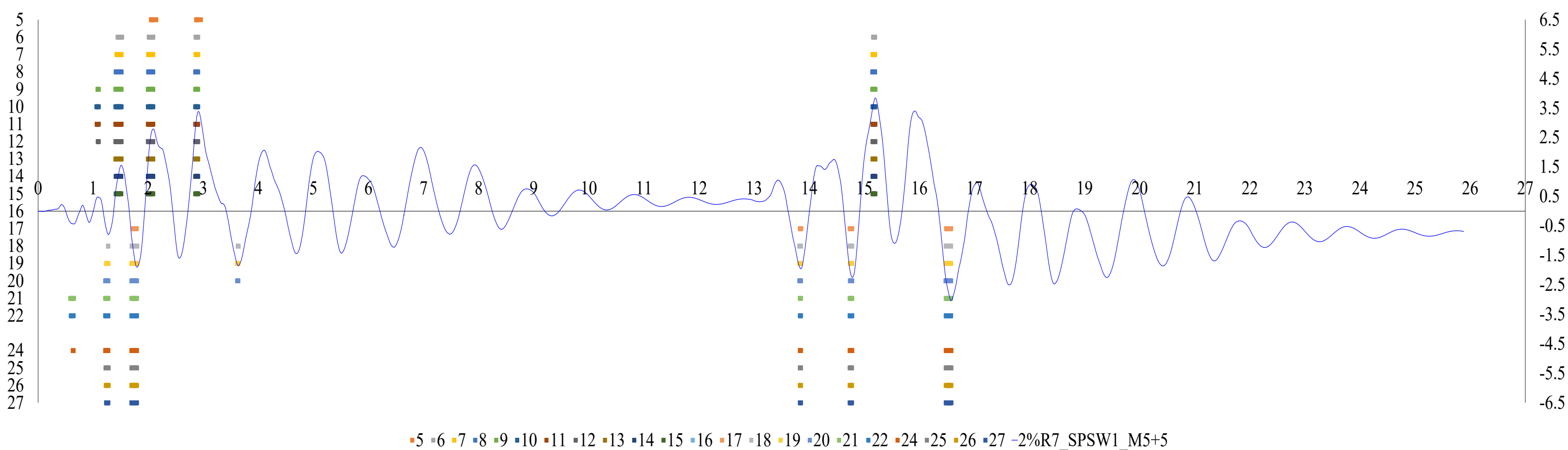
5 6 7 8 9 10 11 12 13 14 15 16 17 18 19 20 21 22 24 25 26 27
6.5 5.5 4.5 3.5 2.5 1.5 0.5 -0.5 -1.5 -2.5 -3.5 -4.5 -5.5 -6.5
0 1 2 3 4 5 6 7 8 9 10 11 12 13 14 15 16 17 18 19 20 21 22 23 24 25 26 27
5 6 7 8 9 10 11 12 13 14 15 16 17 18 19 20 21 22 24 25 26 27 2%R7_SPSW1_M5+5

b)

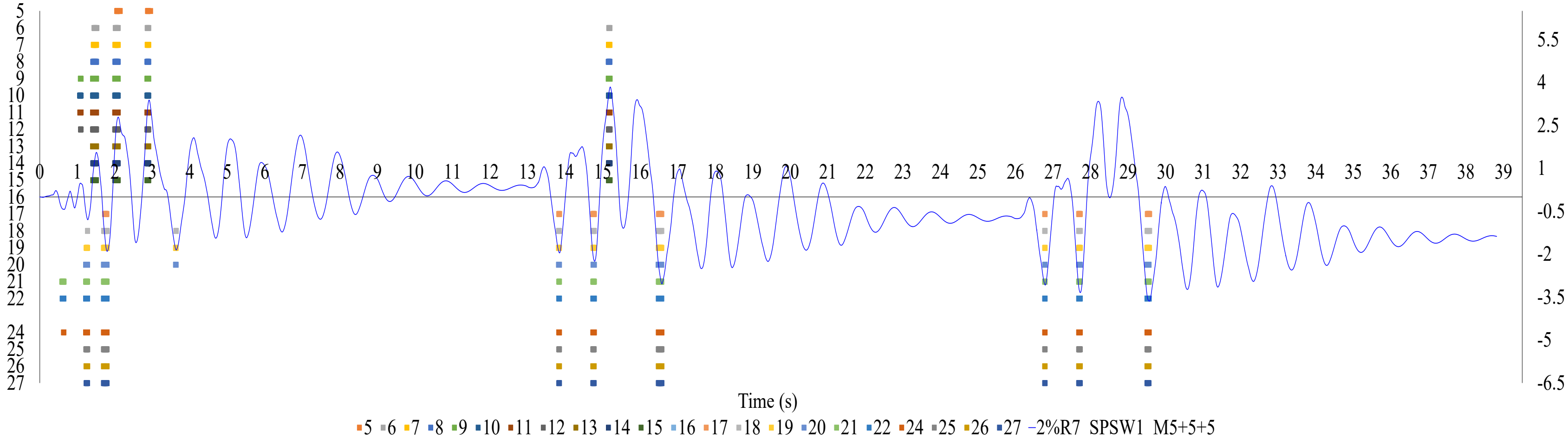

c)

Figure 4-10 Axial hinges "yield bar charts" for the cases of a) M5, b) M5+5, and c) M5+5+5

4.2.6 Cross-comparison of overall behavior

This section condenses the many approaches previously used to understand the behavior of the individual structural components in one graph, in order to provide a thorough cross-comparison of the interaction of all elements involved. The objective was to identify the point in time where the steel web no longer contributed strength to the structural system, and to see whether the response of both the SPSW and the MRF would begin to converge at some point. It was also expected to better understand the role of the steel plate web in preventing large residual drifts.

For the purpose of this section, the approach used in Section 4.2.5 was repeated with a much longer duration of loading. The ground motion time history was prolonged by providing 6 repetitions of the M5 earthquake, with 4 seconds intermittent zero-padding between each consecutive earthquake. Therefore the total duration of seismic loading was around 78 seconds. Yielding of the axial hinges was plotted with respect to time following the same method as in the previous sections. Yielding patterns for each individual fiber present in the flexural fiber hinges, assigned to the HBEs for both the SPSW and the MRF, were also marked respectively in a similar fashion.

Figure 4-11 shows top HBE lateral displacement for SPSW1 and MRF1, with yield response marked for axial hinges in each of the strips within SPSW1 in part a, and for flexural hinges in the HBEs for SPSW1 and MRF1 archetypes in parts b and c respectively. The plot in Figure 4-11 was divided into six segments for ease of visual inspection, with each of these segments presented in Figure 4-12 to Figure 4-17. Each segment had a duration of 13 seconds, and gave a close-up version of the different yield behaviors observed. The same procedure was repeated for ground motion time histories of M8, where input accelerations were also repeated six times with each segment duration of about 112 seconds (42 second ground acceleration followed by zero-padding). The obtained results are later discussed in detail in Section 5.2.

When comparing results from these figures, it was noted that both the MRF1 and the SPSW1 archetypes appear to have certain similarities, with both archetypes engaging in plastic behavior during the stronger portions of the ground motion. As shown in the previous sections, the SPSW archetype faced delays in initiation of yielding as compared to the MRF. The response behavior was notably different at the 7 second mark. At this point, the SPSW1 response depicted a singular yielding spike within the flexural hinges. A similar yielding spike was not observed at that time in the MRF1 response, leading to questions as to the cause of this occurrence. Demands in the axial hinges of the SPSW were scrutinized to understand the nature of this dissimilarity; response from these hinges provided some “snapshots” of the stress conditions in the steel web. It was observed that the steel plate experienced yielding up until approximately the 3.8

second mark. Beyond this point, the stresses within the steel web no longer reached yield levels as the peaks in the input ground motion were of lesser magnitude, and being so, did not re-engage the steel web's interaction in the system. After the 3.8s mark the magnitude of the ground acceleration started decreasing, up until the 7s mark, where a slight increase to the previously declining pattern was experienced. This sudden increase in loading produced new stresses, but, given the fact that the value of overall drift was less than that which had last engaged the steel web (at the 3.8s mark), the steel plate web did not experience further yielding. The steel plate was therefore understood to be "pre-stretched" at the considered point, leaving the boundary frame around it alone to resist the sudden acceleration. The yielding spike within the fiber hinges in the SPSW1 archetype, therefore, was attributed to the above behavior.

Beyond this point, the SPSW1 model behaved as if there was no steel web present. However, as soon as the overall drift became large enough to exceed levels previously produced (at the next consecutive earthquake), the steel plate was observed to reengage, hence never truly acting fully identical to the MRF archetype. The MRF1 model did not exhibit this same behavior, as the response of the frame prior to this point was greater in value, leaving the frame to continue to drift but without yielding, until the next repetition of the M5 earthquake. Note that the residual drifts accumulated with each consecutive peak of maximum drift engaging the frame in new episodes of yielding.

Results from the above case studies indicate that the steel plate web within the SPSW structure never truly stopped contributing strength to the system. It limited the increase in residual drifts for the structure by "catching" the boundary frame at every successive point of maximum drift. It also delayed yielding of the boundary frame. It could thus be reasoned that the steel web continued to provide strength and stability to the structure when subjected to long duration earthquakes. The boundary frame was also crucial to response of the overall SPSW structural system. During those times when the frame lateral response was less than the previous peak, the steel plate was effectively "stretched" or "non-contributing", and all of the earthquake demand was resisted by the boundary frame, for which the HBE plays a major role in limiting drift (as in all moment resisting frames). Design of the HBE section therefore becomes fundamental to overall seismic behavior of the SPSW system.

Note that 3-4% drift is understood to be a usual range for satisfactory seismic performance of SPSWs. Figure 4-18 shows that the SPSW1 displacement response exceeds the 3% drift mark after the 5th earthquake. As initially explained in Section 1, this research did not include the limit states of strength degradation, strain hardening and fracture. However, it can be seen that even if it were possible to overcome these limits, the SPSW would never behave as a bare frame owing to the accumulation of residual drift.

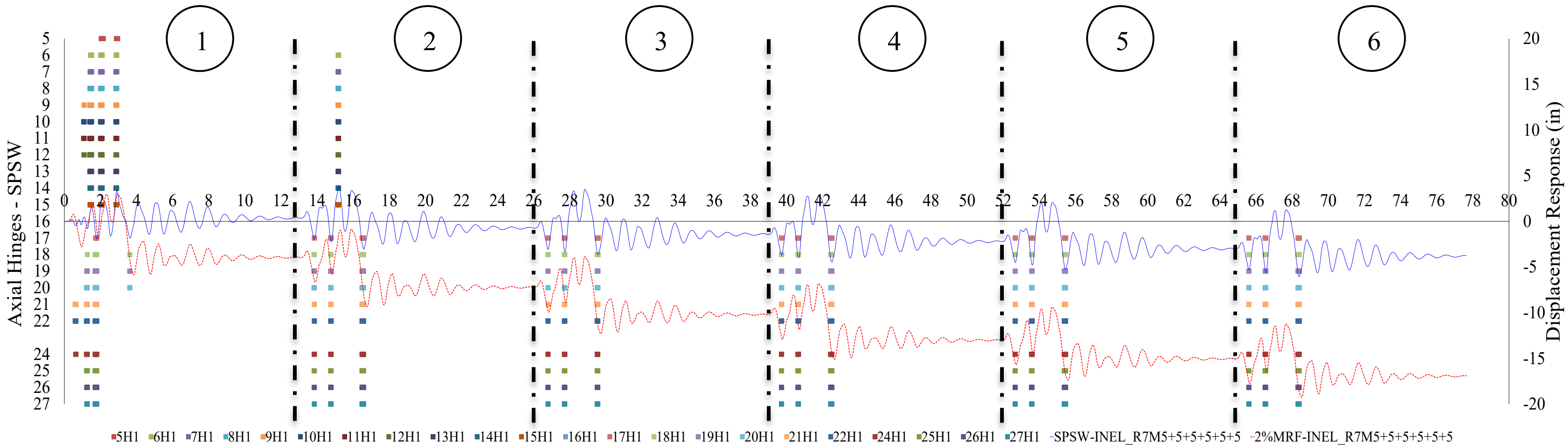
1
2
3
4
5
6
Axial Hinges - SPSW
Displacement Response (in)
0 2 4 6 8 10 12 14 16 18 20 22 24 26 28 30 32 34 36 38 40 42 44 46 48 50 52 54 56 58 60 62 64 66 68 70 72 74 76 78 80
5 6 7 8 9 10 11 12 13 14 15 16 17 18 19 20 21 22 24 25 26 27
20 15 10 5 0 -5 -10 -15 -20
5H1 6H1 7H1 8H1 9H1 10H1 11H1 12H1 13H1 14H1 15H1 16H1 17H1 18H1 19H1 20H1 21H1 22H1 24H1 25H1 26H1 27H1 SPSW-INEL_R7M5+5+5+5+5+5 2%MRF-INEL_R7M5+5+5+5+5+5
a)

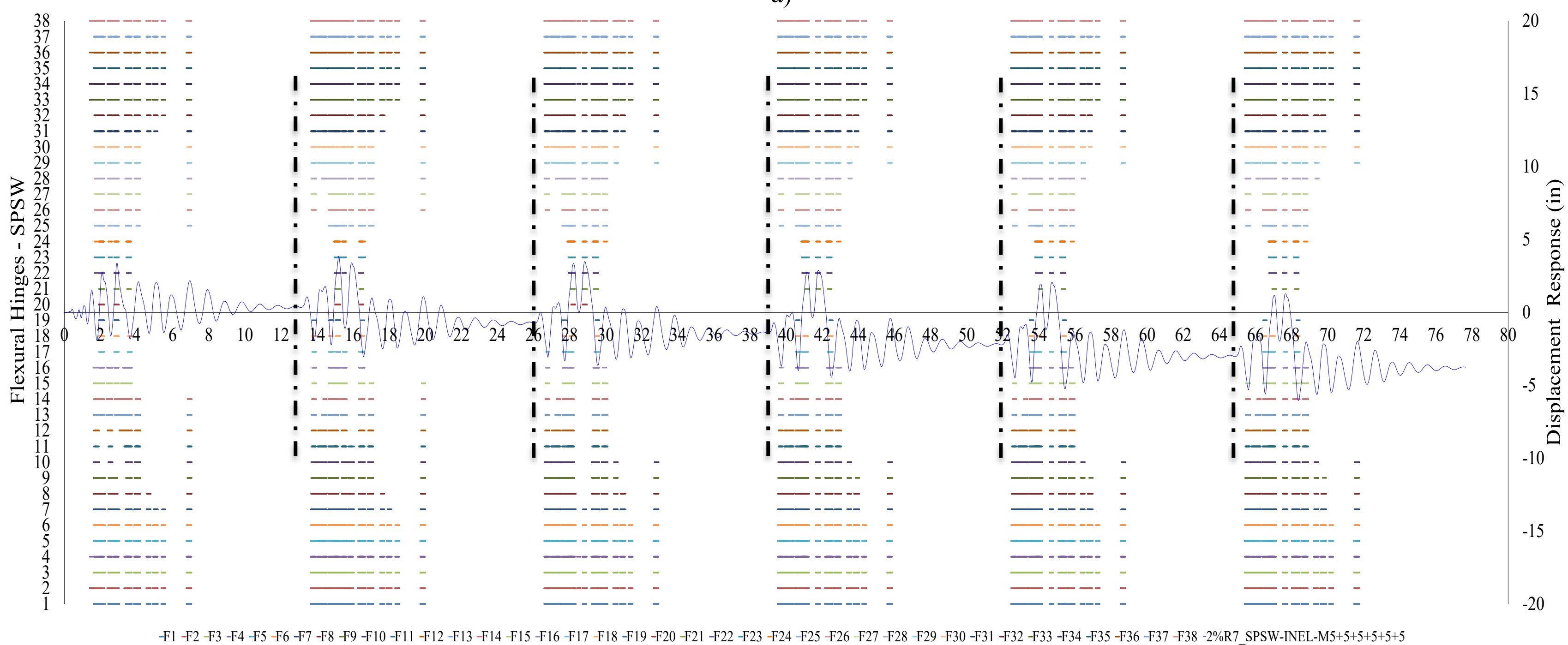
Flexural Hinges - SPSW
Displacement Response (in)
0 2 4 6 8 10 12 14 16 18 20 22 24 26 28 30 32 34 36 38 40 42 44 46 48 50 52 54 56 58 60 62 64 66 68 70 72 74 76 78 80
1 2 3 4 5 6 7 8 9 10 11 12 13 14 15 16 17 18 19 20 21 22 23 24 25 26 27 28 29 30 31 32 33 34 35 36 37 38
20 15 10 5 0 -5 -10 -15 -20
F1 F2 F3 F4 F5 F6 F7 F8 F9 F10 F11 F12 F13 F14 F15 F16 F17 F18 F19 F20 F21 F22 F23 F24 F25 F26 F27 F28 F29 F30 F31 F32 F33 F34 F35 F36 F37 F38 2%R7_SPSW-INEL-M5+5+5+5+5+5
b)

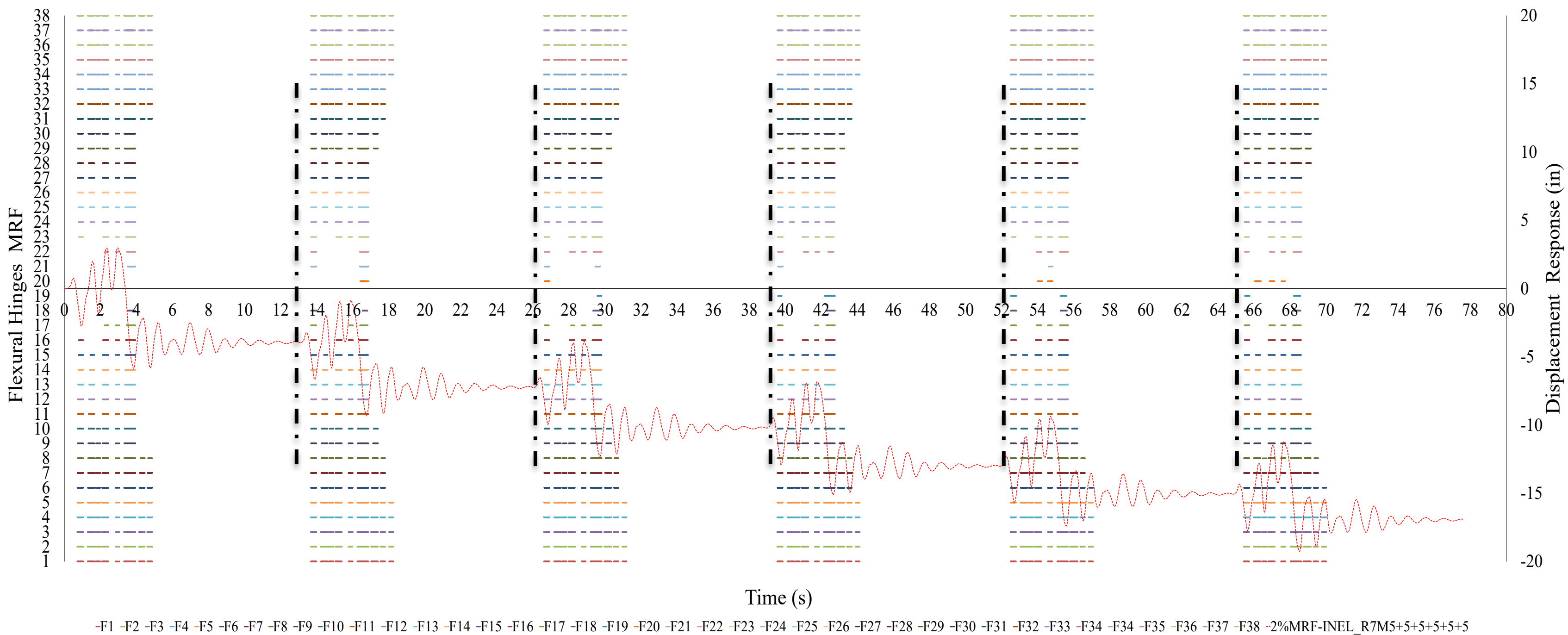

c)

Figure 4-11 M5+5+5+5+5+5 for *R*=7, ζ=2%; Yield Behavior for

a) SPSW Axial Hinges b) SPSW Flexural Hinges, and c) MRF Flexural Hinges

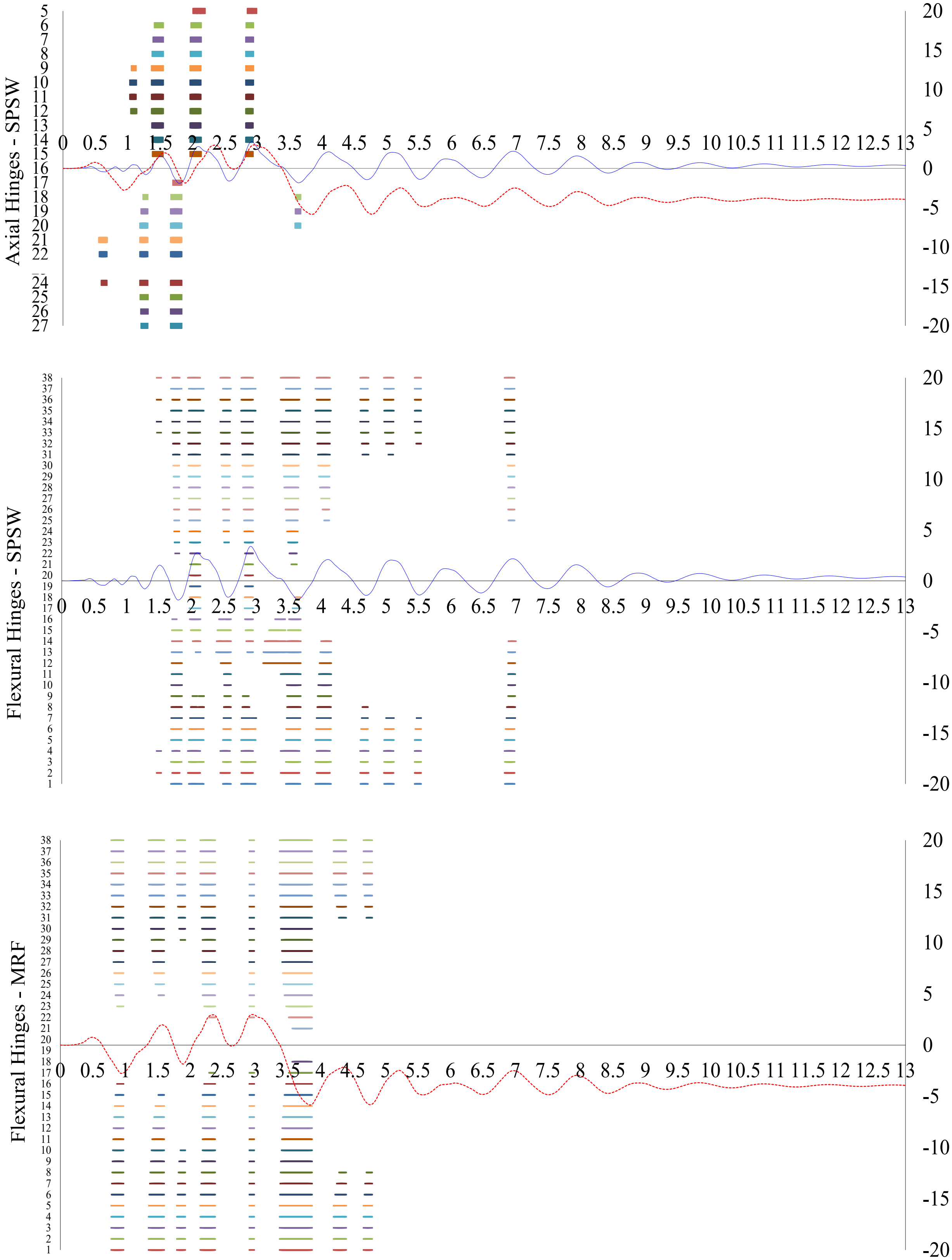

Figure 4-12 Yield Behavior, Segment 1 – 0 to 13 seconds

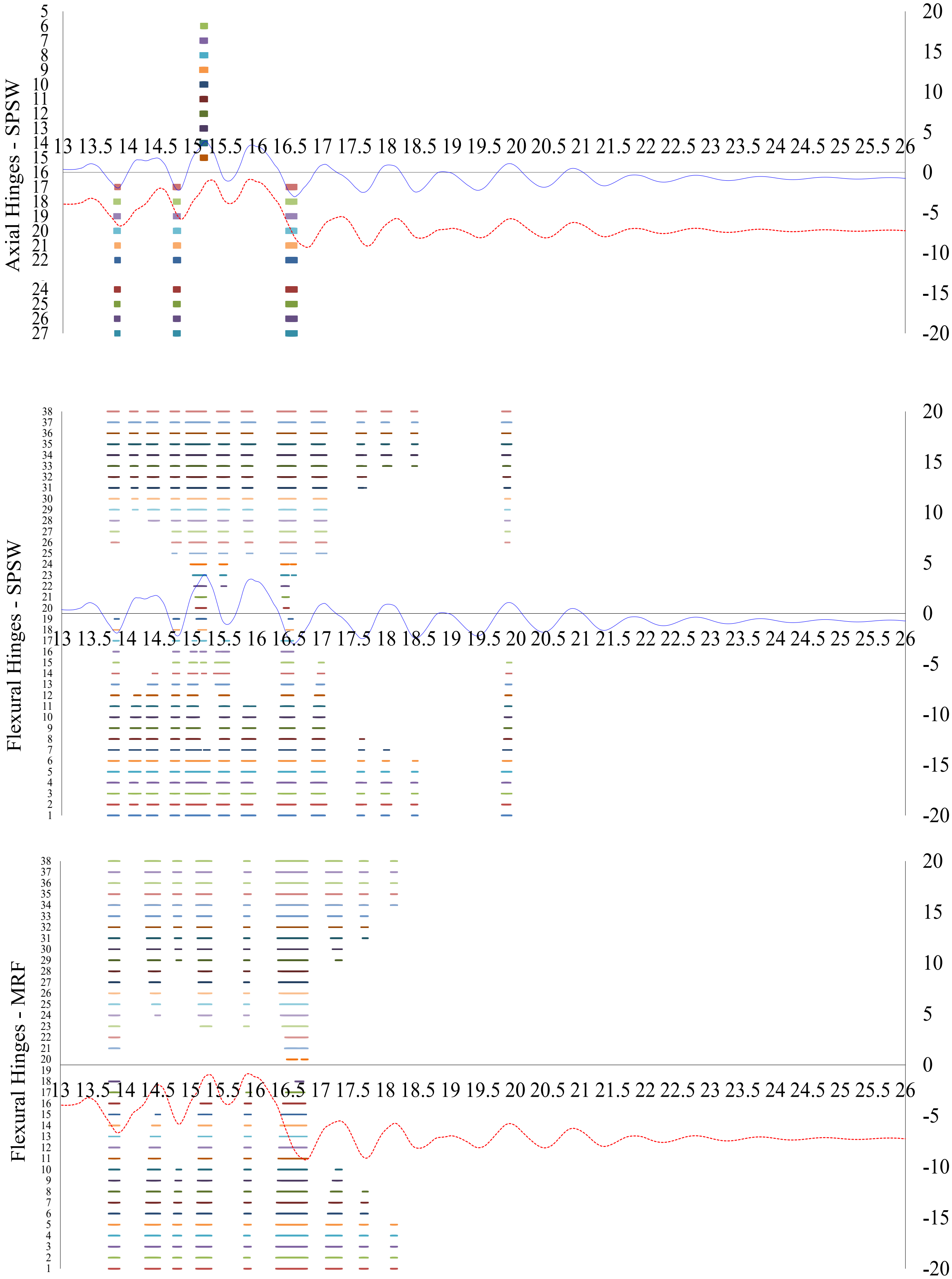

Figure 4-13 Yield Behavior, Segment 2 – 13 to 26 seconds

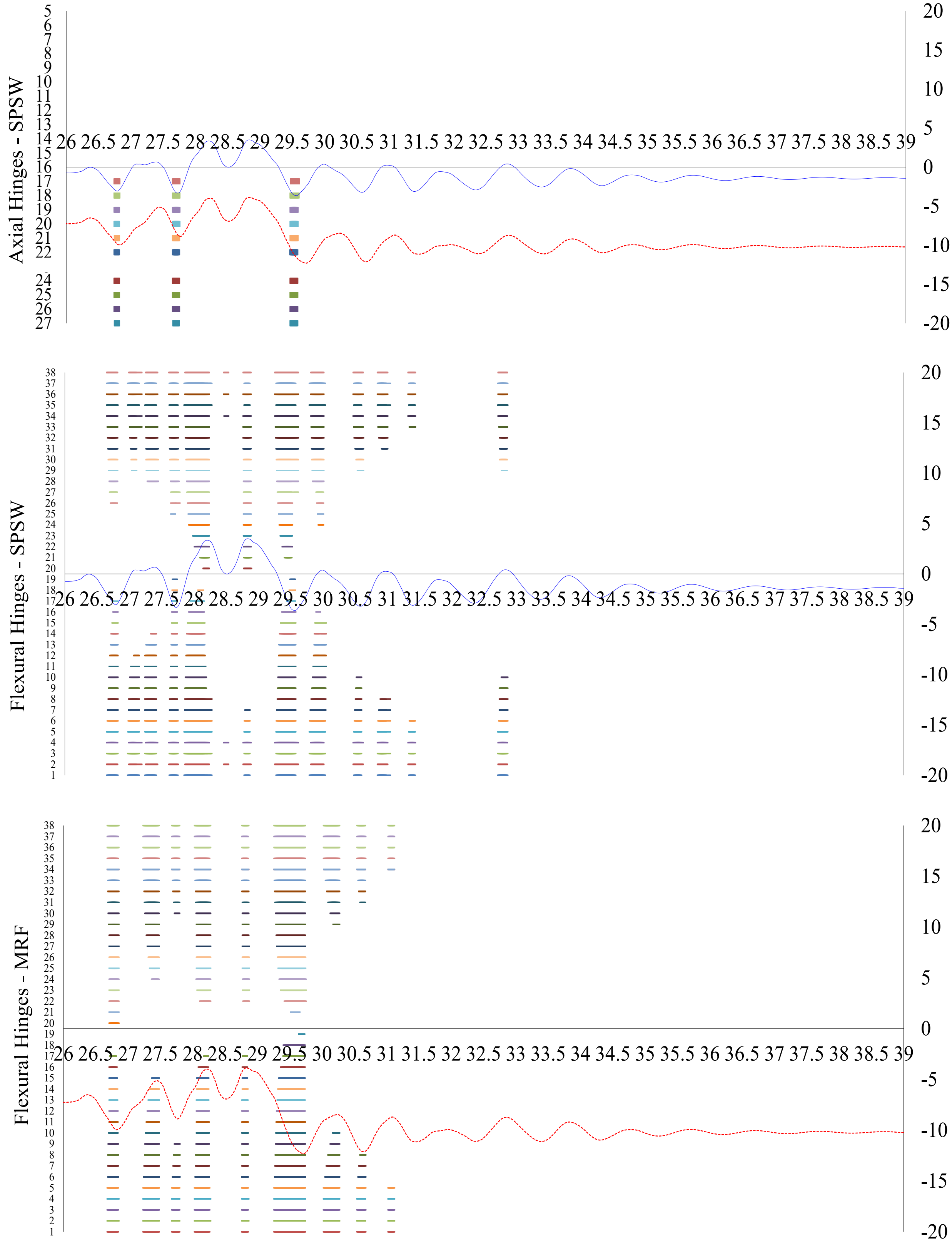

Figure 4-14 Yield Behavior, Segment 3 – 26 to 39 seconds

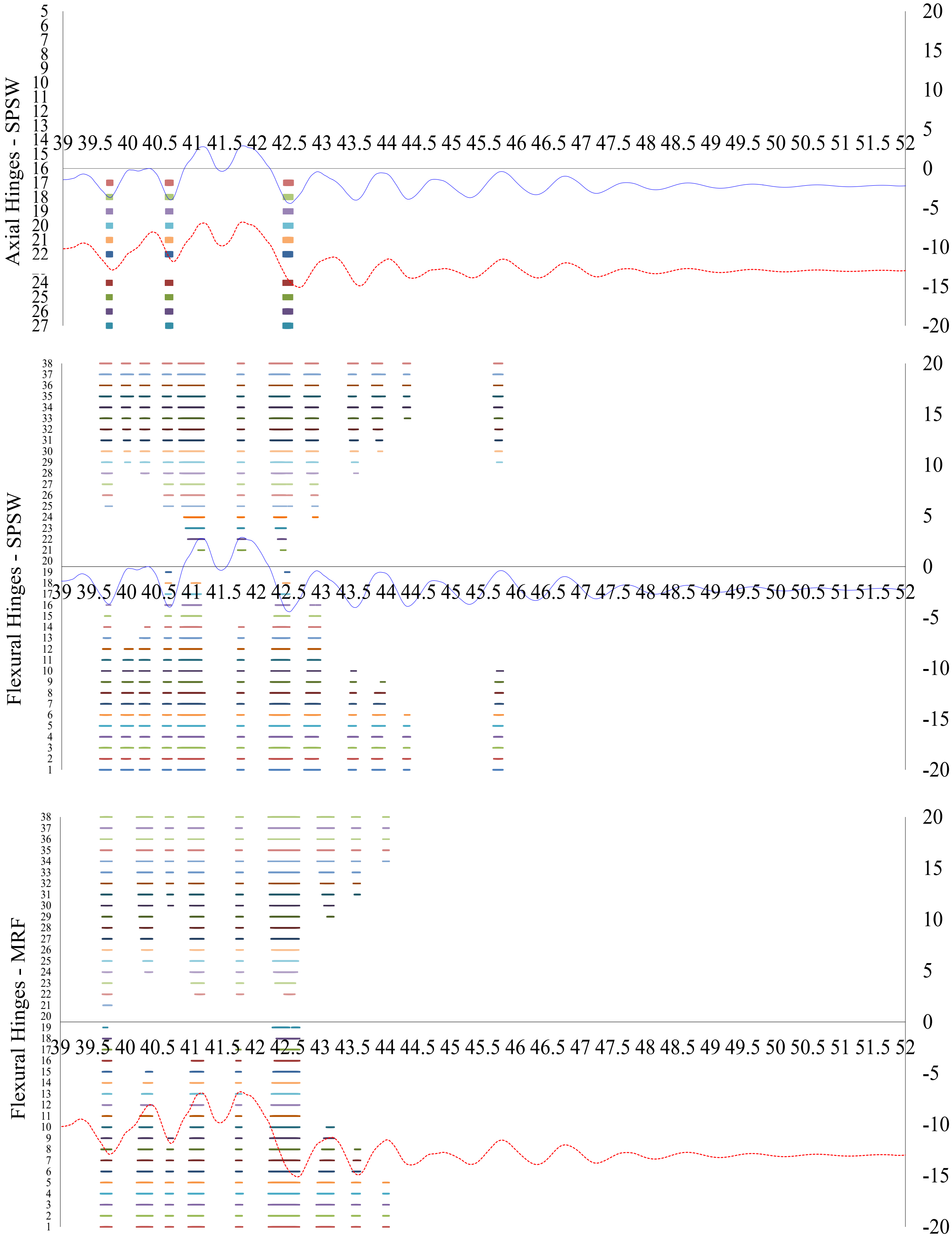

Figure 4-15 Yield Behavior, Segment 4 – 39 to 52 seconds

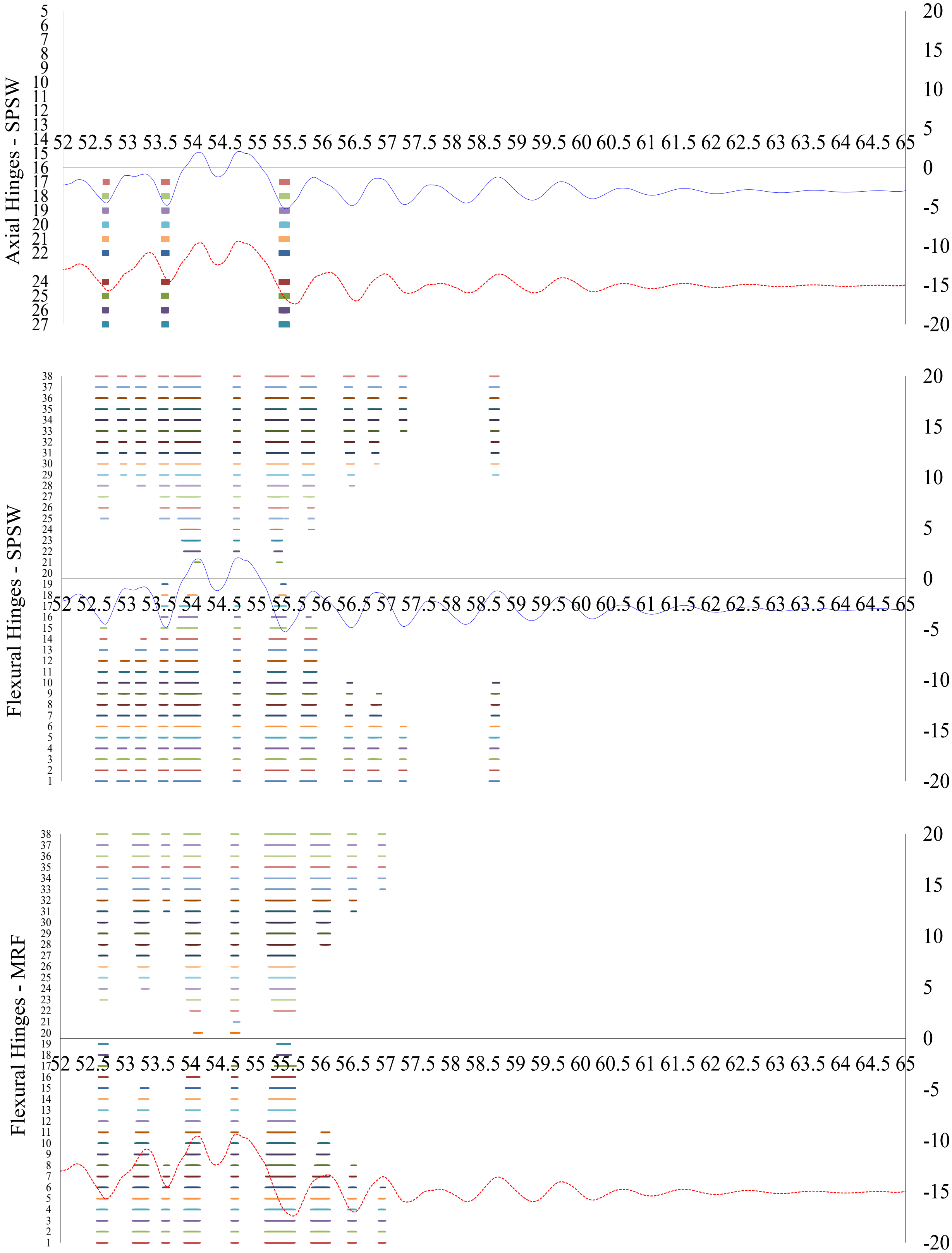

Figure 4-16 Yield Behavior, Segment 5 – 52 to 65 seconds

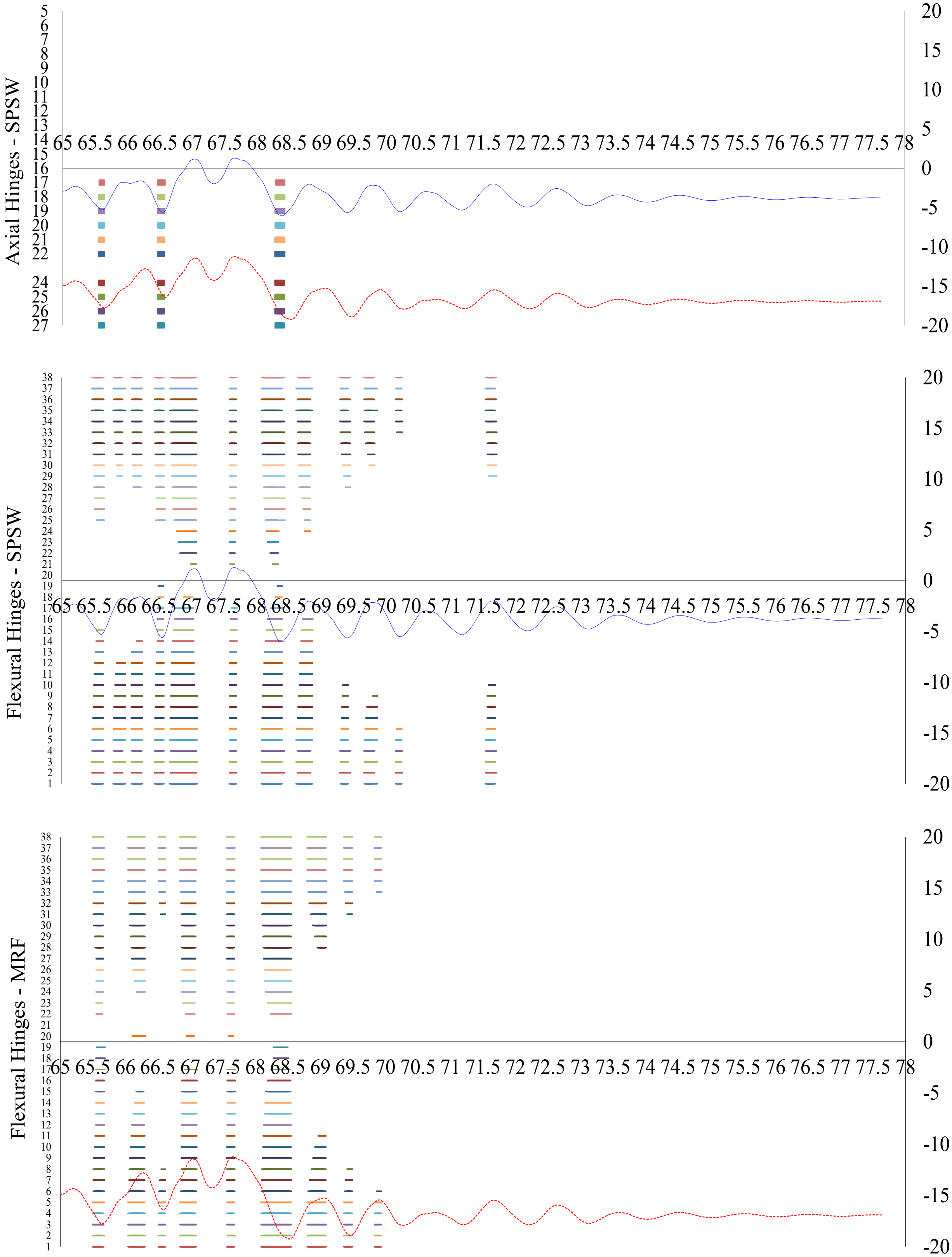

Figure 4-17 Yield Behavior, Segment 6 –65 to 78 seconds

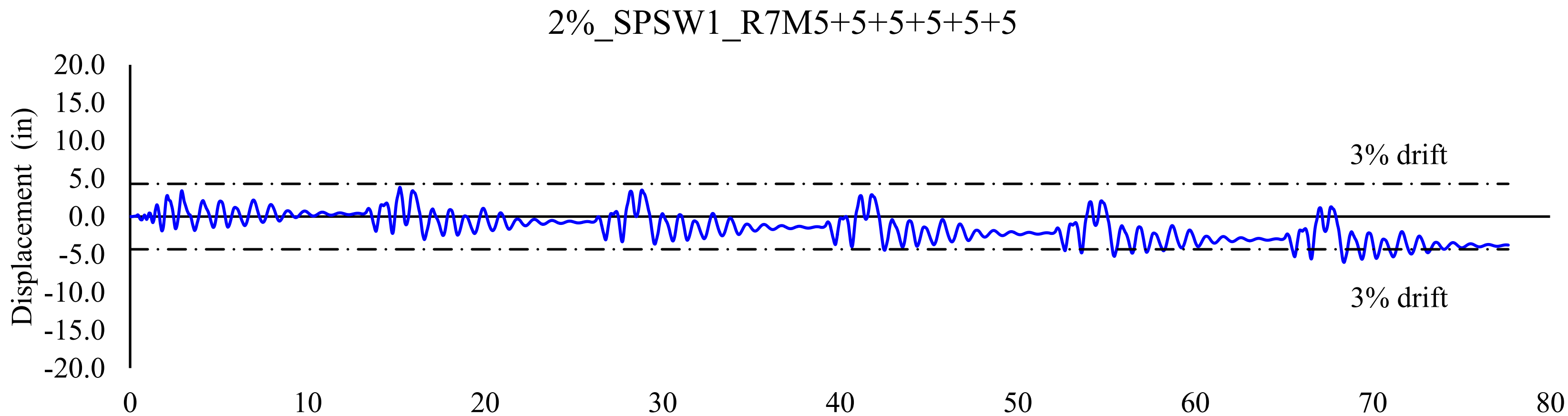

Figure 4-18 SPSW1 Displacement response for ζ = 2%, R= 7, M5+5+5+5+5+5 with 3% drift mark

4.3 Summary

- The Fast Fourier Transform method was found unreliable for obtaining gradual variation in time of the structural system's period given its sensitivity to the duration of the time interval chosen to calculate this "instantaneous" value.
- The RSCTH program matched the same target spectra to all specified durations of earthquakes, resulting in lower values of peak ground acceleration for higher magnitude earthquakes. Synthetically generated ground motion time histories for increasing earthquake magnitudes were therefore found to not be a logical basis of comparison for response.
- Development of stress within fiber and axial hinges was monitored and compared to better understand the progression of plastic yielding in both archetypes.
- Response peaks that engaged the steel web plastically were observed to correspond to movements in the same direction as the residual drift, causing instances of increase in the value of maximum drift.
- A thorough cross-comparison was made by indicating, on the time history response of the SPSW and of the boundary frame alone, the duration from first to last instance of yielding for the various elements in the system, which helped to understand the how the strips limited the increase in residual drifts.
- The steel plate web was seen to continue to offer strength to the system at various times throughout the entire duration of the earthquake, when drifts exceeded preceding drift values. Doing so, it served to control the maximum drift by restricting the boundary frame, minimizing the amplitude of yield excursions, and delaying further yielding.
- Sizing of the HBE remains an important aspect for controlling overall seismic response, as the boundary frame was observed to resist all additional earthquake loads during this intervals when the steel web did not contribute to response.

SECTION 5
SENSITIVITY OF RESULTS OBTAINED

5.1 General

Section 4 above discussed, in sequence, all the analyses performed for the singular case of R = 7, panel aspect ratio of 1:1, and value of damping equal to 2% of critical damping ratio. However, as mentioned in Section 4.1, several different analyses were also performed for cases which considered variations in R-factor, damping ratio, panel aspect ratios, total number of stories in the structure, and the duration of earthquake ground motion the structure was subjected to. Results obtained from these analyses are presented here and serve to improve confidence in the seismic behavior of SPSW under prolonged earthquake loading.

In this section, the results obtained from the above mentioned array of analyses (performed to investigate and compare the sensitivity of various individual factors on the response of SPSWs) are presented as follows. Section 5.2 compares the results for the SPSW and MRF archetypes based on observed changes in residual drifts with increase in number of times the earthquake ground motion time history was repeated, or in other words; as a function of the increase in duration of seismic loading. Section 5.3 then, compares the sensitivity of results when using values of damping ratio equal to either 2% or 5% of the critical damping ratio. Archetypes used for this comparison were designed for a value of *R* equal to 7. However, in total, archetypes were designed for values of *R* equal to 5 and 7 for single story models, and 7 for multi-story models. Keeping all other factors constant, results obtained from analyzing models designed with different values of *R* are compared in Section 5.5 in order to observe sensitivity of the results to various level of ductility demands on the structures while Section 5.45.3 shows the effects of varying panel aspect ratios on the characteristics of response considered here. Results from various analyses for the multi-story SPSW3 were also compared to assess the effects of long duration earthquake loading, as presented in Section 5.6.

While designing the SPSW1 archetype, relatively small length of the HBE members led to higher end moments, resulting in higher shear concentrations; and since there was no additional steel web panel, any resistance to this excessive shear was solely contributed from the boundary frame. Therefore, the design for sizing the HBE members presented challenges in meeting the minimum code-specified shear requirements for the HBE member, leading to difficulties in finding suitable sections during design. By contrast, these issues were not present in SPSW2 or SPSW3, owing to increased width of the structure and multiple stories for each archetype respectively. This sensitivity to design considerations is explained in detail in Section 5.7.

5.2 Sensitivity to Increase in Earthquake Duration

For SPSW1 designed for a value of R = 7, with panel aspect ratio = 1:1, and ζ = 2%, residual drift values were noted at the end of each earthquake in the repetition sequence for the input time histories of moment magnitude of M5 and M8. Figure 5-1 shows the increases in residual drift at each step of the analyses for both moment magnitudes considered. With every subsequent repetition of the input ground acceleration, it can be observed that the residual drifts increase in both the SPSW and MRF cases. However, the overall residual drift in the MRF is of much higher values than that in the SPSW, which is expected given its lesser stiffness. Recall that P-delta effects were not considered here and were not part of the current scope of research.

For the MRF, the increase in residual drift for the M5 earthquake ground motion was observed to grow quite rapidly for the first three repetitions, after which the rate by which the residual drift increased gradually became relatively constant. For the M8 earthquake, this increase was observed to grow relatively constantly only for the last repetition. As was observed in Section 4.2.4, the entire cross-section for the HBE within the MRF model does not fully yield in the first few repetitions, but a comparatively constant increase in drift becomes evident only after all fibers within the cross-section are fully engaged. In comparison, the SPSW demonstrates a lesser rate of change in the additional residual drift as the number of repetitions increase. The steel plate enables the HBE cross-section to fully yield early on through the duration of the earthquake loading, allowing for the increase in residual drift to become a near constant value after each earthquake occurrence, straight from the beginning.

Durations of yielding were also plotted with respect to increase in repetitions of the earthquakes. Figure 5-2 shows the "yield bracket", i.e., the duration between the instance of the first yield and the instance of last unloading for each repetition, marked as D_{YB}. Here the subscripted terms *FHF* and *FHL* stand for "fiber hinge first fiber" and "fiber hinge last fiber" respectively. These "yield bracket" durations were normalized with the duration of the individual earthquake ground motion, marked as D_N, and equal to 9 seconds for the M5, and 42 seconds for the M8 earthquake. It can be seen from Figure 5-2 that for the SPSW archetype, the "yield bracket" for *FHF* was relatively constant, depicting a slight increase only through the first earthquake for both M5 and M8 repetition cases. The SPSW response for *FHL* showed near constant values for the M5 earthquake, but for the M8 earthquake these *FHL* values reduced to zero early in the sequence of repetitions indicating that the entire cross-section did not remain engaged through all repetitions. On the other hand, the MRF behavior mirrors that explained in Section 4.2.4, where, for the M5 earthquake, *FHF* shows relatively constant values, but *FHL* depicts increase in value only after the first repetition; when the entire MRF HBE cross-section yields fully. For the M8 earthquake, the MRF response for *FHL* indicates that, like that within the SPSW flexural hinge, the last fiber was not engaged for long. This behavior can also be observed from Figure 5-4. Then, parts a, b, c, and d of Figure 5-3 show variations in the yield bracket duration as a function of the length of earthquake loading for the steel infill plate, based on the first and last strips to undergo plasticity for both. Here, *AHL* and *AHF* display behavior of "first axial hinge to undergo yielding" and "last axial hinge to undergo yielding" respectively. As for the case of flexural hinges, the purpose of these figures is to help assess the contribution of the steel plate towards seismic response from a standpoint of duration of yielding, however, it was observed that the geometric position of the strip within the archetype was also influential to initiation and continuation of yielding behavior. The first strip to yield did not necessarily continue to remain engaged throughout the earthquake loading, as can be seen in the case of the M8 earthquake repetitions, where the first strip to yield appears to show zero values for *AHF* for the fourth and fifth repetition. Upon detailed investigation, and by plotting Figure 5-4, it was evident that this happened because of the change in direction of drift response for the SPSW system, and does not indicate that the steel plate is no longer responding. Since *AHF* and *ALF* are not entirely representative of plastic yield behavior of the steel plate, these plots were henceforth not considered.

It is important once again to note that these results consider material models with infinite yield plateaus. In actual materials, significant strain hardening would develop in the boundary elements, but strength degradation would eventually develop at large drift, and the drift magnitude would undoubtedly also have direct implications towards the effectiveness of the structural system in resisting earthquake excitation; however, even though both these effects have not been considered here, the results presented here are significant in explaining why SPSWs are effective in resisting long-duration earthquakes in spite of the tension-only behavior of their infill plates.

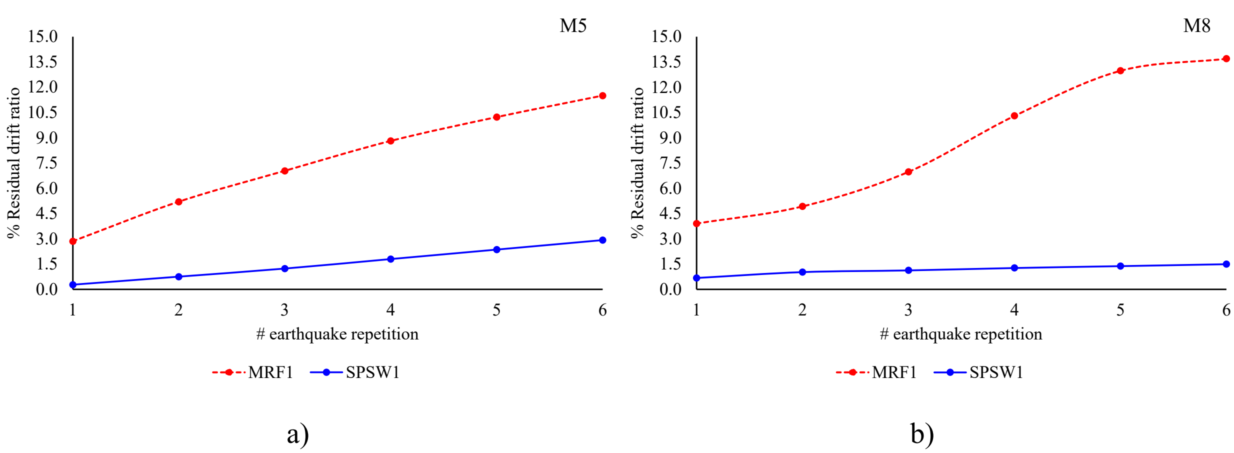

Figure 5-1 %age residual drift for MRF1 and SPSW1 w.r.t. increasing repetitions for a) M5, and b) M8 moment magnitude

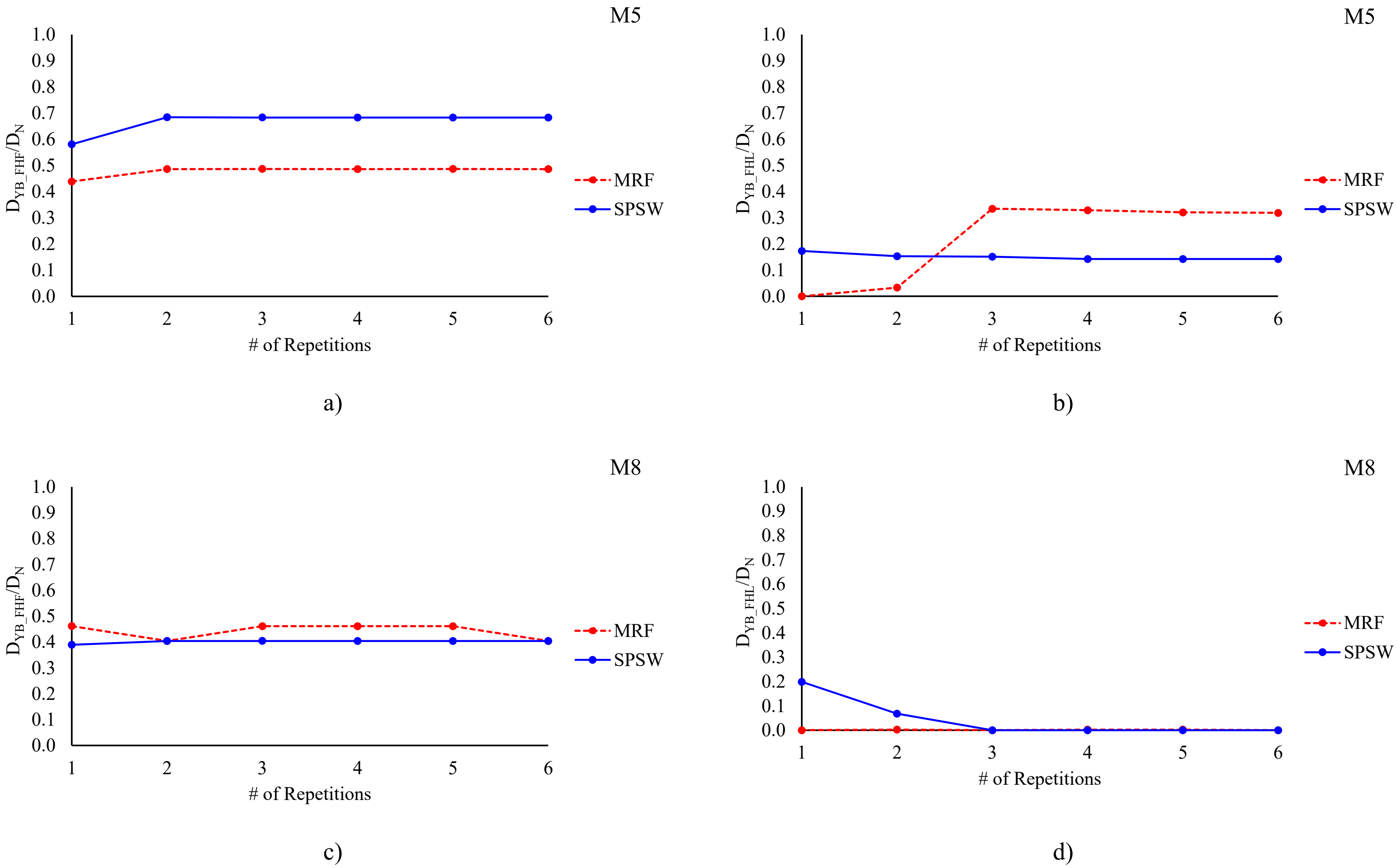

Figure 5-2 Dependency of Yield bracket duration on length of loading for MRF1 and SPSW1 for a) M5 – FHF, b) M5–FHL, c) M8 – FHF, and d) M8 –FHL

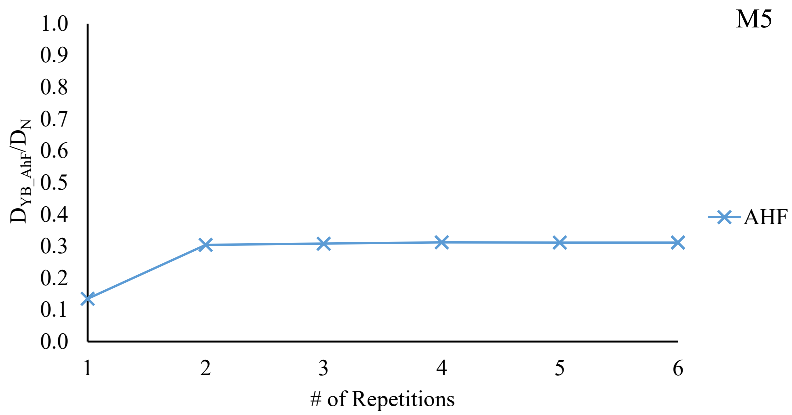

a)

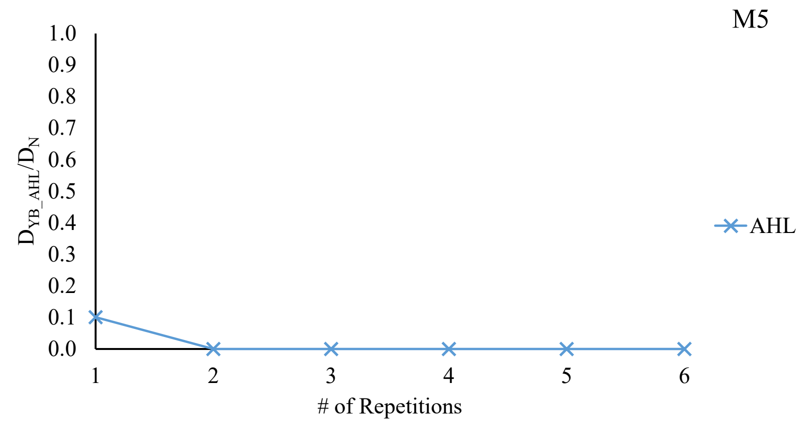

b)

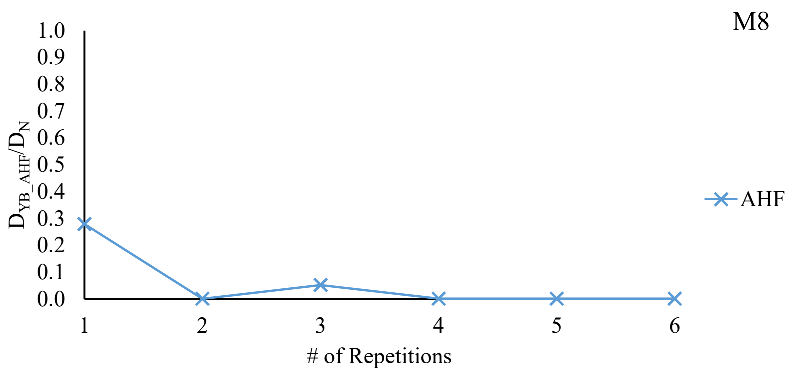

c)

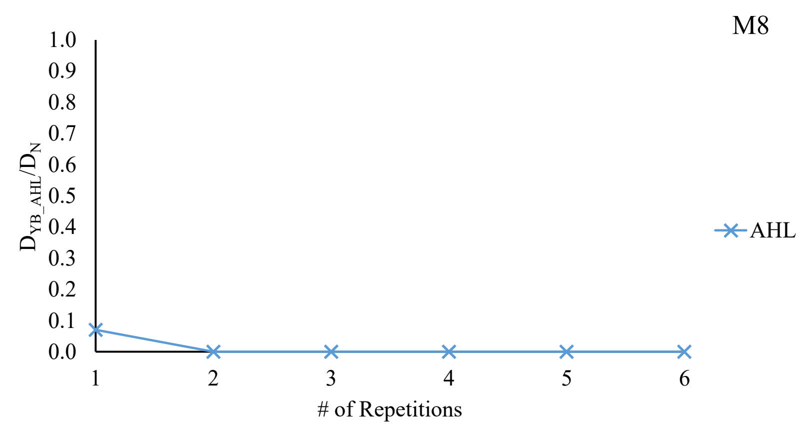

d)

Figure 5-3 Dependency of Yield bracket duration on length of loading for SPSW1 strips for a) M5 – AHF, b) M5– AHL, c) M8 – AHF, and d) M8 – AHL

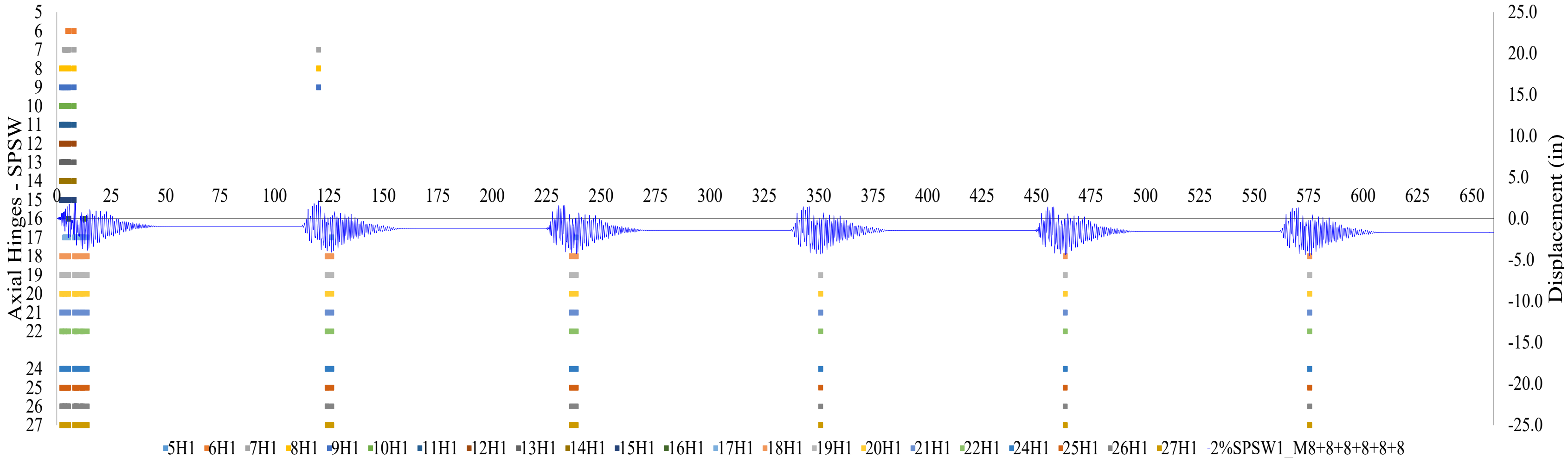
Axial Hinges - SPSW
Displacement (in)
5H1 6H1 7H1 8H1 9H1 10H1 11H1 12H1 13H1 14H1 15H1 16H1 17H1 18H1 19H1 20H1 21H1 22H1 24H1 25H1 26H1 27H1 2%SPSW1_M8+8+8+8+8+8

a)

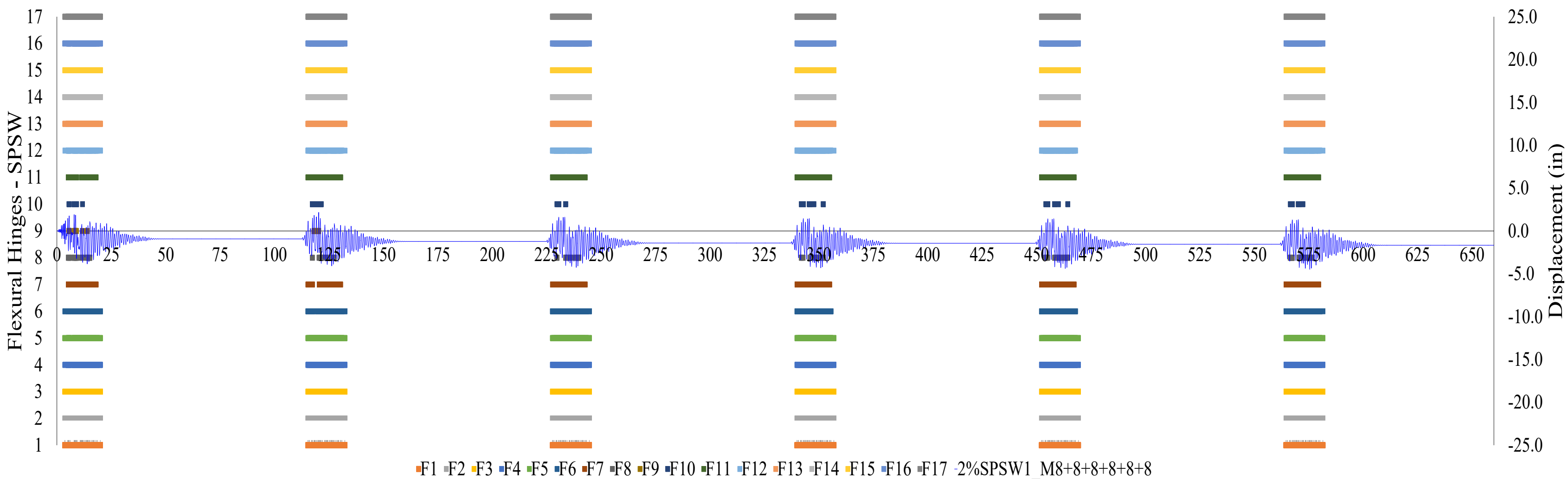
Flexural Hinges - SPSW
Displacement (in)
F1 F2 F3 F4 F5 F6 F7 F8 F9 F10 F11 F12 F13 F14 F15 F16 F17 2%SPSW1_M8+8+8+8+8+8

b)

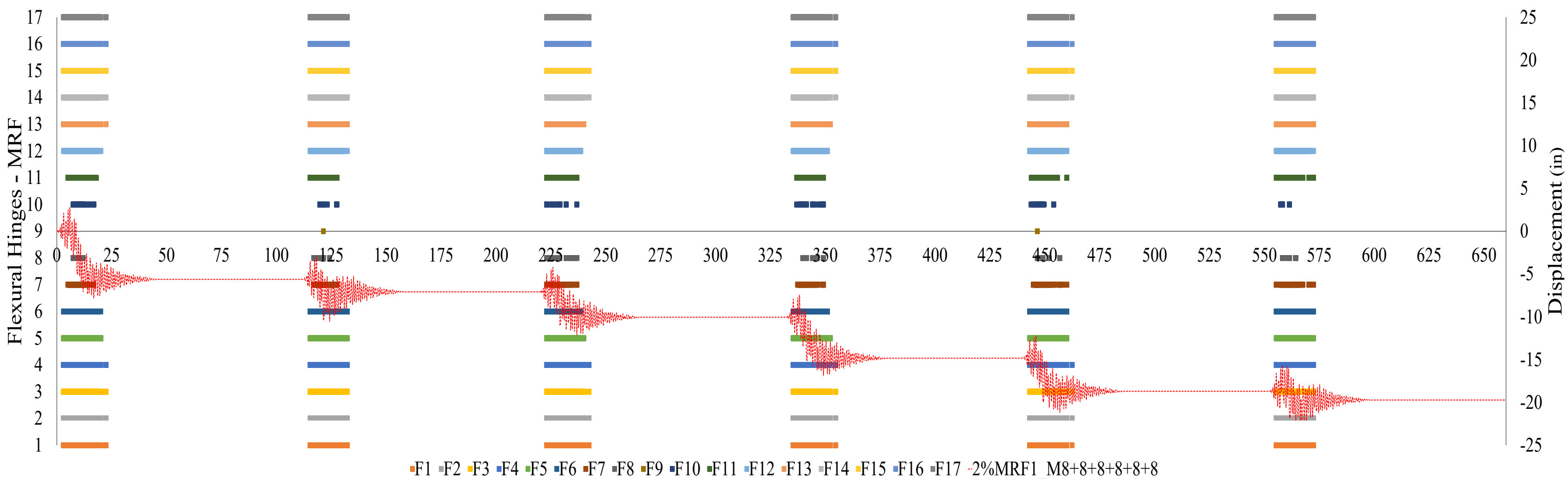

c)

Figure 5-4 M8+8+8+8+8+8, *R*=7, ζ=2%; Yield Behavior for

a) SPSW Axial Hinges b) SPSW Flexural Hinges, and c) MRF Flexural Hinges

5.3 Sensitivity to Damping Ratio

For R = 7, the SPSW1 archetype was analyzed twice with values of damping ratio, ζ taken as 2% and 5% that of critical damping for the input time history of moment magnitude of M5.The values of residual drift for each successive earthquake response were noted and plotted following the method used in Section 5.2. Figure 5-5 plots the increase in residual drift at each consecutive earthquake for both values of damping considered. As can be seen, values of percentage residual drift for ζ = 5% are lesser compared to those obtained for ζ = 2%.

When comparing the dependency of the yield bracket duration on values of damping ratio for both the MRF and SPSW archetypes considered, it was observed from Figure 5-6 that the SPSW flexural hinge initiated yielding earlier than the MRF for ζ = 5%, which contradicts with the delays observed in beginning of plasticity for the SPSW boundary frame for ζ = 2%, relative to the MRF, as mentioned in Section 4.2.4. It is also worth noting that for ζ = 5%, there was lesser difference in values of the ratio D_{YB_FHF}/D_N for the SPSW and MRF archetypes, whereas D_{YB_FHL}/D_N showed that the last fiber for the SPSW flexural hinge was not engaged after the fourth earthquake, and that of the MRF was not engaged at all. This is owing to the limited participation of the now more damped boundary frame, and the reduced engagement of the steel web panel. Figure 5-7 further elaborates this observation, where the "yield bars" plotted for ζ = 2% show more engagement of the plate in contrast with those plotted for ζ = 5%.

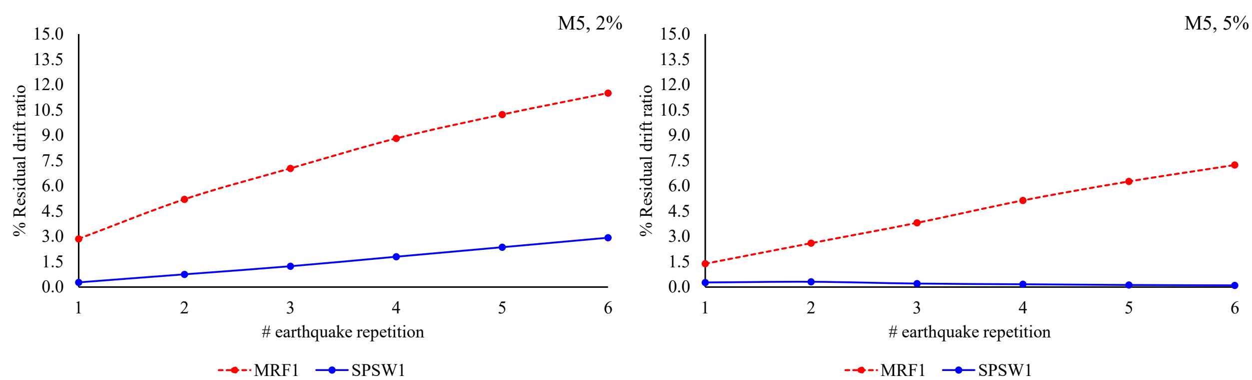

a) b)

Figure 5-5 %age residual drift for MRF1 and SPSW1 w.r.t. increasing repetitions for M5 moment magnitude for a) ζ = 2%, and b) ζ = 5%

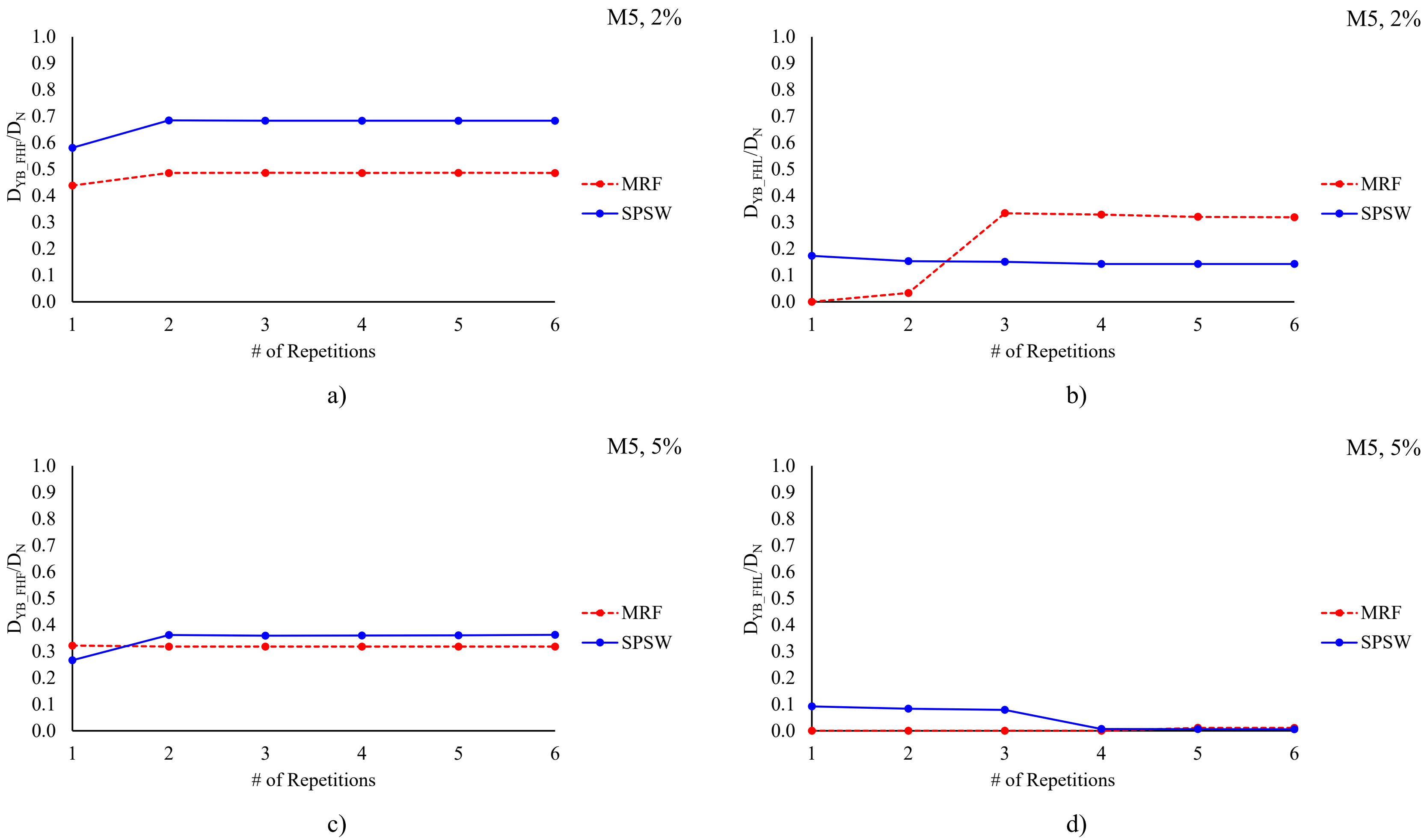

Figure 5-6 Dependency of Yield bracket duration for MRF1 and SPSW1 on value of damping ratio of a) 2% – FHF, b) 2% – FHL, c) 5% – FHF, and d) 5% – FHL

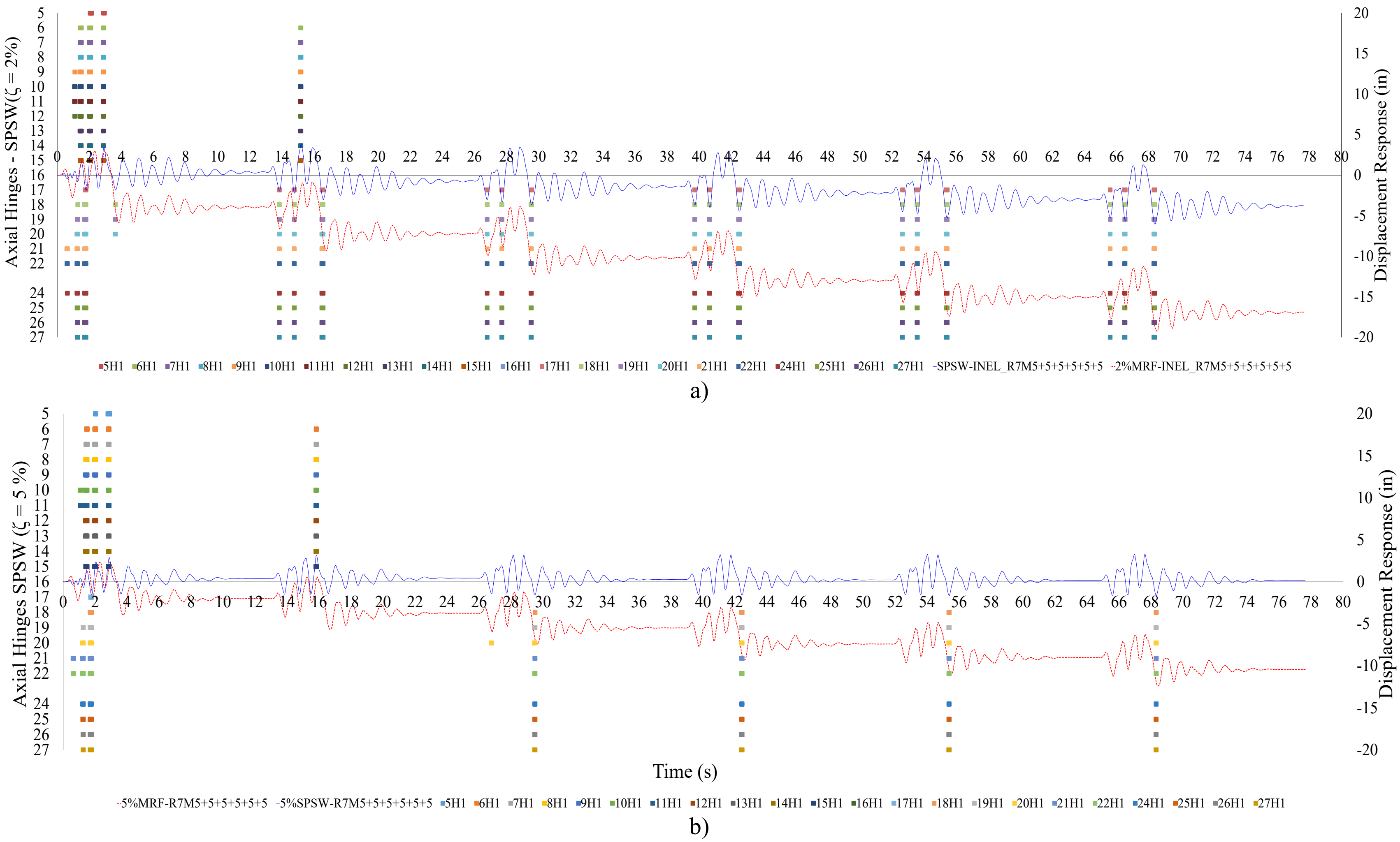

Figure 5-7 Axial Hinges Yield Behavior for SPSW1, *R* = 7, M5+5+5+5+5+5, for a) ζ=2%, and b) ζ=5%

5.4 Sensitivity to Aspect Ratio

In practice, SPSW systems are designed in a multitude of configurations. Archetypes with panel aspect ratio values of 1.0 and 2.0, namely SPSW1 and SPSW2, were considered for the purpose here in order to understand the relationship between seismic behavior of the system and the dimensions of the steel web panel. As previously described, response data from analyses conducted in Section 4 was used to plot trends observed in the accumulation of residual drift. Here, 2% damping was considered for the analysis. Both the SPSW and MRF archetypes were designed for value of $R = 7$.

The SPSW2 response showed a different disposition in contrast to the SPSW1. Comparing Figure 5-8 with Figure 5-1, it was noticed that the SPSW2 showed slightly higher accumulation of residual drift relative to SPSW1. However, this behavior was reverse for the MRF archetypes, where relatively lesser values of addition to residual drift were observed for MRF2 as compared to MRF1. From Figure 5-9 it can be observed that for the M5 earthquake, the first fiber to yield for the SPSW was engaged for lesser duration as compared to that for the MRF. This was not so for the case of 1:1 aspect ratio, where there was a steep increase in residual drift. For M8, the first fibers for both the archetypes follow closely similar trends for both dimensions.

Figure 5-10 depicts the yield behavior of axial hinges in the SPSW2 model for M5 and M8 earthquakes. Comparing Figure 4-11 with Figure 5-10 shows that the larger width of the SPSW2 lessens the demands for the HBE from the wider steel plate, enabling lesser end moments for the HBE sections, and therefore causing lesser engagement for the SPSW2 steel panel relative to SPSW1.

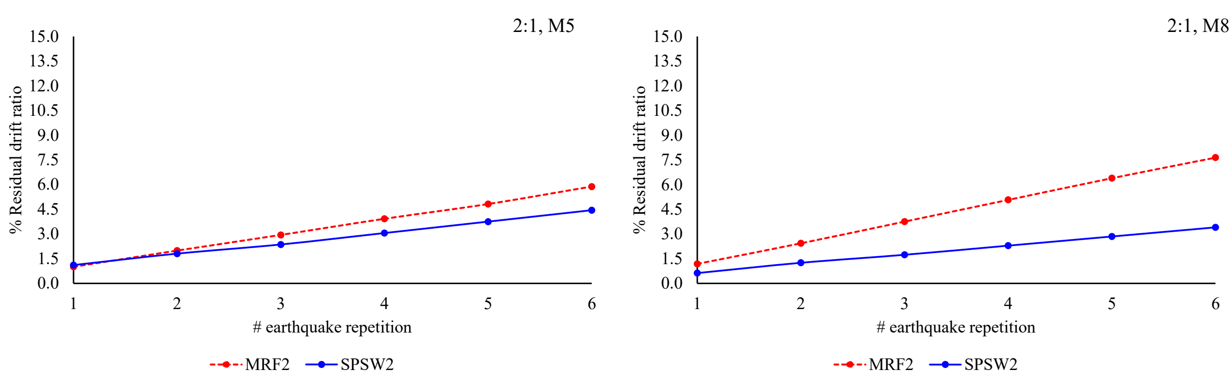

a) b)

Figure 5-8 %age residual drift for MRF2 and SPSW2 w.r.t. increasing repetitions for a) M5, and b) M8

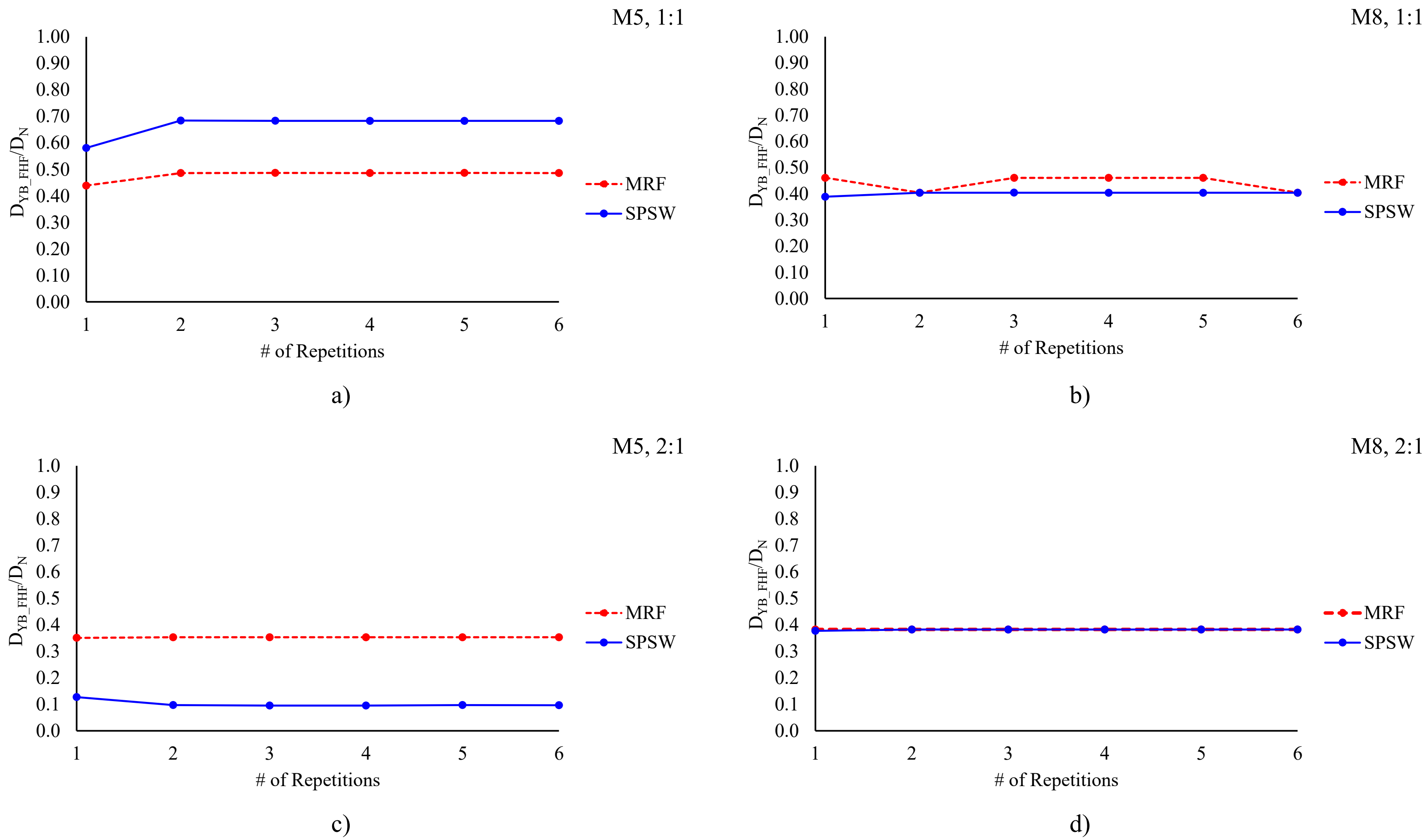

Figure 5-9 Dependency of Yield bracket duration for MRF and SPSW (*R* =7) first fiber on value of aspect ratio of a) 1:1 for M5, b) 1:1 for M8, c) 2:1 for M5, and d) 2:1 for M8

a)

b)

Figure 5-10 Axial Hinge Yield Behavior for SPSW2, *R*=7, ζ=2% for

a) M5+5+5+5+5+5 b) M8+8+8+8+8+8

5.5 Sensitivity to R factor

Two values of the response modification factor, R, were considered for the design and analyses performed here as it allows to investigate how results change as a function of the ductility of the structure. Values of R factors considered in this study were equal to 5 and 7 for both the archetypes with aspect ratios of 1.0 and 2.0. Similar to previous sections, here Figure 5-11 and Figure 5-12 present the percentage residual drift accumulations per earthquake repetition for a variety of configurations, where the former depicts behavior for SPSW1 and the latter for SPSW2.

It can be seen that for decreasing values of R, the residual drift ratio generally decreased. For the case of SPSW1 with an R value of 5, the SPSW and the MRF showed minimal residual drift. Upon investigation of the displacement response, it was seen that for the case of M5 moment magnitude earthquake, both the MRF and SPSW follow closely similar paths. The steel web is excessively engaged for the first two earthquakes, after which both archetypes fall into a similar pattern of displacement. This is displayed in Figure 5-13 along with the yield behavior of the steel plate for SPSW1, $R = 5$.

As shown in Figure 5-12, for the case of M8 earthquake for SPSW2, $R = 5$, it was not possible to extract results for all six repetitions of M8 earthquake for the MRF2 due to computational issues within the software, and therefore only results obtained for first four repetitions have been plotted These results are representative of the trend observed for the MRF2. Figure 5-14 shows displacement response of the SPSW2 and MRF2, both for R along with yielding of the steel plate represented by the behavior of the axial hinges.

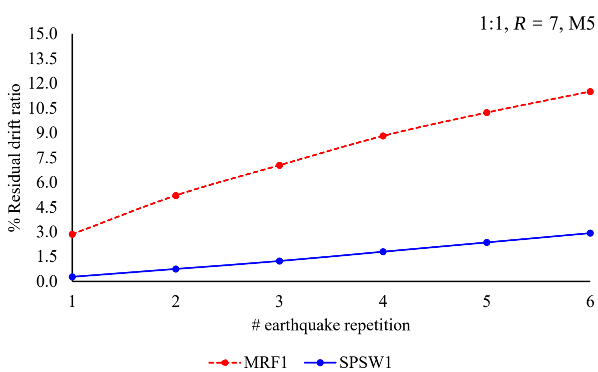

a)

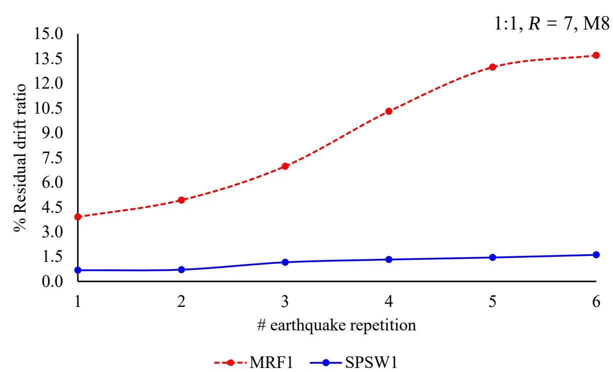

b)

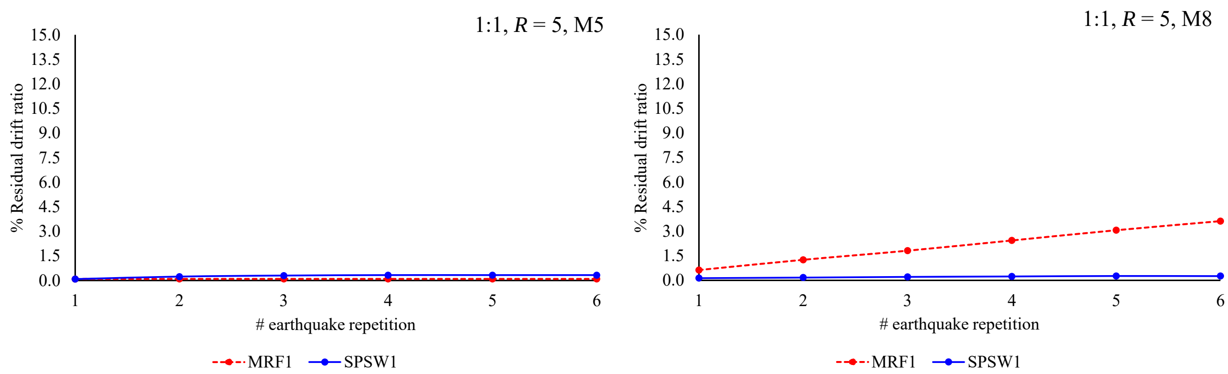

c) d)

Figure 5-11 %age residual drift for MRF1 and SPSW1 w.r.t. increasing repetitions for a) R=7 M5 , b) R=7 M8, c) R=5 M5, and d) R=5 M8

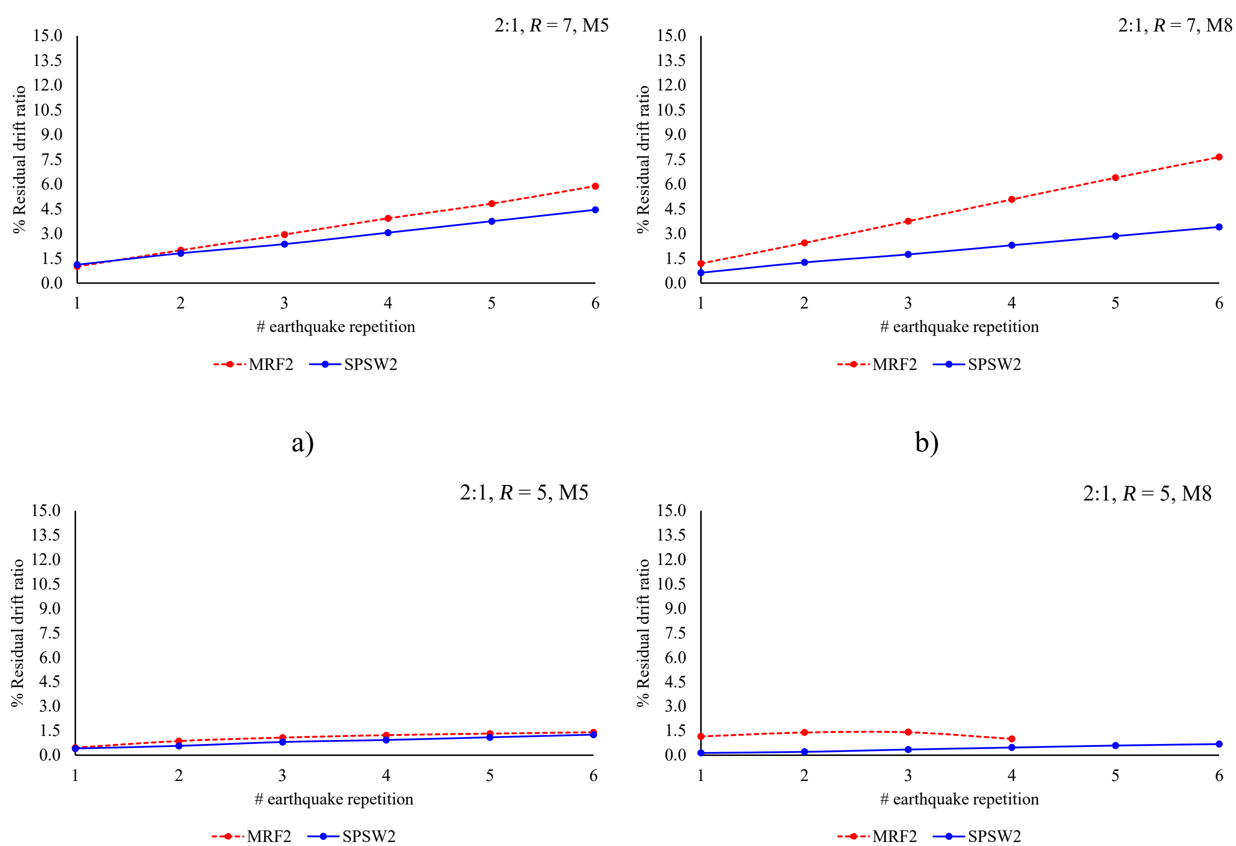

a) b)

c) d)

Figure 5-12 %age residual drift for MRF2 and SPSW2 w.r.t. increasing repetitions for M5 moment magnitude for a) R=7 M5, b) R=7 M8, c) R=5 M5, and d) R=5 M8

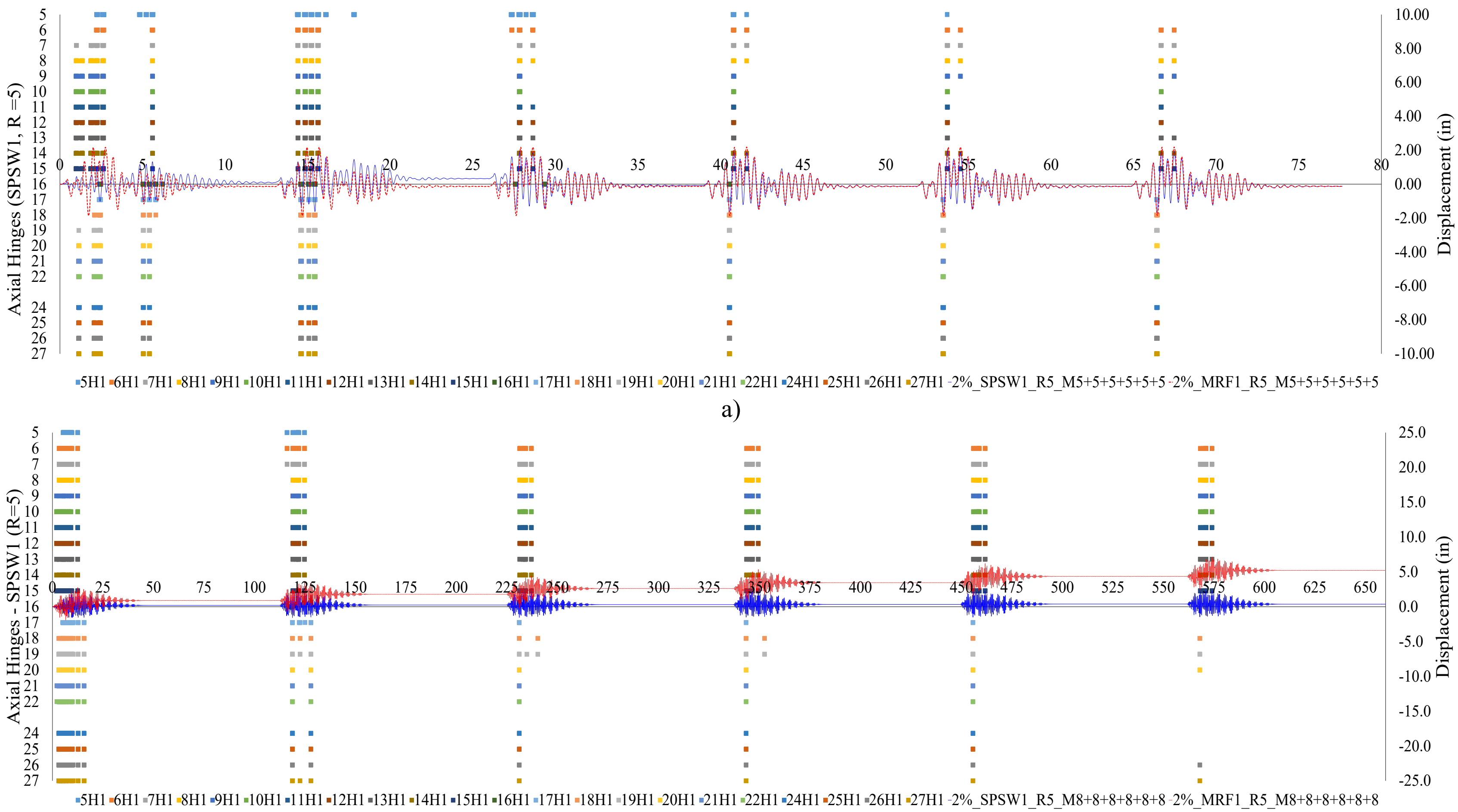

Figure 5-13 Axial Hinge Yield Behavior for SPSW1, *R*=5, ζ=2% for a) M5+5+5+5+5+5 b) M8+8+8+8+8+8

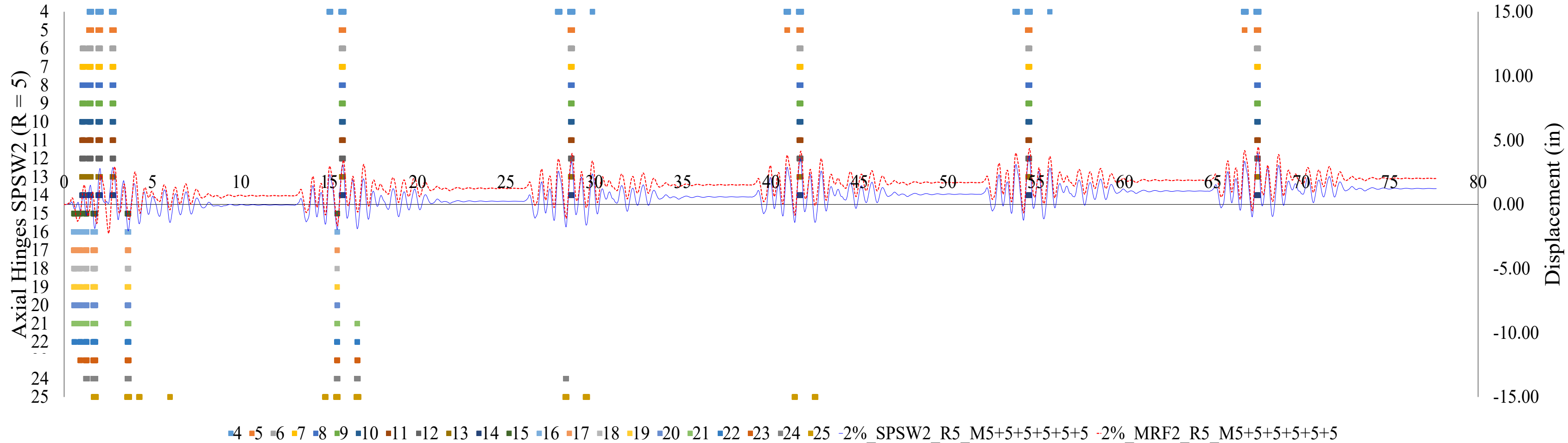

a)

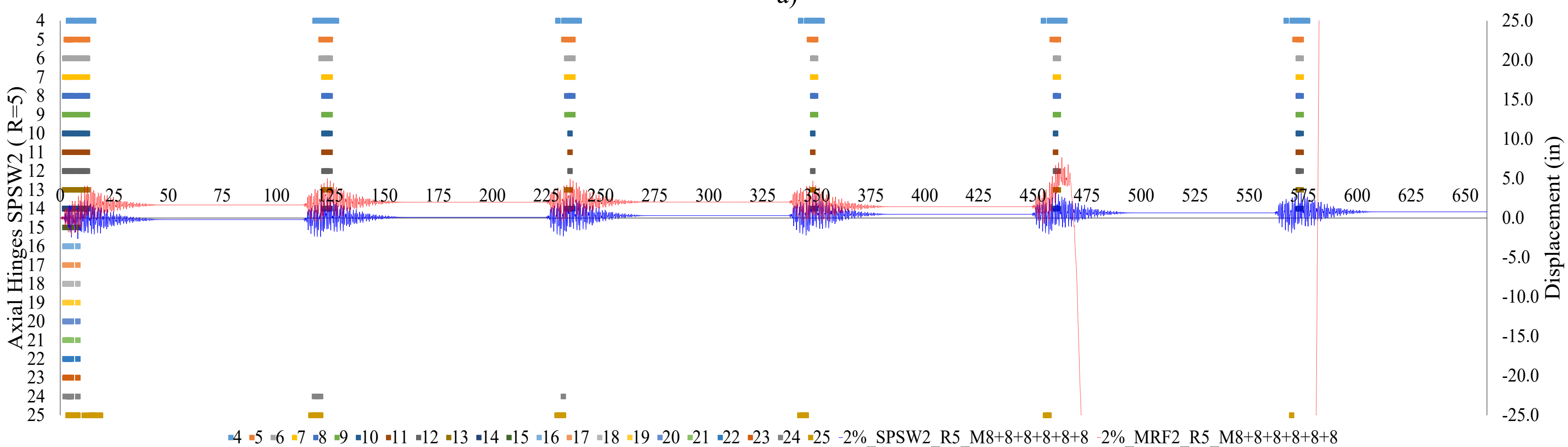

b)

Figure 5-14 Axial Hinge Yield Behavior for SPSW2, R=5, ζ=2% for a) M5+5+5+5+5+5 b) M8+8+8+8+8+8

5.6 Sensitivity to Number of Stories

Analysis of the three story model, namely SPSW3, designed using value of R = 7 and analyzed with ζ = 2%, was also conducted in order to compare behavior under the considered prolonged earthquake durations. Trends observed for story drift are presented in Figure 5-15. As can be seen from the figure, for the M5 earthquake repetitions, the MRF3 archetype does not seem to accumulate much residual drift relative to the SPSW3 structural system. When comparing the response histories of each floor for both the models, it can be seen from Figure 5-17 that even though the SPSW3 shows more percentage residual drift, the values of maximum residual drift per earthquake repetition are much less for the SPSW3 than those for the MRF3. The response oscillations presented in Figure 5-17a are representative of the MRF3 behaving like a single degree of freedom structure. Also, the MRF3 does not appear to damp out quickly. Here, SPSW3_1, SPSW3_2, and SPSW3_3 represent the response histories for the first, second, and top floor respectively; and the same notations are used for the MRF3.

The trends observed for the three story model followed those for the single story, but with lesser values of residual drift. It should be noted that for the M8 earthquake repetitions, the MRF3 archetype faced computational challenges within the software, and was therefore not included in trends plotted here.

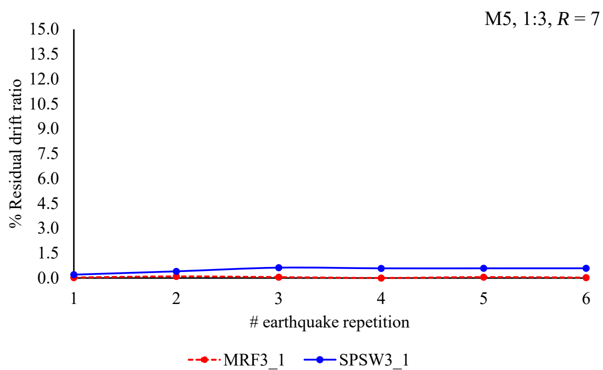

a)

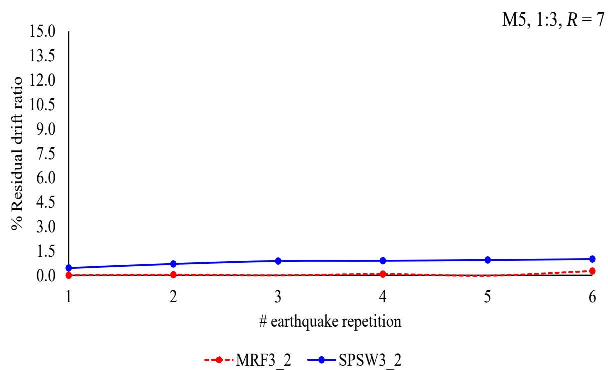

b)

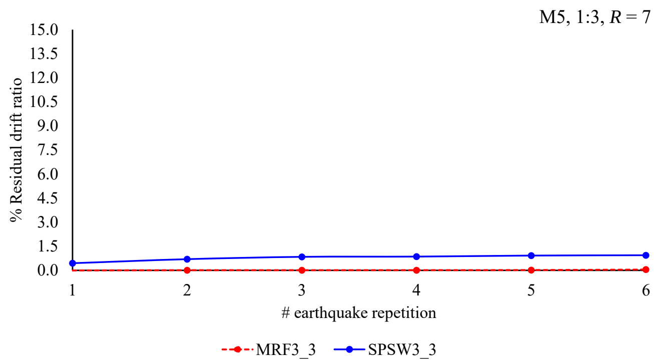

c)

Figure 5-15 %age residual drift for MRF3 and SPSW3 for R =7, w.r.t. increasing M5 repetitions for a) First floor, b) Second floor, and c) Top floor

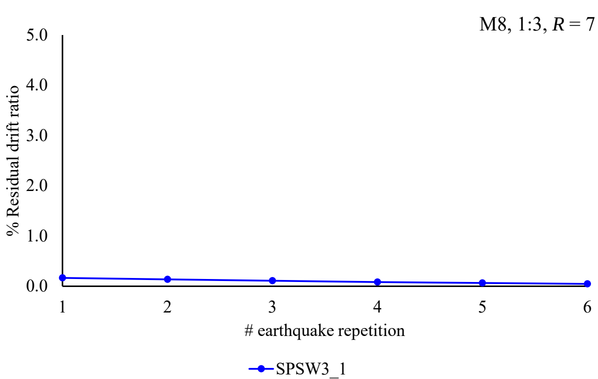

a)

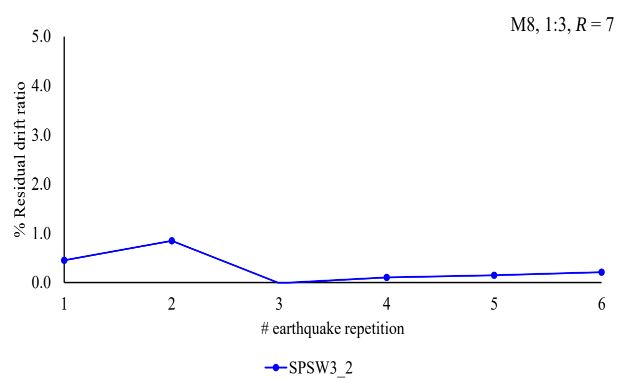

b)

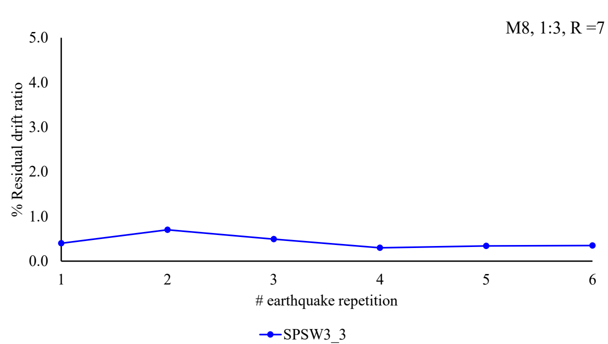

c)

Figure 5-16 %age residual drift for SPSW3 for R =7, w.r.t. increasing M8 repetitions for a) First floor, b) Second floor, and c) Top floor

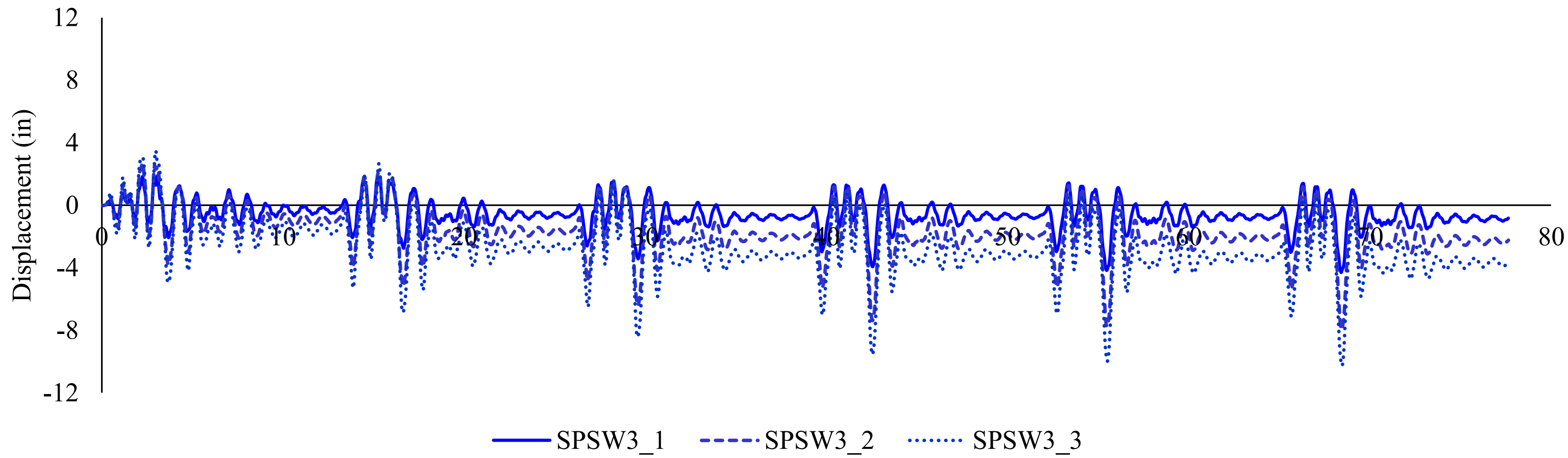

a)

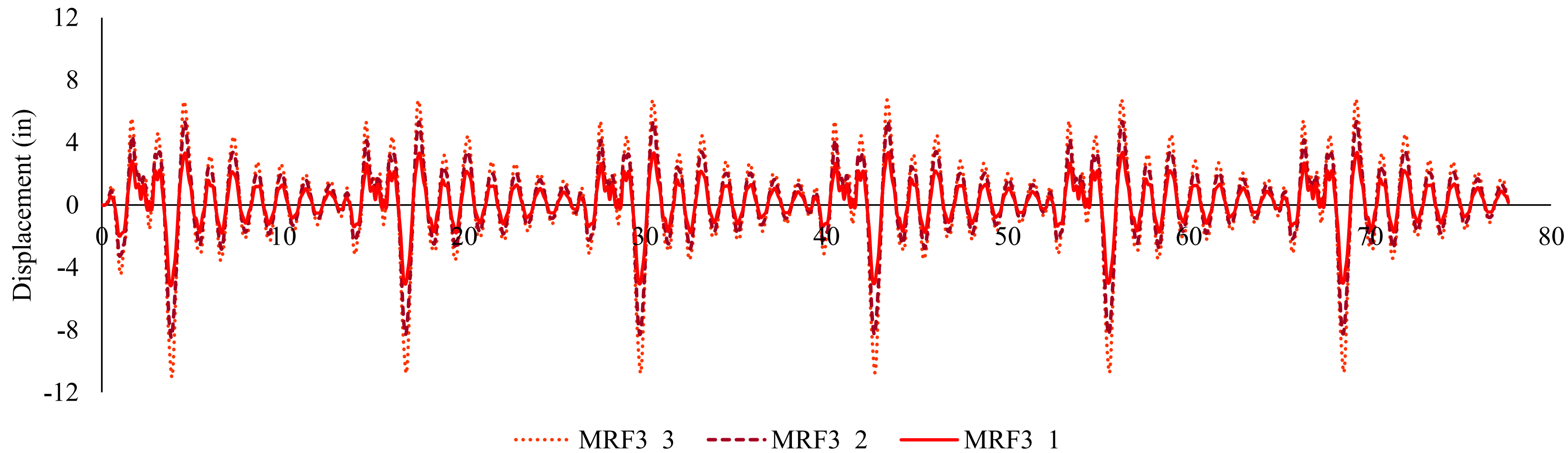

b)

Figure 5-17 Displacement response histories for all three stories for M5 repetitions for a) SPSW3, and b) MRF3

5.7 Sensitivity to Design Considerations

While designing the SPSW1 archetype, corresponding to a bay 12ft wide by 12ft high, certain challenges were presented in finding a suitable design for the boundary frame members which would meet the criterion for shear checks required by the AISC 341. Base shears calculated from the Equivalent Lateral Load procedure from ASCE 7-10 Section 12.8 were used to calculate thickness of the steel plate web. The HBE and VBE sections were then designed in accordance with capacity design principles. Since relatively thick steel panels were required for shear resistance, the resulting HBE and VBE section sizes came out to be quite large. The high base shear loading on a singular web panel implied that all the diagonal tension field action from the steel panel imparted a high shear demand on the HBE. Also, the relatively smaller length of the HBE, L_{cf} = 12ft, resulted in high shear demands due to the plastic moments developing at the HBE ends (i.e., $V = 2M_p/L_{cf}$) moments, making it difficult to satisfy code requirements for shear when using structural steel W-sections from the AISC database.

Consider the case of SPSW1 archetype designed for $R = 7$. From capacity design, and considering 45 degree inclination of the tension field, the horizontal (ω_h) and vertical (ω_v) loads were determined as 4.4 kip/in each. Using the L_{cf} value previously calculated as 125.7 in, the flexural demand came out to be $17463\ kip - in$ at each end. The HBE section was then initially selected as W30x116. In this case, $M_p = F_y \times Z = 50 \times 378 = 18900\ \mathrm{kip-in}$. The probable flexural strength was calculated as $M_{pr} = 1.1 \times R_y \times M_p = 22869\ kip - in$, for which $V_u = \frac{2M_{pr}}{L_{cf}} + \frac{\omega_v L_{cf}}{2} = 334.6 + 382 = 717\ kips$. When comparing this value of shear force with the available capacity for this section, i.e. 528 kips, W30x116 was determined to be less than the required shear strength. It should be noted here that the value of M_{pr} was taken considering plastification of the total depth of the section.

In an attempt to reduce V_u, a simpler approach was taken by considering that only the flange provided flexural strength. Under this assumption in the next iteration, W30x173 was selected, for which the value of $M_{p_{flange}} = 23513\ kip - in$. Proceeding with all the relevant steps under capacity design, the value of the shear demand for the HBE web was estimated as $V_u = \frac{2M_{p_{flange}}}{L_{cf}} + \frac{\omega_v}{Lcf} = 374 + 276 = 650\ kips$. Yet, the available shear strength, $V_n = \mathrm{A_w} \times 0.6 \times \mathrm{F_y} = 550\ \mathrm{kips}$ still did not satisfy the above mentioned requirements, necessitating another iteration.

Then, W36x194 was selected for the subsequent iteration. For this section, $M_{p_{flange}} = 26450\ kip - in$, which resulted in excessive values of V_u once again. As an alternative step towards reduction in V_u, the code prescribed method was attempted by considering the axial force interaction for the calculation of the reduced probable moment, $M_{pr} = 1.1 \times R_y \times F_y \times \left(1 - 0.5\left(\frac{P_{HBE}}{P_y}\right)\right) = 42225\ kip - in$, where the axial reduction factor between parentheses resulted as 0.91. However, it was not possible to obtain compliance with the shear demands with this consideration. Reduced Beam Sections (RBS) were also introduced in an attempt to meet shear requirements. For the case of W36x194, the value of $M_{p_{flange}} = 26457\ kip - in$. Incorporating an RBS section here implied that $M_{pr_{RBS}} = 50\% \times M_p = 13228\ kip - in$. This value was less than the required demand of $17463\ kip - in$ and was therefore not useful in this case.

After evaluating every available compact section in the AISC database using spreadsheets developed for this purpose, it was clear that no section gave satisfactory results; this was attributed to the fact that the requirement for higher plastic moment capacity for HBE sections, led to high values of M_{pr}, which in turn increased the values of V_u dramatically, resulting in noncompliance with AISC shear checks mentioned earlier. In the end, therefore, the HBE obtained in the original design (i.e., W30x116) was considered for analyses conducted for the purpose of studying effects of long duration earthquake motion, disregarding the code requirements for shear.

Theoretically, an alternative approach that can be taken by considering the reductions in the probable plastic moment from combined shear and axial force, in order to reduce the shear demand. However certain challenges are present when modeling an analytical scheme for this method for cyclic loading in SAP2000, as the software cannot account for the combined axial and shear interaction. At any instance in time, the HBE web will have a particular value of shear stress, which will fluctuate corresponding to the fluctuations in the displacement response. For SAP2000 to consider any shear interaction, the HBE web within the flexural hinge would have to be assigned a value of axial stress, σ_w, that would change as a function of the applied shear stresses. Note that using a singular constant value of σ_w could be done for simplicity but would not be a truthful representation of the actual behavior through the entire earthquake

In order to understand and compare trends and sensitivity of the SPSW system to shear and axial interaction, a trial analysis was conducted considering the shear contributions to the HBE web towards the moment resistance, considering a maximum value of σ_w calculated as $\sigma_w = \sqrt{\left(\sigma_y^2 - 3\tau_w^2\right)} = 30.7\ ksi$, where $\tau_w = \frac{V_u}{A_w} = 22.7\ ksi$. Figure 5-18 below presents observed trends in percentage residual drift for such a case, where there appears to be a reduction in drift accumulation relative to SPSW1 with full fiber hinge for $\sigma_y =$

50 ksi. The yield bracket duration for the first yielding fiber for both cases is presented in Figure 5-19. Here, *FF_flange* and *FF_web* stand for "first fiber for full section with σ_y" and "first fiber for web with σ_w" respectively. It can be seen that the HBE for the case of "full section with σ_y" is engaged for relatively longer durations. Comparing Figure 5-20 with Figure 4-11 gives a sense of the relative yield behavior of the axial strips for both cases.

In a multistory SPSW, the previously encountered problem would have less influence, given the fact that the demand applied to the intermediate HBEs within the boundary frames is (for the capacity design part of the design) a function of the difference in thicknesses of the SPSW panels between any two floors in which the HBE is placed. Therefore, in a multistory SPSW, the only floor for which the HBE would have to resist the full yield capacity of a steel web panel would be the top-most level. This level, however, typically resists the least story shear in the structure, requiring relatively less thick panels in the SPSW design.

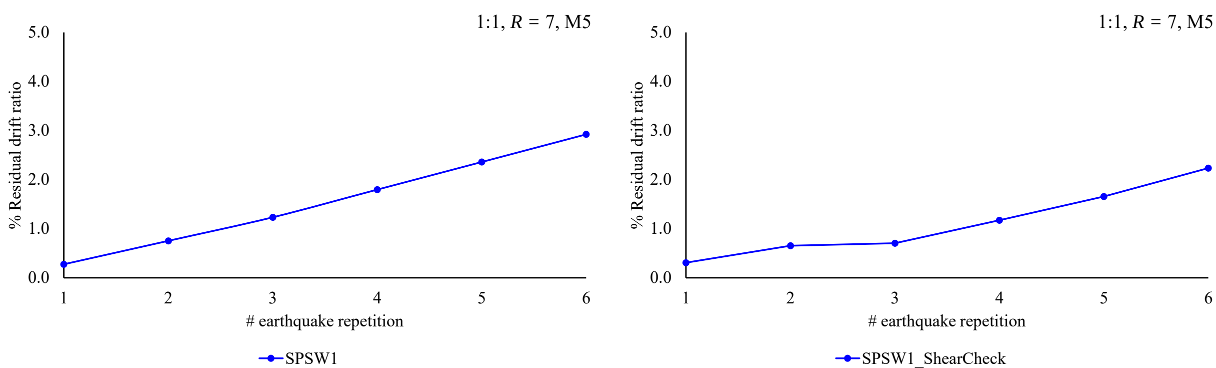

Figure 5-18 %age residual drift for SPSW1 w.r.t. increasing M5 repetitions for a) Full section with σ_y, and b) Web with σ_w

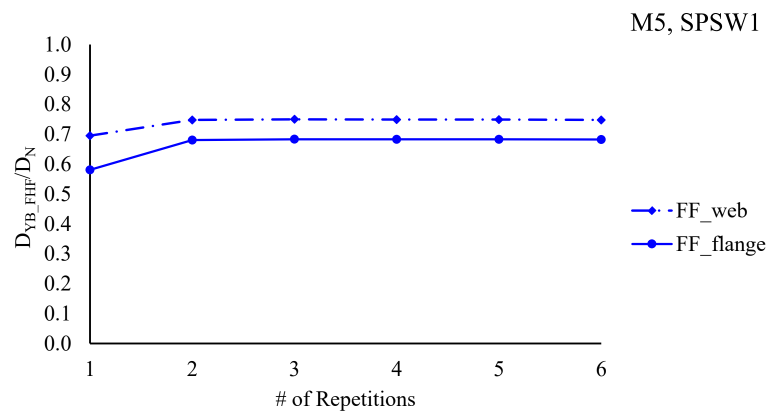

Figure 5-19 Dependency of Yield bracket for SPSW1 with shear interaction on duration

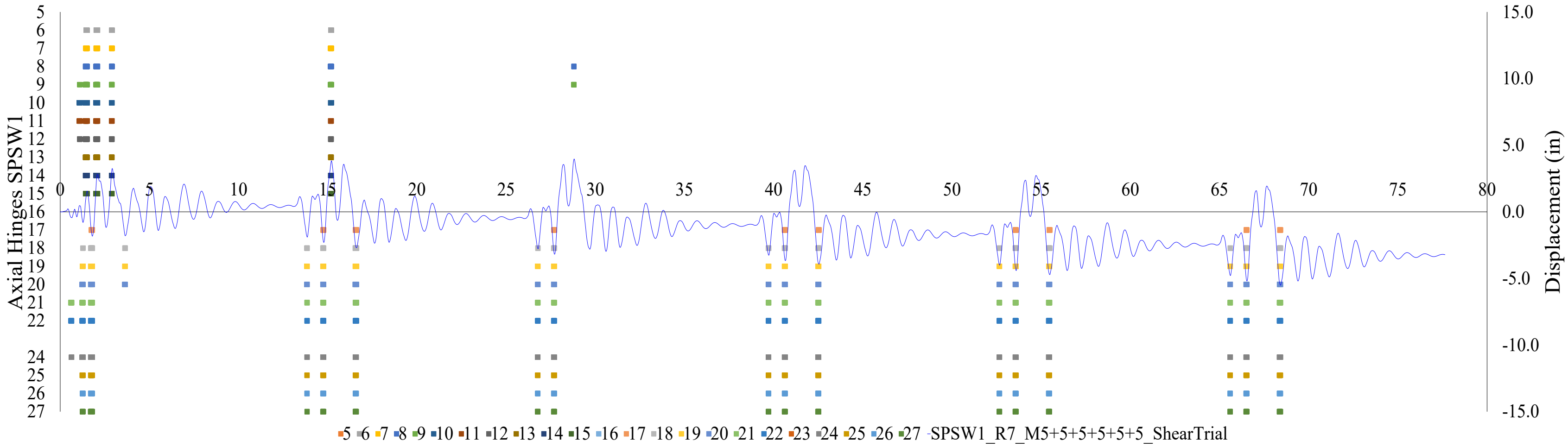

Figure 5-20 Axial Hinge Yield Behavior for *R*=7, ζ=2%, SPSW1 with HBE web with σ_w, for M5+5+5+5+5+5

5.8 Summary

- When comparing drift response with respect to increasing earthquake duration, the SPSW showed less addition to residual drift as compared to the MRF. For the SPSW boundary frame, despite delays observed in initiation of plasticity due to the presence of the steel plate, the entire HBE section was engaged and fully yielded sooner than the MRF section.
- It was seen that increasing values of damping ratio resulted in lesser participation from the more damped boundary frame. Engagement of the steel plate was reduced in such a case. For higher aspect ratios, the residual drift ratios were observed to slightly increase for the SPSW system, whereas these depicted a decreasing tendency with decreasing values of the R factor.
- Multi-story SPSW showed lesser residual drifts as compared to the single story wall.
- For the single story SPSW, challenges in design were met owing to the relatively small length of HBE creating higher end moments, leading to requirement for high values of M_{pr}, which in turn increased the values of V_u. The resulting value of the applied shear was less than the available shear strength of any of the sections present in the AISC database. Considering a simpler, and instantaneous approach toward incorporating combined axial and shear effects on the HBE, a section with axial stress within the web was analyzed. For this section, the residual drift values came out to be lower than that analyzed previously.

SECTION 6
CONCLUSIONS

Using data from analyses performed for the array of considered parameters, it was possible to plot trends in sensitivity of response for various configurations of SPSWs as a function of increasing duration of seismic loading, and to provide some comparison of how some of the factors considered interact with others to affect this response. It was demonstrated that, even as drifts progressively increase, a SPSW never seem to reach a point where it truly behaves as a simple moment resisting frame. The steel plate restricts the boundary frame from drifting freely, limiting plastic residual accumulations. In other words, in all cases considered, the steel plate web within the SPSW continued to contribute to the strength and stability of the system even after long duration of strong ground motion. The presence of this steel plate was observed to also delay the instigation of yielding of the boundary frame.

In addition, it was observed that the HBE members accounted for a significant part of the system's energy dissipation, even when the steel plate yielded beyond past its preceding maximum elongation. This illustrates that the presence of a substantial boundary frame members is important to achieving appropriate performance of the SPSW structural system as a whole, when subjected to earthquake loading (here, for the satisfactory responses observed, the boundary frames were sized to meet the AISC-341-16 requirements).

It was found that the effects of increasing earthquake duration for the SPSW were not as detrimental as for the bare frame. A direct measure of the influence of duration was the residual drift that accumulated from prolonged seismic loading. For a rectangular SPSW, slightly higher drifts were observed to accumulate for higher panel aspect ratios as the earthquake progressively increased in duration. The converse was true for the bare frame. With trends observed for the relationship between earthquake duration and R value, it was found that with respect to the increasing duration of seismic loading, the residual displacements responded correspondingly to changes in R, increasing and decreasing accordingly with the increasing or decreasing values of R. For the multi-story SPSW case considered, the trends were the same but results showed lesser residual drifts when compared to those obtained for the single story wall.

Note that the above findings were obtained for infinitely ductile SPSWs having elasto-plastic material properties, as a first step to determine if the infill of SPSW could fundamentally ever cease to become engaged during seismic response as earthquake duration increases. Considering the fact that this research did not take into consideration the impact of all other limit states of strain hardening, strength degradation, and P-delta effects, for sake of identifying behavior and response on the basis of idealized ductile behavior alone, as mentioned early on in the report, further research is necessary to develop a better understanding of the consequences of these on the behavior of SPSW during long duration earthquakes.

SECTION 7 REFERENCES

Abdelnaby, Adel E. 2012. "Multiple Earthquake Effects on Degrading Reinforced Concrete Structures." University of Illinois at Urbana-Champaign.

AISC. 2016. *Seismic Provisions for Structural Steel Buildings.* Chicago, Illinois: American Institute of Steel Construction, Inc.

ASCE. 2010. "ASCE 7-10 "Minimum Design Loads for Buildings and Other Structures"."

Berman, J. W., and M. Bruneau. 2003b. "Plastic Analysis and Design of Steel Plate Shear Walls." *Journal of Structural Engineering* (ASCE) Vol. 129: 1448–1456.

Bruneau, M., Rafael Sabelli, and Chia-Ming Uang. 2011. *Ductile Design of Steel Structures.* McGraw-Hill Professional Publishing.

Driver, R. G., G. L. Kulak, A. E. Elwi, and D. J. L. Kennedy. 1998a. "Cyclic test of a four-storey steel plate shear wall." *Journal of Structural Engineering* 112-120.

Elgaaly, M., V. Caccese, and C. Du. 1993. "Postbuckling behavior of steel-plate shear walls under cyclic loads." *Journal of Structural Engineering* 119(2): 588–605.

Engineering Seismology Laboratory. 2005. "ESL Software." http://civil.eng.buffalo.edu/engseislab/products.htm#TARSCTHS.

Ericksen, Jason, and Rafael Sabelli. 2008. "A Closer Look at Steel Plate Shear Walls." *Modern Steel Construction*, January.

Federal Emergency Management Agency. 2013. "Prestandard and Commentary for the Seismic Rehabilitation of Buildings."

Federal Emergency Management Agency. 2000. *Recommended Seismic Design Criteria for New Steel Moment-Frame Building.* FEMA-350, NEHRP.

Guo, H. C., J. P. Hao, and Y. H. Liu. 2015. "Behavior of stiffened and unstiffened steel plate shear walls considering joint properties." *Thin-Walled Structures* 97: 53-62.

Housner, G. W. 1965. "Intensity of ground motion shaking near the causative fault." *Proceedings of the Third WCEE.* Auckland, New Zealand. 94-109.

Jeong, G. D., and W. D. Iwan. 1988. "The effect of earthquake duration on the damage of structures." *Earthquake Eng Struct Dyn* 16: 1201–11.

Kawashima, K., and K. Takahashi. 1985. "Duration of strong motion acceleration records." *Proc JSCE 1985.* 161–8.

Krishnan, Swaminathan, and Matthew Muto. 2013. "Sensitivity of the Earthquake Response of Tall Steel Moment Frame Buildings to Ground Motion Features." California Institute of Technology.

Kulak, G. L., D. J.L. Kennedy, and R. G. Driver. 1994. "Discussion of Experimental study of thin steel-plate shear walls under cyclic load by Caccese. V., Elgaaly, M., and Chen, R." *ASCE Journal of Structural Engineering* 120(10): 3072-3073.

Lignos, D. G., Y. Chung, T. Nagae, and M. Nakashima. 2011. "Numerical and experimental evaluation of seismic capacity of high-rise steel buildings subjected to long duration earthquakes." *Computers and Structures* 89: 959–967.

Lopez-Garcia, Diego. n.d. Pontificia Universidad Catolica de Chile, Chile.

Marsh, M. Lee, and Christopher M. Gianotti. 1994. *Structural Response to Long-Duration Earthquakes.* Research Project T9234-09, Washington State Transportation Center (TRAC).

Novikova, E. I., and M. D. Trifunac. 1994. "Duration of ground motion in terms of earthquake magnitude, epicentral distance, site conditions and site geometry." *Earthquake Eng Struct Dyn* 23: 1023–43.

Papageorgiou, Apostolos, and Benedikt Halldorsson. 2004. Response Spectrum Compatible Time Histories. Engineering Seismology Laboratory , State University of New York at Buffalo. http://civil.eng.buffalo.edu/engseislab.

Papageorgiou, Apostolos, and K. Aki. 1983. "A Specific Barrier Model or the Quantitative Description of Inhomogenous Faulting and the Prediction of Strong Ground Motion." *Bull. Seism. Soc. Am.* 693-722.

Purba, R., and M. Bruneau. 2015. "Seismic Performance of Steel Plate Shear Walls Considering Two Different Design Philosophies of Infill Plates. I: Deterioration Model Development." *Journal of Structural Engineering* 141 (6).

Purba, R., and M. Bruneau. 2015. "Seismic Performance of Steel Plate Shear Walls Considering Two Different Design Philosophies of Infill Plates. II: Assessment of Collapse Potential." *Journal of Structural Engineering* Volume 141 (6).

Purba, R., and M. Bruneau. 2014. *Seismic Performance of Steel Plate Shear Walls Considering Various Design Approaches.* MCEER-14-0005, Buffalo: Multidisciplinary Center for Earthquake Engineering Research (MCEER).

Purba, Ronny, and Michel Bruneau. 2010. *Impact of Horizontal Boundary Elements Design on Seismic Behavior of Steel Plate Sher Walls.* MCEER.

Qu, B., and Michel Bruneau. 2007. "Analytical Study on Steel Plate Shear Walls using Dual Strip Model and 3D FE Model." *Workshop of the Asian-Pacific Network of Center in Earthquake Engineering Research.* Hong Kong.

Qu, B., M. Bruneau, C. H. Lin, and K. C. Tsai. 2008. "Testing of full scale two-story steel plate shear wall with reduced beam section connections and composite floors." *Journal of Structural Engineering* 364-373.

Rahnama, M., and L. Manuel. 1996. "The effects of strong motion on seismic demands." *Proceedings of the Eleventh World Conference on Earthquake Engineering.* England. Paper No. 924.

Sabelli, R., and M. Bruneau. 2007. *Steel Design Guide of Steel Plate Shear Walls.* American Institute of Steel Construction.

Sabouri-Ghomi, S., and T. M. Roberts. 1991. "Nonlinear dynamic analysis of thin steel plate shear walls." *Computers and Structures* 39(1/2): 121-127.

Sarieddine, M. 2013. "Effects of Strong-motion Duration on the Response of Reinforced Concrete Frame Buildings." Masters Thesis, Department of Building, Civil and Environmental Engineering at Concordia University, Montreal, Canada.

Suidan, M. T., and R. A. Eubanks. 1973. "Cumulative fatigue damage in seismic structures." *J Struct Div Proc ASCE* 99: 923–43.

Takahashi, Y., Y. Takemoto, T. Takeda, and M. Takagi. 1973. "Experimental study on thin steel shear walls and particular bracings under alternative horizontal load." *Preliminary Report, IABSE Symposium on Resistance and Ultimate Deformability of Structures Acted on by Well-defined Repeated Loads.* Lisbon, Portugal. 185-191.

Thompson, James. 2004. *The effects of long duration earthquakes on concrete bridges with poorly confined columns.* Washington State University.

Thorburn, L. J., G. L. Kulak, and C. J. Montgomery. 1983. "Analysis of steel plate shear walls." Structural Engineering Report, Department of Civil Engineering, University of Alberta, Edmonton, AB.

Timler, P. A., and G. L. Kulak. 1983. *Experimental study of steel plate shear walls.* Structural Engineering Rep. No. 114, Edmonton, Alta: Dept. of Civil Engineering, Univ. of Alberta.

Trifunac, M D, and A. G. Brady. 1975. "A study of the duration of strong earth- quake ground motion." *Bulletin of The Seismological Society of America* 65(3): 581–626.

Trifunac, M D, and E. I. Novikova. 1995. "Duration of earthquake fault motion in California." *Earthquake Eng Struct Dyn* 24: 781–99.

Tromposch, E. W., and G. L. Kulak. 1987. "Cyclic and static behaviour of thin panel steel plate shear walls." Structural Engineering Report No. 145, Department of Civil Engineering, University of Alberta, Edmonton, AB.

U.S. Geological Survey. 2014. "USGS Seismic Design Maps Tool." earthquake.usgs.gov/hazards/designmaps/.

Van de Lindt, J. W., and G. H. Goh. 2004. "Effect of earthquake duration on structural reliability." *Engineering Structures* 26: 1585-1597.

Vanmarcke, E. H., and S-S Lai. 1980. "Strong motion duration and RMS amplitude of earthquake records." *BSSA* 70(4).

Wagner, H. 1931. *Flat sheet metal girders with very thin webs, Part 1 – General theories and assumptions.* Technical Memo. No. 604, Washington, D.C.: National Advisory Committee for Aeronautics.

Xie, Li-Li, and Xiaozhi Zhang. 1988. "Engineering Duration of Strong Motion and its effects on Seismic Damage." *Proceedings of the Ninth World Conference on Earthquake Engineering.* Tokyo, Japan. 307-312.

APPENDIX A

Design of 1:1 SPSW Using ASCE 7-10 Equivalent Lateral Force Procedure, *R* = 7

Location: San Francisco Downtown

Seismic Design Data:

USGS Provided Output (in g units):

$S_S := 1.50$

$S_1 := 0.649$

$S_{DS} := 1.0$

$S_{D1} := 0.432$

$S_{MS} := 1.50$

$S_{M1} := 0.649$

From ASCE 7-10 Table 12.2-1

$R := 7$

$I := 1.0$

$C_d := 6$

$\Omega_o := 2$

Equivalent Lateral Force Procedure – ASCE 7-10 Section 12.8

Seismic Base Shear, V

$$C_s := \frac{S_{DS}}{\left(\frac{R}{I}\right)} = 0.143$$

$W := 1500\text{kip}$

$V := C_s \cdot W = 214.29 \cdot \text{kip}$

Plate Data:

Assumed angle of tension stress

$\alpha := 45deg$

$F_y := 36ksi$

$R_y := 1.3$

$L := 12ft$

$H := 12ft$

L_cf for a start assumed as 12” less than centerline distance between columns

$L_{cf} := L - 12in = 11\ ft$

$\phi := 0.9$

$$t_w := \frac{V}{\phi \cdot 0.42 \cdot F_y \cdot L_{cf} \cdot \sin(2 \cdot \alpha)} = 0.119 \cdot in$$

tw :=

	0	1	2	3
0	Thickness (in)"	0.188	0.25	0.313
1	"ϕV_n(kips)"	336.8	449.1	561.3

Taking plate thickness as

$t_w := 0.1875in$

For Boundary Elements

$F_{yy} := 50ksi$

$R_{yy} := 1.1$

Modulus of Elasticity

$E := 29000ksi$

HBE Data

Trial Section HBE: W30x116

cross-sectional area of HBE

$A_b := 34.2in^2$

depth of HBE

$d_b := 30in$

flange width

$b_{fb} := 10.5in$

flange thickness

$t_{fb} := 0.85in$

web thickness

$t_{wb} := 0.565in$

Inertia of HBE

$I_b := 4930in^4$

Modulus of Plasticity

$Z_{xb} := 378in^3$

Radii of Gyration

$r_{yb} := 2.19in$

$r_{xb} := 12.0in$

Limiting unbraced length (AISC Table 3-2)

$L_{pb} := 7.74ft$

$L_{rb} := 22.6ft$

$Mp_{xb} := 1420kip \cdot ft$

$Mr_{xb} := 864kip \cdot ft$

$Cb_b := 1.14$

VBE Data

Trial Section VBE: W14x398

cross-sectional area of VBE

$A_c := 117in^2$

depth of VBE

$d_c := 18.3in$

flange width

$b_{fc} := 16.6in$

flange thickness

$t_{fc} := 2.85in$

web thickness

$t_{wc} := 1.77in$

Inertia of VBE

$I_c := 6000in^4$

Modulus of Plasticity

$Z_{xc} := 801in^3$

Radii of Gyration

$r_{yc} := 4.31in$

$r_{xc} := 7.16in$

Limiting unbraced length (AISC Table 3-2)

$L_{pc} := 15.2ft$

$L_{rc} := 158ft$

$Mp_{xc} := 3000kip \cdot ft$

$Mr_{xc} := 1720kip \cdot ft$

$Cb_c := 1.14$

Rechecking angle of tension stress

$$\alpha := \tan(\alpha_1)^4 = \frac{1 + \frac{t_w \cdot L}{2 \cdot A_c}}{1 + t_w \cdot H \cdot \left(\frac{1}{A_b} + \frac{H^3}{360 I_c \cdot L}\right)} \text{ solve } \rightarrow \begin{bmatrix} \operatorname{atan}\left[\frac{0.668740304976422024 \cdot \sqrt{in} \cdot (4.80769230769}{(1.5e18 \cdot ft^3 + 6.5789473684210526316e}\right. \\ \operatorname{atan}\left[-\frac{0.668740304976422024i \cdot \sqrt{in} \cdot (4.8076923076}{(1.5e18 \cdot ft^3 + 6.5789473684210526316}\right. \\ \operatorname{atan}\left[\frac{0.668740304976422024i \cdot \sqrt{in} \cdot (4.80769230769}{(1.5e18 \cdot ft^3 + 6.5789473684210526316e}\right. \\ -1.0 \cdot \operatorname{atan}\left[\frac{0.668740304976422024 \cdot \sqrt{in} \cdot (4.807692307}{(1.5e18 \cdot ft^3 + 6.578947368421052631}\right. \end{bmatrix}$$

$$\alpha = \begin{pmatrix} 40.662 \\ -73.882i \\ 73.882i \\ -40.662 \end{pmatrix} \cdot deg$$

$$\alpha := \alpha_0 = 40.662 \cdot deg$$

Calculating horizontal and vertical component of loads from plate web considering full yielding

$$w_{yb} := R_y \cdot F_y \cdot t_w \cdot \cos(\alpha)^2 = 5.049 \cdot \frac{kip}{in}$$

$$w_{xb} := \frac{1}{2} \cdot R_y \cdot F_y \cdot t_w \cdot \sin(2\alpha) = 4.337 \cdot \frac{kip}{in}$$

$$w_{yc} := \frac{1}{2} \cdot R_y \cdot F_y \cdot t_w \cdot \sin(2 \cdot \alpha) = 4.337 \cdot \frac{kip}{in}$$

$$w_{xc} := R_y \cdot F_y \cdot t_w \cdot \sin(\alpha)^2 = 3.726 \cdot \frac{kip}{in}$$

Design of HBE

Design Moment

$$L_{cf} := L - d_c = 125.7 \cdot in$$

$$M_u := w_{yb} \cdot \frac{L_{cf}^2}{4} = 1.995 \times 10^4 \cdot kip \cdot in$$

Axial Force in HBE:

distance between HBE centerlines

$h := 12\text{ft}$

$h_c := h - \frac{1}{2} \cdot d_b = 10.75\text{ ft}$

$P_{HBEvbe} := \frac{1}{2} \cdot R_y \cdot F_y \cdot \sin(\alpha)^2 \cdot t_w \cdot h_c = 240.307 \cdot \text{kip}$

$P_{HBEweb} := R_y \cdot F_y \cdot t_w \cdot L_{cf} \cdot \sin(\alpha)^2 = 468.32 \cdot \text{kip}$

$P_{HBEL} := P_{HBEvbe} + \frac{1}{2} P_{HBEweb} = 474.467 \cdot \text{kip}$

$P_{HBER} := P_{HBEvbe} - \frac{1}{2} P_{HBEweb} = 6.147 \cdot \text{kip}$

$P_u := \max\left(P_{HBEL}, P_{HBER}\right) = 474.467 \cdot \text{kip}$

AISC 341-16 Table D1.1

$P_y := A_b \cdot R_{yy} \cdot F_{yy} = 1.881 \times 10^3 \cdot \text{kip}$

Shear Force in HBE:

$V_{uWebL} := \frac{w_{yb} \cdot L_{cf} + w_{xb} \cdot d_b}{2} = 382.408 \cdot \text{kip}$

$V_{uWebR} := \frac{w_{yb} \cdot L_{cf} - w_{xb} \cdot d_b}{2} = 252.289 \cdot \text{kip}$

$V_{uWeb} := \max\left(V_{uWebR}, V_{uWebL}\right) = 382.408 \cdot \text{kip}$

$V_g := 0\text{kip}$

Reduced Probable flexural strength

Left side

$$M_{pr\_reduced\_L} := \begin{cases} (1.1 \cdot R_{yy} \cdot F_{yy} \cdot Z_{xb}) \cdot \left(1 - 0.5 \cdot \dfrac{P_{HBEL}}{P_y}\right) & \text{if } \dfrac{P_{HBEL}}{P_y} < 0.2 \\ \dfrac{9}{8} \cdot (1.1 \cdot R_{yy} \cdot F_{yy} \cdot Z_{xb}) \cdot \left(1 - \dfrac{P_{HBEL}}{P_y}\right) & \text{otherwise} \end{cases} = 1.924 \times 10^{4} \cdot kip \cdot in$$

Right side

$$M_{pr\_reduced\_R} := \begin{cases} (1.1 \cdot R_{yy} \cdot F_{yy} \cdot Z_{xb}) \cdot \left(1 - 0.5 \cdot \dfrac{P_{HBER}}{P_y}\right) & \text{if } \dfrac{P_{HBER}}{P_y} < 0.2 \\ \dfrac{9}{8} \cdot (1.1 \cdot R_{yy} \cdot F_{yy} \cdot Z_{xb}) \cdot \left(1 - \dfrac{P_{HBER}}{P_y}\right) & \text{otherwise} \end{cases} = 2.283 \times 10^{4} \cdot kip \cdot in$$

$$V_{uHBE} := \frac{(M_{pr\_reduced\_L} + M_{pr\_reduced\_L})}{L_{cf}} = 306.094 \cdot kip$$

$$V_{HBE} := V_{uWeb} + V_g + V_{uHBE} = 688.503 \cdot kip$$

Checks:

1. Check Shear Strength

$$shearcheck1 := \begin{cases} \text{"}\phi v\text{=1"} & \text{if } \dfrac{d_b - 2 \cdot t_{fb}}{t_{wb}} < 2.24 \cdot \sqrt{\dfrac{E}{R_{yy} \cdot F_{yy}}} \\ \text{"no"} & \text{otherwise} \end{cases} = \text{"}\phi v\text{=1"}$$

$$A_w := (d_b - 2 \cdot t_{fb}) \cdot t_{wb} = 15.989 \cdot in^2$$

$$\varphi Vn_b := 1.0 \cdot 0.6 \cdot R_{yy} \cdot F_{yy} \cdot A_w = 527.653 \cdot kip$$

$$V_u := V_{HBE} = 688.503 \cdot kip$$

$$\varphi Vn_b = 527.653 \cdot kip$$

$$shearcheck2 := \begin{cases} \text{"Ok"} & \text{if } \varphi Vn_b > V_u \\ \text{"No"} & \text{otherwise} \end{cases} = \text{"No"}$$

2. Check Compactness

$$\text{flange} := \begin{vmatrix} \text{"Ok"} & \text{if } \dfrac{b_{fb}}{2\cdot t_{fb}} < 0.32\cdot\sqrt{\dfrac{E}{R_{yy}\cdot F_{yy}}} \\ \text{"No"} & \text{otherwise} \end{vmatrix} = \text{"Ok"}$$

$$0.32\cdot\sqrt{\frac{E}{R_{yy}\cdot F_{yy}}} = 7.348$$

$$\frac{b_{fb}}{2\cdot t_{fb}} = 6.176$$

Flange is compact

$$C_a := \frac{P_u}{0.9\cdot P_y} = 0.28$$

$$\text{web} := \begin{vmatrix} \text{"Ok"} & \text{if } \dfrac{d_b - 2\cdot t_{fb}}{t_{wb}} < 0.88\cdot\sqrt{\dfrac{E}{F_{yy}}}\cdot\left(2.68 - C_a\right) \\ \text{"No "} & \text{otherwise} \end{vmatrix} = \text{"Ok"}$$

$$\text{web} := \begin{vmatrix} \text{"Ok"} & \text{if } 0.88\cdot\sqrt{\dfrac{E}{R_{yy}\cdot F_{yy}}}\cdot\left(2.68 - C_a\right) > 1.57\cdot\sqrt{\dfrac{E}{R_{yy}\cdot F_{yy}}} \\ \text{"No "} & \text{otherwise} \end{vmatrix} = \text{"Ok"}$$

$$0.88\cdot\sqrt{\frac{E}{R_{yy}\cdot F_{yy}}}\cdot\left(2.68 - C_a\right) = 48.49$$

$$\frac{d_b - 2\cdot t_{fb}}{t_{wb}} = 50.09$$

$$1.57\cdot\sqrt{\frac{E}{R_{yy}\cdot F_{yy}}} = 36.051$$

Web is compact

3. Check Combined Compression and Flexure

$K := 1$

$$axisbuckling := \begin{cases} \text{"Major axis buckling controls"} & \text{if } \dfrac{K \cdot L}{r_{xb}} > \dfrac{K \cdot L}{r_{yb}} \\ \text{"Minor axis buckling controls"} & \text{otherwise} \end{cases} = \text{"Minor axis buckling controls"}$$

$$\frac{K \cdot L}{r_{xb}} = 12$$

$$\frac{K \cdot L}{r_{yb}} = 65.75$$

$$slenderness := \begin{cases} \dfrac{K \cdot L}{r_{yb}} & \text{if } axisbuckling = \text{"Minor axis buckling controls"} \\ \dfrac{K \cdot L}{r_{xb}} & \text{otherwise} \end{cases} = 65.753$$

$$F_e := \frac{\pi^2 \cdot E}{(slenderness)^2} = 66.2 \cdot ksi$$

$$0.44 \cdot R_{yy} \cdot F_{yy} = 24.2 \cdot ksi$$

$$checkE32 := \begin{cases} \text{"Use E3-2"} & \text{if } \dfrac{\pi^2 \cdot E}{(slenderness)^2} > 0.44 \cdot F_{yy} \\ \text{"Dont use E3-2"} & \text{otherwise} \end{cases} = \text{"Use E3-2"}$$

Using AISC 360 Equation E3-2

$$F_{cr} := 0.658^{\frac{R_{yy} \cdot F_{yy}}{F_e}} \cdot R_{yy} \cdot F_{yy} = 38.846 \cdot ksi$$

$$\varphi Pn_b := 0.9 \cdot F_{cr} \cdot A_b = 1.196 \times 10^3 \cdot kip$$

$$P_c := \varphi Pn_b$$

$$P_r := P_u$$

$$L_{pb} = 7.74 \cdot ft$$

$$L_b := L = 12\,ft$$

$$Mp_{xb} = 1.704 \times 10^4 \cdot kip \cdot in$$

$$\varphi Mn_b := \begin{cases} Mp_{xb} & \text{if } Mp_{xb} < Cb_b \cdot \left[Mp_{xb} - (Mp_{xb} - Mr_{xb}) \cdot \left(\dfrac{L_b - L_{pb}}{L_{rb} - L_{pb}} \right) \right] \\ Cb_b \cdot \left[Mp_{xb} - (Mp_{xb} - Mr_{xb}) \cdot \left(\dfrac{L_b - L_{pb}}{L_{rb} - L_{pb}} \right) \right] & \text{otherwise} \end{cases} = 1.704 \times 10^4 \cdot kip \cdot in$$

$$\frac{P_r}{P_c} = 0.397$$

$$\text{CombinedCheckEq} := \begin{cases} \text{"Use Equation H1-1a"} & \text{if } \dfrac{P_r}{P_c} \geq 0.2 \\ \text{"Use Equation H1-1b"} & \text{otherwise} \end{cases} = \text{"Use Equation H1-1a"}$$

AISC 360-10 Equation H1-1a

$$\text{CombinedCheck} := \begin{cases} \text{"Ok"} & \text{if } 1 > \dfrac{P_r}{P_c} + \dfrac{8}{9} \left(\dfrac{Mr_{xb}}{\varphi Mn_b} \right) \\ \text{"No"} & \text{otherwise} \end{cases} = \text{"Ok"}$$

<u>4. Check moment of inertia</u>

$$I_{required} := \frac{0.003 \cdot t_w \cdot L^4}{h} = 1.68 \times 10^3 \cdot in^4$$

$$I_b = 4.93 \times 10^3 \cdot in^4$$

$$\text{InertiaCheck} := \begin{cases} \text{"Ok"} & \text{if } I_b > I_{required} \\ \text{"No"} & \text{otherwise} \end{cases} = \text{"Ok"}$$

<u>5. Check Web thickness</u>

$$t_{wb} = 0.565 \cdot in$$

$$\frac{t_w \cdot R_y \cdot F_y}{F_{yy}} = 0.176 \cdot in$$

$$\text{WebCheck} := \begin{cases} \text{"Ok"} & \text{if } t_{wb} > \dfrac{t_w \cdot R_y \cdot F_y}{F_{yy}} \\ \text{"No"} & \text{otherwise} \end{cases} = \text{"Ok"}$$

Design of VBE

(there are no adjoining beams)

$M_{pradj} := 0$

$M_{prc} := 1.1 \cdot R_{yy} \cdot F_{yy} \cdot Z_{xc} = 4.846 \times 10^{4} \cdot kip \cdot in$

$L_h := H - d_b = 114 \cdot in$

Resulting compressive force

$$E_{mcomp} := \frac{1}{2} \cdot R_y \cdot F_y \cdot \sin(2 \cdot \alpha) \cdot t_w \cdot h_c + \left(V_{uHBE} + \frac{w_{yb} \cdot L_{cf}}{2}\right) - \left(2 \cdot \frac{M_{pradj}}{L_h}\right) = 1.183 \times 10^{3} \cdot kip$$

$P_{gravity} := 0kip$

$P_{uc} := E_{mcomp} + P_{gravity} = 1.183 \times 10^{3} \cdot kip$

$L_c := h$

Resulting tension force

$$E_{mtens} := \frac{1}{2} \cdot R_y \cdot F_y \cdot \sin(2 \cdot \alpha) \cdot t_w \cdot h_c + \left(V_{uHBE} - \frac{w_{yb} \cdot L_{cf}}{2}\right) - \left(2 \cdot \frac{M_{pradj}}{L_h}\right) = 548.257 \cdot kip$$

Flexure from web tension

$$M_{VBEweb} := w_{xc} \cdot \frac{\left(h_c^{\,2}\right)}{12} = 5.167 \times 10^{3} \cdot kip \cdot in$$

Flexure from VBE compression

$M_{pr} := \max\left(M_{pr\_reduced\_L}, M_{pr\_reduced\_R}\right) = 2.283 \times 10^{4} \cdot kip \cdot in$

$$M_{pb} := \frac{M_{pr}}{1.1 \cdot R_{yy}} + V_u \cdot \left[\frac{1}{2} \cdot \left(d_b + d_c\right)\right] = 3.55 \times 10^{4} \cdot kip \cdot in$$

$$M_{VBEhbe} := \frac{1}{2} \cdot M_{pb} = 1.775 \times 10^{4} \cdot kip \cdot in$$

$M_{uc} := M_{VBEweb} + M_{VBEhbe} = 2.291 \times 10^{4} \cdot kip \cdot in$

Moment magnification

$$P_{ec} := \frac{\pi^2 \cdot E \cdot I_c}{(K \cdot L_c)^2} = 8.282 \times 10^4 \cdot kip$$

$$C_m := 1.0$$

$$B_{1c} := \frac{C_m}{1 - \frac{P_{uc}}{P_{ec}}} = 1.014$$

$$P_{rc} := P_{uc} = 1.183 \times 10^3 \cdot kip$$

$$M_{rc} := B_{1c} \cdot M_{uc} = 2.325 \times 10^4 \cdot kip \cdot in$$

Shear in the VBE is the sum of the effect of web tension and the portion of shear not resisted by the web plate

Shear from web plate

$$V_{VBEweb} := \frac{1}{2} \cdot R_y \cdot F_y \cdot \sin(\alpha) \cdot t_w \cdot h_c = 368.797 \cdot kip$$

Shear from HBE Hinging

$$M_{pc} := M_{VBEhbe} + M_{uc}$$

$$V_{VBEhbe} := \frac{1}{2} \cdot \left(\frac{M_{pc}}{h_c} \right) = 157.609 \cdot kip$$

Shear from horizontal element

$$V_{uc} := V_{VBEweb} + V_{VBEhbe} = 526.405 \cdot kip$$

Design Checks

1. Check Compactness

AISC 341-16 Table D1.1

$$flange_c := \begin{cases} \text{"Ok"} & \text{if } \frac{b_{fc}}{2 \cdot t_{fc}} < 0.32 \cdot \sqrt{\frac{E}{R_{yy} \cdot F_{yy}}} \\ \text{"No"} & \text{otherwise} \end{cases} = \text{"Ok"}$$

$$\frac{b_{fc}}{2 \cdot t_{fc}} = 2.912$$

$$0.32 \cdot \sqrt{\frac{E}{R_{yy} \cdot F_{yy}}} = 7.348$$

Flange is compact

$$C_{ac} := \frac{P_{uc}}{0.9 \cdot F_{yy} \cdot R_{yy} \cdot A_c} = 0.204$$

$$web_c := \begin{cases} \text{"Ok"} & \text{if } \dfrac{d_c - 2 \cdot t_{fc}}{t_{wc}} < 0.88 \cdot \sqrt{\dfrac{E}{R_{yy} \cdot F_{yy}}} \cdot (2.68 - C_{ac}) \\ \text{"No"} & \text{otherwise} \end{cases} = \text{"Ok"}$$

$$web_c := \begin{cases} \text{"Ok"} & \text{if } 0.88 \cdot \sqrt{\dfrac{E}{R_{yy} \cdot F_{yy}}} \cdot (2.68 - C_{ac}) > 1.57 \cdot \sqrt{\dfrac{E}{R_{yy} \cdot F_{yy}}} \\ \text{"No"} & \text{otherwise} \end{cases} = \text{"Ok"}$$

$$\frac{d_c - 2 \cdot t_{fc}}{t_{wc}} = 7.119$$

$$0.88 \cdot \sqrt{\frac{E}{R_{yy} \cdot F_{yy}}} \cdot (2.68 - C_{ac}) = 50.027$$

$$1.57 \cdot \sqrt{\frac{E}{R_{yy} \cdot F_{yy}}} = 36.051$$

Web is compact

2. Check Shear Strength

$$\varphi check := \begin{cases} \text{"}\phi\text{=1"} & \text{if } \dfrac{d_c - 2 \cdot t_{fc}}{t_{wc}} < 2.24 \cdot \sqrt{\dfrac{E}{R_{yy} \cdot F_{yy}}} \\ \text{"No"} & \text{otherwise} \end{cases} = \text{"}\phi\text{=1"}$$

$$\varphi_{vc} := 1$$

$$\varphi Vn_c := \varphi_{vc} \cdot 0.6 \cdot R_{yy} \cdot F_{yy} \cdot (d_c - 2 \cdot t_{fc}) \cdot t_{wc} = 735.966 \cdot kip$$

$$V_{uc} = 526.405 \cdot kip$$

$$shear := \begin{cases} \text{"Ok"} & \text{if } V_{uc} < \varphi Vn_c \\ \text{"No"} & \text{otherwise} \end{cases} = \text{"Ok"}$$

3. Check Combined Compression and Flexure

$$\text{slenderness}_c := \frac{K \cdot L}{r_{yc}}$$

$$F_{ec} := \frac{\pi^2 \cdot E}{\text{slenderness}_c^{\,2}}$$

$$0.44 \cdot R_{yy} \cdot F_{yy} = 24.2 \cdot \text{ksi}$$

$$\text{checkE32}_c := \begin{cases} \text{"Use E3-2"} & \text{if } \dfrac{\pi^2 \cdot E}{\left(\text{slenderness}_c\right)^2} > 0.44 \cdot R_{yy} \cdot F_{yy} \\ \text{"Dont use E3-2"} & \text{otherwise} \end{cases} = \text{"Use E3-2"}$$

Using AISC 360-10 Equation E3-2

$$F_{crc} := 0.658^{\frac{R_{yy} \cdot F_{yy}}{F_{ec}}} \cdot R_{yy} \cdot F_{yy} = 50.277 \cdot \text{ksi}$$

$$\varphi Pn_c := 0.9 \cdot F_{crc} \cdot A_c = 5.294 \times 10^3 \cdot \text{kip}$$

$$P_{cc} := \varphi Pn_c$$

$$L_{bc} := h_c = 10.75 \cdot \text{ft}$$

$$L_{pc} = 15.2 \cdot \text{ft}$$

there is no lateral torsional buckling

$$M_c := 0.9 \cdot R_{yy} \cdot F_{yy} \cdot Z_{xc} = 3.965 \times 10^4 \cdot \text{kip} \cdot \text{in}$$

$$\frac{M_{rc}}{M_c} = 0.586$$

$$\frac{P_{rc}}{P_{cc}} = 0.223$$

$$\text{CombinedCheckEq}_c := \begin{cases} \text{"Use Equation H1-1a"} & \text{if } \dfrac{P_{rc}}{P_{cc}} \ge 0.2 \\ \text{"Use Equation H1-1b"} & \text{otherwise} \end{cases} = \text{"Use Equation H1-1a"}$$

Use AISC 360-10 Eq H1-1a

$$\text{CombinedCheck}_c := \begin{cases} \text{"Ok"} & \text{if } 1 > \dfrac{P_{rc}}{P_{cc}} + \dfrac{8}{9}\left(\dfrac{M_{rc}}{M_c}\right) \\ \text{"No"} & \text{otherwise} \end{cases} = \text{"Ok"}$$

Design of 1:1 SPSW Using ASCE 7-10 Equivalent Lateral Force Procedure - *R* = 5

Location: San Francisco Downtown

Seismic Design Data:

USGS Provided Output (in g units):

$S_S := 1.50$

$S_1 := 0.649$

$S_{DS} := 1.0$

$S_{D1} := 0.432$

$S_{MS} := 1.50$

$S_{M1} := 0.649$

From ASCE 7-10 Table 12.2-1

$R := 5$

$I := 1.0$

$C_d := 6$

$\Omega_o := 2$

Equivalent Lateral Force Procedure – ASCE 7-10 Section 12.8

Seismic Base Shear, V

$$C_s := \frac{S_{DS}}{\left(\frac{R}{I}\right)} = 0.2$$

$W := 2000\text{kip}$

$V := C_s \cdot W = 400 \cdot \text{kip}$

Plate Data:

Assumed angle of tension stress

$\alpha := 45\text{deg}$

$F_y := 36\text{ksi}$

$R_y := 1.3$

$L := 12\text{ft}$

$H := 12\text{ft}$

L_cf for a start assumed as 12” less than centerline distance between columns

$L_{cf} := L - 12\text{in} = 11\ \text{ft}$

$\phi := 0.9$

$$t_w := \frac{V}{\phi \cdot 0.42 \cdot F_y \cdot L_{cf} \cdot \sin(2 \cdot \alpha)} = 0.223 \cdot \text{in}$$

tw :=

	0	1	2	3	4
0	Thickness (in)"	0.125	0.188	0.25	0.313
1	"ϕV_n(kips)"	224.5	336.8	449.1	561.3

Taking plate thickness as

$t_w := 0.25\text{in}$

For Boundary Elements

$F_{yy} := 50\text{ksi}$

$R_{yy} := 1.1$

Modulus of Elasticity

$E := 29000\text{ksi}$

HBE Data

Trial Section HBE: W40x327

cross-sectional area of HBE

$A_b := 96in^2$

depth of HBE

$d_b := 40.8in$

flange width

$b_{fb} := 12.1in$

flange thickness

$t_{fb} := 2.13in$

web thickness

$t_{wb} := 1.18in$

Inertia of HBE

$I_b := 24500in^4$

Modulus of Plasticity

$Z_{xb} := 1410in^3$

Radii of Gyration

$r_{yb} := 2.58in$

$r_{xb} := 16.0in$

Limiting unbraced length (AISC Table 3-2)

$L_{pb} := 9.11ft$

$L_{rb} := 33.6ft$

$Mp_{xb} := 5290kip \cdot ft$

$Mr_{xb} := 3150kip \cdot ft$

$Cb_b := 1.14$

VBE Data

Trial Section VBE: W40x593

cross-sectional area of VBE

$A_c := 174in^2$

depth of VBE

$d_c := 43in$

flange width

$b_{fc} := 16.7in$

flange thickness

$t_{fc} := 3.23in$

web thickness

$t_{wc} := 1.79in$

Inertia of VBE

$I_c := 50400in^4$

Modulus of Plasticity

$Z_{xc} := 2760in^3$

Radii of Gyration

$r_{yc} := 3.80in$

$r_{xc} := 17.0in$

Limiting unbraced length (AISC Table 3-2)

$L_{pc} := 13.4ft$

$L_{rc} := 63.8ft$

$Mp_{xc} := 10400kip \cdot ft$

$Mr_{xc} := 6140kip \cdot ft$

$Cb_c := 1.14$

Rechecking angle of tension stress

$$\alpha := \tan(\alpha_1)^4 = \frac{1+\frac{t_w \cdot L}{2 \cdot A_c}}{1 + t_w \cdot H \cdot \left(\frac{1}{A_b} + \frac{H^3}{360 I_c \cdot L}\right)} \text{ solve } \rightarrow \begin{bmatrix} \operatorname{atan}\left[\frac{0.000053835632709552951949 \cdot \sqrt{in} \cdot (8.62068\ldots}{\left(2.0 \cdot ft^3 + 2625.0 \cdot ft \cdot in^2 \ldots\right.}\right] \\ \operatorname{atan}\left[-\frac{0.000053835632709552951949i \cdot \sqrt{in} \cdot (8.6206\ldots}{\left(2.0 \cdot ft^3 + 2625.0 \cdot ft \cdot in^2 \ldots\right.}\right] \\ \operatorname{atan}\left[\frac{0.000053835632709552951949i \cdot \sqrt{in} \cdot (8.62068\ldots}{\left(2.0 \cdot ft^3 + 2625.0 \cdot ft \cdot in^2 \ldots\right.}\right] \\ -1.0 \cdot \operatorname{atan}\left[\frac{0.000053835632709552951949 \cdot \sqrt{in} \cdot (8.620\ldots}{\left(2.0 \cdot ft^3 + 2625.0 \cdot ft \cdot i\ldots\right.}\right] \end{bmatrix}$$

$$\alpha = \begin{pmatrix} 43.214 \\ -99.353i \\ 99.353i \\ -43.214 \end{pmatrix} \cdot deg$$

$$\alpha := \alpha_0 = 43.214 \cdot deg$$

Calculating horizontal and vertical component of loads from plate web considering full yielding

$$w_{yb} := R_y \cdot F_y \cdot t_w \cdot \cos(\alpha)^2 = 6.214 \cdot \frac{kip}{in}$$

$$w_{xb} := \frac{1}{2} \cdot R_y \cdot F_y \cdot t_w \cdot \sin(2\alpha) = 5.839 \cdot \frac{kip}{in}$$

$$w_{yc} := \frac{1}{2} \cdot R_y \cdot F_y \cdot t_w \cdot \sin(2 \cdot \alpha) = 5.839 \cdot \frac{kip}{in}$$

$$w_{xc} := R_y \cdot F_y \cdot t_w \cdot \sin(\alpha)^2 = 5.486 \cdot \frac{kip}{in}$$

Design of HBE

Design Moment

$$L_{cf} := L - d_c = 101 \cdot in$$

$$M_u := w_{yb} \cdot \frac{L_{cf}^2}{4} = 1.585 \times 10^4 \cdot kip \cdot in$$

Preliminiary Sizing of HBE:

$$h_{0b} := d_b - t_{fb} = 38.67 \cdot in$$

$$A_{fb} := \begin{vmatrix} b_{fb} \cdot t_{fb} \ \text{ if } \ \dfrac{M_u}{0.9 \cdot h_{0b} \cdot F_{yy}} < b_{fb} \cdot t_{fb} \\ \text{"Resize"} \ \text{ otherwise} \end{vmatrix} = 25.773 \cdot in^2$$

Preliminiary HBE Size OK

Axial Force in HBE:

distance between HBE centerlines

$$h := 12ft$$

$$h_c := h - \frac{1}{2} \cdot d_b = 10.3\ ft$$

$$P_{HBEvbe} := \frac{1}{2} \cdot R_y \cdot F_y \cdot \sin(\alpha)^2 \cdot t_w \cdot h_c = 339.009 \cdot kip$$

$$P_{HBEweb} := R_y \cdot F_y \cdot t_w \cdot L_{cf} \cdot \sin(\alpha)^2 = 554.044 \cdot kip$$

$$P_{HBEL} := P_{HBEvbe} + \frac{1}{2} P_{HBEweb} = 616.031 \cdot kip$$

$$P_{HBER} := P_{HBEvbe} - \frac{1}{2} P_{HBEweb} = 61.987 \cdot kip$$

$$P_u := \max\left(P_{HBEL}, P_{HBER}\right) = 616.031 \cdot kip$$

AISC 341-16 Table D1.1

$$P_y := A_b \cdot R_{yy} \cdot F_{yy} = 5.28 \times 10^3 \cdot kip$$

Shear Force in HBE:

$$V_{uWebL} := \frac{w_{yb} \cdot L_{cf} + w_{xb} \cdot d_b}{2} = 432.936 \cdot kip$$

$$V_{uWebR} := \frac{w_{yb} \cdot L_{cf} - w_{xb} \cdot d_b}{2} = 194.72 \cdot kip$$

$$V_{uWeb} := \max\left(V_{uWebR}, V_{uWebL}\right) = 432.936 \cdot kip$$

$$V_g := 0kip$$

Reduced Probable flexural strength

Left side

$$M_{pr\_reduced\_L} := \begin{cases} \left(1.1\cdot R_{yy}\cdot F_{yy}\cdot Z_{xb}\right)\cdot\left(1 - 0.5\cdot\dfrac{P_{HBEL}}{P_y}\right) & \text{if } \dfrac{P_{HBEL}}{P_y} < 0.2 \\ \dfrac{9}{8}\cdot\left(1.1\cdot R_{yy}\cdot F_{yy}\cdot Z_{xb}\right)\cdot\left(1 - \dfrac{P_{HBEL}}{P_y}\right) & \text{otherwise} \end{cases} = 8.033\times 10^{4}\cdot kip\cdot in$$

Right side

$$M_{pr\_reduced\_R} := \begin{cases} \left(1.1\cdot R_{yy}\cdot F_{yy}\cdot Z_{xb}\right)\cdot\left(1 - 0.5\cdot\dfrac{P_{HBER}}{P_y}\right) & \text{if } \dfrac{P_{HBER}}{P_y} < 0.2 \\ \dfrac{9}{8}\cdot\left(1.1\cdot R_{yy}\cdot F_{yy}\cdot Z_{xb}\right)\cdot\left(1 - \dfrac{P_{HBER}}{P_y}\right) & \text{otherwise} \end{cases} = 8.48\times 10^{4}\cdot kip\cdot in$$

$$V_{uHBE} := \frac{\left(M_{pr\_reduced\_L} + M_{pr\_reduced\_L}\right)}{L_{cf}} = 1.591\times 10^{3}\cdot kip$$

$$V_{HBE} := V_{uWeb} + V_g + V_{uHBE} = 2.024\times 10^{3}\cdot kip$$

Checks:

1. Check Shear Strength

$$\text{shearcheck1} := \begin{cases} \text{"}\phi\text{v=1"} & \text{if } \dfrac{d_b - 2\cdot t_{fb}}{t_{wb}} < 2.24\cdot\sqrt{\dfrac{E}{R_{yy}\cdot F_{yy}}} \\ \text{"no"} & \text{otherwise} \end{cases} = \text{"}\phi\text{v=1"}$$

$$A_w := \left(d_b - 2\cdot t_{fb}\right)\cdot t_{wb} = 43.117\cdot in^2$$

$$\varphi Vn_b := 1.0\cdot 0.6\cdot R_{yy}\cdot F_{yy}\cdot A_w = 1.423\times 10^{3}\cdot kip$$

$$V_u := V_{HBE} = 2.024\times 10^{3}\cdot kip$$

$$\varphi Vn_b = 1.423\times 10^{3}\cdot kip$$

$$\text{shearcheck2} := \begin{cases} \text{"Ok"} & \text{if } \varphi Vn_b > V_u \\ \text{"No"} & \text{otherwise} \end{cases} = \text{"No"}$$

2. Check Compactness

$$\text{flange} := \begin{vmatrix} \text{"Ok"} & \text{if } \dfrac{b_{fb}}{2 \cdot t_{fb}} < 0.32 \cdot \sqrt{\dfrac{E}{R_{yy} \cdot F_{yy}}} \\ \text{"No"} & \text{otherwise} \end{vmatrix} = \text{"Ok"}$$

$$0.32 \cdot \sqrt{\frac{E}{R_{yy} \cdot F_{yy}}} = 7.348$$

$$\frac{b_{fb}}{2 \cdot t_{fb}} = 2.84$$

Flange is compact

$$C_a := \frac{P_u}{0.9 \cdot P_y} = 0.13$$

$$\text{web} := \begin{vmatrix} \text{"Ok"} & \text{if } \dfrac{d_b - 2 \cdot t_{fb}}{t_{wb}} < 0.88 \cdot \sqrt{\dfrac{E}{F_{yy}}} \cdot (2.68 - C_a) \\ \text{"No "} & \text{otherwise} \end{vmatrix} = \text{"Ok"}$$

$$\text{web} := \begin{vmatrix} \text{"Ok"} & \text{if } 0.88 \cdot \sqrt{\dfrac{E}{R_{yy} \cdot F_{yy}}} \cdot (2.68 - C_a) > 1.57 \cdot \sqrt{\dfrac{E}{R_{yy} \cdot F_{yy}}} \\ \text{"No "} & \text{otherwise} \end{vmatrix} = \text{"Ok"}$$

$$0.88 \cdot \sqrt{\frac{E}{R_{yy} \cdot F_{yy}}} \cdot (2.68 - C_a) = 51.54$$

$$\frac{d_b - 2 \cdot t_{fb}}{t_{wb}} = 30.97$$

$$1.57 \cdot \sqrt{\frac{E}{R_{yy} \cdot F_{yy}}} = 36.051$$

Web is compact

3. Check Combined Compression and Flexure

$K := 1$

$$\text{axisbuckling} := \begin{cases} \text{"Major axis buckling controls"} & \text{if } \dfrac{K \cdot L}{r_{xb}} > \dfrac{K \cdot L}{r_{yb}} \\ \text{"Minor axis buckling controls"} & \text{otherwise} \end{cases} = \text{"Minor axis buckling controls"}$$

$$\frac{K \cdot L}{r_{xb}} = 9$$

$$\frac{K \cdot L}{r_{yb}} = 55.81$$

$$\text{slenderness} := \begin{cases} \dfrac{K \cdot L}{r_{yb}} & \text{if axisbuckling} = \text{"Minor axis buckling controls"} \\ \dfrac{K \cdot L}{r_{xb}} & \text{otherwise} \end{cases} = 55.814$$

$$F_e := \frac{\pi^2 \cdot E}{(\text{slenderness})^2} = 91.878 \cdot \text{ksi}$$

$$0.44 \cdot R_{yy} \cdot F_{yy} = 24.2 \cdot \text{ksi}$$

$$\text{checkE32} := \begin{cases} \text{"Use E3-2"} & \text{if } \dfrac{\pi^2 \cdot E}{(\text{slenderness})^2} > 0.44 \cdot F_{yy} \\ \text{"Dont use E3-2"} & \text{otherwise} \end{cases} = \text{"Use E3-2"}$$

Using AISC 360 Equation E3-2

$$F_{cr} := 0.658^{\frac{R_{yy} \cdot F_{yy}}{F_e}} \cdot R_{yy} \cdot F_{yy} = 42.81 \cdot \text{ksi}$$

$$\varphi Pn_b := 0.9 \cdot F_{cr} \cdot A_b = 3.699 \times 10^3 \cdot \text{kip}$$

$P_c := \varphi Pn_b$

$P_r := P_u$

$L_{pb} = 9.11 \cdot \text{ft}$

$L_b := L = 12\,\text{ft}$

$Mp_{xb} = 6.348 \times 10^4 \cdot \text{kip} \cdot \text{in}$

$$\varphi Mn_b := \begin{cases} Mp_{xb} & \text{if } Mp_{xb} < Cb_b \cdot \left[Mp_{xb} - \left(Mp_{xb} - Mr_{xb}\right) \cdot \left(\dfrac{L_b - L_{pb}}{L_{rb} - L_{pb}} \right) \right] \\ Cb_b \cdot \left[Mp_{xb} - \left(Mp_{xb} - Mr_{xb}\right) \cdot \left(\dfrac{L_b - L_{pb}}{L_{rb} - L_{pb}} \right) \right] & \text{otherwise} \end{cases} = 6.348 \times 10^4 \cdot kip \cdot in$$

$$\frac{P_r}{P_c} = 0.167$$

$$CombinedCheckEq := \begin{cases} \text{"Use Equation H1-1a"} & \text{if } \dfrac{P_r}{P_c} \geq 0.2 \\ \text{"Use Equation H1-1b"} & \text{otherwise} \end{cases} = \text{"Use Equation H1-1b"}$$

AISC 360-10 Equation H1-1b

$$CombinedCheck := \begin{cases} \text{"Ok"} & \text{if } 1 > \dfrac{P_r}{2P_c} + \left(\dfrac{Mr_{xb}}{\varphi Mn_b} \right) \\ \text{"No"} & \text{otherwise} \end{cases} = \text{"Ok"}$$

4. Check moment of inertia

$$I_{required} := \frac{0.003 \cdot t_w \cdot L^4}{h} = 2.239 \times 10^3 \cdot in^4$$

$$I_b = 2.45 \times 10^4 \cdot in^4$$

$$InertiaCheck := \begin{cases} \text{"Ok"} & \text{if } I_b > I_{required} \\ \text{"No"} & \text{otherwise} \end{cases} = \text{"Ok"}$$

5. Check Web thickness

$$t_{wb} = 1.18 \cdot in$$

$$\frac{t_w \cdot R_y \cdot F_y}{F_{yy}} = 0.234 \cdot in$$

$$WebCheck := \begin{cases} \text{"Ok"} & \text{if } t_{wb} > \dfrac{t_w \cdot R_y \cdot F_y}{F_{yy}} \\ \text{"No"} & \text{otherwise} \end{cases} = \text{"Ok"}$$

Design of VBE

(there are no adjoining beams)

$M_{pradj} := 0$

$M_{prc} := 1.1 \cdot R_{yy} \cdot F_{yy} \cdot Z_{xc} = 1.67 \times 10^{5} \cdot kip \cdot in$

$L_h := H - d_b = 103.2 \cdot in$

Resulting compressive force

$$E_{mcomp} := \frac{1}{2} \cdot R_y \cdot F_y \cdot \sin(2 \cdot \alpha) \cdot t_w \cdot h_c + \left(V_{uHBE} + \frac{w_{yb} \cdot L_{cf}}{2} \right) - \left(2 \cdot \frac{M_{pradj}}{L_h} \right) = 2.626 \times 10^{3} \cdot kip$$

$P_{gravity} := 0kip$

$P_{uc} := E_{mcomp} + P_{gravity} = 2.626 \times 10^{3} \cdot kip$

$L_c := h$

Resulting tension force

$$E_{mtens} := \frac{1}{2} \cdot R_y \cdot F_y \cdot \sin(2 \cdot \alpha) \cdot t_w \cdot h_c + \left(V_{uHBE} - \frac{w_{yb} \cdot L_{cf}}{2} \right) - \left(2 \cdot \frac{M_{pradj}}{L_h} \right) = 1.998 \times 10^{3} \cdot kip$$

Flexure from web tension

$$M_{VBEweb} := w_{xc} \cdot \frac{\left(h_c^{\,2} \right)}{12} = 6.984 \times 10^{3} \cdot kip \cdot in$$

Flexure from VBE compression

$M_{pr} := \max\left(M_{pr\_reduced\_L}, M_{pr\_reduced\_R} \right) = 8.48 \times 10^{4} \cdot kip \cdot in$

$$M_{pb} := \frac{M_{pr}}{1.1 \cdot R_{yy}} + V_u \cdot \left[\frac{1}{2} \cdot \left(d_b + d_c \right) \right] = 1.549 \times 10^{5} \cdot kip \cdot in$$

$$M_{VBEhbe} := \frac{1}{2} \cdot M_{pb} = 7.744 \times 10^{4} \cdot kip \cdot in$$

$M_{uc} := M_{VBEweb} + M_{VBEhbe} = 8.442 \times 10^{4} \cdot kip \cdot in$

Moment magnification

$$P_{ec} := \frac{\pi^2 \cdot E \cdot I_c}{(K \cdot L_c)^2} = 6.957 \times 10^5 \cdot kip$$

$$C_m := 1.0$$

$$B_{1c} := \frac{C_m}{1 - \frac{P_{uc}}{P_{ec}}} = 1.004$$

$$P_{rc} := P_{uc} = 2.626 \times 10^3 \cdot kip$$

$$M_{rc} := B_{1c} \cdot M_{uc} = 8.474 \times 10^4 \cdot kip \cdot in$$

Shear in the VBE is the sum of the effect of web tension and the portion of shear not resisted by the web plate

Shear from web plate

$$V_{VBEweb} := \frac{1}{2} \cdot R_y \cdot F_y \cdot \sin(\alpha) \cdot t_w \cdot h_c = 495.1 \cdot kip$$

Shear from HBE Hinging

$$M_{pc} := M_{VBEhbe} + M_{uc}$$

$$V_{VBEhbe} := \frac{1}{2} \cdot \left(\frac{M_{pc}}{h_c} \right) = 654.768 \cdot kip$$

Shear from horizontal element

$$V_{uc} := V_{VBEweb} + V_{VBEhbe} = 1.15 \times 10^3 \cdot kip$$

Design Checks

1. Check Compactness

AISC 341-16 Table D1.1

$$flange_c := \begin{cases} \text{"Ok"} & \text{if } \frac{b_{fc}}{2 \cdot t_{fc}} < 0.32 \cdot \sqrt{\frac{E}{R_{yy} \cdot F_{yy}}} \\ \text{"No"} & \text{otherwise} \end{cases} = \text{"Ok"}$$

$$\frac{b_{fc}}{2 \cdot t_{fc}} = 2.585$$

$$0.32 \cdot \sqrt{\frac{E}{R_{yy} \cdot F_{yy}}} = 7.348$$

Flange is compact

$$C_{ac} := \frac{P_{uc}}{0.9 \cdot F_{yy} \cdot R_{yy} \cdot A_c} = 0.305$$

$$web_c := \begin{cases} \text{"Ok"} & \text{if } \dfrac{d_c - 2 \cdot t_{fc}}{t_{wc}} < 0.88 \cdot \sqrt{\dfrac{E}{R_{yy} \cdot F_{yy}}} \cdot (2.68 - C_{ac}) \\ \text{"No"} & \text{otherwise} \end{cases} = \text{"Ok"}$$

$$web_c := \begin{cases} \text{"Ok"} & \text{if } 0.88 \cdot \sqrt{\dfrac{E}{R_{yy} \cdot F_{yy}}} \cdot (2.68 - C_{ac}) > 1.57 \cdot \sqrt{\dfrac{E}{R_{yy} \cdot F_{yy}}} \\ \text{"No"} & \text{otherwise} \end{cases} = \text{"Ok"}$$

$$\frac{d_c - 2 \cdot t_{fc}}{t_{wc}} = 20.413$$

$$0.88 \cdot \sqrt{\frac{E}{R_{yy} \cdot F_{yy}}} \cdot (2.68 - C_{ac}) = 47.993$$

$$1.57 \cdot \sqrt{\frac{E}{R_{yy} \cdot F_{yy}}} = 36.051$$

Web is compact

2. Check Shear Strength

$$\varphi check := \begin{cases} \text{"}\phi\text{=1"} & \text{if } \dfrac{d_c - 2 \cdot t_{fc}}{t_{wc}} < 2.24 \cdot \sqrt{\dfrac{E}{R_{yy} \cdot F_{yy}}} \\ \text{"No"} & \text{otherwise} \end{cases} = \text{"}\phi\text{=1"}$$

$$\varphi_{vc} := 1$$

$$\varphi Vn_c := \varphi_{vc} \cdot 0.6 \cdot R_{yy} \cdot F_{yy} \cdot (d_c - 2 \cdot t_{fc}) \cdot t_{wc} = 2.158 \times 10^3 \cdot kip$$

$$V_{uc} = 1.15 \times 10^3 \cdot kip$$

$$shear := \begin{cases} \text{"Ok"} & \text{if } V_{uc} < \varphi Vn_c \\ \text{"No"} & \text{otherwise} \end{cases} = \text{"Ok"}$$

3. Check Combined Compression and Flexure

$$\text{slenderness}_c := \frac{K \cdot L}{r_{yc}}$$

$$F_{ec} := \frac{\pi^2 \cdot E}{\text{slenderness}_c^{\;2}}$$

$$0.44 \cdot R_{yy} \cdot F_{yy} = 24.2 \cdot \text{ksi}$$

$$\text{checkE32}_c := \left| \begin{array}{l} \text{"Use E3-2"} \quad \text{if } \dfrac{\pi^2 \cdot E}{\left(\text{slenderness}_c\right)^2} > 0.44 \cdot R_{yy} \cdot F_{yy} \\ \text{"Dont use E3-2"} \quad \text{otherwise} \end{array} \right. = \text{"Use E3-2"}$$

Using AISC 360-10 Equation E3-2

$$F_{crc} := 0.658^{\frac{R_{yy} \cdot F_{yy}}{F_{ec}}} \cdot R_{yy} \cdot F_{yy} = 49.001 \cdot \text{ksi}$$

$$\varphi Pn_c := 0.9 \cdot F_{crc} \cdot A_c = 7.674 \times 10^3 \cdot \text{kip}$$

$$P_{cc} := \varphi Pn_c$$

$$L_{bc} := h_c = 10.3 \cdot \text{ft}$$

$$L_{pc} = 13.4 \cdot \text{ft}$$

there is no lateral torsional buckling

$$M_c := 0.9 \cdot R_{yy} \cdot F_{yy} \cdot Z_{xc} = 1.366 \times 10^5 \cdot \text{kip} \cdot \text{in}$$

$$\frac{M_{rc}}{M_c} = 0.62$$

$$\frac{P_{rc}}{P_{cc}} = 0.342$$

$$\text{CombinedCheckEq}_c := \left| \begin{array}{l} \text{"Use Equation H1-1a"} \quad \text{if } \dfrac{P_{rc}}{P_{cc}} \geq 0.2 \\ \text{"Use Equation H1-1b"} \quad \text{otherwise} \end{array} \right. = \text{"Use Equation H1-1a"}$$

Use AISC 360-10 Eq H1-1a

$$\text{CombinedCheck}_c := \left| \begin{array}{l} \text{"Ok"} \quad \text{if } 1 > \dfrac{P_{rc}}{P_{cc}} + \dfrac{8}{9}\left(\dfrac{M_{rc}}{M_c}\right) \\ \text{"No"} \quad \text{otherwise} \end{array} \right. = \text{"Ok"}$$

Design of 2:1 SPSW Using ASCE 7-10 Equivalent Lateral Force Procedure, *R* = 7

Location: San Francisco Downtown

Seismic Design Data:

USGS Provided Output (in g units):

$S_S := 1.50$

$S_1 := 0.649$

$S_{DS} := 1.0$

$S_{D1} := 0.432$

$S_{MS} := 1.50$

$S_{M1} := 0.649$

From ASCE 7-10 Table 12.2-1

$R := 7$

$I := 1.0$

$C_d := 6$

$\Omega_o := 2$

Equivalent Lateral Force Procedure – ASCE 7-10 Section 12.8

Seismic Base Shear, V

$$C_s := \frac{S_{DS}}{\left(\frac{R}{I}\right)} = 0.143$$

$W := 2500\text{kip}$

$V := C_s \cdot W = 357.14 \cdot \text{kip}$

Plate Data:

Assumed angle of tension stress

$\alpha := 45deg$

$F_y := 36ksi$

$R_y := 1.3$

$L := 24ft$

$H := 12ft$

L_cf for a start assumed as 12” less than centerline distance between columns

$L_{cf} := L - 12in = 23\ ft$

$\phi := 0.9$

$$t_w := \frac{V}{\phi \cdot 0.42 \cdot F_y \cdot L_{cf} \cdot \sin(2 \cdot \alpha)} = 0.095 \cdot in$$

tw :=

	0	1	2	3	4
0	Thickness (in)"	0.125	0.188	0.25	0.313
1	"ϕV_n(kips)"	224.5	336.8	449.1	561.3

Taking plate thickness as

$t_w := 0.125in$

For Boundary Elements

$F_{yy} := 50ksi$

$R_{yy} := 1.1$

Modulus of Elasticity

$E := 29000ksi$

HBE Data

Trial Section HBE: W36x330

cross-sectional area of HBE

$A_b := 96.9in^2$

depth of HBE

$d_b := 37.7in$

flange width

$b_{fb} := 16.6in$

flange thickness

$t_{fb} := 1.85in$

web thickness

$t_{wb} := 1.02in$

Inertia of HBE

$I_b := 23300in^4$

Modulus of Plasticity

$Z_{xb} := 1410in^3$

Radii of Gyration

$r_{yb} := 3.83in$

$r_{xb} := 15.5in$

Limiting unbraced length (AISC Table 3-2)

$L_{pb} := 13.5ft$

$L_{rb} := 45.5ft$

$Mp_{xb} := 5290kip \cdot ft$

$Mr_{xb} := 3260kip \cdot ft$

$Cb_b := 1.14$

VBE Data

Trial Section VBE: W40x431

cross-sectional area of VBE

$A_c := 127in^2$

depth of VBE

$d_c := 41.3in$

flange width

$b_{fc} := 16.4in$

flange thickness

$t_{fc} := 2.36in$

web thickness

$t_{wc} := 1.34in$

Inertia of VBE

$I_c := 34800in^4$

Modulus of Plasticity

$Z_{xc} := 1960in^3$

Radii of Gyration

$r_{yc} := 3.65in$

$r_{xc} := 16.6in$

Limiting unbraced length (AISC Table 3-2)

$L_{pc} := 12.9ft$

$L_{rc} := 49ft$

$Mp_{xc} := 7350kip \cdot ft$

$Mr_{xc} := 4440kip \cdot ft$

$Cb_c := 1.14$

Rechecking angle of tension stress

$$\alpha := \tan(\alpha_1)^4 = \frac{1 + \frac{t_w \cdot L}{2 \cdot A_c}}{1 + t_w \cdot H \cdot \left(\frac{1}{A_b} + \frac{H^3}{360 I_c \cdot L}\right)} \text{ solve } \rightarrow \begin{bmatrix} \operatorname{atan}\left[\frac{3.4701000819561811999 \cdot \sqrt{in} \cdot (2.36220472440}{(2.5e18 \cdot ft^3 + 4.48916408668730650150}\right. \\ \operatorname{atan}\left[-\frac{3.4701000819561811999i \cdot \sqrt{in} \cdot (2.3622047244}{(2.5e18 \cdot ft^3 + 4.4891640866873065015}\right. \\ \operatorname{atan}\left[\frac{3.4701000819561811999i \cdot \sqrt{in} \cdot (2.3622047244}{(2.5e18 \cdot ft^3 + 4.48916408668730650150}\right. \\ -1.0 \cdot \operatorname{atan}\left[\frac{3.4701000819561811999 \cdot \sqrt{in} \cdot (2.36220472}{(2.5e18 \cdot ft^3 + 4.48916408668730650}\right. \end{bmatrix}$$

$$\alpha = \begin{pmatrix} 44.64 \\ -145.21i \\ 145.21i \\ -44.64 \end{pmatrix} \cdot deg$$

$$\alpha := \alpha_0 = 44.64 \cdot deg$$

Calculating horizontal and vertical component of loads from plate web considering full yielding

$$w_{yb} := R_y \cdot F_y \cdot t_w \cdot \cos(\alpha)^2 = 2.962 \cdot \frac{kip}{in}$$

$$w_{xb} := \frac{1}{2} \cdot R_y \cdot F_y \cdot t_w \cdot \sin(2\alpha) = 2.925 \cdot \frac{kip}{in}$$

$$w_{yc} := \frac{1}{2} \cdot R_y \cdot F_y \cdot t_w \cdot \sin(2 \cdot \alpha) = 2.925 \cdot \frac{kip}{in}$$

$$w_{xc} := R_y \cdot F_y \cdot t_w \cdot \sin(\alpha)^2 = 2.888 \cdot \frac{kip}{in}$$

Design of HBE

Design Moment

$$L_{cf} := L - d_c = 246.7 \cdot in$$

$$M_u := w_{yb} \cdot \frac{L_{cf}^2}{4} = 4.506 \times 10^4 \cdot kip \cdot in$$

Preliminiary Sizing of HBE:

$$h_{0b} := d_b - t_{fb} = 35.85 \cdot in$$

$$A_{fb} := \begin{vmatrix} b_{fb} \cdot t_{fb} \ \text{ if } \ \dfrac{M_u}{0.9 \cdot h_{0b} \cdot F_{yy}} < b_{fb} \cdot t_{fb} \\ \text{"Resize"} \ \text{ otherwise} \end{vmatrix} = 30.71 \cdot in^2$$

Preliminiary HBE Size OK

Axial Force in HBE:

distance between HBE centerlines

$h := 24ft$

$h_c := h - \frac{1}{2} \cdot d_b = 22.429\,ft$

$P_{HBEvbe} := \frac{1}{2} \cdot R_y \cdot F_y \cdot \sin(\alpha)^2 \cdot t_w \cdot h_c = 388.68 \cdot kip$

$P_{HBEweb} := R_y \cdot F_y \cdot t_w \cdot L_{cf} \cdot \sin(\alpha)^2 = 712.52 \cdot kip$

$P_{HBEL} := P_{HBEvbe} + \frac{1}{2} P_{HBEweb} = 744.94 \cdot kip$

$P_{HBER} := P_{HBEvbe} - \frac{1}{2} P_{HBEweb} = 32.42 \cdot kip$

$P_u := \max\left(P_{HBEL}, P_{HBER}\right) = 744.94 \cdot kip$

AISC 341-16 Table D1.1

$P_y := A_b \cdot R_{yy} \cdot F_{yy} = 5.33 \times 10^3 \cdot kip$

Shear Force in HBE:

$V_{uWebL} := \frac{w_{yb} \cdot L_{cf} + w_{xb} \cdot d_b}{2} = 420.469 \cdot kip$

$V_{uWebR} := \frac{w_{yb} \cdot L_{cf} - w_{xb} \cdot d_b}{2} = 310.206 \cdot kip$

$V_{uWeb} := \max\left(V_{uWebR}, V_{uWebL}\right) = 420.469 \cdot kip$

$V_g := 0kip$

Reduced Probable flexural strength

Left side

$$M_{pr\_reduced\_L} := \begin{vmatrix} \left(1.1 \cdot R_{yy} \cdot F_{yy} \cdot Z_{xb}\right) \cdot \left(1 - 0.5 \cdot \dfrac{P_{HBEL}}{P_y}\right) & \text{if } \dfrac{P_{HBEL}}{P_y} < 0.2 \\ \dfrac{9}{8} \cdot \left(1.1 \cdot R_{yy} \cdot F_{yy} \cdot Z_{xb}\right) \cdot \left(1 - \dfrac{P_{HBEL}}{P_y}\right) & \text{otherwise} \end{vmatrix} = 7.934 \times 10^{4} \cdot \text{kip} \cdot \text{in}$$

Right side

$$M_{pr\_reduced\_R} := \begin{vmatrix} \left(1.1 \cdot R_{yy} \cdot F_{yy} \cdot Z_{xb}\right) \cdot \left(1 - 0.5 \cdot \dfrac{P_{HBER}}{P_y}\right) & \text{if } \dfrac{P_{HBER}}{P_y} < 0.2 \\ \dfrac{9}{8} \cdot \left(1.1 \cdot R_{yy} \cdot F_{yy} \cdot Z_{xb}\right) \cdot \left(1 - \dfrac{P_{HBER}}{P_y}\right) & \text{otherwise} \end{vmatrix} = 8.505 \times 10^{4} \cdot \text{kip} \cdot \text{in}$$

$$V_{uHBE} := \frac{\left(M_{pr\_reduced\_L} + M_{pr\_reduced\_L}\right)}{L_{cf}} = 643.236 \cdot \text{kip}$$

$$V_{HBE} := V_{uWeb} + V_g + V_{uHBE} = 1.064 \times 10^{3} \cdot \text{kip}$$

Checks:

1. Check Shear Strength

$$\text{shearcheck1} := \begin{cases} \text{"}\phi\text{v=1"} & \text{if } \dfrac{d_b - 2 \cdot t_{fb}}{t_{wb}} < 2.24 \cdot \sqrt{\dfrac{E}{R_{yy} \cdot F_{yy}}} \\ \text{"no"} & \text{otherwise} \end{cases} = \text{"}\phi\text{v=1"}$$

$$A_w := (d_b - 2 \cdot t_{fb}) \cdot t_{wb} = 34.68 \cdot in^2$$

$$\varphi Vn_b := 1.0 \cdot 0.6 \cdot R_{yy} \cdot F_{yy} \cdot A_w = 1.144 \times 10^3 \cdot kip$$

$$V_u := V_{HBE} = 1.064 \times 10^3 \cdot kip$$

$$\varphi Vn_b = 1.144 \times 10^3 \cdot kip$$

$$\text{shearcheck2} := \begin{cases} \text{"Ok"} & \text{if } \varphi Vn_b > V_u \\ \text{"No"} & \text{otherwise} \end{cases} = \text{"Ok"}$$

2. Check Compactness

$$\text{flange} := \begin{cases} \text{"Ok"} & \text{if } \dfrac{b_{fb}}{2 \cdot t_{fb}} < 0.32 \cdot \sqrt{\dfrac{E}{R_{yy} \cdot F_{yy}}} \\ \text{"No"} & \text{otherwise} \end{cases} = \text{"Ok"}$$

$$0.32 \cdot \sqrt{\frac{E}{R_{yy} \cdot F_{yy}}} = 7.348$$

$$\frac{b_{fb}}{2 \cdot t_{fb}} = 4.486$$

Flange is compact

$$C_a := \frac{P_u}{0.9 \cdot P_y} = 0.155$$

$$web := \begin{array}{|l} \text{"Ok"} \quad \text{if } \dfrac{d_b - 2 \cdot t_{fb}}{t_{wb}} < 0.88 \cdot \sqrt{\dfrac{E}{R_{yy} \cdot F_{yy}}} \cdot (2.68 - C_a) \\ \text{"No "} \quad \text{otherwise} \end{array} = \text{"Ok"}$$

$$web := \begin{array}{|l} \text{"Ok"} \quad \text{if } 0.88 \cdot \sqrt{\dfrac{E}{R_{yy} \cdot F_{yy}}} \cdot (2.68 - C_a) > 1.57 \cdot \sqrt{\dfrac{E}{R_{yy} \cdot F_{yy}}} \\ \text{"No "} \quad \text{otherwise} \end{array} = \text{"Ok"}$$

$$0.88 \cdot \sqrt{\frac{E}{R_{yy} \cdot F_{yy}}} \cdot (2.68 - C_a) = 51.02$$

$$\frac{d_b - 2 \cdot t_{fb}}{t_{wb}} = 33.33$$

$$1.57 \cdot \sqrt{\frac{E}{R_{yy} \cdot F_{yy}}} = 36.051$$

Web is compact

3. Check Combined Compression and Flexure

$$K := 1$$

$$axisbuckling := \begin{array}{|l} \text{"Major axis buckling controls"} \quad \text{if } \dfrac{K \cdot L}{r_{xb}} > \dfrac{K \cdot L}{r_{yb}} \\ \text{"Minor axis buckling controls"} \quad \text{otherwise} \end{array} = \text{"Minor axis buckling controls"}$$

$$\frac{K \cdot L}{r_{xb}} = 18.581$$

$$\frac{K \cdot L}{r_{yb}} = 75.2$$

$$slenderness := \begin{cases} \dfrac{K \cdot L}{r_{yb}} & \text{if } axisbuckling = \text{"Minor axis buckling controls"} \\ \dfrac{K \cdot L}{r_{xb}} & \text{otherwise} \end{cases} = 75.196$$

$$F_e := \frac{\pi^2 \cdot E}{(slenderness)^2} = 50.619 \cdot ksi$$

$$0.44 \cdot R_{yy} \cdot F_{yy} = 24.2 \cdot ksi$$

$$checkE32 := \begin{cases} \text{"Use E3-2"} & \text{if } \dfrac{\pi^2 \cdot E}{(slenderness)^2} > 0.44 \cdot F_{yy} \\ \text{"Dont use E3-2"} & \text{otherwise} \end{cases} = \text{"Use E3-2"}$$

Using AISC 360 Equation E3-2

$$F_{cr} := 0.658^{\frac{R_{yy} \cdot F_{yy}}{F_e}} \cdot R_{yy} \cdot F_{yy} = 34.902 \cdot ksi$$

$$\varphi Pn_b := 0.9 \cdot F_{cr} \cdot A_b = 3.044 \times 10^3 \cdot kip$$

$$P_c := \varphi Pn_b$$
$$P_r := P_u$$

$$\frac{P_r}{P_c} = 0.245$$

$$L_{pb} = 13.5 \cdot ft$$

$$L_b := L = 24\, ft$$

$Mp_{xb} = 6.348 \times 10^4 \cdot kip \cdot in$

$$\varphi Mn_b := \begin{cases} Mp_{xb} & \text{if } Mp_{xb} < Cb_b \cdot \left[Mp_{xb} - \left(Mp_{xb} - Mr_{xb}\right) \cdot \left(\frac{L_b - L_{pb}}{L_{rb} - L_{pb}} \right) \right] \\ Cb_b \cdot \left[Mp_{xb} - \left(Mp_{xb} - Mr_{xb}\right) \cdot \left(\frac{L_b - L_{pb}}{L_{rb} - L_{pb}} \right) \right] & \text{otherwise} \end{cases} = 6.326 \times 10^4 \cdot kip \cdot in$$

$$\frac{P_r}{P_c} = 0.245$$

$$CombinedCheckEq := \begin{cases} \text{"Use Equation H1-1a"} & \text{if } \frac{P_r}{P_c} \geq 0.2 \\ \text{"Use Equation H1-1b"} & \text{otherwise} \end{cases} = \text{"Use Equation H1-1a"}$$

Use AISC 360-10 Equation H1-1a

$$CombinedCheck := \begin{cases} \text{"Ok"} & \text{if } 1 > \frac{P_r}{P_c} + \frac{8}{9}\left(\frac{M_u}{\varphi Mn_b}\right) \\ \text{"No"} & \text{otherwise} \end{cases} = \text{"Ok"}$$

4. Check moment of inertia

$$I_{required} := \frac{0.003 \cdot t_w \cdot L^4}{h} = 8.958 \times 10^3 \cdot in^4$$

$I_b = 2.33 \times 10^4 \cdot in^4$

$$InertiaCheck := \begin{cases} \text{"Ok"} & \text{if } I_b > I_{required} \\ \text{"No"} & \text{otherwise} \end{cases} = \text{"Ok"}$$

5. Check Web thickness

$t_{wb} = 1.02 \cdot in$

$$\frac{t_w \cdot R_y \cdot F_y}{F_{yy}} = 0.117 \cdot in$$

$$WebCheck := \begin{cases} \text{"Ok"} & \text{if } t_{wb} > \frac{t_w \cdot R_y \cdot F_y}{F_{yy}} \\ \text{"No"} & \text{otherwise} \end{cases} = \text{"Ok"}$$

Design of VBE

(there are no adjoining beams)

$M_{pradj} := 0$

$M_{prc} := 1.1 \cdot R_{yy} \cdot F_{yy} \cdot Z_{xc} = 1.186 \times 10^{5} \cdot kip \cdot in$

$L_h := H - d_b = 106.3 \cdot in$

Resulting compressive force

$$E_{mcomp} := \frac{1}{2} \cdot R_y \cdot F_y \cdot \sin(2 \cdot \alpha) \cdot t_w \cdot h_c + \left(V_{uHBE} + \frac{w_{yb} \cdot L_{cf}}{2}\right) - \left(2 \cdot \frac{M_{pradj}}{L_h}\right) = 1.796 \times 10^{3} \cdot kip$$

$P_{gravity} := 0kip$

$P_{uc} := E_{mcomp} + P_{gravity} = 1.796 \times 10^{3} \cdot kip$

$L_c := h$

Resulting tension force

$$E_{mtens} := \frac{1}{2} \cdot R_y \cdot F_y \cdot \sin(2 \cdot \alpha) \cdot t_w \cdot h_c + \left(V_{uHBE} - \frac{w_{yb} \cdot L_{cf}}{2}\right) - \left(2 \cdot \frac{M_{pradj}}{L_h}\right) = 1.065 \times 10^{3} \cdot kip$$

Flexure from web tension

$$M_{VBEweb} := w_{xc} \cdot \frac{\left(h_c^{\,2}\right)}{12} = 1.744 \times 10^{4} \cdot kip \cdot in$$

Flexure from VBE compression

$M_{pr} := \max\left(M_{pr\_reduced\_L}, M_{pr\_reduced\_R}\right) = 8.505 \times 10^{4} \cdot kip \cdot in$

$$M_{pb} := \frac{M_{pr}}{1.1 \cdot R_{yy}} + V_u \cdot \left[\frac{1}{2} \cdot \left(d_b + d_c\right)\right] = 1.123 \times 10^{5} \cdot kip \cdot in$$

$$M_{VBEhbe} := \frac{1}{2} \cdot M_{pb} = 5.615 \times 10^{4} \cdot kip \cdot in$$

$M_{uc} := M_{VBEweb} + M_{VBEhbe} = 7.359 \times 10^{4} \cdot kip \cdot in$

Moment magnification

$$P_{ec} := \frac{\pi^2 \cdot E \cdot I_c}{(K \cdot L_c)^2} = 1.201 \times 10^5 \cdot kip$$

$$C_m := 1.0$$

$$B_{1c} := \frac{C_m}{1 - \frac{P_{uc}}{P_{ec}}} = 1.015$$

$$P_{rc} := P_{uc} = 1.796 \times 10^3 \cdot kip$$

$$M_{rc} := B_{1c} \cdot M_{uc} = 7.47 \times 10^4 \cdot kip \cdot in$$

<u>Shear from web plate</u>

$$V_{VBEweb} := \frac{1}{2} \cdot R_y \cdot F_y \cdot \sin(\alpha) \cdot t_w \cdot h_c = 553.167 \cdot kip$$

<u>Shear from HBE Hinging</u>

$$M_{pc} := M_{VBEhbe} + M_{uc}$$

$$V_{VBEhbe} := \frac{1}{2} \cdot \left(\frac{M_{pc}}{h_c} \right) = 241.013 \cdot kip$$

<u>Shear from horizontal element</u>

$$V_{uc} := V_{VBEweb} + V_{VBEhbe} = 794.18 \cdot kip$$

Design Checks

1. Check Compactness

AISC 341-16 Table D1.1

$$flange_c := \begin{cases} \text{"Ok"} & \text{if } \dfrac{b_{fc}}{2 \cdot t_{fc}} < 0.32 \cdot \sqrt{\dfrac{E}{R_{yy} \cdot F_{yy}}} \\ \text{"No"} & \text{otherwise} \end{cases} = \text{"Ok"}$$

$$\frac{b_{fc}}{2 \cdot t_{fc}} = 3.475$$

$$0.32 \cdot \sqrt{\frac{E}{R_{yy} \cdot F_{yy}}} = 7.348$$

Flange is compact

$$C_{ac} := \frac{P_{uc}}{0.9 \cdot F_{yy} \cdot R_{yy} \cdot A_c} = 0.286$$

$$web_c := \begin{cases} \text{"Ok"} & \text{if } \dfrac{d_c - 2 \cdot t_{fc}}{t_{wc}} < 0.88 \cdot \sqrt{\dfrac{E}{R_{yy} \cdot F_{yy}}} \cdot \left(2.68 - C_{ac}\right) \\ \text{"No"} & \text{otherwise} \end{cases} = \text{"Ok"}$$

$$web_c := \begin{cases} \text{"Ok"} & \text{if } 0.88 \cdot \sqrt{\dfrac{E}{R_{yy} \cdot F_{yy}}} \cdot \left(2.68 - C_{ac}\right) > 1.57 \cdot \sqrt{\dfrac{E}{R_{yy} \cdot F_{yy}}} \\ \text{"No"} & \text{otherwise} \end{cases} = \text{"Ok"}$$

$$\frac{d_c - 2 \cdot t_{fc}}{t_{wc}} = 27.299$$

$$0.88 \cdot \sqrt{\frac{E}{R_{yy} \cdot F_{yy}}} \cdot \left(2.68 - C_{ac}\right) = 48.382$$

$$1.57 \cdot \sqrt{\frac{E}{R_{yy} \cdot F_{yy}}} = 36.051$$

Web is compact

2. Check Shear Strength

$$\varphi check := \begin{cases} \text{"}\phi\text{=1"} & \text{if } \dfrac{d_c - 2 \cdot t_{fc}}{t_{wc}} < 2.24 \cdot \sqrt{\dfrac{E}{R_{yy} \cdot F_{yy}}} \\ \text{"No"} & \text{otherwise} \end{cases} = \text{"}\phi\text{=1"}$$

$$\varphi_{vc} := 1$$

$$\varphi Vn_c := \varphi_{vc} \cdot 0.6 \cdot R_{yy} \cdot F_{yy} \cdot \left(d_c - 2 \cdot t_{fc}\right) \cdot t_{wc} = 1.618 \times 10^3 \cdot kip$$

$$V_{uc} = 794.18 \cdot kip$$

$$shear := \begin{cases} \text{"Ok"} & \text{if } V_{uc} < \varphi Vn_c \\ \text{"No"} & \text{otherwise} \end{cases} = \text{"Ok"}$$

3. Check Combined Compression and Flexure

$$slenderness_c := \frac{K \cdot H}{r_{yc}} = 39.452$$

$$F_{ec} := \frac{\pi^2 \cdot E}{slenderness_c^{\ 2}} = 183.89 \cdot ksi$$

$$0.44 \cdot R_{yy} \cdot F_{yy} = 24.2 \cdot ksi$$

$$checkE32_c := \begin{cases} \text{"Use E3-2"} & \text{if } \dfrac{\pi^2 \cdot E}{\left(slenderness_c\right)^2} > 0.44 \cdot R_{yy} \cdot F_{yy} \\ \text{"Dont use E3-2"} & \text{otherwise} \end{cases} = \text{"Use E3-2"}$$

Using AISC 360-10 Equation E3-2

$$F_{crc} := 0.658^{\frac{R_{yy} \cdot F_{yy}}{F_{ec}}} \cdot R_{yy} \cdot F_{yy} = 48.528 \cdot ksi$$

$$\varphi Pn_c := 0.9 \cdot F_{crc} \cdot A_c = 5.547 \times 10^3 \cdot kip$$

$$P_{cc} := \varphi Pn_c$$

$$L_{bc} := h_c = 22.429 \cdot ft$$

$$L_{pc} = 12.9 \cdot ft$$

there is no lateral torsional buckling

$$M_c := 0.9 \cdot R_{yy} \cdot F_{yy} \cdot Z_{xc} = 8.085 \times 10^3 \cdot kip \cdot ft$$

$$\frac{M_{rc}}{M_c} = 0.77$$

$$\frac{P_{rc}}{P_{cc}} = 0.324$$

$$CombinedCheckEq_c := \left| \begin{array}{ll} \text{"Use Equation H1-1a"} & \text{if } \dfrac{P_{rc}}{P_{cc}} \geq 0.2 \\ \text{"Use Equation H1-1b"} & \text{otherwise} \end{array} \right. = \text{"Use Equation H1-1a"}$$

Use AISC 360-10 Eq H1-1a

$$CombinedCheck_c := \left| \begin{array}{ll} \text{"Ok"} & \text{if } 1.01 > \dfrac{P_{rc}}{P_{cc}} + \dfrac{8}{9}\left(\dfrac{M_{rc}}{M_c}\right) \\ \text{"No"} & \text{otherwise} \end{array} \right. = \text{"Ok"}$$

Design of 2:1 SPSW Using ASCE 7-10 Equivalent Lateral Force Procedure, *R* = 5

Location: San Francisco Downtown

Seismic Design Data:

USGS Provided Output (in g units):

$S_S := 1.50$

$S_1 := 0.649$

$S_{DS} := 1.0$

$S_{D1} := 0.432$

$S_{MS} := 1.50$

$S_{M1} := 0.649$

From ASCE 7-10 Table 12.2-1

$R := 5$

$I := 1.0$

$C_d := 6$

$\Omega_o := 2$

Equivalent Lateral Force Procedure – ASCE 7-10 Section 12.8

Seismic Base Shear, V

$$C_s := \frac{S_{DS}}{\left(\frac{R}{I}\right)} = 0.2$$

$W := 2500\text{kip}$

$V := C_s \cdot W = 500 \cdot \text{kip}$

Plate Data:

Assumed angle of tension stress

$\alpha := 45deg$

$F_y := 36ksi$

$R_y := 1.3$

$L := 24ft$

$H := 12ft$

L_cf for a start assumed as 12" less than centerline distance between columns

$L_{cf} := L - 12in = 23\ ft$

$\phi := 0.9$

$$t_w := \frac{V}{\phi \cdot 0.42 \cdot F_y \cdot L_{cf} \cdot \sin(2 \cdot \alpha)} = 0.133 \cdot in$$

tw :=

	0	1	2	3	4
0	Thickness (in)"	0.125	0.188	0.25	0.313
1	"ϕV_n(kips)"	224.5	336.8	449.1	561.3

Taking plate thickness as

$t_w := 0.1875in$

For Boundary Elements

$F_{yy} := 50ksi$

$R_{yy} := 1.1$

Modulus of Elasticity

$E := 29000ksi$

HBE Data

Trial Section HBE: W40x431

cross-sectional area of HBE

$A_b := 127in^2$

depth of HBE

$d_b := 41.3in$

flange width

$b_{fb} := 16.2in$

flange thickness

$t_{fb} := 2.36in$

web thickness

$t_{wb} := 1.34in$

Inertia of HBE

$I_b := 34800in^4$

Modulus of Plasticity

$Z_{xb} := 1960in^3$

Radii of Gyration

$r_{yb} := 3.65in$

$r_{xb} := 16.6in$

Limiting unbraced length (AISC Table 3-2)

$L_{pb} := 12.9ft$

$L_{rb} := 49.0ft$

$Mp_{xb} := 7350kip \cdot ft$

$Mr_{xb} := 4440kip \cdot ft$

$Cb_b := 1.14$

VBE Data

Trial Section VBE: W36x652

cross-sectional area of VBE

$A_c := 192in^2$

depth of VBE

$d_c := 41.1in$

flange width

$b_{fc} := 17.6in$

flange thickness

$t_{fc} := 3.54in$

web thickness

$t_{wc} := 1.97in$

Inertia of VBE

$I_c := 50600in^4$

Modulus of Plasticity

$Z_{xc} := 2910in^3$

Radii of Gyration

$r_{yc} := 4.1in$

$r_{xc} := 16.2in$

Limiting unbraced length (AISC Table 3-2)

$L_{pc} := 14.5ft$

$L_{rc} := 77.8ft$

$Mp_{xc} := 10900kip \cdot ft$

$Mr_{xc} := 6460kip \cdot ft$

$Cb_c := 1.14$

Rechecking angle of tension stress

$$\alpha := \tan(\alpha_1)^4 = \frac{1 + \dfrac{t_w \cdot L}{2 \cdot A_c}}{1 + t_w \cdot H \cdot \left(\dfrac{1}{A_b} + \dfrac{H^3}{360 I_c \cdot L}\right)} \text{ solve } \rightarrow \begin{bmatrix} \operatorname{atan}\left[\dfrac{26.618652522655572134 \cdot \sqrt{in} \cdot (3.0 \cdot ft + 256.0 \cdot}{\left(1143.0 \cdot ft^3 + 2.277e6 \cdot ft \cdot in^2 + 1.28524e8 \cdot in\right.}\right] \\ \operatorname{atan}\left[-\dfrac{26.618652522655572134i \cdot \sqrt{in} \cdot (3.0 \cdot ft + 256.0}{\left(1143.0 \cdot ft^3 + 2.277e6 \cdot ft \cdot in^2 + 1.28524e8 \cdot in\right.}\right] \\ \operatorname{atan}\left[\dfrac{26.618652522655572134i \cdot \sqrt{in} \cdot (3.0 \cdot ft + 256.0}{\left(1143.0 \cdot ft^3 + 2.277e6 \cdot ft \cdot in^2 + 1.28524e8 \cdot in\right.}\right] \\ -1.0 \cdot \operatorname{atan}\left[\dfrac{26.618652522655572134 \cdot \sqrt{in} \cdot (3.0 \cdot ft + 256}{\left(1143.0 \cdot ft^3 + 2.277e6 \cdot ft \cdot in^2 + 1.28524e8\right.}\right] \end{bmatrix}$$

$$\alpha = \begin{pmatrix} 44.472 \\ -134.247i \\ 134.247i \\ -44.472 \end{pmatrix} \cdot deg$$

$$\alpha := \alpha_0 = 44.472 \cdot deg$$

Calculating horizontal and vertical component of loads from plate web considering full yielding

$$w_{yb} := R_y \cdot F_y \cdot t_w \cdot \cos(\alpha)^2 = 4.468 \cdot \frac{kip}{in}$$

$$w_{xb} := \frac{1}{2} \cdot R_y \cdot F_y \cdot t_w \cdot \sin(2\alpha) = 4.387 \cdot \frac{kip}{in}$$

$$w_{yc} := \frac{1}{2} \cdot R_y \cdot F_y \cdot t_w \cdot \sin(2 \cdot \alpha) = 4.387 \cdot \frac{kip}{in}$$

$$w_{xc} := R_y \cdot F_y \cdot t_w \cdot \sin(\alpha)^2 = 4.307 \cdot \frac{kip}{in}$$

Design of HBE

Design Moment

$$L_{cf} := L - d_c = 246.9 \cdot in$$

$$M_u := w_{yb} \cdot \frac{L_{cf}^{\ 2}}{4} = 68098.305 \cdot kip \cdot in$$

Axial Force in HBE:

distance between HBE centerlines

$$h := 24ft$$

$$h_c := h - \frac{1}{2} \cdot d_b = 22.279\,ft$$

$$P_{HBEvbe} := \frac{1}{2} \cdot R_y \cdot F_y \cdot \sin(\alpha)^2 \cdot t_w \cdot h_c = 575.682 \cdot kip$$

$$P_{HBEweb} := R_y \cdot F_y \cdot t_w \cdot L_{cf} \cdot \sin(\alpha)^2 = 1.063 \times 10^3 \cdot kip$$

$$P_{HBEL} := P_{HBEvbe} + \frac{1}{2} P_{HBEweb} = 1.107 \times 10^3 \cdot kip$$

$$P_{HBER} := P_{HBEvbe} - \frac{1}{2} P_{HBEweb} = 44.035 \cdot kip$$

$$P_u := \max(P_{HBEL}, P_{HBER}) = 1.107 \times 10^3 \cdot kip$$

AISC 341-16 Table D1.1

$$P_y := A_b \cdot R_{yy} \cdot F_{yy} = 6.985 \times 10^3 \cdot kip$$

Shear Force in HBE:

$$V_{uWebL} := \frac{w_{yb} \cdot L_{cf} + w_{xb} \cdot d_b}{2} = 642.213 \cdot kip$$

$$V_{uWebR} := \frac{w_{yb} \cdot L_{cf} - w_{xb} \cdot d_b}{2} = 461.04 \cdot kip$$

$$V_{uWeb} := \max(V_{uWebR}, V_{uWebL}) = 642.213 \cdot kip$$

$$V_g := 0kip$$

Reduced Probable flexural strength

Left side

$$M_{pr\_reduced\_L} := \begin{cases} (1.1 \cdot R_{yy} \cdot F_{yy} \cdot Z_{xb}) \cdot \left(1 - 0.5 \cdot \frac{P_{HBEL}}{P_y}\right) & \text{if } \frac{P_{HBEL}}{P_y} < 0.2 \\ \frac{9}{8} \cdot (1.1 \cdot R_{yy} \cdot F_{yy} \cdot Z_{xb}) \cdot \left(1 - \frac{P_{HBEL}}{P_y}\right) & \text{otherwise} \end{cases} = 1.092 \times 10^5 \cdot kip \cdot in$$

Right side

$$M_{pr\_reduced\_R} := \begin{cases} (1.1 \cdot R_{yy} \cdot F_{yy} \cdot Z_{xb}) \cdot \left(1 - 0.5 \cdot \frac{P_{HBER}}{P_y}\right) & \text{if } \frac{P_{HBER}}{P_y} < 0.2 \\ \frac{9}{8} \cdot (1.1 \cdot R_{yy} \cdot F_{yy} \cdot Z_{xb}) \cdot \left(1 - \frac{P_{HBER}}{P_y}\right) & \text{otherwise} \end{cases} = 118206.225 \cdot kip \cdot in$$

$$V_{uHBE} := \frac{\left(M_{pr\_reduced\_L} + M_{pr\_reduced\_L}\right)}{L_{cf}} = 884.413 \cdot kip$$

$$V_{HBE} := V_{uWeb} + V_g + V_{uHBE} = 1.527 \times 10^3 \cdot kip$$

Checks:

1. Check Shear Strength

$$shearcheck1 := \begin{vmatrix} \text{"}\phi v\text{=1"} \quad \text{if} \quad \dfrac{d_b - 2 \cdot t_{fb}}{t_{wb}} < 2.24 \cdot \sqrt{\dfrac{E}{R_{yy} \cdot F_{yy}}} \\ \text{"no"} \quad \text{otherwise} \end{vmatrix} = \text{"}\phi v\text{=1"}$$

$$A_w := \left(d_b - 2 \cdot t_{fb}\right) \cdot t_{wb} = 49.017 \cdot in^2$$

$$\varphi Vn_b := 1.0 \cdot 0.6 \cdot R_{yy} \cdot F_{yy} \cdot A_w = 1.618 \times 10^3 \cdot kip$$

$$V_u := V_{HBE} = 1.527 \times 10^3 \cdot kip$$

$$\varphi Vn_b = 1.618 \times 10^3 \cdot kip$$

$$shearcheck2 := \begin{vmatrix} \text{"Ok"} \quad \text{if} \quad \varphi Vn_b > V_u \\ \text{"No"} \quad \text{otherwise} \end{vmatrix} = \text{"Ok"}$$

2. Check Compactness

$$flange := \begin{array}{|ll} \text{"Ok"} & \text{if } \dfrac{b_{fb}}{2 \cdot t_{fb}} < 0.32 \cdot \sqrt{\dfrac{E}{R_{yy} \cdot F_{yy}}} \\ \text{"No"} & \text{otherwise} \end{array} = \text{"Ok"}$$

$$0.32 \cdot \sqrt{\frac{E}{R_{yy} \cdot F_{yy}}} = 7.348$$

$$\frac{b_{fb}}{2 \cdot t_{fb}} = 3.432$$

Flange is compact

$$C_a := \frac{P_u}{0.9 \cdot P_y} = 0.176$$

$$web := \begin{array}{|ll} \text{"Ok"} & \text{if } \dfrac{d_b - 2 \cdot t_{fb}}{t_{wb}} < 0.88 \cdot \sqrt{\dfrac{E}{R_{yy} \cdot F_{yy}}} \cdot (2.68 - C_a) \\ \text{"No "} & \text{otherwise} \end{array} = \text{"Ok"}$$

$$web := \begin{array}{|ll} \text{"Ok"} & \text{if } 0.88 \cdot \sqrt{\dfrac{E}{R_{yy} \cdot F_{yy}}} \cdot (2.68 - C_a) > 1.57 \cdot \sqrt{\dfrac{E}{R_{yy} \cdot F_{yy}}} \\ \text{"No "} & \text{otherwise} \end{array} = \text{"Ok"}$$

$$0.88 \cdot \sqrt{\frac{E}{R_{yy} \cdot F_{yy}}} \cdot (2.68 - C_a) = 50.6$$

$$\frac{d_b - 2 \cdot t_{fb}}{t_{wb}} = 27.3$$

$$1.57 \cdot \sqrt{\frac{E}{R_{yy} \cdot F_{yy}}} = 36.051$$

Web is compact

3. Check Combined Compression and Flexure

$K := 1$

$$axisbuckling := \begin{cases} \text{"Major axis buckling controls"} & \text{if } \dfrac{K \cdot L}{r_{xb}} > \dfrac{K \cdot L}{r_{yb}} \\ \text{"Minor axis buckling controls"} & \text{otherwise} \end{cases} = \text{"Minor axis buckling controls"}$$

$$\frac{K \cdot L}{r_{xb}} = 17.349$$

$$\frac{K \cdot L}{r_{yb}} = 78.9$$

$$slenderness := \begin{cases} \dfrac{K \cdot L}{r_{yb}} & \text{if } axisbuckling = \text{"Minor axis buckling controls"} \\ \dfrac{K \cdot L}{r_{xb}} & \text{otherwise} \end{cases} = 78.904$$

$$F_e := \frac{\pi^2 \cdot E}{(slenderness)^2} = 45.973 \cdot ksi$$

$$0.44 \cdot R_{yy} \cdot F_{yy} = 24.2 \cdot ksi$$

$$checkE32 := \begin{cases} \text{"Use E3-2"} & \text{if } \dfrac{\pi^2 \cdot E}{(slenderness)^2} > 0.44 \cdot F_{yy} \\ \text{"Dont use E3-2"} & \text{otherwise} \end{cases} = \text{"Use E3-2"}$$

Using AISC 360 Equation E3-2

$$F_{cr} := 0.658^{\frac{R_{yy} \cdot F_{yy}}{F_e}} \cdot R_{yy} \cdot F_{yy} = 33.335 \cdot ksi$$

$$\varphi Pn_b := 0.9 \cdot F_{cr} \cdot A_b = 3.81 \times 10^3 \cdot kip$$

$P_c := \varphi Pn_b$

$P_r := P_u = 1.107 \times 10^3 \cdot kip$

$\frac{P_r}{P_c} = 0.291$

$L_{pb} = 12.9 \cdot ft$

$L_b := L_{cf} = 20.575\,ft$

$Mp_{xb} = 8.82 \times 10^4 \cdot kip \cdot in$

$$\varphi Mn_b := \begin{cases} Mp_{xb} & \text{if } Mp_{xb} < Cb_b \cdot \left[Mp_{xb} - \left(Mp_{xb} - Mr_{xb}\right) \cdot \left(\frac{L_b - L_{pb}}{L_{rb} - L_{pb}}\right)\right] \\ Cb_b \cdot \left[Mp_{xb} - \left(Mp_{xb} - Mr_{xb}\right) \cdot \left(\frac{L_b - L_{pb}}{L_{rb} - L_{pb}}\right)\right] & \text{otherwise} \end{cases} = 88200 \cdot kip \cdot in$$

$\frac{P_r}{P_c} = 0.291$

$$CombinedCheckEq := \begin{cases} \text{"Use Equation H1-1a"} & \text{if } \frac{P_r}{P_c} \geq 0.2 \\ \text{"Use Equation H1-1b"} & \text{otherwise} \end{cases} = \text{"Use Equation H1-1a"}$$

Use AISC 360-10 Equation H1-1a

$$CombinedCheck := \begin{cases} \text{"Ok"} & \text{if } 1 > \frac{P_r}{P_c} + \frac{8}{9}\left(\frac{M_u}{\varphi Mn_b}\right) \\ \text{"No"} & \text{otherwise} \end{cases} = \text{"Ok"}$$

4. Check moment of inertia

$$I_{required} := \frac{0.003 \cdot t_w \cdot L^4}{h} = 1.344 \times 10^4 \cdot in^4$$

$I_b = 3.48 \times 10^4 \cdot in^4$

$$InertiaCheck := \begin{cases} \text{"Ok"} & \text{if } I_b > I_{required} \\ \text{"No"} & \text{otherwise} \end{cases} = \text{"Ok"}$$

5. Check Web thickness

$t_{wb} = 1.34 \cdot in$

$\frac{t_w \cdot R_y \cdot F_y}{F_{yy}} = 0.176 \cdot in$

$$WebCheck := \begin{cases} \text{"Ok"} & \text{if } t_{wb} > \frac{t_w \cdot R_y \cdot F_y}{F_{yy}} \\ \text{"No"} & \text{otherwise} \end{cases} = \text{"Ok"}$$

Design of VBE

(there are no adjoining beams)

$M_{pradj} := 0$

$M_{prc} := 1.1 \cdot R_{yy} \cdot F_{yy} \cdot Z_{xc} = 1.761 \times 10^5 \cdot kip \cdot in$

$L_h := H - d_b = 102.7 \cdot in$

Resulting compressive force

$$E_{mcomp} := \frac{1}{2} \cdot R_y \cdot F_y \cdot \sin(2 \cdot \alpha) \cdot t_w \cdot h_c + \left(V_{uHBE} + \frac{w_{yb} \cdot L_{cf}}{2}\right) - \left(2 \cdot \frac{M_{pradj}}{L_h}\right) = 2.609 \times 10^3 \cdot kip$$

$P_{gravity} := 0 kip$

$P_{uc} := E_{mcomp} + P_{gravity} = 2.609 \times 10^3 \cdot kip$

$L_c := h$

Resulting tension force

$$E_{mtens} := \frac{1}{2} \cdot R_y \cdot F_y \cdot \sin(2 \cdot \alpha) \cdot t_w \cdot h_c + \left(V_{uHBE} - \frac{w_{yb} \cdot L_{cf}}{2}\right) - \left(2 \cdot \frac{M_{pradj}}{L_h}\right) = 1.506 \times 10^3 \cdot kip$$

Flexure from web tension

$$M_{VBEweb} := w_{xc} \cdot \frac{\left(h_c^2\right)}{12} = 2.565 \times 10^4 \cdot kip \cdot in$$

Flexure from VBE compression

$$M_{pr} := \max\left(M_{pr\_reduced\_L}, M_{pr\_reduced\_R}\right) = 1.182 \times 10^{5} \cdot kip \cdot in$$

$$M_{pb} := \frac{M_{pr}}{1.1 \cdot R_{yy}} + V_u \cdot \left[\frac{1}{2} \cdot \left(d_b + d_c\right)\right] = 1.606 \times 10^{5} \cdot kip \cdot in$$

$$M_{VBEhbe} := \frac{1}{2} \cdot M_{pb} = 8.029 \times 10^{4} \cdot kip \cdot in$$

$$M_{uc} := M_{VBEweb} + M_{VBEhbe} = 1.059 \times 10^{5} \cdot kip \cdot in$$

Moment magnification

$$P_{ec} := \frac{\pi^2 \cdot E \cdot I_c}{\left(K \cdot L_c\right)^2} = 1.746 \times 10^{5} \cdot kip$$

$$C_m := 1.0$$

$$B_{1c} := \frac{C_m}{1 - \frac{P_{uc}}{P_{ec}}} = 1.015$$

$$P_{rc} := P_{uc} = 2.609 \times 10^{3} \cdot kip$$

$$M_{rc} := B_{1c} \cdot M_{uc} = 1.076 \times 10^{5} \cdot kip \cdot in$$

Shear from web plate

$$V_{VBEweb} := \frac{1}{2} \cdot R_y \cdot F_y \cdot \sin(\alpha) \cdot t_w \cdot h_c = 821.75 \cdot kip$$

Shear from HBE Hinging

$$M_{pc} := M_{VBEhbe} + M_{uc} = 1.862 \times 10^{5} \cdot kip \cdot in$$

$$V_{VBEhbe} := \frac{1}{2} \cdot \left(\frac{M_{pc}}{h_c}\right) = 348.307 \cdot kip$$

Shear from horizontal element

$$V_{uc} := V_{VBEweb} + V_{VBEhbe} = 1.17 \times 10^{3} \cdot kip$$

Design Checks

1. Check Compactness

AISC 341-16 Table D1.1

$$flange_c := \begin{cases} \text{"Ok"} & \text{if } \frac{b_{fc}}{2 \cdot t_{fc}} < 0.32 \cdot \sqrt{\frac{E}{R_{yy} \cdot F_{yy}}} \\ \text{"No"} & \text{otherwise} \end{cases} = \text{"Ok"}$$

$$\frac{b_{fc}}{2 \cdot t_{fc}} = 2.486$$

$$0.32 \cdot \sqrt{\frac{E}{R_{yy} \cdot F_{yy}}} = 7.348$$

Flange is compact

$$C_{ac} := \frac{P_{uc}}{0.9 \cdot F_{yy} \cdot R_{yy} \cdot A_c} = 0.274$$

$$web_c := \begin{cases} \text{"Ok"} & \text{if } \frac{d_c - 2 \cdot t_{fc}}{t_{wc}} < 0.88 \cdot \sqrt{\frac{E}{R_{yy} \cdot F_{yy}}} \cdot \left(2.68 - C_{ac}\right) \\ \text{"No"} & \text{otherwise} \end{cases} = \text{"Ok"}$$

$$web_c := \begin{cases} \text{"Ok"} & \text{if } 0.88 \cdot \sqrt{\frac{E}{R_{yy} \cdot F_{yy}}} \cdot \left(2.68 - C_{ac}\right) > 1.57 \cdot \sqrt{\frac{E}{R_{yy} \cdot F_{yy}}} \\ \text{"No"} & \text{otherwise} \end{cases} = \text{"Ok"}$$

$$\frac{d_c - 2 \cdot t_{fc}}{t_{wc}} = 17.269 \qquad 0.88 \cdot \sqrt{\frac{E}{R_{yy} \cdot F_{yy}}} \cdot \left(2.68 - C_{ac}\right) = 48.608 \qquad 1.57 \cdot \sqrt{\frac{E}{R_{yy} \cdot F_{yy}}} = 36.051$$

Web is compact

2. Check Shear Strength

$$\varphi check := \begin{cases} \text{"}\phi\text{=1"} & \text{if } \frac{d_c - 2 \cdot t_{fc}}{t_{wc}} < 2.24 \cdot \sqrt{\frac{E}{R_{yy} \cdot F_{yy}}} \\ \text{"No"} & \text{otherwise} \end{cases} = \text{"}\phi\text{=1"}$$

$$\varphi_{vc} := 1$$

$$\varphi Vn_c := \varphi_{vc} \cdot 0.6 \cdot R_{yy} \cdot F_{yy} \cdot \left(d_c - 2 \cdot t_{fc}\right) \cdot t_{wc} = 2.212 \times 10^3 \cdot kip$$

$V_{uc} = 1.17 \times 10^3 \cdot kip$

$$shear := \begin{cases} \text{"Ok"} & \text{if } V_{uc} < \varphi Vn_c \\ \text{"No"} & \text{otherwise} \end{cases} = \text{"Ok"}$$

3. Check Combined Compression and Flexure

$$slenderness_c := \frac{K \cdot H}{r_{yc}} = 35.122$$

$$F_{ec} := \frac{\pi^2 \cdot E}{slenderness_c^{\,2}} = 232.028 \cdot ksi$$

$$0.44 \cdot R_{yy} \cdot F_{yy} = 24.2 \cdot ksi$$

$$checkE32_c := \begin{cases} \text{"Use E3-2"} & \text{if } \dfrac{\pi^2 \cdot E}{\left(slenderness_c\right)^2} > 0.44 \cdot R_{yy} \cdot F_{yy} \\ \text{"Dont use E3-2"} & \text{otherwise} \end{cases} = \text{"Use E3-2"}$$

Using AISC 360-10 Equation E3-2

$$F_{crc} := 0.658^{\frac{R_{yy} \cdot F_{yy}}{F_{ec}}} \cdot R_{yy} \cdot F_{yy} = 49.805 \cdot ksi$$

$$\varphi Pn_c := 0.9 \cdot F_{crc} \cdot A_c = 8.606 \times 10^3 \cdot kip$$

$$P_{cc} := \varphi Pn_c$$

$$L_{bc} := H - d_b = 8.558 \cdot ft$$

$$L_{pc} = 14.5 \cdot ft$$

$$\varphi Mn_c := \begin{cases} Mp_{xc} & \text{if } Mp_{xc} < Cb_c \cdot \left[Mp_{xc} - \left(Mp_{xc} - Mr_{xc}\right) \cdot \left(\dfrac{L_{bc} - L_{pc}}{L_{rc} - L_{pc}} \right) \right] \\ Cb_c \cdot \left[Mp_{xc} - \left(Mp_{xc} - Mr_{xc}\right) \cdot \left(\dfrac{L_{bc} - L_{pc}}{L_{rc} - L_{pc}} \right) \right] & \text{otherwise} \end{cases} = 130800 \cdot kip \cdot in$$

$$M_c := 0.9 \cdot R_{yy} \cdot F_{yy} \cdot Z_{xc} = 1.44 \times 10^5 \cdot kip \cdot in$$

$$\frac{M_{rc}}{M_c} = 0.747$$

$$\frac{P_{rc}}{P_{cc}} = 0.303$$

$$CombinedCheckEq_c := \begin{array}{|l} \text{"Use Equation H1-1a"} \quad \text{if } \dfrac{P_{rc}}{P_{cc}} \geq 0.2 \\ \text{"Use Equation H1-1b"} \quad \text{otherwise} \end{array} = \text{"Use Equation H1-1a"}$$

Use AISC 360-10 Eq H1-1a

$$CombinedCheck_c := \begin{array}{|l} \text{"Ok"} \quad \text{if } 1 > \dfrac{P_{rc}}{P_{cc}} + \dfrac{8}{9}\left(\dfrac{M_{rc}}{M_c}\right) \\ \text{"No"} \quad \text{otherwise} \end{array} = \text{"Ok"}$$

Design of 1:3 SPSW Using ASCE 7-10 Equivalent Lateral Force Procedure, *R* = 7

Location: San Francisco Downtown

Seismic Design Data:

USGS Provided Output (in g units):

$S_S := 1.50$

$S_1 := 0.649$

$S_{DS} := 1.0$

$S_{D1} := 0.432$

$S_{MS} := 1.50$

$S_{M1} := 0.649$

From ASCE 7-10 Table 12.2-1

$R := 7$

$I := 1.0$

$C_d := 6$

$\Omega_o := 2$

Equivalent Lateral Force Procedure – ASCE 7-10 Section 12.8

Seismic Base Shear, V

$$C_s := \frac{S_{DS}}{\left(\frac{R}{I}\right)} = 0.143$$

$h_1 := 12ft$ $\quad h_2 := 24ft$ $\quad h_3 := 36ft$

$w_1 := 2000kip$ $\quad w_2 := 2000kip$ $\quad w_3 := 2000kip$

$W := w_1 + w_2 + w_3$

$V := C_s \cdot W = 857.14 \cdot kip$

$$F_1 := \frac{V \cdot w_1 \cdot h_1}{w_1 \cdot h_1 + w_2 \cdot h_2 + w_3 \cdot h_3} = 142.857 \cdot kip$$

$$F_2 := \frac{V \cdot w_2 \cdot h_2}{w_1 \cdot h_1 + w_2 \cdot h_2 + w_3 \cdot h_3} = 285.714 \cdot kip$$

$$F_3 := \frac{V \cdot w_3 \cdot h_3}{w_1 \cdot h_1 + w_2 \cdot h_2 + w_3 \cdot h_3} = 428.571 \cdot kip$$

$V_1 := V = 857.143 \cdot kip$

$V_2 := V - F_1 = 714.286 \cdot kip$

$V_3 := V - F_1 - F_2 = 428.571 \cdot kip$

Plate Data:

Assumed angle of tension stress

$\alpha := 45deg$

$F_y := 36ksi$

$R_y := 1.3$

$L := 12ft$

$H := 12ft$

L_cf for a start assumed as 12” less than centerline distance between columns

$L_{cf} := L - 12in = 11\ ft$

$\phi := 0.9$

$$t_{www} := \frac{V}{\phi \cdot 0.42 \cdot F_y \cdot L_{cf} \cdot \sin(2 \cdot \alpha)} = 0.477 \cdot in$$

tw :=

	0	1	2	3	4
0	Thickness (in)"	0.313	0.375	0.438	0.5
1	"ϕV_n(kips)"	561.3	673.6	785.9	898.1

Taking plate thickness as

$t_{w1} := 0.5in$ $V_1 = 857.143 \cdot kip$ $\varphi Vn_1 := t_{w1} \cdot 0.42 \cdot F_y \cdot L_{cf} \cdot \sin(2 \cdot \alpha) \cdot 0.9 = 898.128 \cdot kip$

$t_{w2} := 0.4375in$ $V_2 = 714.286 \cdot kip$ $\varphi Vn_2 := t_{w2} \cdot 0.42 \cdot F_y \cdot L_{cf} \cdot \sin(2 \cdot \alpha) \cdot 0.9 = 785.862 \cdot kip$

$t_{w3} := 0.25in$ $V_3 = 428.571 \cdot kip$ $\varphi Vn_3 := t_{w3} \cdot 0.42 \cdot F_y \cdot L_{cf} \cdot \sin(2 \cdot \alpha) \cdot 0.9 = 449.064 \cdot kip$

For Boundary Elements

$F_{yy} := 50ksi$

$R_{yy} := 1.1$

Modulus of Elasticity

$E := 29000ksi$

First Floor

HBE Data

Trial Section HBE: W40x199

cross-sectional area of HBE

$A_b := 58.5in^2$

depth of HBE

$d_b := 38.7in$

flange width

$b_{fb} := 15.8in$

flange thickness

$t_{fb} := 1.07in$

web thickness

$t_{wb} := 0.65in$

Inertia of HBE

$I_b := 14900in^4$

Modulus of Plasticity

$Z_{xb} := 869in^3$

Radii of Gyration

$r_{yb} := 3.45in$

$r_{xb} := 16.0in$

Limiting unbraced length (AISC Table 3-2)

$L_{pb} := 12.2ft$

$L_{rb} := 34.3ft$

$Mp_{xb} := 3260kip\cdot ft$

$Mr_{xb} := 2020kip\cdot ft$

$Cb_b := 1.14$

VBE Data

Trial Section VBE: W40x431

cross-sectional area of VBE

$A_c := 127in^2$

depth of VBE

$d_c := 41.3in$

flange width

$b_{fc} := 16.2in$

flange thickness

$t_{fc} := 2.36in$

web thickness

$t_{wc} := 1.34in$

Inertia of VBE

$I_c := 34800in^4$

Modulus of Plasticity

$Z_{xc} := 1960in^3$

Radii of Gyration

$r_{yc} := 3.65in$

$r_{xc} := 16.6in$

Limiting unbraced length (AISC Table 3-2)

$L_{pc} := 12.9ft$

$L_{rc} := 49ft$

$Mp_{xc} := 7350kip\cdot ft$

$Mr_{xc} := 4440kip\cdot ft$

$Cb_c := 1.14$

Rechecking angle of tension stress

$$\alpha := \tan(\alpha_1)^4 = \frac{1 + \dfrac{t_{w1}\cdot L}{2\cdot A_c}}{1 + t_{w1}\cdot H\cdot\left(\dfrac{1}{A_b} + \dfrac{H^3}{360 I_c\cdot L}\right)} \text{ solve } \rightarrow \begin{bmatrix} \operatorname{atan}\left[\dfrac{3.4701000819561811999\cdot\sqrt{in}\cdot(2.362204724}{\left(1.0e19\cdot ft^3 + 1.4871794871794871795\right.}\right. \\ \operatorname{atan}\left[-\dfrac{3.4701000819561811999i\cdot\sqrt{in}\cdot(2.36220472}{\left(1.0e19\cdot ft^3 + 1.48717948717948717\right.}\right. \\ \operatorname{atan}\left[\dfrac{3.4701000819561811999i\cdot\sqrt{in}\cdot(2.362204724}{\left(1.0e19\cdot ft^3 + 1.4871794871794871795\right.}\right. \\ -1.0\cdot\operatorname{atan}\left[\dfrac{3.4701000819561811999\cdot\sqrt{in}\cdot(2.3622047}{\left(1.0e19\cdot ft^3 + 1.48717948717948717\right.}\right. \end{bmatrix}$$

$$\alpha = \begin{pmatrix} 40.685 \\ -74.031i \\ 74.031i \\ -40.685 \end{pmatrix}\cdot deg$$

$$\alpha := \alpha_0 = 40.685\cdot deg$$

Calculating horizontal and vertical component of loads from plate web considering full yielding

$$w_{yb} := R_y \cdot F_y \cdot \left(t_{w1} - t_{w2}\right) \cdot \cos(\alpha)^2 = 1.682 \cdot \frac{kip}{in}$$

$$w_{xb} := \frac{1}{2} \cdot R_y \cdot F_y \cdot \left(t_{w1} - t_{w2}\right) \cdot \sin(2\alpha) = 1.446 \cdot \frac{kip}{in}$$

$$w_{yc} := \frac{1}{2} \cdot R_y \cdot F_y \cdot \left(t_{w1} - t_{w2}\right) \cdot \sin(2 \cdot \alpha) = 1.446 \cdot \frac{kip}{in}$$

$$w_{xc} := R_y \cdot F_y \cdot \left(t_{w1} - t_{w2}\right) \cdot \sin(\alpha)^2 = 1.243 \cdot \frac{kip}{in}$$

Design of HBE

Design Moment

$$L_{cf} := L - d_c = 102.7 \cdot in$$

$$M_u := w_{yb} \cdot \frac{L_{cf}^2}{4} = 4435.056 \cdot kip \cdot in$$

Preliminiary Sizing of HBE:

$$h_{0b} := d_b - t_{fb} = 37.63 \cdot in$$

$$A_{fb} := \begin{array}{|l} b_{fb} \cdot t_{fb} \ \text{ if } \ \dfrac{M_u}{0.9 \cdot h_{0b} \cdot F_{yy}} < b_{fb} \cdot t_{fb} \\ \text{"Resize"} \ \text{ otherwise} \end{array} = 16.906 \cdot in^2$$

Preliminiary HBE Size OK

Axial Force in HBE:

distance between HBE centerlines

$h := 12ft$

$h_c := h - \frac{1}{2} \cdot d_b = 10.387\, ft$

$P_{HBEvbe} := \frac{1}{2} \cdot R_y \cdot F_y \cdot \sin(\alpha)^2 \cdot (t_{w1} + t_{w2}) \cdot h_c = 1162.078 \cdot kip$

$P_{HBEweb} := R_y \cdot F_y \cdot (t_{w1} + t_{w2}) \cdot L_{cf} \cdot \sin(\alpha)^2 = 1914.888 \cdot kip$

$P_{HBEL} := P_{HBEvbe} + \frac{1}{2} P_{HBEweb} = 2119.522 \cdot kip$

$P_{HBER} := P_{HBEvbe} - \frac{1}{2} P_{HBEweb} = 204.634 \cdot kip$

$P_u := \max(P_{HBEL}, P_{HBER}) = 2119.522 \cdot kip$

AISC 341-16 Table D1.1

$P_y := A_b \cdot R_{yy} \cdot F_{yy} = 3217.5 \cdot kip$

Shear Force in HBE:

$V_{uWebL} := \frac{w_{yb} \cdot L_{cf} + w_{xb} \cdot d_b}{2} = 114.348 \cdot kip$

$V_{uWebR} := \frac{w_{yb} \cdot L_{cf} - w_{xb} \cdot d_b}{2} = 58.39 \cdot kip$

$V_{uWeb} := \max(V_{uWebR}, V_{uWebL}) = 114.348 \cdot kip$

$V_g := 0kip$

Reduced Probable flexural strength

Left side

$$M_{pr\_reduced\_L} := \begin{cases} \left(1.1 \cdot R_{yy} \cdot F_{yy} \cdot Z_{xb}\right) \cdot \left(1 - 0.5 \cdot \dfrac{P_{HBEL}}{P_y}\right) & \text{if } \dfrac{P_{HBEL}}{P_y} < 0.2 \\ \dfrac{9}{8} \cdot \left(1.1 \cdot R_{yy} \cdot F_{yy} \cdot Z_{xb}\right) \cdot \left(1 - \dfrac{P_{HBEL}}{P_y}\right) & \text{otherwise} \end{cases} = 20183.798 \cdot kip \cdot in$$

Right side

$$M_{pr\_reduced\_R} := \begin{cases} \left(1.1 \cdot R_{yy} \cdot F_{yy} \cdot Z_{xb}\right) \cdot \left(1 - 0.5 \cdot \dfrac{P_{HBER}}{P_y}\right) & \text{if } \dfrac{P_{HBER}}{P_y} < 0.2 \\ \dfrac{9}{8} \cdot \left(1.1 \cdot R_{yy} \cdot F_{yy} \cdot Z_{xb}\right) \cdot \left(1 - \dfrac{P_{HBER}}{P_y}\right) & \text{otherwise} \end{cases} = 50902.624 \cdot kip \cdot in$$

$$V_{uHBE} := \frac{\left(M_{pr\_reduced\_L} + M_{pr\_reduced\_R}\right)}{L_{cf}} = 692.175 \cdot kip$$

$$V_{HBE} := V_{uWeb} + V_g + V_{uHBE} = 806.524 \cdot kip$$

Checks:

1. Check Shear Strength

$$\text{shearcheck1} := \begin{cases} \text{"}\phi\text{v=1"} & \text{if } \dfrac{d_b - 2 \cdot t_{fb}}{t_{wb}} < 2.24 \cdot \sqrt{\dfrac{E}{R_{yy} \cdot F_{yy}}} \\ \text{"no"} & \text{otherwise} \end{cases} = \text{"no"}$$

$$A_w := \left(d_b - 2 \cdot t_{fb}\right) \cdot t_{wb} = 23.764 \cdot in^2$$

$$\varphi Vn_b := 1.0 \cdot 0.6 \cdot R_{yy} \cdot F_{yy} \cdot A_w = 784.212 \cdot kip$$

$$V_u := V_{HBE} = 806.524 \cdot kip$$

$$\varphi Vn_b = 784.212 \cdot kip$$

$$\text{shearcheck2} := \begin{cases} \text{"Ok"} & \text{if } \varphi Vn_b > V_u \\ \text{"No"} & \text{otherwise} \end{cases} = \text{"No"}$$

2. Check Combined Compression and Flexure

$K := 1$

$$axisbuckling := \begin{cases} \text{"Major axis buckling controls"} & \text{if } \frac{K \cdot L}{r_{xb}} > \frac{K \cdot L}{r_{yb}} \\ \text{"Minor axis buckling controls"} & \text{otherwise} \end{cases} = \text{"Minor axis buckling controls"}$$

$$\frac{K \cdot L}{r_{xb}} = 9$$

$$\frac{K \cdot L}{r_{yb}} = 41.74$$

$$slenderness := \begin{cases} \frac{K \cdot L}{r_{yb}} & \text{if } axisbuckling = \text{"Minor axis buckling controls"} \\ \frac{K \cdot L}{r_{xb}} & \text{otherwise} \end{cases} = 41.739$$

$$F_e := \frac{\pi^2 \cdot E}{(slenderness)^2} = 164.29 \cdot ksi$$

$$0.44 \cdot R_{yy} \cdot F_{yy} = 24.2 \cdot ksi$$

$$checkE32 := \begin{cases} \text{"Use E3-2"} & \text{if } \frac{\pi^2 \cdot E}{(slenderness)^2} > 0.44 \cdot F_{yy} \\ \text{"Dont use E3-2"} & \text{otherwise} \end{cases} = \text{"Use E3-2"}$$

Using AISC 360 Equation E3-2

$$F_{cr} := 0.658^{\frac{R_{yy} \cdot F_{yy}}{F_e}} \cdot R_{yy} \cdot F_{yy} = 47.809 \cdot ksi$$

$$\varphi Pn_b := 0.9 \cdot F_{cr} \cdot A_b = 2517.143 \cdot kip$$

$$P_c := \varphi Pn_b$$

$$P_r := P_u$$

$$L_{pb} = 12.2 \cdot ft$$

$$L_b := L = 12\,ft$$

$$Mp_{xb} = 39120 \cdot kip \cdot in$$

$$\varphi Mn_b := \begin{cases} Mp_{xb} & \text{if } Mp_{xb} < Cb_b \cdot \left[Mp_{xb} - \left(Mp_{xb} - Mr_{xb}\right) \cdot \left(\dfrac{L_b - L_{pb}}{L_{rb} - L_{pb}} \right) \right] \\ Cb_b \cdot \left[Mp_{xb} - \left(Mp_{xb} - Mr_{xb}\right) \cdot \left(\dfrac{L_b - L_{pb}}{L_{rb} - L_{pb}} \right) \right] & \text{otherwise} \end{cases} = 39120 \cdot kip \cdot in$$

$$\frac{P_r}{P_c} = 0.842$$

$$CombinedCheckEq := \begin{cases} \text{"Use Equation H1-1a"} & \text{if } \dfrac{P_r}{P_c} \ge 0.2 \\ \text{"Use Equation H1-1b"} & \text{otherwise} \end{cases} = \text{"Use Equation H1-1a"}$$

AISC 360-10 Equation H1-1a

$$CombinedCheck := \begin{cases} \text{"Ok"} & \text{if } 1 > \dfrac{P_r}{P_c} + \dfrac{8}{9}\left(\dfrac{M_u}{\varphi Mn_b}\right) \\ \text{"No"} & \text{otherwise} \end{cases} = \text{"Ok"}$$

3. Check moment of inertia

$$I_{required} := \frac{0.003 \cdot t_{w1} \cdot L^4}{h} = 4478.976 \cdot in^4$$

$$I_b = 14900 \cdot in^4$$

$$InertiaCheck := \begin{cases} \text{"Ok"} & \text{if } I_b > I_{required} \\ \text{"No"} & \text{otherwise} \end{cases} = \text{"Ok"}$$

4. Check Web thickness

$$t_{wb} = 0.65 \cdot in$$

$$\frac{t_{w1} \cdot R_y \cdot F_y}{F_{yy}} = 0.468 \cdot in$$

$$WebCheck := \begin{cases} \text{"Ok"} & \text{if } t_{wb} > \dfrac{t_{w1} \cdot R_y \cdot F_y}{F_{yy}} \\ \text{"No"} & \text{otherwise} \end{cases} = \text{"Ok"}$$

Design of VBE

(there are no adjoining beams)

$$M_{pradj} := 0$$

$$M_{prc} := 1.1 \cdot R_{yy} \cdot F_{yy} \cdot Z_{xc} = 1.186 \times 10^{5} \cdot kip \cdot in$$

$$L_h := H - d_b = 105.3 \cdot in$$

Resulting compressive force

$$E_{mcomp} := \frac{1}{2} \cdot R_y \cdot F_y \cdot \sin(2 \cdot \alpha) \cdot \left(t_{w1} + t_{w2}\right) \cdot h_c + \left(V_{uHBE} + \frac{w_{yb} \cdot L_{cf}}{2}\right) - \left(2 \cdot \frac{M_{pradj}}{L_h}\right) = 3482.089 \cdot kip$$

$$P_{gravity} := 0 kip$$

$$P_{uc} := E_{mcomp} + P_{gravity} = 3482.089 \cdot kip$$

$$L_c := h$$

Resulting tension force

$$E_{mtens} := \frac{1}{2} \cdot R_y \cdot F_y \cdot \sin(2 \cdot \alpha) \cdot \left(t_{w1} + t_{w2}\right) \cdot h_c + \left(V_{uHBE} - \frac{w_{yb} \cdot L_{cf}}{2}\right) - \left(2 \cdot \frac{M_{pradj}}{L_h}\right) = 3309.351 \cdot kip$$

Flexure from web tension

$$M_{VBEweb} := w_{xc} \cdot \frac{\left(h_c^{\ 2}\right)}{12} = 1609.478 \cdot kip \cdot in$$

Flexure from VBE compression

$$M_{pr} := \max\left(M_{pr\_reduced\_L}, M_{pr\_reduced\_R}\right) = 50902.624 \cdot kip \cdot in$$

$$M_{pb} := \frac{M_{pr}}{1.1 \cdot R_{yy}} + V_u \cdot \left[\frac{1}{2} \cdot \left(d_b + d_c\right)\right] = 74329.227 \cdot kip \cdot in$$

$$M_{VBEhbe} := \frac{1}{2} \cdot M_{pb} = 37164.613 \cdot kip \cdot in$$

$$M_{uc} := M_{VBEweb} + M_{VBEhbe} = 38774.091 \cdot kip \cdot in$$

Moment magnification

$$P_{ec} := \frac{\pi^2 \cdot E \cdot I_c}{\left(K \cdot L_c\right)^2} = 4.803 \times 10^5 \cdot kip$$

$$C_m := 1.0$$

$$B_{1c} := \frac{C_m}{1 - \frac{P_{uc}}{P_{ec}}} = 1.007$$

$$P_{rc} := P_{uc} = 3482.089 \cdot kip$$

$$M_{rc} := B_{1c} \cdot M_{uc} = 39057.223 \cdot kip \cdot in$$

Shear in the VBE is the sum of the effect of web tension and the portion of shear not resisted by the web plate

Shear from web plate

$$V_{VBEweb} := \frac{1}{2} \cdot R_y \cdot F_y \cdot \sin(\alpha) \cdot \left(t_{w1} - t_{w2}\right) \cdot h_c = 118.841 \cdot kip$$

Shear from HBE Hinging

$$M_{pc} := M_{VBEhbe} + M_{uc} = 75938.705 \cdot kip \cdot in$$

$$V_{VBEhbe} := \frac{1}{2} \cdot \left(\frac{M_{pc}}{h_c}\right) = 304.608 \cdot kip$$

Shear from horizontal element

$$V_{uc} := V_{VBEweb} + V_{VBEhbe} = 423.449 \cdot kip$$

Design Checks

1. Check Compactness

AISC 341-16 Table D1.1

$$flange_c := \begin{cases} \text{"Ok"} & \text{if } \frac{b_{fc}}{2 \cdot t_{fc}} < 0.32 \cdot \sqrt{\frac{E}{R_{yy} \cdot F_{yy}}} \\ \text{"No"} & \text{otherwise} \end{cases} = \text{"Ok"}$$

$$\frac{b_{fc}}{2 \cdot t_{fc}} = 3.432$$

$$0.32 \cdot \sqrt{\frac{E}{R_{yy} \cdot F_{yy}}} = 7.348$$

Flange is compact

$$C_{ac} := \frac{P_{uc}}{0.9 \cdot F_{yy} \cdot R_{yy} \cdot A_c} = 0.554$$

$$web_c := \begin{cases} \text{"Ok"} & \text{if } \dfrac{d_c - 2 \cdot t_{fc}}{t_{wc}} < 0.88 \cdot \sqrt{\dfrac{E}{R_{yy} \cdot F_{yy}}} \cdot (2.68 - C_{ac}) \\ \text{"No"} & \text{otherwise} \end{cases} = \text{"Ok"}$$

$$web_c := \begin{cases} \text{"Ok"} & \text{if } 0.88 \cdot \sqrt{\dfrac{E}{R_{yy} \cdot F_{yy}}} \cdot (2.68 - C_{ac}) > 1.57 \cdot \sqrt{\dfrac{E}{R_{yy} \cdot F_{yy}}} \\ \text{"No"} & \text{otherwise} \end{cases} = \text{"Ok"}$$

$$\frac{d_c - 2 \cdot t_{fc}}{t_{wc}} = 27.299$$

$$0.88 \cdot \sqrt{\frac{E}{R_{yy} \cdot F_{yy}}} \cdot (2.68 - C_{ac}) = 42.962$$

$$1.57 \cdot \sqrt{\frac{E}{R_{yy} \cdot F_{yy}}} = 36.051$$

Web is compact

2. Check Shear Strength

$$\varphi check := \begin{cases} \text{"}\phi\text{=1"} & \text{if } \dfrac{d_c - 2 \cdot t_{fc}}{t_{wc}} < 2.24 \cdot \sqrt{\dfrac{E}{R_{yy} \cdot F_{yy}}} \\ \text{"No"} & \text{otherwise} \end{cases} = \text{"}\phi\text{=1"}$$

$$\varphi_{vc} := 1$$

$$\varphi Vn_c := \varphi_{vc} \cdot 0.6 \cdot R_{yy} \cdot F_{yy} \cdot (d_c - 2 \cdot t_{fc}) \cdot t_{wc} = 1617.568 \cdot kip$$

$$V_{uc} = 423.449 \cdot kip$$

$$shear := \begin{cases} \text{"Ok"} & \text{if } V_{uc} < \varphi Vn_c \\ \text{"No"} & \text{otherwise} \end{cases} = \text{"Ok"}$$

3. Check Combined Compression and Flexure

$$\text{slenderness}_c := \frac{K \cdot L}{r_{yc}}$$

$$F_{ec} := \frac{\pi^2 \cdot E}{\text{slenderness}_c^{\,2}}$$

$$0.44 \cdot R_{yy} \cdot F_{yy} = 24.2 \cdot \text{ksi}$$

$$\text{checkE32}_c := \begin{cases} \text{"Use E3-2"} & \text{if } \dfrac{\pi^2 \cdot E}{\left(\text{slenderness}_c\right)^2} > 0.44 \cdot R_{yy} \cdot F_{yy} \\ \text{"Dont use E3-2"} & \text{otherwise} \end{cases} = \text{"Use E3-2"}$$

Using AISC 360-10 Equation E3-2

$$F_{crc} := 0.658^{\frac{R_{yy} \cdot F_{yy}}{F_{ec}}} \cdot R_{yy} \cdot F_{yy} = 48.528 \cdot \text{ksi}$$

$$\varphi Pn_c := 0.9 \cdot F_{crc} \cdot A_c = 5546.791 \cdot \text{kip}$$

$$P_{cc} := \varphi Pn_c$$

$$L_{bc} := h_c = 10.387 \cdot \text{ft}$$

$$L_{pc} = 12.9 \cdot \text{ft}$$

there is no lateral torsional buckling

$$M_c := 0.9 \cdot R_{yy} \cdot F_{yy} \cdot Z_{xc} = 8085 \cdot \text{kip} \cdot \text{ft}$$

$$\frac{M_{rc}}{M_c} = 0.403$$

$$\frac{P_{rc}}{P_{cc}} = 0.628$$

$$\text{CombinedCheckEq}_c := \begin{cases} \text{"Use Equation H1-1a"} & \text{if } \dfrac{P_{rc}}{P_{cc}} \geq 0.2 \\ \text{"Use Equation H1-1b"} & \text{otherwise} \end{cases} = \text{"Use Equation H1-1a"}$$

Use AISC 360-10 Eq H1-1a

$$\text{CombinedCheck}_c := \begin{cases} \text{"Ok"} & \text{if } 1 > \dfrac{P_{rc}}{P_{cc}} + \dfrac{8}{9}\left(\dfrac{M_{rc}}{M_c}\right) \\ \text{"No"} & \text{otherwise} \end{cases} = \text{"Ok"}$$

Second Floor

HBE Data

Trial Section HBE: W40x199

cross-sectional area of HBE

$A_b := 58.5in^2$

depth of HBE

$d_b := 38.7in$

flange width

$b_{fb} := 15.8in$

flange thickness

$t_{fb} := 1.07in$

web thickness

$t_{wb} := 0.65in$

Inertia of HBE

$I_b := 14900in^4$

Modulus of Plasticity

$Z_{xb} := 869in^3$

Radii of Gyration

$r_{yb} := 3.45in$

$r_{xb} := 16in$

Limiting unbraced length (AISC Table 3-2)

$L_{pb} := 12.2ft$

$L_{rb} := 34.3ft$

$Mp_{xb} := 3260kip \cdot ft$

$Mr_{xb} := 2020kip \cdot ft$

$Cb_b := 1.14$

VBE Data

Trial Section VBE: W40x431

cross-sectional area of VBE

$A_c := 107in^2$

depth of VBE

$d_c := 40.6in$

flange width

$b_{fc} := 16in$

flange thickness

$t_{fc} := 2.01in$

web thickness

$t_{wc} := 1.12in$

Inertia of VBE

$I_c := 28900in^4$

Modulus of Plasticity

$Z_{xc} := 1640in^3$

Radii of Gyration

$r_{yc} := 3.60in$

$r_{xc} := 16.5in$

Limiting unbraced length (AISC Table 3-2)

$L_{pc} := 12.7ft$

$L_{rc} := 44ft$

$Mp_{xc} := 6150kip \cdot ft$

$Mr_{xc} := 3730kip \cdot ft$

$Cb_c := 1.14$

Rechecking angle of tension stress

$$\alpha := \tan(\alpha_1)^4 = \frac{1 + \dfrac{t_{w2} \cdot L}{2 \cdot A_c}}{1 + t_{w2} \cdot H \cdot \left(\dfrac{1}{A_b} + \dfrac{H^3}{360 I_c \cdot L}\right)} \text{ solve } \rightarrow \begin{bmatrix} \operatorname{atan}\left[\dfrac{5.8309518948453004709 \cdot \sqrt{in} \cdot (2.453271028}{(8.4e20 \cdot ft^3 + 1.037435897435897435 9}\right. \\ \operatorname{atan}\left[-\dfrac{5.8309518948453004709i \cdot \sqrt{in} \cdot (2.45327102}{(8.4e20 \cdot ft^3 + 1.037435897435897435 9}\right. \\ \operatorname{atan}\left[\dfrac{5.8309518948453004709i \cdot \sqrt{in} \cdot (2.453271028}{(8.4e20 \cdot ft^3 + 1.037435897435897435 9}\right. \\ -1.0 \cdot \operatorname{atan}\left[\dfrac{5.8309518948453004709 \cdot \sqrt{in} \cdot (2.4532710}{(8.4e20 \cdot ft^3 + 1.03743589743589743}\right. \end{bmatrix}$$

$$\alpha = \begin{pmatrix} 41.204 \\ -77.718i \\ 77.718i \\ -41.204 \end{pmatrix} \cdot deg$$

$$\alpha := \alpha_0 = 41.204 \cdot deg$$

Calculating horizontal and vertical component of loads from plate web considering full yielding

$$w_{yb} := R_y \cdot F_y \cdot (t_{w2} - t_{w3}) \cdot \cos(\alpha)^2 = 4.967 \cdot \frac{kip}{in}$$

$$w_{xb} := \frac{1}{2} \cdot R_y \cdot F_y \cdot (t_{w2} - t_{w3}) \cdot \sin(2\alpha) = 4.349 \cdot \frac{kip}{in}$$

$$w_{yc} := \frac{1}{2} \cdot R_y \cdot F_y \cdot (t_{w2} - t_{w3}) \cdot \sin(2 \cdot \alpha) = 4.349 \cdot \frac{kip}{in}$$

$$w_{xc} := R_y \cdot F_y \cdot (t_{w2} - t_{w3}) \cdot \sin(\alpha)^2 = 3.808 \cdot \frac{kip}{in}$$

Design of HBE

Design Moment

$$L_{cf} := L - d_c = 103.4 \cdot in$$

$$M_u := w_{yb} \cdot \frac{L_{cf}^2}{4} = 13276.596 \cdot kip \cdot in$$

Preliminiary Sizing of HBE:

$$h_{0b} := d_b - t_{fb} = 37.63 \cdot in$$

$$A_{fb} := \left| \begin{array}{ll} b_{fb} \cdot t_{fb} & \text{if } \dfrac{M_u}{0.9 \cdot h_{0b} \cdot F_{yy}} < b_{fb} \cdot t_{fb} \\ \text{"Resize"} & \text{otherwise} \end{array} \right. = 16.906 \cdot in^2$$

Preliminiary HBE Size OK

Axial Force in HBE:

distance between HBE centerlines

$h := 12ft$

$h_c := h - \frac{1}{2} \cdot d_b = 10.387\ ft$

$P_{HBEvbe} := \frac{1}{2} \cdot R_y \cdot F_y \cdot \sin(\alpha)^2 \cdot (t_{w2} + t_{w3}) \cdot h_c = 870.193 \cdot kip$

$P_{HBEweb} := R_y \cdot F_y \cdot (t_{w2} + t_{w3}) \cdot L_{cf} \cdot \sin(\alpha)^2 = 1443.69 \cdot kip$

$P_{HBEL} := P_{HBEvbe} + \frac{1}{2} P_{HBEweb} = 1592.038 \cdot kip$

$P_{HBER} := P_{HBEvbe} - \frac{1}{2} P_{HBEweb} = 148.348 \cdot kip$

$P_u := \max(P_{HBEL}, P_{HBER}) = 1592.038 \cdot kip$

AISC 341-16 Table D1.1

$P_y := A_b \cdot R_{yy} \cdot F_{yy} = 3217.5 \cdot kip$

Shear Force in HBE:

$V_{uWebL} := \frac{w_{yb} \cdot L_{cf} + w_{xb} \cdot d_b}{2} = 340.955 \cdot kip$

$V_{uWebR} := \frac{w_{yb} \cdot L_{cf} - w_{xb} \cdot d_b}{2} = 172.647 \cdot kip$

$V_{uWeb} := \max(V_{uWebR}, V_{uWebL}) = 340.955 \cdot kip$

$V_g := 0kip$

Reduced Probable flexural strength

Left side

$$M_{pr\_reduced\_L} := \begin{cases} (1.1 \cdot R_{yy} \cdot F_{yy} \cdot Z_{xb}) \cdot \left(1 - 0.5 \cdot \frac{P_{HBEL}}{P_y}\right) & \text{if } \frac{P_{HBEL}}{P_y} < 0.2 \\ \frac{9}{8} \cdot (1.1 \cdot R_{yy} \cdot F_{yy} \cdot Z_{xb}) \cdot \left(1 - \frac{P_{HBEL}}{P_y}\right) & \text{otherwise} \end{cases} = 29880.365 \cdot kip \cdot in$$

Right side

$$M_{pr\_reduced\_R} := \begin{cases} (1.1 \cdot R_{yy} \cdot F_{yy} \cdot Z_{xb}) \cdot \left(1 - 0.5 \cdot \frac{P_{HBER}}{P_y}\right) & \text{if } \frac{P_{HBER}}{P_y} < 0.2 \\ \frac{9}{8} \cdot (1.1 \cdot R_{yy} \cdot F_{yy} \cdot Z_{xb}) \cdot \left(1 - \frac{P_{HBER}}{P_y}\right) & \text{otherwise} \end{cases} = 51362.482 \cdot kip \cdot in$$

$$V_{uHBE} := \frac{(M_{pr\_reduced\_L} + M_{pr\_reduced\_R})}{L_{cf}} = 785.714 \cdot kip$$

$$V_{HBE} := V_{uWeb} + V_g + V_{uHBE} = 1126.669 \cdot kip$$

Checks:

1. Check Shear Strength

$$shearcheck1 := \begin{cases} \text{"}\phi v=1\text{"} & \text{if } \frac{d_b - 2 \cdot t_{fb}}{t_{wb}} < 2.24 \cdot \sqrt{\frac{E}{R_{yy} \cdot F_{yy}}} \\ \text{"no"} & \text{otherwise} \end{cases} = \text{"no"}$$

$$A_w := (d_b - 2 \cdot t_{fb}) \cdot t_{wb} = 23.764 \cdot in^2$$

$$\varphi Vn_b := 1.0 \cdot 0.6 \cdot R_{yy} \cdot F_{yy} \cdot A_w = 784.212 \cdot kip$$

$$V_u := V_{HBE} = 1126.669 \cdot kip$$

$$\varphi Vn_b = 784.212 \cdot kip$$

$$shearcheck2 := \begin{cases} \text{"Ok"} & \text{if } \varphi Vn_b > V_u \\ \text{"No"} & \text{otherwise} \end{cases} = \text{"No"}$$

2. Check Combined Compression and Flexure

$K := 1$

$$axisbuckling := \begin{cases} \text{"Major axis buckling controls"} & \text{if } \frac{K \cdot L}{r_{xb}} > \frac{K \cdot L}{r_{yb}} \\ \text{"Minor axis buckling controls"} & \text{otherwise} \end{cases} = \text{"Minor axis buckling controls"}$$

$$\frac{K \cdot L}{r_{xb}} = 9$$

$$\frac{K \cdot L}{r_{yb}} = 41.74$$

$$slenderness := \begin{cases} \frac{K \cdot L}{r_{yb}} & \text{if axisbuckling} = \text{"Minor axis buckling controls"} \\ \frac{K \cdot L}{r_{xb}} & \text{otherwise} \end{cases} = 41.739$$

$$F_e := \frac{\pi^2 \cdot E}{(slenderness)^2} = 164.29 \cdot ksi$$

$$0.44 \cdot R_{yy} \cdot F_{yy} = 24.2 \cdot ksi$$

$$checkE32 := \begin{cases} \text{"Use E3-2"} & \text{if } \frac{\pi^2 \cdot E}{(slenderness)^2} > 0.44 \cdot F_{yy} \\ \text{"Dont use E3-2"} & \text{otherwise} \end{cases} = \text{"Use E3-2"}$$

Using AISC 360 Equation E3-2

$$F_{cr} := 0.658^{\frac{R_{yy} \cdot F_{yy}}{F_e}} \cdot R_{yy} \cdot F_{yy} = 47.809 \cdot ksi$$

$$\varphi Pn_b := 0.9 \cdot F_{cr} \cdot A_b = 2517.143 \cdot kip$$

$$P_c := \varphi Pn_b$$

$$P_r := P_u$$

$$L_{pb} = 12.2 \cdot ft$$

$$L_b := L = 12\,ft$$

$$Mp_{xb} = 39120 \cdot kip \cdot in$$

$$\varphi Mn_b := \begin{cases} Mp_{xb} & \text{if } Mp_{xb} < Cb_b \cdot \left[Mp_{xb} - (Mp_{xb} - Mr_{xb}) \cdot \left(\dfrac{L_b - L_{pb}}{L_{rb} - L_{pb}} \right) \right] \\ Cb_b \cdot \left[Mp_{xb} - (Mp_{xb} - Mr_{xb}) \cdot \left(\dfrac{L_b - L_{pb}}{L_{rb} - L_{pb}} \right) \right] & \text{otherwise} \end{cases} = 39120 \cdot kip \cdot in$$

$$\frac{P_r}{P_c} = 0.632$$

$$CombinedCheckEq := \begin{cases} \text{"Use Equation H1-1a"} & \text{if } \dfrac{P_r}{P_c} \geq 0.2 \\ \text{"Use Equation H1-1b"} & \text{otherwise} \end{cases} = \text{"Use Equation H1-1a"}$$

AISC 360-10 Equation H1-1a

$$CombinedCheck := \begin{cases} \text{"Ok"} & \text{if } 1 > \dfrac{P_r}{P_c} + \dfrac{8}{9}\left(\dfrac{M_u}{\varphi Mn_b} \right) \\ \text{"No"} & \text{otherwise} \end{cases} = \text{"Ok"}$$

3. Check moment of inertia

$$I_{required} := \frac{0.003 \cdot t_{w2} \cdot L^4}{h} = 3919.104 \cdot in^4$$

$$I_b = 14900 \cdot in^4$$

$$InertiaCheck := \begin{cases} \text{"Ok"} & \text{if } I_b > I_{required} \\ \text{"No"} & \text{otherwise} \end{cases} = \text{"Ok"}$$

4. Check Web thickness

$$t_{wb} = 0.65 \cdot in$$

$$\frac{t_{w2} \cdot R_y \cdot F_y}{F_{yy}} = 0.409 \cdot in$$

$$WebCheck := \begin{cases} \text{"Ok"} & \text{if } t_{wb} > \dfrac{t_{w2} \cdot R_y \cdot F_y}{F_{yy}} \\ \text{"No"} & \text{otherwise} \end{cases} = \text{"Ok"}$$

Design of VBE

(there are no adjoining beams)

$M_{pradj} := 0$

$M_{prc} := 1.1 \cdot R_{yy} \cdot F_{yy} \cdot Z_{xc} = 99220 \cdot kip \cdot in$

$L_h := H - d_b = 105.3 \cdot in$

Resulting compressive force

$$E_{mcomp} := \frac{1}{2} \cdot R_y \cdot F_y \cdot \sin(2 \cdot \alpha) \cdot \left(t_{w2} + t_{w3}\right) \cdot h_c + \left(V_{uHBE} + \frac{w_{yb} \cdot L_{cf}}{2}\right) - \left(2 \cdot \frac{M_{pradj}}{L_h}\right) = 3030.245 \cdot kip$$

$P_{gravity} := 0kip$

$P_{uc} := E_{mcomp} + P_{gravity} = 3030.245 \cdot kip$

$L_c := h$

Resulting tension force

$$E_{mtens} := \frac{1}{2} \cdot R_y \cdot F_y \cdot \sin(2 \cdot \alpha) \cdot \left(t_{w2} + t_{w3}\right) \cdot h_c + \left(V_{uHBE} - \frac{w_{yb} \cdot L_{cf}}{2}\right) - \left(2 \cdot \frac{M_{pradj}}{L_h}\right) = 2516.644 \cdot kip$$

Flexure from web tension

$$M_{VBEweb} := w_{xc} \cdot \frac{\left(h_c^{\,2}\right)}{12} = 4930.435 \cdot kip \cdot in$$

Flexure from VBE compression

$M_{pr} := \max\left(M_{pr\_reduced\_L}, M_{pr\_reduced\_R}\right) = 51362.482 \cdot kip \cdot in$

$$M_{pb} := \frac{M_{pr}}{1.1 \cdot R_{yy}} + V_u \cdot \left[\frac{1}{2} \cdot \left(d_b + d_c\right)\right] = 87120.754 \cdot kip \cdot in$$

$$M_{VBEhbe} := \frac{1}{2} \cdot M_{pb} = 43560.377 \cdot kip \cdot in$$

$M_{uc} := M_{VBEweb} + M_{VBEhbe} = 48490.812 \cdot kip \cdot in$

Moment magnification

$$P_{ec} := \frac{\pi^2 \cdot E \cdot I_c}{(K \cdot L_c)^2} = 3.989 \times 10^5 \cdot kip$$

$$C_m := 1.0$$

$$B_{1c} := \frac{C_m}{1 - \frac{P_{uc}}{P_{ec}}} = 1.008$$

$$P_{rc} := P_{uc} = 3030.245 \cdot kip$$

$$M_{rc} := B_{1c} \cdot M_{uc} = 48861.987 \cdot kip \cdot in$$

Shear in the VBE is the sum of the effect of web tension and the portion of shear not resisted by the web plate

Shear from web plate

$$V_{VBEweb} := \frac{1}{2} \cdot R_y \cdot F_y \cdot \sin(\alpha) \cdot \left(t_{w2} - t_{w3}\right) \cdot h_c = 360.269 \cdot kip$$

Shear from HBE Hinging

$$M_{pc} := M_{VBEhbe} + M_{uc} = 92051.189 \cdot kip \cdot in$$

$$V_{VBEhbe} := \frac{1}{2} \cdot \left(\frac{M_{pc}}{h_c}\right) = 369.239 \cdot kip$$

Shear from horizontal element

$$V_{uc} := V_{VBEweb} + V_{VBEhbe} = 729.508 \cdot kip$$

Design Checks

1. Check Compactness

AISC 341-16 Table D1.1

$$flange_c := \begin{cases} \text{"Ok"} & \text{if } \frac{b_{fc}}{2 \cdot t_{fc}} < 0.32 \cdot \sqrt{\frac{E}{R_{yy} \cdot F_{yy}}} \\ \text{"No"} & \text{otherwise} \end{cases} = \text{"Ok"}$$

$$\frac{b_{fc}}{2 \cdot t_{fc}} = 3.98$$

$$0.32 \cdot \sqrt{\frac{E}{R_{yy} \cdot F_{yy}}} = 7.348$$

Flange is compact

$$C_{ac} := \frac{P_{uc}}{0.9 \cdot F_{yy} \cdot R_{yy} \cdot A_c} = 0.572$$

$$web_c := \begin{vmatrix} \text{"Ok"} & \text{if } \dfrac{d_c - 2 \cdot t_{fc}}{t_{wc}} < 0.88 \cdot \sqrt{\dfrac{E}{R_{yy} \cdot F_{yy}}} \cdot (2.68 - C_{ac}) \\ \text{"No"} & \text{otherwise} \end{vmatrix} = \text{"Ok"}$$

$$web_c := \begin{vmatrix} \text{"Ok"} & \text{if } 0.88 \cdot \sqrt{\dfrac{E}{R_{yy} \cdot F_{yy}}} \cdot (2.68 - C_{ac}) > 1.57 \cdot \sqrt{\dfrac{E}{R_{yy} \cdot F_{yy}}} \\ \text{"No"} & \text{otherwise} \end{vmatrix} = \text{"Ok"}$$

$$\frac{d_c - 2 \cdot t_{fc}}{t_{wc}} = 32.661$$

$$0.88 \cdot \sqrt{\frac{E}{R_{yy} \cdot F_{yy}}} \cdot (2.68 - C_{ac}) = 42.594$$

$$1.57 \cdot \sqrt{\frac{E}{R_{yy} \cdot F_{yy}}} = 36.051$$

Web is compact

2. Check Shear Strength

$$\varphi check := \begin{vmatrix} \text{"}\phi\text{=1"} & \text{if } \dfrac{d_c - 2 \cdot t_{fc}}{t_{wc}} < 2.24 \cdot \sqrt{\dfrac{E}{R_{yy} \cdot F_{yy}}} \\ \text{"No"} & \text{otherwise} \end{vmatrix} = \text{"}\phi\text{=1"}$$

$$\varphi_{vc} := 1$$

$$\varphi Vn_c := \varphi_{vc} \cdot 0.6 \cdot R_{yy} \cdot F_{yy} \cdot (d_c - 2 \cdot t_{fc}) \cdot t_{wc} = 1351.997 \cdot kip$$

$$V_{uc} = 729.508 \cdot kip$$

$$shear := \begin{vmatrix} \text{"Ok"} & \text{if } V_{uc} < \varphi Vn_c \\ \text{"No"} & \text{otherwise} \end{vmatrix} = \text{"Ok"}$$

3. Check Combined Compression and Flexure

$$slenderness_c := \frac{K \cdot L}{r_{yc}}$$

$$F_{ec} := \frac{\pi^2 \cdot E}{slenderness_c^{\,2}}$$

$$0.44 \cdot R_{yy} \cdot F_{yy} = 24.2 \cdot ksi$$

$$checkE32_c := \begin{cases} \text{"Use E3-2"} & \text{if } \dfrac{\pi^2 \cdot E}{\left(slenderness_c\right)^2} > 0.44 \cdot R_{yy} \cdot F_{yy} \\ \text{"Dont use E3-2"} & \text{otherwise} \end{cases} = \text{"Use E3-2"}$$

Using AISC 360-10 Equation E3-2

$$F_{crc} := 0.658^{\frac{R_{yy} \cdot F_{yy}}{F_{ec}}} \cdot R_{yy} \cdot F_{yy} = 48.359 \cdot ksi$$

$$\varphi Pn_c := 0.9 \cdot F_{crc} \cdot A_c = 4656.946 \cdot kip$$

$$P_{cc} := \varphi Pn_c$$

$$L_{bc} := h_c = 10.387 \cdot ft$$

$$L_{pc} = 12.7 \cdot ft$$

there is no lateral torsional buckling

$$M_c := 0.9 \cdot R_{yy} \cdot F_{yy} \cdot Z_{xc} = 6765 \cdot kip \cdot ft$$

$$\frac{M_{rc}}{M_c} = 0.602$$

$$\frac{P_{rc}}{P_{cc}} = 0.651$$

$$CombinedCheckEq_c := \begin{cases} \text{"Use Equation H1-1a"} & \text{if } \dfrac{P_{rc}}{P_{cc}} \geq 0.2 \\ \text{"Use Equation H1-1b"} & \text{otherwise} \end{cases} = \text{"Use Equation H1-1a"}$$

Use AISC 360-10 Eq H1-1a

$$CombinedCheck_c := \begin{cases} \text{"Ok"} & \text{if } 1 > \dfrac{P_{rc}}{P_{cc}} + \dfrac{8}{9}\left(\dfrac{M_{rc}}{M_c}\right) \\ \text{"No"} & \text{otherwise} \end{cases} = \text{"No"}$$

Third Floor

HBE Data

Trial Section HBE: W40x149

cross-sectional area of HBE

$A_b := 43.8 in^2$

depth of HBE

$d_b := 38.2 in$

flange width

$b_{fb} := 11.8 in$

flange thickness

$t_{fb} := 0.83 in$

web thickness

$t_{wb} := 0.63 in$

Inertia of HBE

$I_b := 9800 in^4$

Modulus of Plasticity

$Z_{xb} := 598 in^3$

Radii of Gyration

$r_{yb} := 2.29 in$

$r_{xb} := 15 in$

Limiting unbraced length (AISC Table 3-2)

$L_{pb} := 8.09 ft$

$L_{rb} := 23.5 ft$

$Mp_{xb} := 2240 kip \cdot ft$

$Mr_{xb} := 1350 kip \cdot ft$

$Cb_b := 1.14$

VBE Data

Trial Section VBE: W40x324

cross-sectional area of VBE

$A_c := 95.3 in^2$

depth of VBE

$d_c := 40.2 in$

flange width

$b_{fc} := 15.9 in$

flange thickness

$t_{fc} := 1.81 in$

web thickness

$t_{wc} := 1 in$

Inertia of VBE

$I_c := 25600 in^4$

Modulus of Plasticity

$Z_{xc} := 1460 in^3$

Radii of Gyration

$r_{yc} := 3.58 in$

$r_{xc} := 16.4 in$

Limiting unbraced length (AISC Table 3-2)

$L_{pc} := 12.6 ft$

$L_{rc} := 41.3 ft$

$Mp_{xc} := 5480 kip \cdot ft$

$Mr_{xc} := 3360 kip \cdot ft$

$Cb_c := 1.14$

Rechecking angle of tension stress

$$\alpha := \tan(\alpha_1)^4 = \frac{1 + \frac{t_{w3}\cdot L}{2\cdot A_c}}{1 + t_{w3}\cdot H\cdot\left(\frac{1}{A_b} + \frac{H^3}{360I_c\cdot L}\right)} \text{ solve } \rightarrow \begin{bmatrix} \operatorname{atan}\left[\frac{1.4142135623730950488\cdot\sqrt{in}\cdot(3.934942287}{(4.6875e17\cdot ft^3 + 6.849315068493150 68}\right] \\ \operatorname{atan}\left[-\frac{1.4142135623730950488i\cdot\sqrt{in}\cdot(3.93494228}{(4.6875e17\cdot ft^3 + 6.8493150684931506}\right] \\ \operatorname{atan}\left[\frac{1.4142135623730950488i\cdot\sqrt{in}\cdot(3.934942287}{(4.6875e17\cdot ft^3 + 6.849315068493150 68}\right] \\ -1.0\cdot\operatorname{atan}\left[\frac{1.4142135623730950488\cdot\sqrt{in}\cdot(3.9349422}{(4.6875e17\cdot ft^3 + 6.84931506849315}\right] \end{bmatrix}$$

$$\alpha = \begin{pmatrix} 41.639 \\ -81.211i \\ 81.211i \\ -41.639 \end{pmatrix}\cdot deg$$

$$\alpha := \alpha_0 = 41.639\cdot deg$$

Calculating horizontal and vertical component of loads from plate web considering full yielding

$$w_{yb} := R_y \cdot F_y \cdot \left(t_{w3}\right) \cdot \cos(\alpha)^2 = 6.535 \cdot \frac{kip}{in}$$

$$w_{xb} := \frac{1}{2} \cdot R_y \cdot F_y \cdot \left(t_{w3}\right) \cdot \sin(2\alpha) = 5.81 \cdot \frac{kip}{in}$$

$$w_{yc} := \frac{1}{2} \cdot R_y \cdot F_y \cdot \left(t_{w3}\right) \cdot \sin(2 \cdot \alpha) = 5.81 \cdot \frac{kip}{in}$$

$$w_{xc} := R_y \cdot F_y \cdot \left(t_{w3}\right) \cdot \sin(\alpha)^2 = 5.165 \cdot \frac{kip}{in}$$

Design of HBE

Design Moment

$$L_{cf} := L - d_c = 103.8 \cdot in$$

$$M_u := w_{yb} \cdot \frac{L_{cf}^{\,2}}{4} = 17602.137 \cdot kip \cdot in$$

Axial Force in HBE:

distance between HBE centerlines

$h := 12ft$

$h_c := h - \frac{1}{2} \cdot d_b = 10.408\ ft$

$P_{HBEvbe} := \frac{1}{2} \cdot R_y \cdot F_y \cdot \sin(\alpha)^2 \cdot (t_{w3}) \cdot h_c = 322.568 \cdot kip$

$P_{HBEweb} := R_y \cdot F_y \cdot (t_{w3}) \cdot L_{cf} \cdot \sin(\alpha)^2 = 536.15 \cdot kip$

$P_{HBEL} := P_{HBEvbe} + \frac{1}{2} P_{HBEweb} = 590.643 \cdot kip$

$P_{HBER} := P_{HBEvbe} - \frac{1}{2} P_{HBEweb} = 54.493 \cdot kip$

$P_u := \max(P_{HBEL}, P_{HBER}) = 590.643 \cdot kip$

AISC 341-16 Table D1.1

$P_y := A_b \cdot R_{yy} \cdot F_{yy} = 2409 \cdot kip$

Shear Force in HBE:

$V_{uWebL} := \frac{w_{yb} \cdot L_{cf} + w_{xb} \cdot d_b}{2} = 450.122 \cdot kip$

$V_{uWebR} := \frac{w_{yb} \cdot L_{cf} - w_{xb} \cdot d_b}{2} = 228.188 \cdot kip$

$V_{uWeb} := \max(V_{uWebR}, V_{uWebL}) = 450.122 \cdot kip$

$V_g := 0kip$

Reduced Probable flexural strength

Left side

$$M_{pr\_reduced\_L} := \begin{cases} \left(1.1\cdot R_{yy}\cdot F_{yy}\cdot Z_{xb}\right)\cdot\left(1 - 0.5\cdot\dfrac{P_{HBEL}}{P_y}\right) & \text{if } \dfrac{P_{HBEL}}{P_y} < 0.2 \\ \dfrac{9}{8}\cdot\left(1.1\cdot R_{yy}\cdot F_{yy}\cdot Z_{xb}\right)\cdot\left(1 - \dfrac{P_{HBEL}}{P_y}\right) & \text{otherwise} \end{cases} = 30722.131\cdot kip\cdot in$$

Right side

$$M_{pr\_reduced\_R} := \begin{cases} \left(1.1\cdot R_{yy}\cdot F_{yy}\cdot Z_{xb}\right)\cdot\left(1 - 0.5\cdot\dfrac{P_{HBER}}{P_y}\right) & \text{if } \dfrac{P_{HBER}}{P_y} < 0.2 \\ \dfrac{9}{8}\cdot\left(1.1\cdot R_{yy}\cdot F_{yy}\cdot Z_{xb}\right)\cdot\left(1 - \dfrac{P_{HBER}}{P_y}\right) & \text{otherwise} \end{cases} = 35769.804\cdot kip\cdot in$$

$$V_{uHBE} := \frac{\left(M_{pr\_reduced\_L} + M_{pr\_reduced\_R}\right)}{L_{cf}} = 640.577\cdot kip$$

$$V_{HBE} := V_{uWeb} + V_g + V_{uHBE} = 1090.699\cdot kip$$

Checks:

1. Check Shear Strength

$$shearcheck1 := \begin{cases} \text{"}\phi v\text{=1"} & \text{if } \dfrac{d_b - 2\cdot t_{fb}}{t_{wb}} < 2.24\cdot\sqrt{\dfrac{E}{R_{yy}\cdot F_{yy}}} \\ \text{"no"} & \text{otherwise} \end{cases} = \text{"no"}$$

$$A_w := \left(d_b - 2\cdot t_{fb}\right)\cdot t_{wb} = 23.02\cdot in^2$$

$$\varphi Vn_b := 1.0\cdot 0.6\cdot R_{yy}\cdot F_{yy}\cdot A_w = 759.667\cdot kip$$

$$V_u := V_{HBE} = 1090.699\cdot kip$$

$$\varphi Vn_b = 759.667\cdot kip$$

$$shearcheck2 := \begin{cases} \text{"Ok"} & \text{if } \varphi Vn_b > V_u \\ \text{"No"} & \text{otherwise} \end{cases} = \text{"No"}$$

2. Check Compactness

$$flange := \begin{cases} \text{"Ok"} & \text{if } \dfrac{b_{fb}}{2 \cdot t_{fb}} < 0.32 \cdot \sqrt{\dfrac{E}{R_{yy} \cdot F_{yy}}} \\ \text{"No"} & \text{otherwise} \end{cases} = \text{"Ok"}$$

$$0.32 \cdot \sqrt{\frac{E}{R_{yy} \cdot F_{yy}}} = 7.348$$

$$\frac{b_{fb}}{2 \cdot t_{fb}} = 7.108$$

Flange is compact

$$C_a := \frac{P_u}{0.9 \cdot P_y} = 0.272$$

$$web := \begin{cases} \text{"Ok"} & \text{if } \dfrac{d_b - 2 \cdot t_{fb}}{t_{wb}} < 0.88 \cdot \sqrt{\dfrac{E}{F_{yy}}} \cdot (2.68 - C_a) \\ \text{"No "} & \text{otherwise} \end{cases} = \text{"No "}$$

$$web := \begin{cases} \text{"Ok"} & \text{if } 0.88 \cdot \sqrt{\dfrac{E}{R_{yy} \cdot F_{yy}}} \cdot (2.68 - C_a) > 1.57 \cdot \sqrt{\dfrac{E}{R_{yy} \cdot F_{yy}}} \\ \text{"No "} & \text{otherwise} \end{cases} = \text{"Ok"}$$

$$0.88 \cdot \sqrt{\frac{E}{R_{yy} \cdot F_{yy}}} \cdot (2.68 - C_a) = 48.65$$

$$\frac{d_b - 2 \cdot t_{fb}}{t_{wb}} = 58$$

$$1.57 \cdot \sqrt{\frac{E}{R_{yy} \cdot F_{yy}}} = 36.051$$

Web is compact

3. Check Combined Compression and Flexure

$K := 1$

$$axisbuckling := \left| \begin{array}{ll} \text{"Major axis buckling controls"} & \text{if } \frac{K\cdot L}{r_{xb}} > \frac{K\cdot L}{r_{yb}} \\ \text{"Minor axis buckling controls"} & \text{otherwise} \end{array} \right. = \text{"Minor axis buckling controls"}$$

$$\frac{K\cdot L}{r_{xb}} = 9.6$$

$$\frac{K\cdot L}{r_{yb}} = 62.88$$

$$slenderness := \left| \begin{array}{ll} \frac{K\cdot L}{r_{yb}} & \text{if } axisbuckling = \text{"Minor axis buckling controls"} \\ \frac{K\cdot L}{r_{xb}} & \text{otherwise} \end{array} \right. = 62.882$$

$$F_e := \frac{\pi^2 \cdot E}{(slenderness)^2} = 72.384\cdot ksi$$

$$0.44\cdot R_{yy}\cdot F_{yy} = 24.2\cdot ksi$$

$$checkE32 := \left| \begin{array}{ll} \text{"Use E3-2"} & \text{if } \frac{\pi^2 \cdot E}{(slenderness)^2} > 0.44\cdot F_{yy} \\ \text{"Dont use E3-2"} & \text{otherwise} \end{array} \right. = \text{"Use E3-2"}$$

Using AISC 360 Equation E3-2

$$F_{cr} := 0.658^{\frac{R_{yy}\cdot F_{yy}}{F_e}} \cdot R_{yy}\cdot F_{yy} = 40.017\cdot ksi$$

$$\varphi Pn_b := 0.9\cdot F_{cr}\cdot A_b = 1577.47\cdot kip$$

$$P_c := \varphi Pn_b$$

$$P_r := P_u$$

$$L_{pb} = 8.09\cdot ft$$

$$L_b := L = 12\,ft$$

$$Mp_{xb} = 26880\cdot kip\cdot in$$

$$\varphi Mn_b := \begin{cases} Mp_{xb} & \text{if } Mp_{xb} < Cb_b \cdot \left[Mp_{xb} - \left(Mp_{xb} - Mr_{xb} \right) \cdot \left(\dfrac{L_b - L_{pb}}{L_{rb} - L_{pb}} \right) \right] \\ Cb_b \cdot \left[Mp_{xb} - \left(Mp_{xb} - Mr_{xb} \right) \cdot \left(\dfrac{L_b - L_{pb}}{L_{rb} - L_{pb}} \right) \right] & \text{otherwise} \end{cases} = 26880 \cdot kip \cdot in$$

$$\frac{P_r}{P_c} = 0.374$$

$$CombinedCheckEq := \begin{cases} \text{"Use Equation H1-1a"} & \text{if } \dfrac{P_r}{P_c} \geq 0.2 \\ \text{"Use Equation H1-1b"} & \text{otherwise} \end{cases} = \text{"Use Equation H1-1a"}$$

AISC 360-10 Equation H1-1a

$$CombinedCheck := \begin{cases} \text{"Ok"} & \text{if } 1 > \dfrac{P_r}{P_c} + \dfrac{8}{9} \left(\dfrac{M_u}{\varphi Mn_b} \right) \\ \text{"No"} & \text{otherwise} \end{cases} = \text{"Ok"}$$

4. Check moment of inertia

$$I_{required} := \frac{0.003 \cdot t_{w3} \cdot L^4}{h} = 2239.488 \cdot in^4$$

$$I_b = 9800 \cdot in^4$$

$$InertiaCheck := \begin{cases} \text{"Ok"} & \text{if } I_b > I_{required} \\ \text{"No"} & \text{otherwise} \end{cases} = \text{"Ok"}$$

5. Check Web thickness

$$t_{wb} = 0.63 \cdot in$$

$$\frac{t_{w3} \cdot R_y \cdot F_y}{F_{yy}} = 0.234 \cdot in$$

$$WebCheck := \begin{cases} \text{"Ok"} & \text{if } t_{wb} > \dfrac{t_{w3} \cdot R_y \cdot F_y}{F_{yy}} \\ \text{"No"} & \text{otherwise} \end{cases} = \text{"Ok"}$$

Design of VBE

(there are no adjoining beams)

$M_{pradj} := 0$

$M_{prc} := 1.1 \cdot R_{yy} \cdot F_{yy} \cdot Z_{xc} = 88330 \cdot kip \cdot in$

$L_h := H - d_b = 105.8 \cdot in$

Resulting compressive force

$$E_{mcomp} := \frac{1}{2} \cdot R_y \cdot F_y \cdot \sin(2 \cdot \alpha) \cdot \left(t_{w3}\right) \cdot h_c + \left(V_{uHBE} + \frac{w_{yb} \cdot L_{cf}}{2}\right) - \left(2 \cdot \frac{M_{pradj}}{L_h}\right) = 1705.374 \cdot kip$$

$P_{gravity} := 0kip$

$P_{uc} := E_{mcomp} + P_{gravity} = 1705.374 \cdot kip$

$L_c := h$

Resulting tension force

$$E_{mtens} := \frac{1}{2} \cdot R_y \cdot F_y \cdot \sin(2 \cdot \alpha) \cdot \left(t_{w3}\right) \cdot h_c + \left(V_{uHBE} - \frac{w_{yb} \cdot L_{cf}}{2}\right) - \left(2 \cdot \frac{M_{pradj}}{L_h}\right) = 1027.064 \cdot kip$$

Flexure from web tension

$$M_{VBEweb} := w_{xc} \cdot \frac{\left(h_c^{\,2}\right)}{12} = 6714.796 \cdot kip \cdot in$$

Flexure from VBE compression

$M_{pr} := \max\left(M_{pr\_reduced\_L}, M_{pr\_reduced\_R}\right) = 35769.804 \cdot kip \cdot in$

$$M_{pb} := \frac{M_{pr}}{1.1 \cdot R_{yy}} + V_u \cdot \left[\frac{1}{2} \cdot \left(d_b + d_c\right)\right] = 72317.228 \cdot kip \cdot in$$

$$M_{VBEhbe} := \frac{1}{2} \cdot M_{pb} = 36158.614 \cdot kip \cdot in$$

$M_{uc} := M_{VBEweb} + M_{VBEhbe} = 42873.41 \cdot kip \cdot in$

Moment magnification

$$P_{ec} := \frac{\pi^2 \cdot E \cdot I_c}{(K \cdot L_c)^2} = 3.534 \times 10^5 \cdot kip$$

$$C_m := 1.0$$

$$B_{1c} := \frac{C_m}{1 - \frac{P_{uc}}{P_{ec}}} = 1.005$$

$$P_{rc} := P_{uc} = 1705.374 \cdot kip$$

$$M_{rc} := B_{1c} \cdot M_{uc} = 43081.329 \cdot kip \cdot in$$

Shear in the VBE is the sum of the effect of web tension and the portion of shear not resisted by the web plate

Shear from web plate

$$V_{VBEweb} := \frac{1}{2} \cdot R_y \cdot F_y \cdot \sin(\alpha) \cdot (t_{w3}) \cdot h_c = 485.478 \cdot kip$$

Shear from HBE Hinging

$$M_{pc} := M_{VBEhbe} + M_{uc} = 79032.023 \cdot kip \cdot in$$

$$V_{VBEhbe} := \frac{1}{2} \cdot \left(\frac{M_{pc}}{h_c}\right) = 316.381 \cdot kip$$

Shear from horizontal element

$$V_{uc} := V_{VBEweb} + V_{VBEhbe} = 801.86 \cdot kip$$

Design Checks

1. Check Compactness

AISC 341-16 Table D1.1

$$flange_c := \begin{cases} \text{"Ok"} & \text{if } \frac{b_{fc}}{2 \cdot t_{fc}} < 0.32 \cdot \sqrt{\frac{E}{R_{yy} \cdot F_{yy}}} \\ \text{"No"} & \text{otherwise} \end{cases} = \text{"Ok"}$$

$$\frac{b_{fc}}{2 \cdot t_{fc}} = 4.392$$

$$0.32 \cdot \sqrt{\frac{E}{R_{yy} \cdot F_{yy}}} = 7.348$$

Flange is compact

$$C_{ac} := \frac{P_{uc}}{0.9 \cdot F_{yy} \cdot R_{yy} \cdot A_c} = 0.362$$

$$web_c := \begin{cases} \text{"Ok"} & \text{if } \dfrac{d_c - 2 \cdot t_{fc}}{t_{wc}} < 0.88 \cdot \sqrt{\dfrac{E}{R_{yy} \cdot F_{yy}}} \cdot (2.68 - C_{ac}) \\ \text{"No"} & \text{otherwise} \end{cases} = \text{"Ok"}$$

$$web_c := \begin{cases} \text{"Ok"} & \text{if } 0.88 \cdot \sqrt{\dfrac{E}{R_{yy} \cdot F_{yy}}} \cdot (2.68 - C_{ac}) > 1.57 \cdot \sqrt{\dfrac{E}{R_{yy} \cdot F_{yy}}} \\ \text{"No"} & \text{otherwise} \end{cases} = \text{"Ok"}$$

$$\frac{d_c - 2 \cdot t_{fc}}{t_{wc}} = 36.58$$

$$0.88 \cdot \sqrt{\frac{E}{R_{yy} \cdot F_{yy}}} \cdot (2.68 - C_{ac}) = 46.85$$

$$1.57 \cdot \sqrt{\frac{E}{R_{yy} \cdot F_{yy}}} = 36.051$$

Web is compact

2. Check Shear Strength

$$\varphi check := \begin{cases} \text{"}\phi\text{=1"} & \text{if } \dfrac{d_c - 2 \cdot t_{fc}}{t_{wc}} < 2.24 \cdot \sqrt{\dfrac{E}{R_{yy} \cdot F_{yy}}} \\ \text{"No"} & \text{otherwise} \end{cases} = \text{"}\phi\text{=1"}$$

$$\varphi_{vc} := 1$$

$$\varphi Vn_c := \varphi_{vc} \cdot 0.6 \cdot R_{yy} \cdot F_{yy} \cdot (d_c - 2 \cdot t_{fc}) \cdot t_{wc} = 1207.14 \cdot kip$$

$$V_{uc} = 801.86 \cdot kip$$

$$shear := \begin{cases} \text{"Ok"} & \text{if } V_{uc} < \varphi Vn_c \\ \text{"No"} & \text{otherwise} \end{cases} = \text{"Ok"}$$

3. Check Combined Compression and Flexure

$$slenderness_c := \frac{K \cdot L}{r_{yc}}$$

$$F_{ec} := \frac{\pi^2 \cdot E}{slenderness_c^{\,2}}$$

$$0.44 \cdot R_{yy} \cdot F_{yy} = 24.2 \cdot ksi$$

$$checkE32_c := \begin{cases} \text{"Use E3-2"} & \text{if } \dfrac{\pi^2 \cdot E}{\left(slenderness_c\right)^2} > 0.44 \cdot R_{yy} \cdot F_{yy} \\ \text{"Dont use E3-2"} & \text{otherwise} \end{cases} = \text{"Use E3-2"}$$

Using AISC 360-10 Equation E3-2

$$F_{crc} := 0.658^{\frac{R_{yy} \cdot F_{yy}}{F_{ec}}} \cdot R_{yy} \cdot F_{yy} = 48.289 \cdot ksi$$

$$\varphi Pn_c := 0.9 \cdot F_{crc} \cdot A_c = 4141.752 \cdot kip$$

$$P_{cc} := \varphi Pn_c$$

$$L_{bc} := h_c = 10.408 \cdot ft$$

$$L_{pc} = 12.6 \cdot ft$$

there is no lateral torsional buckling

$$M_c := 0.9 \cdot R_{yy} \cdot F_{yy} \cdot Z_{xc} = 6022.5 \cdot kip \cdot ft$$

$$\frac{M_{rc}}{M_c} = 0.596$$

$$\frac{P_{rc}}{P_{cc}} = 0.412$$

$$CombinedCheckEq_c := \begin{cases} \text{"Use Equation H1-1a"} & \text{if } \dfrac{P_{rc}}{P_{cc}} \geq 0.2 \\ \text{"Use Equation H1-1b"} & \text{otherwise} \end{cases} = \text{"Use Equation H1-1a"}$$

Use AISC 360-10 Eq H1-1a

$$CombinedCheck_c := \begin{cases} \text{"Ok"} & \text{if } 1 > \dfrac{P_{rc}}{P_{cc}} + \dfrac{8}{9}\left(\dfrac{M_{rc}}{M_c}\right) \\ \text{"No"} & \text{otherwise} \end{cases} = \text{"Ok"}$$

APPENDIX B

B.1. General

The axial strips, as mentioned earlier, were assigned zero compression strength within SAP2000 to mimic the behavior of the slender steel web panel under seismic loading conditions. The *Axial-P* hinge was assigned to each of these diagonal strips, which by definition, only allows for tension and compression yielding. In order to restrict these hinges from yielding under compression (owing to buckling caused by compressive stresses within the steel plate), a near-zero compression limit was assigned to the axial strips. Note that the material model used for the plate in this study followed ASTM A36 standards, with a simplified elasto-plastic stress-strain model having a constant plastic plateau for up to very large strains. For this modification to work, the program was required to log values of the last deformation before entering the next consecutive compression loading regime, allowing the strips to recover all previously logged deformation values before entering the tension regime again. Figure B-1 shows a schematic idealization of the expected strip hysteresis as presented by Purba and Bruneau in 2010. A test-run was conducted with a simple portal frame with a singular diagonal axial strip in order to validate the above mentioned behavior. This is explained in Section B-2.

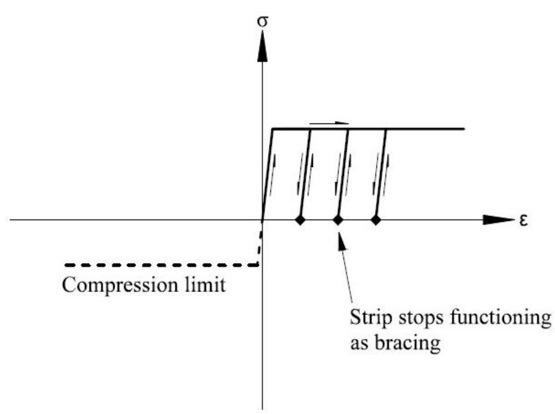

Figure B-1 Generic Strip Hysteretic Behavior (Purba and Bruneau 2010)

B.2. Case Study

As shown in Figure B-2a, a simple moment resisting frame was braced with a singular diagonal axial strip to be used as a case study for validation of previously mentioned behavior. The diagonal strip, using ASTM A36 material with F_y = 36 ksi, was assigned a compression limit of -0.01 (near-zero value). An *Axial-P* hinge was assigned to the strip at mid-length. For a forcing function, a nonlinear time history load case was set up using a cosine function of amplitude 1. This was an idealistic representation of the typical conditions under seismic loading. Figure B-2b depicts the considered loading time history.

As can be observed from Figure B-3, the axial hinge is only engaged during the tension regime of the forcing function. Correlating the time steps where the cosine function undergoes compressive action, it could be seen that there was no stress developing within the diagonal strip. In addition, the strip was re-engaged as soon as the function entered into tension domain, starting from exactly the same value of deformation where the previous tension regime had logged off. This case study verified the behavior of the *Axial-P* hinge in reference to modifications mentioned Section 3.3.2.

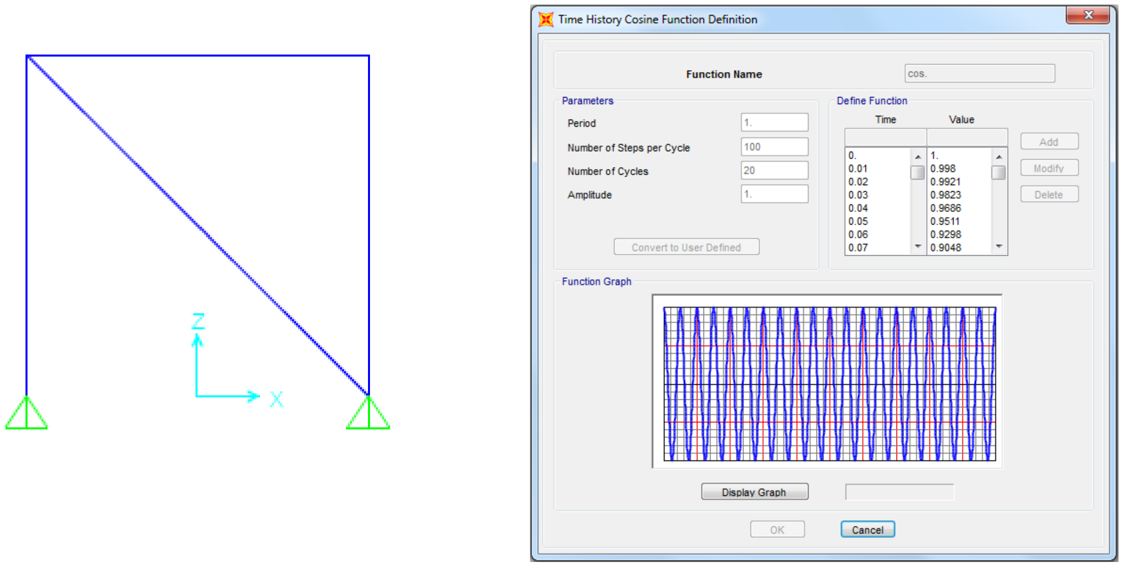

a) b)

Figure B-2 a) Case Study set-up for axial hinge action verification, and b) Cosine Function Time History as defined within SAP2000

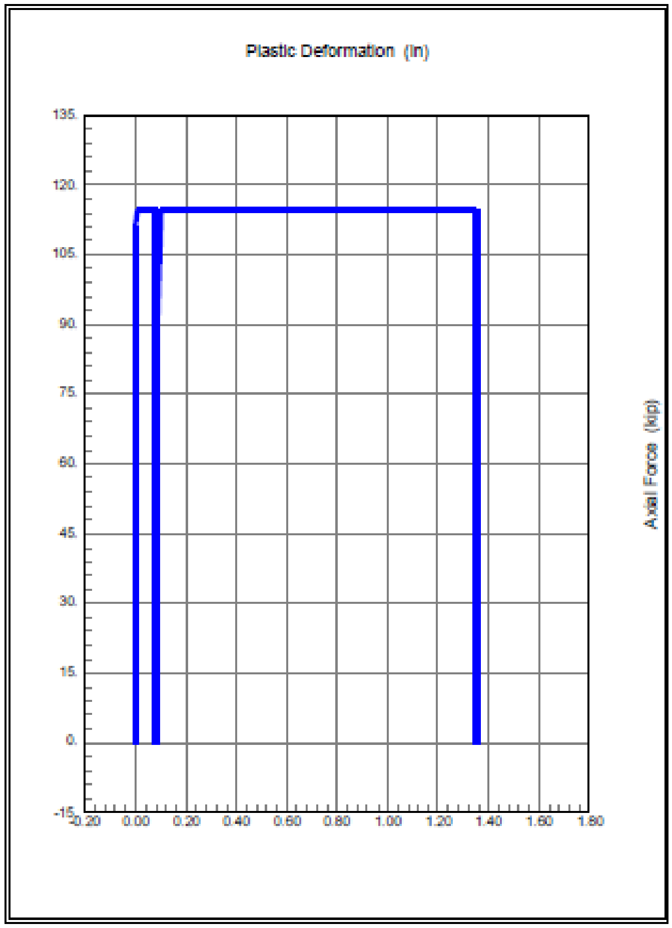

Figure B-3 Axial Hinge Force-Displacement behavior

APPENDIX C

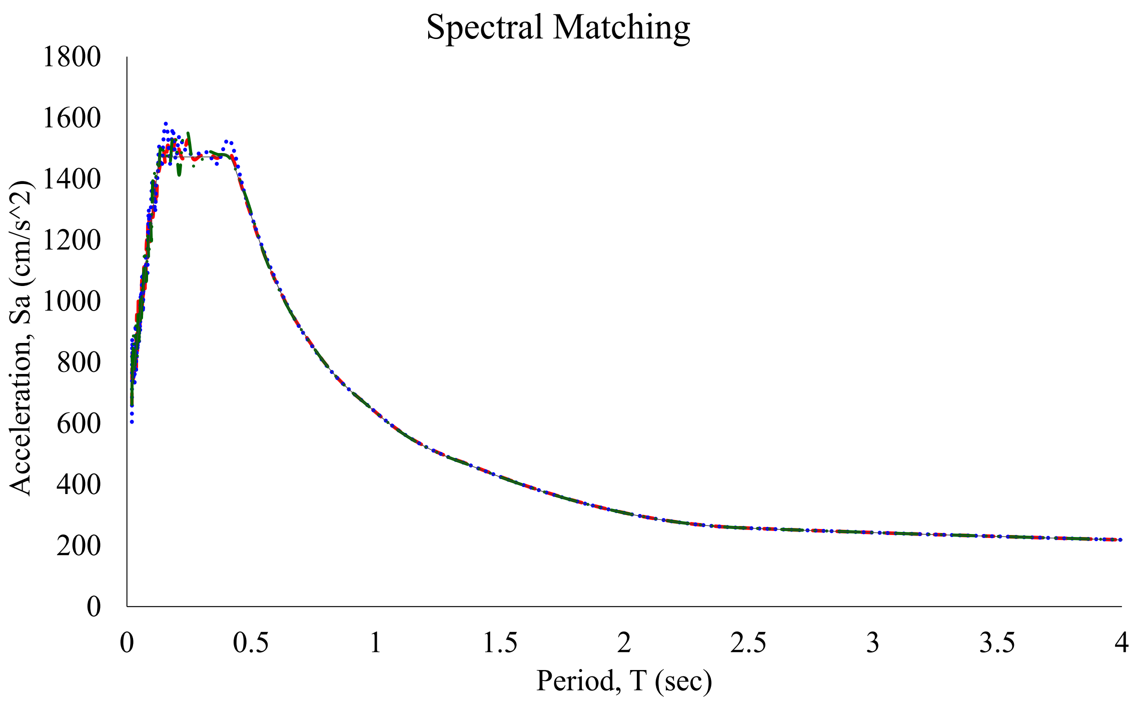

Figure C-1 Spectral matching for synthetic ground motions with target spectrum

APPENDIX D

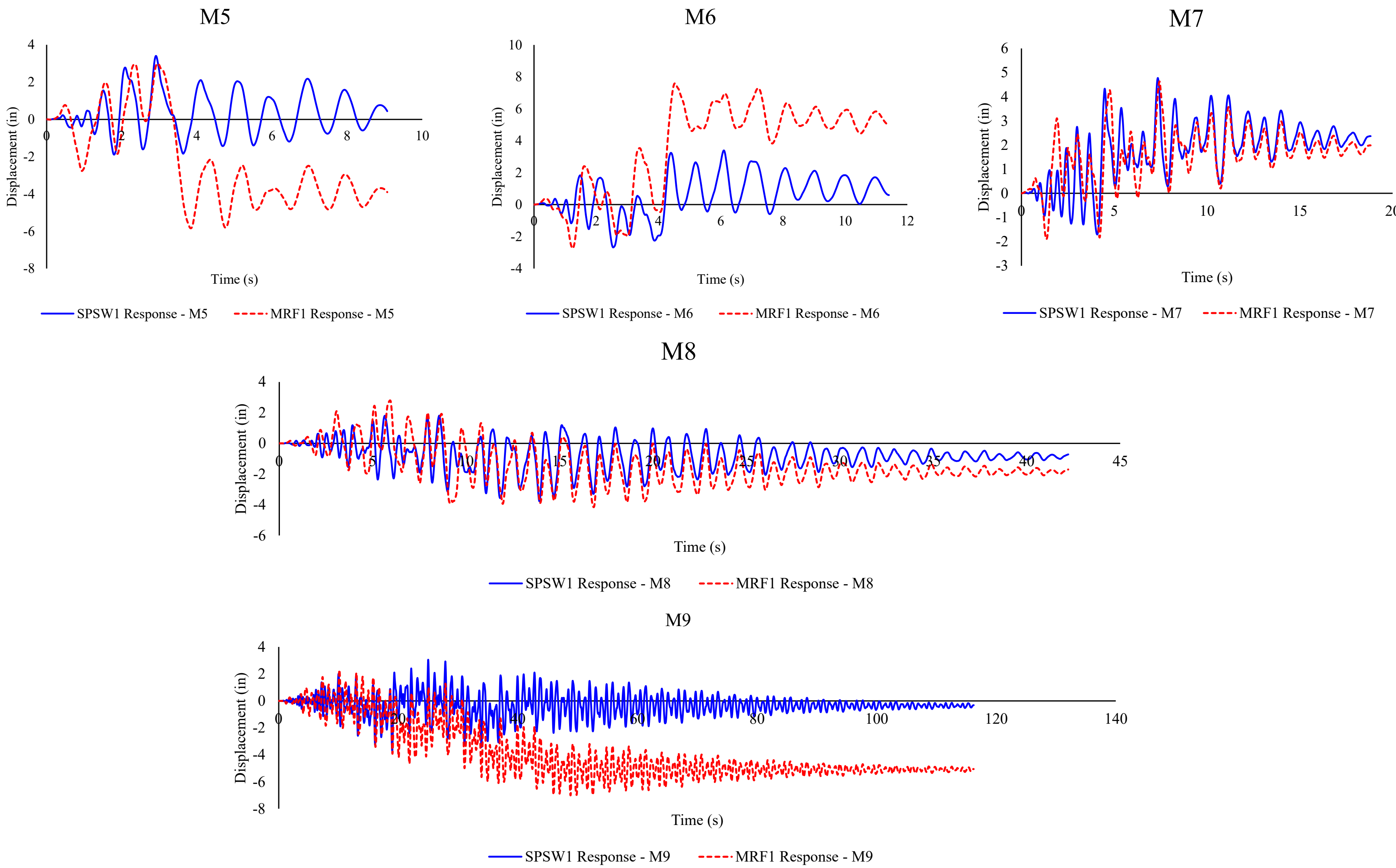

Figure D-1 Drift response for SPSW1 compared with that of MRF1 for M5 to M9

MCEER Technical Reports

MCEER publishes technical reports on a variety of subjects written by authors funded through MCEER. These reports can be downloaded from the MCEER website at http://www.buffalo.edu/mceer. They can also be requested through NTIS, P.O. Box 1425, Springfield, Virginia 22151. NTIS accession numbers are shown in parenthesis, if available.

NCEER-87-0001 "First-Year Program in Research, Education and Technology Transfer," 3/5/87, (PB88-134275, A04, MF-A01).

NCEER-87-0002 "Experimental Evaluation of Instantaneous Optimal Algorithms for Structural Control," by R.C. Lin, T.T. Soong and A.M. Reinhorn, 4/20/87, (PB88-134341, A04, MF-A01).

NCEER-87-0003 "Experimentation Using the Earthquake Simulation Facilities at University at Buffalo," by A.M. Reinhorn and R.L. Ketter, not available.

NCEER-87-0004 "The System Characteristics and Performance of a Shaking Table," by J.S. Hwang, K.C. Chang and G.C. Lee, 6/1/87, (PB88-134259, A03, MF-A01). This report is available only through NTIS (see address given above).

NCEER-87-0005 "A Finite Element Formulation for Nonlinear Viscoplastic Material Using a Q Model," by O. Gyebi and G. Dasgupta, 11/2/87, (PB88-213764, A08, MF-A01).

NCEER-87-0006 "Symbolic Manipulation Program (SMP) - Algebraic Codes for Two and Three Dimensional Finite Element Formulations," by X. Lee and G. Dasgupta, 11/9/87, (PB88-218522, A05, MF-A01).

NCEER-87-0007 "Instantaneous Optimal Control Laws for Tall Buildings Under Seismic Excitations," by J.N. Yang, A. Akbarpour and P. Ghaemmaghami, 6/10/87, (PB88-134333, A06, MF-A01). This report is only available through NTIS (see address given above).

NCEER-87-0008 "IDARC: Inelastic Damage Analysis of Reinforced Concrete Frame - Shear-Wall Structures," by Y.J. Park, A.M. Reinhorn and S.K. Kunnath, 7/20/87, (PB88-134325, A09, MF-A01). This report is only available through NTIS (see address given above).

NCEER-87-0009 "Liquefaction Potential for New York State: A Preliminary Report on Sites in Manhattan and Buffalo," by M. Budhu, V. Vijayakumar, R.F. Giese and L. Baumgras, 8/31/87, (PB88-163704, A03, MF-A01). This report is available only through NTIS (see address given above).

NCEER-87-0010 "Vertical and Torsional Vibration of Foundations in Inhomogeneous Media," by A.S. Veletsos and K.W. Dotson, 6/1/87, (PB88-134291, A03, MF-A01). This report is only available through NTIS (see address given above).

NCEER-87-0011 "Seismic Probabilistic Risk Assessment and Seismic Margins Studies for Nuclear Power Plants," by Howard H.M. Hwang, 6/15/87, (PB88-134267, A03, MF-A01). This report is only available through NTIS (see address given above).

NCEER-87-0012 "Parametric Studies of Frequency Response of Secondary Systems Under Ground-Acceleration Excitations," by Y. Yong and Y.K. Lin, 6/10/87, (PB88-134309, A03, MF-A01). This report is only available through NTIS (see address given above).

NCEER-87-0013 "Frequency Response of Secondary Systems Under Seismic Excitation," by J.A. HoLung, J. Cai and Y.K. Lin, 7/31/87, (PB88-134317, A05, MF-A01). This report is only available through NTIS (see address given above).

NCEER-87-0014 "Modelling Earthquake Ground Motions in Seismically Active Regions Using Parametric Time Series Methods," by G.W. Ellis and A.S. Cakmak, 8/25/87, (PB88-134283, A08, MF-A01). This report is only available through NTIS (see address given above).

NCEER-87-0015 "Detection and Assessment of Seismic Structural Damage," by E. DiPasquale and A.S. Cakmak, 8/25/87, (PB88-163712, A05, MF-A01). This report is only available through NTIS (see address given above).

NCEER-87-0016 "Pipeline Experiment at Parkfield, California," by J. Isenberg and E. Richardson, 9/15/87, (PB88-163720, A03, MF-A01). This report is available only through NTIS (see address given above).

NCEER-87-0017 "Digital Simulation of Seismic Ground Motion," by M. Shinozuka, G. Deodatis and T. Harada, 8/31/87, (PB88-155197, A04, MF-A01). This report is available only through NTIS (see address given above).

NCEER-87-0018 "Practical Considerations for Structural Control: System Uncertainty, System Time Delay and Truncation of Small Control Forces," J.N. Yang and A. Akbarpour, 8/10/87, (PB88-163738, A08, MF-A01). This report is only available through NTIS (see address given above).

NCEER-87-0019 "Modal Analysis of Nonclassically Damped Structural Systems Using Canonical Transformation," by J.N. Yang, S. Sarkani and F.X. Long, 9/27/87, (PB88-187851, A04, MF-A01).

NCEER-87-0020 "A Nonstationary Solution in Random Vibration Theory," by J.R. Red-Horse and P.D. Spanos, 11/3/87, (PB88-163746, A03, MF-A01).

NCEER-87-0021 "Horizontal Impedances for Radially Inhomogeneous Viscoelastic Soil Layers," by A.S. Veletsos and K.W. Dotson, 10/15/87, (PB88-150859, A04, MF-A01).

NCEER-87-0022 "Seismic Damage Assessment of Reinforced Concrete Members," by Y.S. Chung, C. Meyer and M. Shinozuka, 10/9/87, (PB88-150867, A05, MF-A01). This report is available only through NTIS (see address given above).

NCEER-87-0023 "Active Structural Control in Civil Engineering," by T.T. Soong, 11/11/87, (PB88-187778, A03, MF-A01).

NCEER-87-0024 "Vertical and Torsional Impedances for Radially Inhomogeneous Viscoelastic Soil Layers," by K.W. Dotson and A.S. Veletsos, 12/87, (PB88-187786, A03, MF-A01).

NCEER-87-0025 "Proceedings from the Symposium on Seismic Hazards, Ground Motions, Soil-Liquefaction and Engineering Practice in Eastern North America," October 20-22, 1987, edited by K.H. Jacob, 12/87, (PB88-188115, A23, MF-A01). This report is available only through NTIS (see address given above).

NCEER-87-0026 "Report on the Whittier-Narrows, California, Earthquake of October 1, 1987," by J. Pantelic and A. Reinhorn, 11/87, (PB88-187752, A03, MF-A01). This report is available only through NTIS (see address given above).

NCEER-87-0027 "Design of a Modular Program for Transient Nonlinear Analysis of Large 3-D Building Structures," by S. Srivastav and J.F. Abel, 12/30/87, (PB88-187950, A05, MF-A01). This report is only available through NTIS (see address given above).

NCEER-87-0028 "Second-Year Program in Research, Education and Technology Transfer," 3/8/88, (PB88-219480, A04, MF-A01).

NCEER-88-0001 "Workshop on Seismic Computer Analysis and Design of Buildings With Interactive Graphics," by W. McGuire, J.F. Abel and C.H. Conley, 1/18/88, (PB88-187760, A03, MF-A01). This report is only available through NTIS (see address given above).

NCEER-88-0002 "Optimal Control of Nonlinear Flexible Structures," by J.N. Yang, F.X. Long and D. Wong, 1/22/88, (PB88-213772, A06, MF-A01).

NCEER-88-0003 "Substructuring Techniques in the Time Domain for Primary-Secondary Structural Systems," by G.D. Manolis and G. Juhn, 2/10/88, (PB88-213780, A04, MF-A01).

NCEER-88-0004 "Iterative Seismic Analysis of Primary-Secondary Systems," by A. Singhal, L.D. Lutes and P.D. Spanos, 2/23/88, (PB88-213798, A04, MF-A01).

NCEER-88-0005 "Stochastic Finite Element Expansion for Random Media," by P.D. Spanos and R. Ghanem, 3/14/88, (PB88-213806, A03, MF-A01).

NCEER-88-0006 "Combining Structural Optimization and Structural Control," by F.Y. Cheng and C.P. Pantelides, 1/10/88, (PB88-213814, A05, MF-A01).

NCEER-88-0007 "Seismic Performance Assessment of Code-Designed Structures," by H.H-M. Hwang, J-W. Jaw and H-J. Shau, 3/20/88, (PB88-219423, A04, MF-A01). This report is only available through NTIS (see address given above).

NCEER-88-0008 "Reliability Analysis of Code-Designed Structures Under Natural Hazards," by H.H-M. Hwang, H. Ushiba and M. Shinozuka, 2/29/88, (PB88-229471, A07, MF-A01). This report is only available through NTIS (see address given above).

NCEER-88-0009 "Seismic Fragility Analysis of Shear Wall Structures," by J-W Jaw and H.H-M. Hwang, 4/30/88, (PB89-102867, A04, MF-A01).

NCEER-88-0010 "Base Isolation of a Multi-Story Building Under a Harmonic Ground Motion - A Comparison of Performances of Various Systems," by F-G Fan, G. Ahmadi and I.G. Tadjbakhsh, 5/18/88, (PB89-122238, A06, MF-A01). This report is only available through NTIS (see address given above).

NCEER-88-0011 "Seismic Floor Response Spectra for a Combined System by Green's Functions," by F.M. Lavelle, L.A. Bergman and P.D. Spanos, 5/1/88, (PB89-102875, A03, MF-A01).

NCEER-88-0012 "A New Solution Technique for Randomly Excited Hysteretic Structures," by G.Q. Cai and Y.K. Lin, 5/16/88, (PB89-102883, A03, MF-A01).

NCEER-88-0013 "A Study of Radiation Damping and Soil-Structure Interaction Effects in the Centrifuge," by K. Weissman, supervised by J.H. Prevost, 5/24/88, (PB89-144703, A06, MF-A01).

NCEER-88-0014 "Parameter Identification and Implementation of a Kinematic Plasticity Model for Frictional Soils," by J.H. Prevost and D.V. Griffiths, not available.

NCEER-88-0015 "Two- and Three- Dimensional Dynamic Finite Element Analyses of the Long Valley Dam," by D.V. Griffiths and J.H. Prevost, 6/17/88, (PB89-144711, A04, MF-A01).

NCEER-88-0016 "Damage Assessment of Reinforced Concrete Structures in Eastern United States," by A.M. Reinhorn, M.J. Seidel, S.K. Kunnath and Y.J. Park, 6/15/88, (PB89-122220, A04, MF-A01). This report is only available through NTIS (see address given above).

NCEER-88-0017 "Dynamic Compliance of Vertically Loaded Strip Foundations in Multilayered Viscoelastic Soils," by S. Ahmad and A.S.M. Israil, 6/17/88, (PB89-102891, A04, MF-A01).

NCEER-88-0018 "An Experimental Study of Seismic Structural Response With Added Viscoelastic Dampers," by R.C. Lin, Z. Liang, T.T. Soong and R.H. Zhang, 6/30/88, (PB89-122212, A05, MF-A01). This report is available only through NTIS (see address given above).

NCEER-88-0019 "Experimental Investigation of Primary - Secondary System Interaction," by G.D. Manolis, G. Juhn and A.M. Reinhorn, 5/27/88, (PB89-122204, A04, MF-A01).

NCEER-88-0020 "A Response Spectrum Approach For Analysis of Nonclassically Damped Structures," by J.N. Yang, S. Sarkani and F.X. Long, 4/22/88, (PB89-102909, A04, MF-A01).

NCEER-88-0021 "Seismic Interaction of Structures and Soils: Stochastic Approach," by A.S. Veletsos and A.M. Prasad, 7/21/88, (PB89-122196, A04, MF-A01). This report is only available through NTIS (see address given above).

NCEER-88-0022 "Identification of the Serviceability Limit State and Detection of Seismic Structural Damage," by E. DiPasquale and A.S. Cakmak, 6/15/88, (PB89-122188, A05, MF-A01). This report is available only through NTIS (see address given above).

NCEER-88-0023 "Multi-Hazard Risk Analysis: Case of a Simple Offshore Structure," by B.K. Bhartia and E.H. Vanmarcke, 7/21/88, (PB89-145213, A05, MF-A01).

NCEER-88-0024 "Automated Seismic Design of Reinforced Concrete Buildings," by Y.S. Chung, C. Meyer and M. Shinozuka, 7/5/88, (PB89-122170, A06, MF-A01). This report is available only through NTIS (see address given above).

NCEER-88-0025 "Experimental Study of Active Control of MDOF Structures Under Seismic Excitations," by L.L. Chung, R.C. Lin, T.T. Soong and A.M. Reinhorn, 7/10/88, (PB89-122600, A04, MF-A01).

NCEER-88-0026 "Earthquake Simulation Tests of a Low-Rise Metal Structure," by J.S. Hwang, K.C. Chang, G.C. Lee and R.L. Ketter, 8/1/88, (PB89-102917, A04, MF-A01).

NCEER-88-0027 "Systems Study of Urban Response and Reconstruction Due to Catastrophic Earthquakes," by F. Kozin and H.K. Zhou, 9/22/88, (PB90-162348, A04, MF-A01).

NCEER-88-0028 "Seismic Fragility Analysis of Plane Frame Structures," by H.H-M. Hwang and Y.K. Low, 7/31/88, (PB89-131445, A06, MF-A01).

NCEER-88-0029 "Response Analysis of Stochastic Structures," by A. Kardara, C. Bucher and M. Shinozuka, 9/22/88, (PB89-174429, A04, MF-A01).

NCEER-88-0030 "Nonnormal Accelerations Due to Yielding in a Primary Structure," by D.C.K. Chen and L.D. Lutes, 9/19/88, (PB89-131437, A04, MF-A01).

NCEER-88-0031 "Design Approaches for Soil-Structure Interaction," by A.S. Veletsos, A.M. Prasad and Y. Tang, 12/30/88, (PB89-174437, A03, MF-A01). This report is available only through NTIS (see address given above).

NCEER-88-0032 "A Re-evaluation of Design Spectra for Seismic Damage Control," by C.J. Turkstra and A.G. Tallin, 11/7/88, (PB89-145221, A05, MF-A01).

NCEER-88-0033 "The Behavior and Design of Noncontact Lap Splices Subjected to Repeated Inelastic Tensile Loading," by V.E. Sagan, P. Gergely and R.N. White, 12/8/88, (PB89-163737, A08, MF-A01).

NCEER-88-0034 "Seismic Response of Pile Foundations," by S.M. Mamoon, P.K. Banerjee and S. Ahmad, 11/1/88, (PB89-145239, A04, MF-A01).

NCEER-88-0035 "Modeling of R/C Building Structures With Flexible Floor Diaphragms (IDARC2)," by A.M. Reinhorn, S.K. Kunnath and N. Panahshahi, 9/7/88, (PB89-207153, A07, MF-A01).

NCEER-88-0036 "Solution of the Dam-Reservoir Interaction Problem Using a Combination of FEM, BEM with Particular Integrals, Modal Analysis, and Substructuring," by C-S. Tsai, G.C. Lee and R.L. Ketter, 12/31/88, (PB89-207146, A04, MF-A01).

NCEER-88-0037 "Optimal Placement of Actuators for Structural Control," by F.Y. Cheng and C.P. Pantelides, 8/15/88, (PB89-162846, A05, MF-A01).

NCEER-88-0038 "Teflon Bearings in Aseismic Base Isolation: Experimental Studies and Mathematical Modeling," by A. Mokha, M.C. Constantinou and A.M. Reinhorn, 12/5/88, (PB89-218457, A10, MF-A01). This report is available only through NTIS (see address given above).

NCEER-88-0039 "Seismic Behavior of Flat Slab High-Rise Buildings in the New York City Area," by P. Weidlinger and M. Ettouney, 10/15/88, (PB90-145681, A04, MF-A01).

NCEER-88-0040 "Evaluation of the Earthquake Resistance of Existing Buildings in New York City," by P. Weidlinger and M. Ettouney, 10/15/88, not available.

NCEER-88-0041 "Small-Scale Modeling Techniques for Reinforced Concrete Structures Subjected to Seismic Loads," by W. Kim, A. El-Attar and R.N. White, 11/22/88, (PB89-189625, A05, MF-A01).

NCEER-88-0042 "Modeling Strong Ground Motion from Multiple Event Earthquakes," by G.W. Ellis and A.S. Cakmak, 10/15/88, (PB89-174445, A03, MF-A01).

NCEER-88-0043 "Nonstationary Models of Seismic Ground Acceleration," by M. Grigoriu, S.E. Ruiz and E. Rosenblueth, 7/15/88, (PB89-189617, A04, MF-A01).

NCEER-88-0044 "SARCF User's Guide: Seismic Analysis of Reinforced Concrete Frames," by Y.S. Chung, C. Meyer and M. Shinozuka, 11/9/88, (PB89-174452, A08, MF-A01).

NCEER-88-0045 "First Expert Panel Meeting on Disaster Research and Planning," edited by J. Pantelic and J. Stoyle, 9/15/88, (PB89-174460, A05, MF-A01).

NCEER-88-0046 "Preliminary Studies of the Effect of Degrading Infill Walls on the Nonlinear Seismic Response of Steel Frames," by C.Z. Chrysostomou, P. Gergely and J.F. Abel, 12/19/88, (PB89-208383, A05, MF-A01).

NCEER-88-0047 "Reinforced Concrete Frame Component Testing Facility - Design, Construction, Instrumentation and Operation," by S.P. Pessiki, C. Conley, T. Bond, P. Gergely and R.N. White, 12/16/88, (PB89-174478, A04, MF-A01).

NCEER-89-0001 "Effects of Protective Cushion and Soil Compliancy on the Response of Equipment Within a Seismically Excited Building," by J.A. HoLung, 2/16/89, (PB89-207179, A04, MF-A01).

NCEER-89-0002 "Statistical Evaluation of Response Modification Factors for Reinforced Concrete Structures," by H.H-M. Hwang and J-W. Jaw, 2/17/89, (PB89-207187, A05, MF-A01).

NCEER-89-0003 "Hysteretic Columns Under Random Excitation," by G-Q. Cai and Y.K. Lin, 1/9/89, (PB89-196513, A03, MF-A01).

NCEER-89-0004 "Experimental Study of `Elephant Foot Bulge' Instability of Thin-Walled Metal Tanks," by Z-H. Jia and R.L. Ketter, 2/22/89, (PB89-207195, A03, MF-A01).

NCEER-89-0005 "Experiment on Performance of Buried Pipelines Across San Andreas Fault," by J. Isenberg, E. Richardson and T.D. O'Rourke, 3/10/89, (PB89-218440, A04, MF-A01). This report is available only through NTIS (see address given above).

NCEER-89-0006 "A Knowledge-Based Approach to Structural Design of Earthquake-Resistant Buildings," by M. Subramani, P. Gergely, C.H. Conley, J.F. Abel and A.H. Zaghw, 1/15/89, (PB89-218465, A06, MF-A01).

NCEER-89-0007 "Liquefaction Hazards and Their Effects on Buried Pipelines," by T.D. O'Rourke and P.A. Lane, 2/1/89, (PB89-218481, A09, MF-A01).

NCEER-89-0008 "Fundamentals of System Identification in Structural Dynamics," by H. Imai, C-B. Yun, O. Maruyama and M. Shinozuka, 1/26/89, (PB89-207211, A04, MF-A01).

NCEER-89-0009 "Effects of the 1985 Michoacan Earthquake on Water Systems and Other Buried Lifelines in Mexico," by A.G. Ayala and M.J. O'Rourke, 3/8/89, (PB89-207229, A06, MF-A01).

NCEER-89-R010 "NCEER Bibliography of Earthquake Education Materials," by K.E.K. Ross, Second Revision, 9/1/89, (PB90-125352, A05, MF-A01). This report is replaced by NCEER-92-0018.

NCEER-89-0011 "Inelastic Three-Dimensional Response Analysis of Reinforced Concrete Building Structures (IDARC-3D), Part I - Modeling," by S.K. Kunnath and A.M. Reinhorn, 4/17/89, (PB90-114612, A07, MF-A01). This report is available only through NTIS (see address given above).

NCEER-89-0012 "Recommended Modifications to ATC-14," by C.D. Poland and J.O. Malley, 4/12/89, (PB90-108648, A15, MF-A01).

NCEER-89-0013 "Repair and Strengthening of Beam-to-Column Connections Subjected to Earthquake Loading," by M. Corazao and A.J. Durrani, 2/28/89, (PB90-109885, A06, MF-A01).

NCEER-89-0014 "Program EXKAL2 for Identification of Structural Dynamic Systems," by O. Maruyama, C-B. Yun, M. Hoshiya and M. Shinozuka, 5/19/89, (PB90-109877, A09, MF-A01).

NCEER-89-0015 "Response of Frames With Bolted Semi-Rigid Connections, Part I - Experimental Study and Analytical Predictions," by P.J. DiCorso, A.M. Reinhorn, J.R. Dickerson, J.B. Radziminski and W.L. Harper, 6/1/89, not available.

NCEER-89-0016 "ARMA Monte Carlo Simulation in Probabilistic Structural Analysis," by P.D. Spanos and M.P. Mignolet, 7/10/89, (PB90-109893, A03, MF-A01).

NCEER-89-P017 "Preliminary Proceedings from the Conference on Disaster Preparedness - The Place of Earthquake Education in Our Schools," Edited by K.E.K. Ross, 6/23/89, (PB90-108606, A03, MF-A01).

NCEER-89-0017 "Proceedings from the Conference on Disaster Preparedness - The Place of Earthquake Education in Our Schools," Edited by K.E.K. Ross, 12/31/89, (PB90-207895, A012, MF-A02). This report is available only through NTIS (see address given above).

NCEER-89-0018 "Multidimensional Models of Hysteretic Material Behavior for Vibration Analysis of Shape Memory Energy Absorbing Devices, by E.J. Graesser and F.A. Cozzarelli, 6/7/89, (PB90-164146, A04, MF-A01).

NCEER-89-0019 "Nonlinear Dynamic Analysis of Three-Dimensional Base Isolated Structures (3D-BASIS)," by S. Nagarajaiah, A.M. Reinhorn and M.C. Constantinou, 8/3/89, (PB90-161936, A06, MF-A01). This report has been replaced by NCEER-93-0011.

NCEER-89-0020 "Structural Control Considering Time-Rate of Control Forces and Control Rate Constraints," by F.Y. Cheng and C.P. Pantelides, 8/3/89, (PB90-120445, A04, MF-A01).

NCEER-89-0021 "Subsurface Conditions of Memphis and Shelby County," by K.W. Ng, T-S. Chang and H-H.M. Hwang, 7/26/89, (PB90-120437, A03, MF-A01).

NCEER-89-0022 "Seismic Wave Propagation Effects on Straight Jointed Buried Pipelines," by K. Elhmadi and M.J. O'Rourke, 8/24/89, (PB90-162322, A10, MF-A02).

NCEER-89-0023 "Workshop on Serviceability Analysis of Water Delivery Systems," edited by M. Grigoriu, 3/6/89, (PB90-127424, A03, MF-A01).

NCEER-89-0024 "Shaking Table Study of a 1/5 Scale Steel Frame Composed of Tapered Members," by K.C. Chang, J.S. Hwang and G.C. Lee, 9/18/89, (PB90-160169, A04, MF-A01).

NCEER-89-0025 "DYNA1D: A Computer Program for Nonlinear Seismic Site Response Analysis - Technical Documentation," by Jean H. Prevost, 9/14/89, (PB90-161944, A07, MF-A01). This report is available only through NTIS (see address given above).

NCEER-89-0026 "1:4 Scale Model Studies of Active Tendon Systems and Active Mass Dampers for Aseismic Protection," by A.M. Reinhorn, T.T. Soong, R.C. Lin, Y.P. Yang, Y. Fukao, H. Abe and M. Nakai, 9/15/89, (PB90-173246, A10, MF-A02). This report is available only through NTIS (see address given above).

NCEER-89-0027 "Scattering of Waves by Inclusions in a Nonhomogeneous Elastic Half Space Solved by Boundary Element Methods," by P.K. Hadley, A. Askar and A.S. Cakmak, 6/15/89, (PB90-145699, A07, MF-A01).

NCEER-89-0028 "Statistical Evaluation of Deflection Amplification Factors for Reinforced Concrete Structures," by H.H.M. Hwang, J-W. Jaw and A.L. Ch'ng, 8/31/89, (PB90-164633, A05, MF-A01).

NCEER-89-0029 "Bedrock Accelerations in Memphis Area Due to Large New Madrid Earthquakes," by H.H.M. Hwang, C.H.S. Chen and G. Yu, 11/7/89, (PB90-162330, A04, MF-A01).

NCEER-89-0030 "Seismic Behavior and Response Sensitivity of Secondary Structural Systems," by Y.Q. Chen and T.T. Soong, 10/23/89, (PB90-164658, A08, MF-A01).

NCEER-89-0031 "Random Vibration and Reliability Analysis of Primary-Secondary Structural Systems," by Y. Ibrahim, M. Grigoriu and T.T. Soong, 11/10/89, (PB90-161951, A04, MF-A01).

NCEER-89-0032 "Proceedings from the Second U.S. - Japan Workshop on Liquefaction, Large Ground Deformation and Their Effects on Lifelines, September 26-29, 1989," Edited by T.D. O'Rourke and M. Hamada, 12/1/89, (PB90-209388, A22, MF-A03).

NCEER-89-0033 "Deterministic Model for Seismic Damage Evaluation of Reinforced Concrete Structures," by J.M. Bracci, A.M. Reinhorn, J.B. Mander and S.K. Kunnath, 9/27/89, (PB91-108803, A06, MF-A01).

NCEER-89-0034 "On the Relation Between Local and Global Damage Indices," by E. DiPasquale and A.S. Cakmak, 8/15/89, (PB90-173865, A05, MF-A01).

NCEER-89-0035 "Cyclic Undrained Behavior of Nonplastic and Low Plasticity Silts," by A.J. Walker and H.E. Stewart, 7/26/89, (PB90-183518, A10, MF-A01).

NCEER-89-0036 "Liquefaction Potential of Surficial Deposits in the City of Buffalo, New York," by M. Budhu, R. Giese and L. Baumgrass, 1/17/89, (PB90-208455, A04, MF-A01).

NCEER-89-0037 "A Deterministic Assessment of Effects of Ground Motion Incoherence," by A.S. Veletsos and Y. Tang, 7/15/89, (PB90-164294, A03, MF-A01).

NCEER-89-0038 "Workshop on Ground Motion Parameters for Seismic Hazard Mapping," July 17-18, 1989, edited by R.V. Whitman, 12/1/89, (PB90-173923, A04, MF-A01).

NCEER-89-0039 "Seismic Effects on Elevated Transit Lines of the New York City Transit Authority," by C.J. Costantino, C.A. Miller and E. Heymsfield, 12/26/89, (PB90-207887, A06, MF-A01).

NCEER-89-0040 "Centrifugal Modeling of Dynamic Soil-Structure Interaction," by K. Weissman, Supervised by J.H. Prevost, 5/10/89, (PB90-207879, A07, MF-A01).

NCEER-89-0041 "Linearized Identification of Buildings With Cores for Seismic Vulnerability Assessment," by I-K. Ho and A.E. Aktan, 11/1/89, (PB90-251943, A07, MF-A01).

NCEER-90-0001 "Geotechnical and Lifeline Aspects of the October 17, 1989 Loma Prieta Earthquake in San Francisco," by T.D. O'Rourke, H.E. Stewart, F.T. Blackburn and T.S. Dickerman, 1/90, (PB90-208596, A05, MF-A01).

NCEER-90-0002 "Nonnormal Secondary Response Due to Yielding in a Primary Structure," by D.C.K. Chen and L.D. Lutes, 2/28/90, (PB90-251976, A07, MF-A01).

NCEER-90-0003 "Earthquake Education Materials for Grades K-12," by K.E.K. Ross, 4/16/90, (PB91-251984, A05, MF-A05). This report has been replaced by NCEER-92-0018.

NCEER-90-0004 "Catalog of Strong Motion Stations in Eastern North America," by R.W. Busby, 4/3/90, (PB90-251984, A05, MF-A01).

NCEER-90-0005 "NCEER Strong-Motion Data Base: A User Manual for the GeoBase Release (Version 1.0 for the Sun3)," by P. Friberg and K. Jacob, 3/31/90 (PB90-258062, A04, MF-A01).

NCEER-90-0006 "Seismic Hazard Along a Crude Oil Pipeline in the Event of an 1811-1812 Type New Madrid Earthquake," by H.H.M. Hwang and C-H.S. Chen, 4/16/90, (PB90-258054, A04, MF-A01).

NCEER-90-0007 "Site-Specific Response Spectra for Memphis Sheahan Pumping Station," by H.H.M. Hwang and C.S. Lee, 5/15/90, (PB91-108811, A05, MF-A01).

NCEER-90-0008 "Pilot Study on Seismic Vulnerability of Crude Oil Transmission Systems," by T. Ariman, R. Dobry, M. Grigoriu, F. Kozin, M. O'Rourke, T. O'Rourke and M. Shinozuka, 5/25/90, (PB91-108837, A06, MF-A01).

NCEER-90-0009 "A Program to Generate Site Dependent Time Histories: EQGEN," by G.W. Ellis, M. Srinivasan and A.S. Cakmak, 1/30/90, (PB91-108829, A04, MF-A01).

NCEER-90-0010 "Active Isolation for Seismic Protection of Operating Rooms," by M.E. Talbott, Supervised by M. Shinozuka, 6/8/9, (PB91-110205, A05, MF-A01).

NCEER-90-0011 "Program LINEARID for Identification of Linear Structural Dynamic Systems," by C-B. Yun and M. Shinozuka, 6/25/90, (PB91-110312, A08, MF-A01).

NCEER-90-0012 "Two-Dimensional Two-Phase Elasto-Plastic Seismic Response of Earth Dams," by A.N. Yiagos, Supervised by J.H. Prevost, 6/20/90, (PB91-110197, A13, MF-A02).

NCEER-90-0013 "Secondary Systems in Base-Isolated Structures: Experimental Investigation, Stochastic Response and Stochastic Sensitivity," by G.D. Manolis, G. Juhn, M.C. Constantinou and A.M. Reinhorn, 7/1/90, (PB91-110320, A08, MF-A01).

NCEER-90-0014 "Seismic Behavior of Lightly-Reinforced Concrete Column and Beam-Column Joint Details," by S.P. Pessiki, C.H. Conley, P. Gergely and R.N. White, 8/22/90, (PB91-108795, A11, MF-A02).

NCEER-90-0015 "Two Hybrid Control Systems for Building Structures Under Strong Earthquakes," by J.N. Yang and A. Danielians, 6/29/90, (PB91-125393, A04, MF-A01).

NCEER-90-0016 "Instantaneous Optimal Control with Acceleration and Velocity Feedback," by J.N. Yang and Z. Li, 6/29/90, (PB91-125401, A03, MF-A01).

NCEER-90-0017 "Reconnaissance Report on the Northern Iran Earthquake of June 21, 1990," by M. Mehrain, 10/4/90, (PB91-125377, A03, MF-A01).

NCEER-90-0018 "Evaluation of Liquefaction Potential in Memphis and Shelby County," by T.S. Chang, P.S. Tang, C.S. Lee and H. Hwang, 8/10/90, (PB91-125427, A09, MF-A01).

NCEER-90-0019 "Experimental and Analytical Study of a Combined Sliding Disc Bearing and Helical Steel Spring Isolation System," by M.C. Constantinou, A.S. Mokha and A.M. Reinhorn, 10/4/90, (PB91-125385, A06, MF-A01). This report is available only through NTIS (see address given above).

NCEER-90-0020 "Experimental Study and Analytical Prediction of Earthquake Response of a Sliding Isolation System with a Spherical Surface," by A.S. Mokha, M.C. Constantinou and A.M. Reinhorn, 10/11/90, (PB91-125419, A05, MF-A01).

NCEER-90-0021 "Dynamic Interaction Factors for Floating Pile Groups," by G. Gazetas, K. Fan, A. Kaynia and E. Kausel, 9/10/90, (PB91-170381, A05, MF-A01).

NCEER-90-0022 "Evaluation of Seismic Damage Indices for Reinforced Concrete Structures," by S. Rodriguez-Gomez and A.S. Cakmak, 9/30/90, PB91-171322, A06, MF-A01).

NCEER-90-0023 "Study of Site Response at a Selected Memphis Site," by H. Desai, S. Ahmad, E.S. Gazetas and M.R. Oh, 10/11/90, (PB91-196857, A03, MF-A01).

NCEER-90-0024 "A User's Guide to Strongmo: Version 1.0 of NCEER's Strong-Motion Data Access Tool for PCs and Terminals," by P.A. Friberg and C.A.T. Susch, 11/15/90, (PB91-171272, A03, MF-A01).

NCEER-90-0025 "A Three-Dimensional Analytical Study of Spatial Variability of Seismic Ground Motions," by L-L. Hong and A.H.-S. Ang, 10/30/90, (PB91-170399, A09, MF-A01).

NCEER-90-0026 "MUMOID User's Guide - A Program for the Identification of Modal Parameters," by S. Rodriguez-Gomez and E. DiPasquale, 9/30/90, (PB91-171298, A04, MF-A01).

NCEER-90-0027 "SARCF-II User's Guide - Seismic Analysis of Reinforced Concrete Frames," by S. Rodriguez-Gomez, Y.S. Chung and C. Meyer, 9/30/90, (PB91-171280, A05, MF-A01).

NCEER-90-0028 "Viscous Dampers: Testing, Modeling and Application in Vibration and Seismic Isolation," by N. Makris and M.C. Constantinou, 12/20/90 (PB91-190561, A06, MF-A01).

NCEER-90-0029 "Soil Effects on Earthquake Ground Motions in the Memphis Area," by H. Hwang, C.S. Lee, K.W. Ng and T.S. Chang, 8/2/90, (PB91-190751, A05, MF-A01).

NCEER-91-0001 "Proceedings from the Third Japan-U.S. Workshop on Earthquake Resistant Design of Lifeline Facilities and Countermeasures for Soil Liquefaction, December 17-19, 1990," edited by T.D. O'Rourke and M. Hamada, 2/1/91, (PB91-179259, A99, MF-A04).

NCEER-91-0002 "Physical Space Solutions of Non-Proportionally Damped Systems," by M. Tong, Z. Liang and G.C. Lee, 1/15/91, (PB91-179242, A04, MF-A01).

NCEER-91-0003 "Seismic Response of Single Piles and Pile Groups," by K. Fan and G. Gazetas, 1/10/91, (PB92-174994, A04, MF-A01).

NCEER-91-0004 "Damping of Structures: Part 1 - Theory of Complex Damping," by Z. Liang and G. Lee, 10/10/91, (PB92-197235, A12, MF-A03).

NCEER-91-0005 "3D-BASIS - Nonlinear Dynamic Analysis of Three Dimensional Base Isolated Structures: Part II," by S. Nagarajaiah, A.M. Reinhorn and M.C. Constantinou, 2/28/91, (PB91-190553, A07, MF-A01). This report has been replaced by NCEER-93-0011.

NCEER-91-0006 "A Multidimensional Hysteretic Model for Plasticity Deforming Metals in Energy Absorbing Devices," by E.J. Graesser and F.A. Cozzarelli, 4/9/91, (PB92-108364, A04, MF-A01).

NCEER-91-0007 "A Framework for Customizable Knowledge-Based Expert Systems with an Application to a KBES for Evaluating the Seismic Resistance of Existing Buildings," by E.G. Ibarra-Anaya and S.J. Fenves, 4/9/91, (PB91-210930, A08, MF-A01).

NCEER-91-0008 "Nonlinear Analysis of Steel Frames with Semi-Rigid Connections Using the Capacity Spectrum Method," by G.G. Deierlein, S-H. Hsieh, Y-J. Shen and J.F. Abel, 7/2/91, (PB92-113828, A05, MF-A01).

NCEER-91-0009 "Earthquake Education Materials for Grades K-12," by K.E.K. Ross, 4/30/91, (PB91-212142, A06, MF-A01). This report has been replaced by NCEER-92-0018.

NCEER-91-0010 "Phase Wave Velocities and Displacement Phase Differences in a Harmonically Oscillating Pile," by N. Makris and G. Gazetas, 7/8/91, (PB92-108356, A04, MF-A01).

NCEER-91-0011 "Dynamic Characteristics of a Full-Size Five-Story Steel Structure and a 2/5 Scale Model," by K.C. Chang, G.C. Yao, G.C. Lee, D.S. Hao and Y.C. Yeh," 7/2/91, (PB93-116648, A06, MF-A02).

NCEER-91-0012 "Seismic Response of a 2/5 Scale Steel Structure with Added Viscoelastic Dampers," by K.C. Chang, T.T. Soong, S-T. Oh and M.L. Lai, 5/17/91, (PB92-110816, A05, MF-A01).

NCEER-91-0013 "Earthquake Response of Retaining Walls; Full-Scale Testing and Computational Modeling," by S. Alampalli and A-W.M. Elgamal, 6/20/91, not available.

NCEER-91-0014 "3D-BASIS-M: Nonlinear Dynamic Analysis of Multiple Building Base Isolated Structures," by P.C. Tsopelas, S. Nagarajaiah, M.C. Constantinou and A.M. Reinhorn, 5/28/91, (PB92-113885, A09, MF-A02).

NCEER-91-0015 "Evaluation of SEAOC Design Requirements for Sliding Isolated Structures," by D. Theodossiou and M.C. Constantinou, 6/10/91, (PB92-114602, A11, MF-A03).

NCEER-91-0016 "Closed-Loop Modal Testing of a 27-Story Reinforced Concrete Flat Plate-Core Building," by H.R. Somaprasad, T. Toksoy, H. Yoshiyuki and A.E. Aktan, 7/15/91, (PB92-129980, A07, MF-A02).

NCEER-91-0017 "Shake Table Test of a 1/6 Scale Two-Story Lightly Reinforced Concrete Building," by A.G. El-Attar, R.N. White and P. Gergely, 2/28/91, (PB92-222447, A06, MF-A02).

NCEER-91-0018 "Shake Table Test of a 1/8 Scale Three-Story Lightly Reinforced Concrete Building," by A.G. El-Attar, R.N. White and P. Gergely, 2/28/91, (PB93-116630, A08, MF-A02).

NCEER-91-0019 "Transfer Functions for Rigid Rectangular Foundations," by A.S. Veletsos, A.M. Prasad and W.H. Wu, 7/31/91, not available.

NCEER-91-0020 "Hybrid Control of Seismic-Excited Nonlinear and Inelastic Structural Systems," by J.N. Yang, Z. Li and A. Danielians, 8/1/91, (PB92-143171, A06, MF-A02).

NCEER-91-0021 "The NCEER-91 Earthquake Catalog: Improved Intensity-Based Magnitudes and Recurrence Relations for U.S. Earthquakes East of New Madrid," by L. Seeber and J.G. Armbruster, 8/28/91, (PB92-176742, A06, MF-A02).

NCEER-91-0022 "Proceedings from the Implementation of Earthquake Planning and Education in Schools: The Need for Change - The Roles of the Changemakers," by K.E.K. Ross and F. Winslow, 7/23/91, (PB92-129998, A12, MF-A03).

NCEER-91-0023 "A Study of Reliability-Based Criteria for Seismic Design of Reinforced Concrete Frame Buildings," by H.H.M. Hwang and H-M. Hsu, 8/10/91, (PB92-140235, A09, MF-A02).

NCEER-91-0024 "Experimental Verification of a Number of Structural System Identification Algorithms," by R.G. Ghanem, H. Gavin and M. Shinozuka, 9/18/91, (PB92-176577, A18, MF-A04).

NCEER-91-0025 "Probabilistic Evaluation of Liquefaction Potential," by H.H.M. Hwang and C.S. Lee," 11/25/91, (PB92-143429, A05, MF-A01).

NCEER-91-0026 "Instantaneous Optimal Control for Linear, Nonlinear and Hysteretic Structures - Stable Controllers," by J.N. Yang and Z. Li, 11/15/91, (PB92-163807, A04, MF-A01).

NCEER-91-0027 "Experimental and Theoretical Study of a Sliding Isolation System for Bridges," by M.C. Constantinou, A. Kartoum, A.M. Reinhorn and P. Bradford, 11/15/91, (PB92-176973, A10, MF-A03).

NCEER-92-0001 "Case Studies of Liquefaction and Lifeline Performance During Past Earthquakes, Volume 1: Japanese Case Studies," Edited by M. Hamada and T. O'Rourke, 2/17/92, (PB92-197243, A18, MF-A04).

NCEER-92-0002 "Case Studies of Liquefaction and Lifeline Performance During Past Earthquakes, Volume 2: United States Case Studies," Edited by T. O'Rourke and M. Hamada, 2/17/92, (PB92-197250, A20, MF-A04).

NCEER-92-0003 "Issues in Earthquake Education," Edited by K. Ross, 2/3/92, (PB92-222389, A07, MF-A02).

NCEER-92-0004 "Proceedings from the First U.S. - Japan Workshop on Earthquake Protective Systems for Bridges," Edited by I.G. Buckle, 2/4/92, (PB94-142239, A99, MF-A06).

NCEER-92-0005 "Seismic Ground Motion from a Haskell-Type Source in a Multiple-Layered Half-Space," A.P. Theoharis, G. Deodatis and M. Shinozuka, 1/2/92, not available.

NCEER-92-0006 "Proceedings from the Site Effects Workshop," Edited by R. Whitman, 2/29/92, (PB92-197201, A04, MF-A01).

NCEER-92-0007 "Engineering Evaluation of Permanent Ground Deformations Due to Seismically-Induced Liquefaction," by M.H. Baziar, R. Dobry and A-W.M. Elgamal, 3/24/92, (PB92-222421, A13, MF-A03).

NCEER-92-0008 "A Procedure for the Seismic Evaluation of Buildings in the Central and Eastern United States," by C.D. Poland and J.O. Malley, 4/2/92, (PB92-222439, A20, MF-A04).

NCEER-92-0009 "Experimental and Analytical Study of a Hybrid Isolation System Using Friction Controllable Sliding Bearings," by M.Q. Feng, S. Fujii and M. Shinozuka, 5/15/92, (PB93-150282, A06, MF-A02).

NCEER-92-0010 "Seismic Resistance of Slab-Column Connections in Existing Non-Ductile Flat-Plate Buildings," by A.J. Durrani and Y. Du, 5/18/92, (PB93-116812, A06, MF-A02).

NCEER-92-0011 "The Hysteretic and Dynamic Behavior of Brick Masonry Walls Upgraded by Ferrocement Coatings Under Cyclic Loading and Strong Simulated Ground Motion," by H. Lee and S.P. Prawel, 5/11/92, not available.

NCEER-92-0012 "Study of Wire Rope Systems for Seismic Protection of Equipment in Buildings," by G.F. Demetriades, M.C. Constantinou and A.M. Reinhorn, 5/20/92, (PB93-116655, A08, MF-A02).

NCEER-92-0013 "Shape Memory Structural Dampers: Material Properties, Design and Seismic Testing," by P.R. Witting and F.A. Cozzarelli, 5/26/92, (PB93-116663, A05, MF-A01).

NCEER-92-0014 "Longitudinal Permanent Ground Deformation Effects on Buried Continuous Pipelines," by M.J. O'Rourke, and C. Nordberg, 6/15/92, (PB93-116671, A08, MF-A02).

NCEER-92-0015 "A Simulation Method for Stationary Gaussian Random Functions Based on the Sampling Theorem," by M. Grigoriu and S. Balopoulou, 6/11/92, (PB93-127496, A05, MF-A01).

NCEER-92-0016 "Gravity-Load-Designed Reinforced Concrete Buildings: Seismic Evaluation of Existing Construction and Detailing Strategies for Improved Seismic Resistance," by G.W. Hoffmann, S.K. Kunnath, A.M. Reinhorn and J.B. Mander, 7/15/92, (PB94-142007, A08, MF-A02).

NCEER-92-0017 "Observations on Water System and Pipeline Performance in the Limón Area of Costa Rica Due to the April 22, 1991 Earthquake," by M. O'Rourke and D. Ballantyne, 6/30/92, (PB93-126811, A06, MF-A02).

NCEER-92-0018 "Fourth Edition of Earthquake Education Materials for Grades K-12," Edited by K.E.K. Ross, 8/10/92, (PB93-114023, A07, MF-A02).

NCEER-92-0019 "Proceedings from the Fourth Japan-U.S. Workshop on Earthquake Resistant Design of Lifeline Facilities and Countermeasures for Soil Liquefaction," Edited by M. Hamada and T.D. O'Rourke, 8/12/92, (PB93-163939, A99, MF-E11).

NCEER-92-0020 "Active Bracing System: A Full Scale Implementation of Active Control," by A.M. Reinhorn, T.T. Soong, R.C. Lin, M.A. Riley, Y.P. Wang, S. Aizawa and M. Higashino, 8/14/92, (PB93-127512, A06, MF-A02).

NCEER-92-0021 "Empirical Analysis of Horizontal Ground Displacement Generated by Liquefaction-Induced Lateral Spreads," by S.F. Bartlett and T.L. Youd, 8/17/92, (PB93-188241, A06, MF-A02).

NCEER-92-0022 "IDARC Version 3.0: Inelastic Damage Analysis of Reinforced Concrete Structures," by S.K. Kunnath, A.M. Reinhorn and R.F. Lobo, 8/31/92, (PB93-227502, A07, MF-A02).

NCEER-92-0023 "A Semi-Empirical Analysis of Strong-Motion Peaks in Terms of Seismic Source, Propagation Path and Local Site Conditions, by M. Kamiyama, M.J. O'Rourke and R. Flores-Berrones, 9/9/92, (PB93-150266, A08, MF-A02).

NCEER-92-0024 "Seismic Behavior of Reinforced Concrete Frame Structures with Nonductile Details, Part I: Summary of Experimental Findings of Full Scale Beam-Column Joint Tests," by A. Beres, R.N. White and P. Gergely, 9/30/92, (PB93-227783, A05, MF-A01).

NCEER-92-0025 "Experimental Results of Repaired and Retrofitted Beam-Column Joint Tests in Lightly Reinforced Concrete Frame Buildings," by A. Beres, S. El-Borgi, R.N. White and P. Gergely, 10/29/92, (PB93-227791, A05, MF-A01).

NCEER-92-0026 "A Generalization of Optimal Control Theory: Linear and Nonlinear Structures," by J.N. Yang, Z. Li and S. Vongchavalitkul, 11/2/92, (PB93-188621, A05, MF-A01).

NCEER-92-0027 "Seismic Resistance of Reinforced Concrete Frame Structures Designed Only for Gravity Loads: Part I - Design and Properties of a One-Third Scale Model Structure," by J.M. Bracci, A.M. Reinhorn and J.B. Mander, 12/1/92, (PB94-104502, A08, MF-A02).

NCEER-92-0028 "Seismic Resistance of Reinforced Concrete Frame Structures Designed Only for Gravity Loads: Part II - Experimental Performance of Subassemblages," by L.E. Aycardi, J.B. Mander and A.M. Reinhorn, 12/1/92, (PB94-104510, A08, MF-A02).

NCEER-92-0029 "Seismic Resistance of Reinforced Concrete Frame Structures Designed Only for Gravity Loads: Part III - Experimental Performance and Analytical Study of a Structural Model," by J.M. Bracci, A.M. Reinhorn and J.B. Mander, 12/1/92, (PB93-227528, A09, MF-A01).

NCEER-92-0030 "Evaluation of Seismic Retrofit of Reinforced Concrete Frame Structures: Part I - Experimental Performance of Retrofitted Subassemblages," by D. Choudhuri, J.B. Mander and A.M. Reinhorn, 12/8/92, (PB93-198307, A07, MF-A02).

NCEER-92-0031 "Evaluation of Seismic Retrofit of Reinforced Concrete Frame Structures: Part II - Experimental Performance and Analytical Study of a Retrofitted Structural Model," by J.M. Bracci, A.M. Reinhorn and J.B. Mander, 12/8/92, (PB93-198315, A09, MF-A03).

NCEER-92-0032 "Experimental and Analytical Investigation of Seismic Response of Structures with Supplemental Fluid Viscous Dampers," by M.C. Constantinou and M.D. Symans, 12/21/92, (PB93-191435, A10, MF-A03). This report is available only through NTIS (see address given above).

NCEER-92-0033 "Reconnaissance Report on the Cairo, Egypt Earthquake of October 12, 1992," by M. Khater, 12/23/92, (PB93-188621, A03, MF-A01).

NCEER-92-0034 "Low-Level Dynamic Characteristics of Four Tall Flat-Plate Buildings in New York City," by H. Gavin, S. Yuan, J. Grossman, E. Pekelis and K. Jacob, 12/28/92, (PB93-188217, A07, MF-A02).

NCEER-93-0001 "An Experimental Study on the Seismic Performance of Brick-Infilled Steel Frames With and Without Retrofit," by J.B. Mander, B. Nair, K. Wojtkowski and J. Ma, 1/29/93, (PB93-227510, A07, MF-A02).

NCEER-93-0002 "Social Accounting for Disaster Preparedness and Recovery Planning," by S. Cole, E. Pantoja and V. Razak, 2/22/93, (PB94-142114, A12, MF-A03).

NCEER-93-0003 "Assessment of 1991 NEHRP Provisions for Nonstructural Components and Recommended Revisions," by T.T. Soong, G. Chen, Z. Wu, R-H. Zhang and M. Grigoriu, 3/1/93, (PB93-188639, A06, MF-A02).

NCEER-93-0004 "Evaluation of Static and Response Spectrum Analysis Procedures of SEAOC/UBC for Seismic Isolated Structures," by C.W. Winters and M.C. Constantinou, 3/23/93, (PB93-198299, A10, MF-A03).

NCEER-93-0005 "Earthquakes in the Northeast - Are We Ignoring the Hazard? A Workshop on Earthquake Science and Safety for Educators," edited by K.E.K. Ross, 4/2/93, (PB94-103066, A09, MF-A02).

NCEER-93-0006 "Inelastic Response of Reinforced Concrete Structures with Viscoelastic Braces," by R.F. Lobo, J.M. Bracci, K.L. Shen, A.M. Reinhorn and T.T. Soong, 4/5/93, (PB93-227486, A05, MF-A02).

NCEER-93-0007 "Seismic Testing of Installation Methods for Computers and Data Processing Equipment," by K. Kosar, T.T. Soong, K.L. Shen, J.A. HoLung and Y.K. Lin, 4/12/93, (PB93-198299, A07, MF-A02).

NCEER-93-0008 "Retrofit of Reinforced Concrete Frames Using Added Dampers," by A. Reinhorn, M. Constantinou and C. Li, not available.

NCEER-93-0009 "Seismic Behavior and Design Guidelines for Steel Frame Structures with Added Viscoelastic Dampers," by K.C. Chang, M.L. Lai, T.T. Soong, D.S. Hao and Y.C. Yeh, 5/1/93, (PB94-141959, A07, MF-A02).

NCEER-93-0010 "Seismic Performance of Shear-Critical Reinforced Concrete Bridge Piers," by J.B. Mander, S.M. Waheed, M.T.A. Chaudhary and S.S. Chen, 5/12/93, (PB93-227494, A08, MF-A02).

NCEER-93-0011 "3D-BASIS-TABS: Computer Program for Nonlinear Dynamic Analysis of Three Dimensional Base Isolated Structures," by S. Nagarajaiah, C. Li, A.M. Reinhorn and M.C. Constantinou, 8/2/93, (PB94-141819, A09, MF-A02).

NCEER-93-0012 "Effects of Hydrocarbon Spills from an Oil Pipeline Break on Ground Water," by O.J. Helweg and H.H.M. Hwang, 8/3/93, (PB94-141942, A06, MF-A02).

NCEER-93-0013 "Simplified Procedures for Seismic Design of Nonstructural Components and Assessment of Current Code Provisions," by M.P. Singh, L.E. Suarez, E.E. Matheu and G.O. Maldonado, 8/4/93, (PB94-141827, A09, MF-A02).

NCEER-93-0014 "An Energy Approach to Seismic Analysis and Design of Secondary Systems," by G. Chen and T.T. Soong, 8/6/93, (PB94-142767, A11, MF-A03).

NCEER-93-0015 "Proceedings from School Sites: Becoming Prepared for Earthquakes - Commemorating the Third Anniversary of the Loma Prieta Earthquake," Edited by F.E. Winslow and K.E.K. Ross, 8/16/93, (PB94-154275, A16, MF-A02).

NCEER-93-0016 "Reconnaissance Report of Damage to Historic Monuments in Cairo, Egypt Following the October 12, 1992 Dahshur Earthquake," by D. Sykora, D. Look, G. Croci, E. Karaesmen and E. Karaesmen, 8/19/93, (PB94-142221, A08, MF-A02).

NCEER-93-0017 "The Island of Guam Earthquake of August 8, 1993," by S.W. Swan and S.K. Harris, 9/30/93, (PB94-141843, A04, MF-A01).

NCEER-93-0018 "Engineering Aspects of the October 12, 1992 Egyptian Earthquake," by A.W. Elgamal, M. Amer, K. Adalier and A. Abul-Fadl, 10/7/93, (PB94-141983, A05, MF-A01).

NCEER-93-0019 "Development of an Earthquake Motion Simulator and its Application in Dynamic Centrifuge Testing," by I. Krstelj, Supervised by J.H. Prevost, 10/23/93, (PB94-181773, A-10, MF-A03).

NCEER-93-0020 "NCEER-Taisei Corporation Research Program on Sliding Seismic Isolation Systems for Bridges: Experimental and Analytical Study of a Friction Pendulum System (FPS)," by M.C. Constantinou, P. Tsopelas, Y-S. Kim and S. Okamoto, 11/1/93, (PB94-142775, A08, MF-A02).

NCEER-93-0021 "Finite Element Modeling of Elastomeric Seismic Isolation Bearings," by L.J. Billings, Supervised by R. Shepherd, 11/8/93, not available.

NCEER-93-0022 "Seismic Vulnerability of Equipment in Critical Facilities: Life-Safety and Operational Consequences," by K. Porter, G.S. Johnson, M.M. Zadeh, C. Scawthorn and S. Eder, 11/24/93, (PB94-181765, A16, MF-A03).

NCEER-93-0023 "Hokkaido Nansei-oki, Japan Earthquake of July 12, 1993, by P.I. Yanev and C.R. Scawthorn, 12/23/93, (PB94-181500, A07, MF-A01).

NCEER-94-0001 "An Evaluation of Seismic Serviceability of Water Supply Networks with Application to the San Francisco Auxiliary Water Supply System," by I. Markov, Supervised by M. Grigoriu and T. O'Rourke, 1/21/94, (PB94-204013, A07, MF-A02).

NCEER-94-0002 "NCEER-Taisei Corporation Research Program on Sliding Seismic Isolation Systems for Bridges: Experimental and Analytical Study of Systems Consisting of Sliding Bearings, Rubber Restoring Force Devices and Fluid Dampers," Volumes I and II, by P. Tsopelas, S. Okamoto, M.C. Constantinou, D. Ozaki and S. Fujii, 2/4/94, (PB94-181740, A09, MF-A02 and PB94-181757, A12, MF-A03).

NCEER-94-0003 "A Markov Model for Local and Global Damage Indices in Seismic Analysis," by S. Rahman and M. Grigoriu, 2/18/94, (PB94-206000, A12, MF-A03).

NCEER-94-0004 "Proceedings from the NCEER Workshop on Seismic Response of Masonry Infills," edited by D.P. Abrams, 3/1/94, (PB94-180783, A07, MF-A02).

NCEER-94-0005 "The Northridge, California Earthquake of January 17, 1994: General Reconnaissance Report," edited by J.D. Goltz, 3/11/94, (PB94-193943, A10, MF-A03).

NCEER-94-0006 "Seismic Energy Based Fatigue Damage Analysis of Bridge Columns: Part I - Evaluation of Seismic Capacity," by G.A. Chang and J.B. Mander, 3/14/94, (PB94-219185, A11, MF-A03).

NCEER-94-0007 "Seismic Isolation of Multi-Story Frame Structures Using Spherical Sliding Isolation Systems," by T.M. Al-Hussaini, V.A. Zayas and M.C. Constantinou, 3/17/94, (PB94-193745, A09, MF-A02).

NCEER-94-0008 "The Northridge, California Earthquake of January 17, 1994: Performance of Highway Bridges," edited by I.G. Buckle, 3/24/94, (PB94-193851, A06, MF-A02).

NCEER-94-0009 "Proceedings of the Third U.S.-Japan Workshop on Earthquake Protective Systems for Bridges," edited by I.G. Buckle and I. Friedland, 3/31/94, (PB94-195815, A99, MF-A06).

NCEER-94-0010 "3D-BASIS-ME: Computer Program for Nonlinear Dynamic Analysis of Seismically Isolated Single and Multiple Structures and Liquid Storage Tanks," by P.C. Tsopelas, M.C. Constantinou and A.M. Reinhorn, 4/12/94, (PB94-204922, A09, MF-A02).

NCEER-94-0011 "The Northridge, California Earthquake of January 17, 1994: Performance of Gas Transmission Pipelines," by T.D. O'Rourke and M.C. Palmer, 5/16/94, (PB94-204989, A05, MF-A01).

NCEER-94-0012 "Feasibility Study of Replacement Procedures and Earthquake Performance Related to Gas Transmission Pipelines," by T.D. O'Rourke and M.C. Palmer, 5/25/94, (PB94-206638, A09, MF-A02).

NCEER-94-0013 "Seismic Energy Based Fatigue Damage Analysis of Bridge Columns: Part II - Evaluation of Seismic Demand," by G.A. Chang and J.B. Mander, 6/1/94, (PB95-18106, A08, MF-A02).

NCEER-94-0014 "NCEER-Taisei Corporation Research Program on Sliding Seismic Isolation Systems for Bridges: Experimental and Analytical Study of a System Consisting of Sliding Bearings and Fluid Restoring Force/Damping Devices," by P. Tsopelas and M.C. Constantinou, 6/13/94, (PB94-219144, A10, MF-A03).

NCEER-94-0015 "Generation of Hazard-Consistent Fragility Curves for Seismic Loss Estimation Studies," by H. Hwang and J-R. Huo, 6/14/94, (PB95-181996, A09, MF-A02).

NCEER-94-0016 "Seismic Study of Building Frames with Added Energy-Absorbing Devices," by W.S. Pong, C.S. Tsai and G.C. Lee, 6/20/94, (PB94-219136, A10, A03).

NCEER-94-0017 "Sliding Mode Control for Seismic-Excited Linear and Nonlinear Civil Engineering Structures," by J. Yang, J. Wu, A. Agrawal and Z. Li, 6/21/94, (PB95-138483, A06, MF-A02).

NCEER-94-0018 "3D-BASIS-TABS Version 2.0: Computer Program for Nonlinear Dynamic Analysis of Three Dimensional Base Isolated Structures," by A.M. Reinhorn, S. Nagarajaiah, M.C. Constantinou, P. Tsopelas and R. Li, 6/22/94, (PB95-182176, A08, MF-A02).

NCEER-94-0019 "Proceedings of the International Workshop on Civil Infrastructure Systems: Application of Intelligent Systems and Advanced Materials on Bridge Systems," Edited by G.C. Lee and K.C. Chang, 7/18/94, (PB95-252474, A20, MF-A04).

NCEER-94-0020 "Study of Seismic Isolation Systems for Computer Floors," by V. Lambrou and M.C. Constantinou, 7/19/94, (PB95-138533, A10, MF-A03).

NCEER-94-0021 "Proceedings of the U.S.-Italian Workshop on Guidelines for Seismic Evaluation and Rehabilitation of Unreinforced Masonry Buildings," Edited by D.P. Abrams and G.M. Calvi, 7/20/94, (PB95-138749, A13, MF-A03).

NCEER-94-0022 "NCEER-Taisei Corporation Research Program on Sliding Seismic Isolation Systems for Bridges: Experimental and Analytical Study of a System Consisting of Lubricated PTFE Sliding Bearings and Mild Steel Dampers," by P. Tsopelas and M.C. Constantinou, 7/22/94, (PB95-182184, A08, MF-A02).

NCEER-94-0023 "Development of Reliability-Based Design Criteria for Buildings Under Seismic Load," by Y.K. Wen, H. Hwang and M. Shinozuka, 8/1/94, (PB95-211934, A08, MF-A02).

NCEER-94-0024 "Experimental Verification of Acceleration Feedback Control Strategies for an Active Tendon System," by S.J. Dyke, B.F. Spencer, Jr., P. Quast, M.K. Sain, D.C. Kaspari, Jr. and T.T. Soong, 8/29/94, (PB95-212320, A05, MF-A01).

NCEER-94-0025 "Seismic Retrofitting Manual for Highway Bridges," Edited by I.G. Buckle and I.F. Friedland, published by the Federal Highway Administration (PB95-212676, A15, MF-A03).

NCEER-94-0026 "Proceedings from the Fifth U.S.-Japan Workshop on Earthquake Resistant Design of Lifeline Facilities and Countermeasures Against Soil Liquefaction," Edited by T.D. O'Rourke and M. Hamada, 11/7/94, (PB95-220802, A99, MF-E08).

NCEER-95-0001 "Experimental and Analytical Investigation of Seismic Retrofit of Structures with Supplemental Damping: Part 1 - Fluid Viscous Damping Devices," by A.M. Reinhorn, C. Li and M.C. Constantinou, 1/3/95, (PB95-266599, A09, MF-A02).

NCEER-95-0002 "Experimental and Analytical Study of Low-Cycle Fatigue Behavior of Semi-Rigid Top-And-Seat Angle Connections," by G. Pekcan, J.B. Mander and S.S. Chen, 1/5/95, (PB95-220042, A07, MF-A02).

NCEER-95-0003 "NCEER-ATC Joint Study on Fragility of Buildings," by T. Anagnos, C. Rojahn and A.S. Kiremidjian, 1/20/95, (PB95-220026, A06, MF-A02).

NCEER-95-0004 "Nonlinear Control Algorithms for Peak Response Reduction," by Z. Wu, T.T. Soong, V. Gattulli and R.C. Lin, 2/16/95, (PB95-220349, A05, MF-A01).

NCEER-95-0005 "Pipeline Replacement Feasibility Study: A Methodology for Minimizing Seismic and Corrosion Risks to Underground Natural Gas Pipelines," by R.T. Eguchi, H.A. Seligson and D.G. Honegger, 3/2/95, (PB95-252326, A06, MF-A02).

NCEER-95-0006 "Evaluation of Seismic Performance of an 11-Story Frame Building During the 1994 Northridge Earthquake," by F. Naeim, R. DiSulio, K. Benuska, A. Reinhorn and C. Li, not available.

NCEER-95-0007 "Prioritization of Bridges for Seismic Retrofitting," by N. Basöz and A.S. Kiremidjian, 4/24/95, (PB95-252300, A08, MF-A02).

NCEER-95-0008 "Method for Developing Motion Damage Relationships for Reinforced Concrete Frames," by A. Singhal and A.S. Kiremidjian, 5/11/95, (PB95-266607, A06, MF-A02).

NCEER-95-0009 "Experimental and Analytical Investigation of Seismic Retrofit of Structures with Supplemental Damping: Part II - Friction Devices," by C. Li and A.M. Reinhorn, 7/6/95, (PB96-128087, A11, MF-A03).

NCEER-95-0010 "Experimental Performance and Analytical Study of a Non-Ductile Reinforced Concrete Frame Structure Retrofitted with Elastomeric Spring Dampers," by G. Pekcan, J.B. Mander and S.S. Chen, 7/14/95, (PB96-137161, A08, MF-A02).

NCEER-95-0011 "Development and Experimental Study of Semi-Active Fluid Damping Devices for Seismic Protection of Structures," by M.D. Symans and M.C. Constantinou, 8/3/95, (PB96-136940, A23, MF-A04).

NCEER-95-0012 "Real-Time Structural Parameter Modification (RSPM): Development of Innervated Structures," by Z. Liang, M. Tong and G.C. Lee, 4/11/95, (PB96-137153, A06, MF-A01).

NCEER-95-0013 "Experimental and Analytical Investigation of Seismic Retrofit of Structures with Supplemental Damping: Part III - Viscous Damping Walls," by A.M. Reinhorn and C. Li, 10/1/95, (PB96-176409, A11, MF-A03).

NCEER-95-0014 "Seismic Fragility Analysis of Equipment and Structures in a Memphis Electric Substation," by J-R. Huo and H.H.M. Hwang, 8/10/95, (PB96-128087, A09, MF-A02).

NCEER-95-0015 "The Hanshin-Awaji Earthquake of January 17, 1995: Performance of Lifelines," Edited by M. Shinozuka, 11/3/95, (PB96-176383, A15, MF-A03).

NCEER-95-0016 "Highway Culvert Performance During Earthquakes," by T.L. Youd and C.J. Beckman, available as NCEER-96-0015.

NCEER-95-0017 "The Hanshin-Awaji Earthquake of January 17, 1995: Performance of Highway Bridges," Edited by I.G. Buckle, 12/1/95, not available.

NCEER-95-0018 "Modeling of Masonry Infill Panels for Structural Analysis," by A.M. Reinhorn, A. Madan, R.E. Valles, Y. Reichmann and J.B. Mander, 12/8/95, (PB97-110886, MF-A01, A06).

NCEER-95-0019 "Optimal Polynomial Control for Linear and Nonlinear Structures," by A.K. Agrawal and J.N. Yang, 12/11/95, (PB96-168737, A07, MF-A02).

NCEER-95-0020 "Retrofit of Non-Ductile Reinforced Concrete Frames Using Friction Dampers," by R.S. Rao, P. Gergely and R.N. White, 12/22/95, (PB97-133508, A10, MF-A02).

NCEER-95-0021 "Parametric Results for Seismic Response of Pile-Supported Bridge Bents," by G. Mylonakis, A. Nikolaou and G. Gazetas, 12/22/95, (PB97-100242, A12, MF-A03).

NCEER-95-0022 "Kinematic Bending Moments in Seismically Stressed Piles," by A. Nikolaou, G. Mylonakis and G. Gazetas, 12/23/95, (PB97-113914, MF-A03, A13).

NCEER-96-0001 "Dynamic Response of Unreinforced Masonry Buildings with Flexible Diaphragms," by A.C. Costley and D.P. Abrams," 10/10/96, (PB97-133573, MF-A03, A15).

NCEER-96-0002 "State of the Art Review: Foundations and Retaining Structures," by I. Po Lam, not available.

NCEER-96-0003 "Ductility of Rectangular Reinforced Concrete Bridge Columns with Moderate Confinement," by N. Wehbe, M. Saiidi, D. Sanders and B. Douglas, 11/7/96, (PB97-133557, A06, MF-A02).

NCEER-96-0004 "Proceedings of the Long-Span Bridge Seismic Research Workshop," edited by I.G. Buckle and I.M. Friedland, not available.

NCEER-96-0005 "Establish Representative Pier Types for Comprehensive Study: Eastern United States," by J. Kulicki and Z. Prucz, 5/28/96, (PB98-119217, A07, MF-A02).

NCEER-96-0006 "Establish Representative Pier Types for Comprehensive Study: Western United States," by R. Imbsen, R.A. Schamber and T.A. Osterkamp, 5/28/96, (PB98-118607, A07, MF-A02).

NCEER-96-0007 "Nonlinear Control Techniques for Dynamical Systems with Uncertain Parameters," by R.G. Ghanem and M.I. Bujakov, 5/27/96, (PB97-100259, A17, MF-A03).

NCEER-96-0008 "Seismic Evaluation of a 30-Year Old Non-Ductile Highway Bridge Pier and Its Retrofit," by J.B. Mander, B. Mahmoodzadegan, S. Bhadra and S.S. Chen, 5/31/96, (PB97-110902, MF-A03, A10).

NCEER-96-0009 "Seismic Performance of a Model Reinforced Concrete Bridge Pier Before and After Retrofit," by J.B. Mander, J.H. Kim and C.A. Ligozio, 5/31/96, (PB97-110910, MF-A02, A10).

NCEER-96-0010 "IDARC2D Version 4.0: A Computer Program for the Inelastic Damage Analysis of Buildings," by R.E. Valles, A.M. Reinhorn, S.K. Kunnath, C. Li and A. Madan, 6/3/96, (PB97-100234, A17, MF-A03).

NCEER-96-0011 "Estimation of the Economic Impact of Multiple Lifeline Disruption: Memphis Light, Gas and Water Division Case Study," by S.E. Chang, H.A. Seligson and R.T. Eguchi, 8/16/96, (PB97-133490, A11, MF-A03).

NCEER-96-0012 "Proceedings from the Sixth Japan-U.S. Workshop on Earthquake Resistant Design of Lifeline Facilities and Countermeasures Against Soil Liquefaction, Edited by M. Hamada and T. O'Rourke, 9/11/96, (PB97-133581, A99, MF-A06).

NCEER-96-0013 "Chemical Hazards, Mitigation and Preparedness in Areas of High Seismic Risk: A Methodology for Estimating the Risk of Post-Earthquake Hazardous Materials Release," by H.A. Seligson, R.T. Eguchi, K.J. Tierney and K. Richmond, 11/7/96, (PB97-133565, MF-A02, A08).

NCEER-96-0014 "Response of Steel Bridge Bearings to Reversed Cyclic Loading," by J.B. Mander, D-K. Kim, S.S. Chen and G.J. Premus, 11/13/96, (PB97-140735, A12, MF-A03).

NCEER-96-0015 "Highway Culvert Performance During Past Earthquakes," by T.L. Youd and C.J. Beckman, 11/25/96, (PB97-133532, A06, MF-A01).

NCEER-97-0001 "Evaluation, Prevention and Mitigation of Pounding Effects in Building Structures," by R.E. Valles and A.M. Reinhorn, 2/20/97, (PB97-159552, A14, MF-A03).

NCEER-97-0002 "Seismic Design Criteria for Bridges and Other Highway Structures," by C. Rojahn, R. Mayes, D.G. Anderson, J. Clark, J.H. Hom, R.V. Nutt and M.J. O'Rourke, 4/30/97, (PB97-194658, A06, MF-A03).

NCEER-97-0003 “Proceedings of the U.S.-Italian Workshop on Seismic Evaluation and Retrofit,” Edited by D.P. Abrams and G.M. Calvi, 3/19/97, (PB97-194666, A13, MF-A03).

NCEER-97-0004 "Investigation of Seismic Response of Buildings with Linear and Nonlinear Fluid Viscous Dampers," by A.A. Seleemah and M.C. Constantinou, 5/21/97, (PB98-109002, A15, MF-A03).

NCEER-97-0005 "Proceedings of the Workshop on Earthquake Engineering Frontiers in Transportation Facilities," edited by G.C. Lee and I.M. Friedland, 8/29/97, (PB98-128911, A25, MR-A04).

NCEER-97-0006 "Cumulative Seismic Damage of Reinforced Concrete Bridge Piers," by S.K. Kunnath, A. El-Bahy, A. Taylor and W. Stone, 9/2/97, (PB98-108814, A11, MF-A03).

NCEER-97-0007 "Structural Details to Accommodate Seismic Movements of Highway Bridges and Retaining Walls," by R.A. Imbsen, R.A. Schamber, E. Thorkildsen, A. Kartoum, B.T. Martin, T.N. Rosser and J.M. Kulicki, 9/3/97, (PB98-108996, A09, MF-A02).

NCEER-97-0008 "A Method for Earthquake Motion-Damage Relationships with Application to Reinforced Concrete Frames," by A. Singhal and A.S. Kiremidjian, 9/10/97, (PB98-108988, A13, MF-A03).

NCEER-97-0009 "Seismic Analysis and Design of Bridge Abutments Considering Sliding and Rotation," by K. Fishman and R. Richards, Jr., 9/15/97, (PB98-108897, A06, MF-A02).

NCEER-97-0010 "Proceedings of the FHWA/NCEER Workshop on the National Representation of Seismic Ground Motion for New and Existing Highway Facilities," edited by I.M. Friedland, M.S. Power and R.L. Mayes, 9/22/97, (PB98-128903, A21, MF-A04).

NCEER-97-0011 "Seismic Analysis for Design or Retrofit of Gravity Bridge Abutments," by K.L. Fishman, R. Richards, Jr. and R.C. Divito, 10/2/97, (PB98-128937, A08, MF-A02).

NCEER-97-0012 "Evaluation of Simplified Methods of Analysis for Yielding Structures," by P. Tsopelas, M.C. Constantinou, C.A. Kircher and A.S. Whittaker, 10/31/97, (PB98-128929, A10, MF-A03).

NCEER-97-0013 "Seismic Design of Bridge Columns Based on Control and Repairability of Damage," by C-T. Cheng and J.B. Mander, 12/8/97, (PB98-144249, A11, MF-A03).

NCEER-97-0014 "Seismic Resistance of Bridge Piers Based on Damage Avoidance Design," by J.B. Mander and C-T. Cheng, 12/10/97, (PB98-144223, A09, MF-A02).

NCEER-97-0015 “Seismic Response of Nominally Symmetric Systems with Strength Uncertainty,” by S. Balopoulou and M. Grigoriu, 12/23/97, (PB98-153422, A11, MF-A03).

NCEER-97-0016 “Evaluation of Seismic Retrofit Methods for Reinforced Concrete Bridge Columns,” by T.J. Wipf, F.W. Klaiber and F.M. Russo, 12/28/97, (PB98-144215, A12, MF-A03).

NCEER-97-0017 “Seismic Fragility of Existing Conventional Reinforced Concrete Highway Bridges,” by C.L. Mullen and A.S. Cakmak, 12/30/97, (PB98-153406, A08, MF-A02).

NCEER-97-0018 “Loss Asssessment of Memphis Buildings,” edited by D.P. Abrams and M. Shinozuka, 12/31/97, (PB98-144231, A13, MF-A03).

NCEER-97-0019 “Seismic Evaluation of Frames with Infill Walls Using Quasi-static Experiments,” by K.M. Mosalam, R.N. White and P. Gergely, 12/31/97, (PB98-153455, A07, MF-A02).

NCEER-97-0020 “Seismic Evaluation of Frames with Infill Walls Using Pseudo-dynamic Experiments,” by K.M. Mosalam, R.N. White and P. Gergely, 12/31/97, (PB98-153430, A07, MF-A02).

NCEER-97-0021 “Computational Strategies for Frames with Infill Walls: Discrete and Smeared Crack Analyses and Seismic Fragility,” by K.M. Mosalam, R.N. White and P. Gergely, 12/31/97, (PB98-153414, A10, MF-A02).

NCEER-97-0022 "Proceedings of the NCEER Workshop on Evaluation of Liquefaction Resistance of Soils," edited by T.L. Youd and I.M. Idriss, 12/31/97, (PB98-155617, A15, MF-A03).

MCEER-98-0001 "Extraction of Nonlinear Hysteretic Properties of Seismically Isolated Bridges from Quick-Release Field Tests," by Q. Chen, B.M. Douglas, E.M. Maragakis and I.G. Buckle, 5/26/98, (PB99-118838, A06, MF-A01).

MCEER-98-0002 "Methodologies for Evaluating the Importance of Highway Bridges," by A. Thomas, S. Eshenaur and J. Kulicki, 5/29/98, (PB99-118846, A10, MF-A02).

MCEER-98-0003 "Capacity Design of Bridge Piers and the Analysis of Overstrength," by J.B. Mander, A. Dutta and P. Goel, 6/1/98, (PB99-118853, A09, MF-A02).

MCEER-98-0004 "Evaluation of Bridge Damage Data from the Loma Prieta and Northridge, California Earthquakes," by N. Basoz and A. Kiremidjian, 6/2/98, (PB99-118861, A15, MF-A03).

MCEER-98-0005 "Screening Guide for Rapid Assessment of Liquefaction Hazard at Highway Bridge Sites," by T. L. Youd, 6/16/98, (PB99-118879, A06, not available on microfiche).

MCEER-98-0006 "Structural Steel and Steel/Concrete Interface Details for Bridges," by P. Ritchie, N. Kauhl and J. Kulicki, 7/13/98, (PB99-118945, A06, MF-A01).

MCEER-98-0007 "Capacity Design and Fatigue Analysis of Confined Concrete Columns," by A. Dutta and J.B. Mander, 7/14/98, (PB99-118960, A14, MF-A03).

MCEER-98-0008 "Proceedings of the Workshop on Performance Criteria for Telecommunication Services Under Earthquake Conditions," edited by A.J. Schiff, 7/15/98, (PB99-118952, A08, MF-A02).

MCEER-98-0009 "Fatigue Analysis of Unconfined Concrete Columns," by J.B. Mander, A. Dutta and J.H. Kim, 9/12/98, (PB99-123655, A10, MF-A02).

MCEER-98-0010 "Centrifuge Modeling of Cyclic Lateral Response of Pile-Cap Systems and Seat-Type Abutments in Dry Sands," by A.D. Gadre and R. Dobry, 10/2/98, (PB99-123606, A13, MF-A03).

MCEER-98-0011 "IDARC-BRIDGE: A Computational Platform for Seismic Damage Assessment of Bridge Structures," by A.M. Reinhorn, V. Simeonov, G. Mylonakis and Y. Reichman, 10/2/98, (PB99-162919, A15, MF-A03).

MCEER-98-0012 "Experimental Investigation of the Dynamic Response of Two Bridges Before and After Retrofitting with Elastomeric Bearings," by D.A. Wendichansky, S.S. Chen and J.B. Mander, 10/2/98, (PB99-162927, A15, MF-A03).

MCEER-98-0013 "Design Procedures for Hinge Restrainers and Hinge Sear Width for Multiple-Frame Bridges," by R. Des Roches and G.L. Fenves, 11/3/98, (PB99-140477, A13, MF-A03).

MCEER-98-0014 "Response Modification Factors for Seismically Isolated Bridges," by M.C. Constantinou and J.K. Quarshie, 11/3/98, (PB99-140485, A14, MF-A03).

MCEER-98-0015 "Proceedings of the U.S.-Italy Workshop on Seismic Protective Systems for Bridges," edited by I.M. Friedland and M.C. Constantinou, 11/3/98, (PB2000-101711, A22, MF-A04).

MCEER-98-0016 "Appropriate Seismic Reliability for Critical Equipment Systems: Recommendations Based on Regional Analysis of Financial and Life Loss," by K. Porter, C. Scawthorn, C. Taylor and N. Blais, 11/10/98, (PB99-157265, A08, MF-A02).

MCEER-98-0017 "Proceedings of the U.S. Japan Joint Seminar on Civil Infrastructure Systems Research," edited by M. Shinozuka and A. Rose, 11/12/98, (PB99-156713, A16, MF-A03).

MCEER-98-0018 "Modeling of Pile Footings and Drilled Shafts for Seismic Design," by I. PoLam, M. Kapuskar and D. Chaudhuri, 12/21/98, (PB99-157257, A09, MF-A02).

MCEER-99-0001 "Seismic Evaluation of a Masonry Infilled Reinforced Concrete Frame by Pseudodynamic Testing," by S.G. Buonopane and R.N. White, 2/16/99, (PB99-162851, A09, MF-A02).

MCEER-99-0002 "Response History Analysis of Structures with Seismic Isolation and Energy Dissipation Systems: Verification Examples for Program SAP2000," by J. Scheller and M.C. Constantinou, 2/22/99, (PB99-162869, A08, MF-A02).

MCEER-99-0003 "Experimental Study on the Seismic Design and Retrofit of Bridge Columns Including Axial Load Effects," by A. Dutta, T. Kokorina and J.B. Mander, 2/22/99, (PB99-162877, A09, MF-A02).

MCEER-99-0004 "Experimental Study of Bridge Elastomeric and Other Isolation and Energy Dissipation Systems with Emphasis on Uplift Prevention and High Velocity Near-source Seismic Excitation," by A. Kasalanati and M. C. Constantinou, 2/26/99, (PB99-162885, A12, MF-A03).

MCEER-99-0005 "Truss Modeling of Reinforced Concrete Shear-flexure Behavior," by J.H. Kim and J.B. Mander, 3/8/99, (PB99-163693, A12, MF-A03).

MCEER-99-0006 "Experimental Investigation and Computational Modeling of Seismic Response of a 1:4 Scale Model Steel Structure with a Load Balancing Supplemental Damping System," by G. Pekcan, J.B. Mander and S.S. Chen, 4/2/99, (PB99-162893, A11, MF-A03).

MCEER-99-0007 "Effect of Vertical Ground Motions on the Structural Response of Highway Bridges," by M.R. Button, C.J. Cronin and R.L. Mayes, 4/10/99, (PB2000-101411, A10, MF-A03).

MCEER-99-0008 "Seismic Reliability Assessment of Critical Facilities: A Handbook, Supporting Documentation, and Model Code Provisions," by G.S. Johnson, R.E. Sheppard, M.D. Quilici, S.J. Eder and C.R. Scawthorn, 4/12/99, (PB2000-101701, A18, MF-A04).

MCEER-99-0009 "Impact Assessment of Selected MCEER Highway Project Research on the Seismic Design of Highway Structures," by C. Rojahn, R. Mayes, D.G. Anderson, J.H. Clark, D'Appolonia Engineering, S. Gloyd and R.V. Nutt, 4/14/99, (PB99-162901, A10, MF-A02).

MCEER-99-0010 "Site Factors and Site Categories in Seismic Codes," by R. Dobry, R. Ramos and M.S. Power, 7/19/99, (PB2000-101705, A08, MF-A02).

MCEER-99-0011 "Restrainer Design Procedures for Multi-Span Simply-Supported Bridges," by M.J. Randall, M. Saiidi, E. Maragakis and T. Isakovic, 7/20/99, (PB2000-101702, A10, MF-A02).

MCEER-99-0012 "Property Modification Factors for Seismic Isolation Bearings," by M.C. Constantinou, P. Tsopelas, A. Kasalanati and E. Wolff, 7/20/99, (PB2000-103387, A11, MF-A03).

MCEER-99-0013 "Critical Seismic Issues for Existing Steel Bridges," by P. Ritchie, N. Kauhl and J. Kulicki, 7/20/99, (PB2000-101697, A09, MF-A02).

MCEER-99-0014 "Nonstructural Damage Database," by A. Kao, T.T. Soong and A. Vender, 7/24/99, (PB2000-101407, A06, MF-A01).

MCEER-99-0015 "Guide to Remedial Measures for Liquefaction Mitigation at Existing Highway Bridge Sites," by H.G. Cooke and J. K. Mitchell, 7/26/99, (PB2000-101703, A11, MF-A03).

MCEER-99-0016 "Proceedings of the MCEER Workshop on Ground Motion Methodologies for the Eastern United States," edited by N. Abrahamson and A. Becker, 8/11/99, (PB2000-103385, A07, MF-A02).

MCEER-99-0017 "Quindío, Colombia Earthquake of January 25, 1999: Reconnaissance Report," by A.P. Asfura and P.J. Flores, 10/4/99, (PB2000-106893, A06, MF-A01).

MCEER-99-0018 "Hysteretic Models for Cyclic Behavior of Deteriorating Inelastic Structures," by M.V. Sivaselvan and A.M. Reinhorn, 11/5/99, (PB2000-103386, A08, MF-A02).

MCEER-99-0019 "Proceedings of the 7th U.S.- Japan Workshop on Earthquake Resistant Design of Lifeline Facilities and Countermeasures Against Soil Liquefaction," edited by T.D. O'Rourke, J.P. Bardet and M. Hamada, 11/19/99, (PB2000-103354, A99, MF-A06).

MCEER-99-0020 "Development of Measurement Capability for Micro-Vibration Evaluations with Application to Chip Fabrication Facilities," by G.C. Lee, Z. Liang, J.W. Song, J.D. Shen and W.C. Liu, 12/1/99, (PB2000-105993, A08, MF-A02).

MCEER-99-0021 "Design and Retrofit Methodology for Building Structures with Supplemental Energy Dissipating Systems," by G. Pekcan, J.B. Mander and S.S. Chen, 12/31/99, (PB2000-105994, A11, MF-A03).

MCEER-00-0001 "The Marmara, Turkey Earthquake of August 17, 1999: Reconnaissance Report," edited by C. Scawthorn; with major contributions by M. Bruneau, R. Eguchi, T. Holzer, G. Johnson, J. Mander, J. Mitchell, W. Mitchell, A. Papageorgiou, C. Scaethorn, and G. Webb, 3/23/00, (PB2000-106200, A11, MF-A03).

MCEER-00-0002 "Proceedings of the MCEER Workshop for Seismic Hazard Mitigation of Health Care Facilities," edited by G.C. Lee, M. Ettouney, M. Grigoriu, J. Hauer and J. Nigg, 3/29/00, (PB2000-106892, A08, MF-A02).

MCEER-00-0003 "The Chi-Chi, Taiwan Earthquake of September 21, 1999: Reconnaissance Report," edited by G.C. Lee and C.H. Loh, with major contributions by G.C. Lee, M. Bruneau, I.G. Buckle, S.E. Chang, P.J. Flores, T.D. O'Rourke, M. Shinozuka, T.T. Soong, C-H. Loh, K-C. Chang, Z-J. Chen, J-S. Hwang, M-L. Lin, G-Y. Liu, K-C. Tsai, G.C. Yao and C-L. Yen, 4/30/00, (PB2001-100980, A10, MF-A02).

MCEER-00-0004 "Seismic Retrofit of End-Sway Frames of Steel Deck-Truss Bridges with a Supplemental Tendon System: Experimental and Analytical Investigation," by G. Pekcan, J.B. Mander and S.S. Chen, 7/1/00, (PB2001-100982, A10, MF-A02).

MCEER-00-0005 "Sliding Fragility of Unrestrained Equipment in Critical Facilities," by W.H. Chong and T.T. Soong, 7/5/00, (PB2001-100983, A08, MF-A02).

MCEER-00-0006 "Seismic Response of Reinforced Concrete Bridge Pier Walls in the Weak Direction," by N. Abo-Shadi, M. Saiidi and D. Sanders, 7/17/00, (PB2001-100981, A17, MF-A03).

MCEER-00-0007 "Low-Cycle Fatigue Behavior of Longitudinal Reinforcement in Reinforced Concrete Bridge Columns," by J. Brown and S.K. Kunnath, 7/23/00, (PB2001-104392, A08, MF-A02).

MCEER-00-0008 "Soil Structure Interaction of Bridges for Seismic Analysis," I. PoLam and H. Law, 9/25/00, (PB2001-105397, A08, MF-A02).

MCEER-00-0009 "Proceedings of the First MCEER Workshop on Mitigation of Earthquake Disaster by Advanced Technologies (MEDAT-1), edited by M. Shinozuka, D.J. Inman and T.D. O'Rourke, 11/10/00, (PB2001-105399, A14, MF-A03).

MCEER-00-0010 "Development and Evaluation of Simplified Procedures for Analysis and Design of Buildings with Passive Energy Dissipation Systems, Revision 01," by O.M. Ramirez, M.C. Constantinou, C.A. Kircher, A.S. Whittaker, M.W. Johnson, J.D. Gomez and C. Chrysostomou, 11/16/01, (PB2001-105523, A23, MF-A04).

MCEER-00-0011 "Dynamic Soil-Foundation-Structure Interaction Analyses of Large Caissons," by C-Y. Chang, C-M. Mok, Z-L. Wang, R. Settgast, F. Waggoner, M.A. Ketchum, H.M. Gonnermann and C-C. Chin, 12/30/00, (PB2001-104373, A07, MF-A02).

MCEER-00-0012 "Experimental Evaluation of Seismic Performance of Bridge Restrainers," by A.G. Vlassis, E.M. Maragakis and M. Saiid Saiidi, 12/30/00, (PB2001-104354, A09, MF-A02).

MCEER-00-0013 "Effect of Spatial Variation of Ground Motion on Highway Structures," by M. Shinozuka, V. Saxena and G. Deodatis, 12/31/00, (PB2001-108755, A13, MF-A03).

MCEER-00-0014 "A Risk-Based Methodology for Assessing the Seismic Performance of Highway Systems," by S.D. Werner, C.E. Taylor, J.E. Moore, II, J.S. Walton and S. Cho, 12/31/00, (PB2001-108756, A14, MF-A03).

MCEER-01-0001 "Experimental Investigation of P-Delta Effects to Collapse During Earthquakes," by D. Vian and M. Bruneau, 6/25/01, (PB2002-100534, A17, MF-A03).

MCEER-01-0002 "Proceedings of the Second MCEER Workshop on Mitigation of Earthquake Disaster by Advanced Technologies (MEDAT-2)," edited by M. Bruneau and D.J. Inman, 7/23/01, (PB2002-100434, A16, MF-A03).

MCEER-01-0003 "Sensitivity Analysis of Dynamic Systems Subjected to Seismic Loads," by C. Roth and M. Grigoriu, 9/18/01, (PB2003-100884, A12, MF-A03).

MCEER-01-0004 "Overcoming Obstacles to Implementing Earthquake Hazard Mitigation Policies: Stage 1 Report," by D.J. Alesch and W.J. Petak, 12/17/01, (PB2002-107949, A07, MF-A02).

MCEER-01-0005 "Updating Real-Time Earthquake Loss Estimates: Methods, Problems and Insights," by C.E. Taylor, S.E. Chang and R.T. Eguchi, 12/17/01, (PB2002-107948, A05, MF-A01).

MCEER-01-0006 "Experimental Investigation and Retrofit of Steel Pile Foundations and Pile Bents Under Cyclic Lateral Loadings," by A. Shama, J. Mander, B. Blabac and S. Chen, 12/31/01, (PB2002-107950, A13, MF-A03).

MCEER-02-0001 "Assessment of Performance of Bolu Viaduct in the 1999 Duzce Earthquake in Turkey" by P.C. Roussis, M.C. Constantinou, M. Erdik, E. Durukal and M. Dicleli, 5/8/02, (PB2003-100883, A08, MF-A02).

MCEER-02-0002 "Seismic Behavior of Rail Counterweight Systems of Elevators in Buildings," by M.P. Singh, Rildova and L.E. Suarez, 5/27/02. (PB2003-100882, A11, MF-A03).

MCEER-02-0003 "Development of Analysis and Design Procedures for Spread Footings," by G. Mylonakis, G. Gazetas, S. Nikolaou and A. Chauncey, 10/02/02, (PB2004-101636, A13, MF-A03, CD-A13).

MCEER-02-0004 "Bare-Earth Algorithms for Use with SAR and LIDAR Digital Elevation Models," by C.K. Huyck, R.T. Eguchi and B. Houshmand, 10/16/02, (PB2004-101637, A07, CD-A07).

MCEER-02-0005 "Review of Energy Dissipation of Compression Members in Concentrically Braced Frames," by K.Lee and M. Bruneau, 10/18/02, (PB2004-101638, A10, CD-A10).

MCEER-03-0001 "Experimental Investigation of Light-Gauge Steel Plate Shear Walls for the Seismic Retrofit of Buildings" by J. Berman and M. Bruneau, 5/2/03, (PB2004-101622, A10, MF-A03, CD-A10).

MCEER-03-0002 "Statistical Analysis of Fragility Curves," by M. Shinozuka, M.Q. Feng, H. Kim, T. Uzawa and T. Ueda, 6/16/03, (PB2004-101849, A09, CD-A09).

MCEER-03-0003 "Proceedings of the Eighth U.S.-Japan Workshop on Earthquake Resistant Design f Lifeline Facilities and Countermeasures Against Liquefaction," edited by M. Hamada, J.P. Bardet and T.D. O'Rourke, 6/30/03, (PB2004-104386, A99, CD-A99).

MCEER-03-0004 "Proceedings of the PRC-US Workshop on Seismic Analysis and Design of Special Bridges," edited by L.C. Fan and G.C. Lee, 7/15/03, (PB2004-104387, A14, CD-A14).

MCEER-03-0005 "Urban Disaster Recovery: A Framework and Simulation Model," by S.B. Miles and S.E. Chang, 7/25/03, (PB2004-104388, A07, CD-A07).

MCEER-03-0006 "Behavior of Underground Piping Joints Due to Static and Dynamic Loading," by R.D. Meis, M. Maragakis and R. Siddharthan, 11/17/03, (PB2005-102194, A13, MF-A03, CD-A00).

MCEER-04-0001 "Experimental Study of Seismic Isolation Systems with Emphasis on Secondary System Response and Verification of Accuracy of Dynamic Response History Analysis Methods," by E. Wolff and M. Constantinou, 1/16/04 (PB2005-102195, A99, MF-E08, CD-A00).

MCEER-04-0002 "Tension, Compression and Cyclic Testing of Engineered Cementitious Composite Materials," by K. Kesner and S.L. Billington, 3/1/04, (PB2005-102196, A08, CD-A08).

MCEER-04-0003 "Cyclic Testing of Braces Laterally Restrained by Steel Studs to Enhance Performance During Earthquakes," by O.C. Celik, J.W. Berman and M. Bruneau, 3/16/04, (PB2005-102197, A13, MF-A03, CD-A00).

MCEER-04-0004 "Methodologies for Post Earthquake Building Damage Detection Using SAR and Optical Remote Sensing: Application to the August 17, 1999 Marmara, Turkey Earthquake," by C.K. Huyck, B.J. Adams, S. Cho, R.T. Eguchi, B. Mansouri and B. Houshmand, 6/15/04, (PB2005-104888, A10, CD-A00).

MCEER-04-0005 "Nonlinear Structural Analysis Towards Collapse Simulation: A Dynamical Systems Approach," by M.V. Sivaselvan and A.M. Reinhorn, 6/16/04, (PB2005-104889, A11, MF-A03, CD-A00).

MCEER-04-0006 "Proceedings of the Second PRC-US Workshop on Seismic Analysis and Design of Special Bridges," edited by G.C. Lee and L.C. Fan, 6/25/04, (PB2005-104890, A16, CD-A00).

MCEER-04-0007 "Seismic Vulnerability Evaluation of Axially Loaded Steel Built-up Laced Members," by K. Lee and M. Bruneau, 6/30/04, (PB2005-104891, A16, CD-A00).

MCEER-04-0008 "Evaluation of Accuracy of Simplified Methods of Analysis and Design of Buildings with Damping Systems for Near-Fault and for Soft-Soil Seismic Motions," by E.A. Pavlou and M.C. Constantinou, 8/16/04, (PB2005-104892, A08, MF-A02, CD-A00).

MCEER-04-0009 "Assessment of Geotechnical Issues in Acute Care Facilities in California," by M. Lew, T.D. O'Rourke, R. Dobry and M. Koch, 9/15/04, (PB2005-104893, A08, CD-A00).

MCEER-04-0010 "Scissor-Jack-Damper Energy Dissipation System," by A.N. Sigaher-Boyle and M.C. Constantinou, 12/1/04 (PB2005-108221).

MCEER-04-0011 "Seismic Retrofit of Bridge Steel Truss Piers Using a Controlled Rocking Approach," by M. Pollino and M. Bruneau, 12/20/04 (PB2006-105795).

MCEER-05-0001 "Experimental and Analytical Studies of Structures Seismically Isolated with an Uplift-Restraint Isolation System," by P.C. Roussis and M.C. Constantinou, 1/10/05 (PB2005-108222).

MCEER-05-0002 "A Versatile Experimentation Model for Study of Structures Near Collapse Applied to Seismic Evaluation of Irregular Structures," by D. Kusumastuti, A.M. Reinhorn and A. Rutenberg, 3/31/05 (PB2006-101523).

MCEER-05-0003 "Proceedings of the Third PRC-US Workshop on Seismic Analysis and Design of Special Bridges," edited by L.C. Fan and G.C. Lee, 4/20/05, (PB2006-105796).

MCEER-05-0004 "Approaches for the Seismic Retrofit of Braced Steel Bridge Piers and Proof-of-Concept Testing of an Eccentrically Braced Frame with Tubular Link," by J.W. Berman and M. Bruneau, 4/21/05 (PB2006-101524).

MCEER-05-0005 "Simulation of Strong Ground Motions for Seismic Fragility Evaluation of Nonstructural Components in Hospitals," by A. Wanitkorkul and A. Filiatrault, 5/26/05 (PB2006-500027).

MCEER-05-0006 "Seismic Safety in California Hospitals: Assessing an Attempt to Accelerate the Replacement or Seismic Retrofit of Older Hospital Facilities," by D.J. Alesch, L.A. Arendt and W.J. Petak, 6/6/05 (PB2006-105794).

MCEER-05-0007 "Development of Seismic Strengthening and Retrofit Strategies for Critical Facilities Using Engineered Cementitious Composite Materials," by K. Kesner and S.L. Billington, 8/29/05 (PB2006-111701).

MCEER-05-0008 "Experimental and Analytical Studies of Base Isolation Systems for Seismic Protection of Power Transformers," by N. Murota, M.Q. Feng and G-Y. Liu, 9/30/05 (PB2006-111702).

MCEER-05-0009 "3D-BASIS-ME-MB: Computer Program for Nonlinear Dynamic Analysis of Seismically Isolated Structures," by P.C. Tsopelas, P.C. Roussis, M.C. Constantinou, R. Buchanan and A.M. Reinhorn, 10/3/05 (PB2006-111703).

MCEER-05-0010 "Steel Plate Shear Walls for Seismic Design and Retrofit of Building Structures," by D. Vian and M. Bruneau, 12/15/05 (PB2006-111704).

MCEER-05-0011 "The Performance-Based Design Paradigm," by M.J. Astrella and A. Whittaker, 12/15/05 (PB2006-111705).

MCEER-06-0001 "Seismic Fragility of Suspended Ceiling Systems," H. Badillo-Almaraz, A.S. Whittaker, A.M. Reinhorn and G.P. Cimellaro, 2/4/06 (PB2006-111706).

MCEER-06-0002 "Multi-Dimensional Fragility of Structures," by G.P. Cimellaro, A.M. Reinhorn and M. Bruneau, 3/1/06 (PB2007-106974, A09, MF-A02, CD A00).

MCEER-06-0003 "Built-Up Shear Links as Energy Dissipators for Seismic Protection of Bridges," by P. Dusicka, A.M. Itani and I.G. Buckle, 3/15/06 (PB2006-111708).

MCEER-06-0004 "Analytical Investigation of the Structural Fuse Concept," by R.E. Vargas and M. Bruneau, 3/16/06 (PB2006-111709).

MCEER-06-0005 "Experimental Investigation of the Structural Fuse Concept," by R.E. Vargas and M. Bruneau, 3/17/06 (PB2006-111710).

MCEER-06-0006 "Further Development of Tubular Eccentrically Braced Frame Links for the Seismic Retrofit of Braced Steel Truss Bridge Piers," by J.W. Berman and M. Bruneau, 3/27/06 (PB2007-105147).

MCEER-06-0007 "REDARS Validation Report," by S. Cho, C.K. Huyck, S. Ghosh and R.T. Eguchi, 8/8/06 (PB2007-106983).

MCEER-06-0008 "Review of Current NDE Technologies for Post-Earthquake Assessment of Retrofitted Bridge Columns," by J.W. Song, Z. Liang and G.C. Lee, 8/21/06 (PB2007-106984).

MCEER-06-0009 "Liquefaction Remediation in Silty Soils Using Dynamic Compaction and Stone Columns," by S. Thevanayagam, G.R. Martin, R. Nashed, T. Shenthan, T. Kanagalingam and N. Ecemis, 8/28/06 (PB2007-106985).

MCEER-06-0010 "Conceptual Design and Experimental Investigation of Polymer Matrix Composite Infill Panels for Seismic Retrofitting," by W. Jung, M. Chiewanichakorn and A.J. Aref, 9/21/06 (PB2007-106986).

MCEER-06-0011 "A Study of the Coupled Horizontal-Vertical Behavior of Elastomeric and Lead-Rubber Seismic Isolation Bearings," by G.P. Warn and A.S. Whittaker, 9/22/06 (PB2007-108679).

MCEER-06-0012 "Proceedings of the Fourth PRC-US Workshop on Seismic Analysis and Design of Special Bridges: Advancing Bridge Technologies in Research, Design, Construction and Preservation," Edited by L.C. Fan, G.C. Lee and L. Ziang, 10/12/06 (PB2007-109042).

MCEER-06-0013 "Cyclic Response and Low Cycle Fatigue Characteristics of Plate Steels," by P. Dusicka, A.M. Itani and I.G. Buckle, 11/1/06 06 (PB2007-106987).

MCEER-06-0014 "Proceedings of the Second US-Taiwan Bridge Engineering Workshop," edited by W.P. Yen, J. Shen, J-Y. Chen and M. Wang, 11/15/06 (PB2008-500041).

MCEER-06-0015 "User Manual and Technical Documentation for the REDARS^{TM} Import Wizard," by S. Cho, S. Ghosh, C.K. Huyck and S.D. Werner, 11/30/06 (PB2007-114766).

MCEER-06-0016 "Hazard Mitigation Strategy and Monitoring Technologies for Urban and Infrastructure Public Buildings: Proceedings of the China-US Workshops," edited by X.Y. Zhou, A.L. Zhang, G.C. Lee and M. Tong, 12/12/06 (PB2008-500018).

MCEER-07-0001 "Static and Kinetic Coefficients of Friction for Rigid Blocks," by C. Kafali, S. Fathali, M. Grigoriu and A.S. Whittaker, 3/20/07 (PB2007-114767).

MCEER-07-0002 "Hazard Mitigation Investment Decision Making: Organizational Response to Legislative Mandate," by L.A. Arendt, D.J. Alesch and W.J. Petak, 4/9/07 (PB2007-114768).

MCEER-07-0003 "Seismic Behavior of Bidirectional-Resistant Ductile End Diaphragms with Unbonded Braces in Straight or Skewed Steel Bridges," by O. Celik and M. Bruneau, 4/11/07 (PB2008-105141).

MCEER-07-0004 "Modeling Pile Behavior in Large Pile Groups Under Lateral Loading," by A.M. Dodds and G.R. Martin, 4/16/07(PB2008-105142).

MCEER-07-0005 "Experimental Investigation of Blast Performance of Seismically Resistant Concrete-Filled Steel Tube Bridge Piers," by S. Fujikura, M. Bruneau and D. Lopez-Garcia, 4/20/07 (PB2008-105143).

MCEER-07-0006 "Seismic Analysis of Conventional and Isolated Liquefied Natural Gas Tanks Using Mechanical Analogs," by I.P. Christovasilis and A.S. Whittaker, 5/1/07, not available.

MCEER-07-0007 "Experimental Seismic Performance Evaluation of Isolation/Restraint Systems for Mechanical Equipment – Part 1: Heavy Equipment Study," by S. Fathali and A. Filiatrault, 6/6/07 (PB2008-105144).

MCEER-07-0008 "Seismic Vulnerability of Timber Bridges and Timber Substructures," by A.A. Sharma, J.B. Mander, I.M. Friedland and D.R. Allicock, 6/7/07 (PB2008-105145).

MCEER-07-0009 "Experimental and Analytical Study of the XY-Friction Pendulum (XY-FP) Bearing for Bridge Applications," by C.C. Marin-Artieda, A.S. Whittaker and M.C. Constantinou, 6/7/07 (PB2008-105191).

MCEER-07-0010 "Proceedings of the PRC-US Earthquake Engineering Forum for Young Researchers," Edited by G.C. Lee and X.Z. Qi, 6/8/07 (PB2008-500058).

MCEER-07-0011 "Design Recommendations for Perforated Steel Plate Shear Walls," by R. Purba and M. Bruneau, 6/18/07, (PB2008-105192).

MCEER-07-0012 "Performance of Seismic Isolation Hardware Under Service and Seismic Loading," by M.C. Constantinou, A.S. Whittaker, Y. Kalpakidis, D.M. Fenz and G.P. Warn, 8/27/07, (PB2008-105193).

MCEER-07-0013 "Experimental Evaluation of the Seismic Performance of Hospital Piping Subassemblies," by E.R. Goodwin, E. Maragakis and A.M. Itani, 9/4/07, (PB2008-105194).

MCEER-07-0014 "A Simulation Model of Urban Disaster Recovery and Resilience: Implementation for the 1994 Northridge Earthquake," by S. Miles and S.E. Chang, 9/7/07, (PB2008-106426).

MCEER-07-0015 "Statistical and Mechanistic Fragility Analysis of Concrete Bridges," by M. Shinozuka, S. Banerjee and S-H. Kim, 9/10/07, (PB2008-106427).

MCEER-07-0016 "Three-Dimensional Modeling of Inelastic Buckling in Frame Structures," by M. Schachter and AM. Reinhorn, 9/13/07, (PB2008-108125).

MCEER-07-0017 "Modeling of Seismic Wave Scattering on Pile Groups and Caissons," by I. Po Lam, H. Law and C.T. Yang, 9/17/07 (PB2008-108150).

MCEER-07-0018 "Bridge Foundations: Modeling Large Pile Groups and Caissons for Seismic Design," by I. Po Lam, H. Law and G.R. Martin (Coordinating Author), 12/1/07 (PB2008-111190).

MCEER-07-0019 "Principles and Performance of Roller Seismic Isolation Bearings for Highway Bridges," by G.C. Lee, Y.C. Ou, Z. Liang, T.C. Niu and J. Song, 12/10/07 (PB2009-110466).

MCEER-07-0020 "Centrifuge Modeling of Permeability and Pinning Reinforcement Effects on Pile Response to Lateral Spreading," by L.L Gonzalez-Lagos, T. Abdoun and R. Dobry, 12/10/07 (PB2008-111191).

MCEER-07-0021 "Damage to the Highway System from the Pisco, Perú Earthquake of August 15, 2007," by J.S. O'Connor, L. Mesa and M. Nykamp, 12/10/07, (PB2008-108126).

MCEER-07-0022 "Experimental Seismic Performance Evaluation of Isolation/Restraint Systems for Mechanical Equipment – Part 2: Light Equipment Study," by S. Fathali and A. Filiatrault, 12/13/07 (PB2008-111192).

MCEER-07-0023 "Fragility Considerations in Highway Bridge Design," by M. Shinozuka, S. Banerjee and S.H. Kim, 12/14/07 (PB2008-111193).

MCEER-07-0024 "Performance Estimates for Seismically Isolated Bridges," by G.P. Warn and A.S. Whittaker, 12/30/07 (PB2008-112230).

MCEER-08-0001 "Seismic Performance of Steel Girder Bridge Superstructures with Conventional Cross Frames," by L.P. Carden, A.M. Itani and I.G. Buckle, 1/7/08, (PB2008-112231).

MCEER-08-0002 "Seismic Performance of Steel Girder Bridge Superstructures with Ductile End Cross Frames with Seismic Isolators," by L.P. Carden, A.M. Itani and I.G. Buckle, 1/7/08 (PB2008-112232).

MCEER-08-0003 "Analytical and Experimental Investigation of a Controlled Rocking Approach for Seismic Protection of Bridge Steel Truss Piers," by M. Pollino and M. Bruneau, 1/21/08 (PB2008-112233).

MCEER-08-0004 "Linking Lifeline Infrastructure Performance and Community Disaster Resilience: Models and Multi-Stakeholder Processes," by S.E. Chang, C. Pasion, K. Tatebe and R. Ahmad, 3/3/08 (PB2008-112234).

MCEER-08-0005 "Modal Analysis of Generally Damped Linear Structures Subjected to Seismic Excitations," by J. Song, Y-L. Chu, Z. Liang and G.C. Lee, 3/4/08 (PB2009-102311).

MCEER-08-0006 "System Performance Under Multi-Hazard Environments," by C. Kafali and M. Grigoriu, 3/4/08 (PB2008-112235).

MCEER-08-0007 "Mechanical Behavior of Multi-Spherical Sliding Bearings," by D.M. Fenz and M.C. Constantinou, 3/6/08 (PB2008-112236).

MCEER-08-0008 "Post-Earthquake Restoration of the Los Angeles Water Supply System," by T.H.P. Tabucchi and R.A. Davidson, 3/7/08 (PB2008-112237).

MCEER-08-0009 "Fragility Analysis of Water Supply Systems," by A. Jacobson and M. Grigoriu, 3/10/08 (PB2009-105545).

MCEER-08-0010 "Experimental Investigation of Full-Scale Two-Story Steel Plate Shear Walls with Reduced Beam Section Connections," by B. Qu, M. Bruneau, C-H. Lin and K-C. Tsai, 3/17/08 (PB2009-106368).

MCEER-08-0011 "Seismic Evaluation and Rehabilitation of Critical Components of Electrical Power Systems," S. Ersoy, B. Feizi, A. Ashrafi and M. Ala Saadeghvaziri, 3/17/08 (PB2009-105546).

MCEER-08-0012 "Seismic Behavior and Design of Boundary Frame Members of Steel Plate Shear Walls," by B. Qu and M. Bruneau, 4/26/08 . (PB2009-106744).

MCEER-08-0013 "Development and Appraisal of a Numerical Cyclic Loading Protocol for Quantifying Building System Performance," by A. Filiatrault, A. Wanitkorkul and M. Constantinou, 4/27/08 (PB2009-107906).

MCEER-08-0014 "Structural and Nonstructural Earthquake Design: The Challenge of Integrating Specialty Areas in Designing Complex, Critical Facilities," by W.J. Petak and D.J. Alesch, 4/30/08 (PB2009-107907).

MCEER-08-0015 "Seismic Performance Evaluation of Water Systems," by Y. Wang and T.D. O'Rourke, 5/5/08 (PB2009-107908).

MCEER-08-0016 "Seismic Response Modeling of Water Supply Systems," by P. Shi and T.D. O'Rourke, 5/5/08 (PB2009-107910).

MCEER-08-0017 "Numerical and Experimental Studies of Self-Centering Post-Tensioned Steel Frames," by D. Wang and A. Filiatrault, 5/12/08 (PB2009-110479).

MCEER-08-0018 "Development, Implementation and Verification of Dynamic Analysis Models for Multi-Spherical Sliding Bearings," by D.M. Fenz and M.C. Constantinou, 8/15/08 (PB2009-107911).

MCEER-08-0019 "Performance Assessment of Conventional and Base Isolated Nuclear Power Plants for Earthquake Blast Loadings," by Y.N. Huang, A.S. Whittaker and N. Luco, 10/28/08 (PB2009-107912).

MCEER-08-0020 "Remote Sensing for Resilient Multi-Hazard Disaster Response – Volume I: Introduction to Damage Assessment Methodologies," by B.J. Adams and R.T. Eguchi, 11/17/08 (PB2010-102695).

MCEER-08-0021 "Remote Sensing for Resilient Multi-Hazard Disaster Response – Volume II: Counting the Number of Collapsed Buildings Using an Object-Oriented Analysis: Case Study of the 2003 Bam Earthquake," by L. Gusella, C.K. Huyck and B.J. Adams, 11/17/08 (PB2010-100925).

MCEER-08-0022 "Remote Sensing for Resilient Multi-Hazard Disaster Response – Volume III: Multi-Sensor Image Fusion Techniques for Robust Neighborhood-Scale Urban Damage Assessment," by B.J. Adams and A. McMillan, 11/17/08 (PB2010-100926).

MCEER-08-0023 "Remote Sensing for Resilient Multi-Hazard Disaster Response – Volume IV: A Study of Multi-Temporal and Multi-Resolution SAR Imagery for Post-Katrina Flood Monitoring in New Orleans," by A. McMillan, J.G. Morley, B.J. Adams and S. Chesworth, 11/17/08 (PB2010-100927).

MCEER-08-0024 "Remote Sensing for Resilient Multi-Hazard Disaster Response – Volume V: Integration of Remote Sensing Imagery and VIEWS^{TM} Field Data for Post-Hurricane Charley Building Damage Assessment," by J.A. Womble, K. Mehta and B.J. Adams, 11/17/08 (PB2009-115532).

MCEER-08-0025 "Building Inventory Compilation for Disaster Management: Application of Remote Sensing and Statistical Modeling," by P. Sarabandi, A.S. Kiremidjian, R.T. Eguchi and B. J. Adams, 11/20/08 (PB2009-110484).

MCEER-08-0026 "New Experimental Capabilities and Loading Protocols for Seismic Qualification and Fragility Assessment of Nonstructural Systems," by R. Retamales, G. Mosqueda, A. Filiatrault and A. Reinhorn, 11/24/08 (PB2009-110485).

MCEER-08-0027 "Effects of Heating and Load History on the Behavior of Lead-Rubber Bearings," by I.V. Kalpakidis and M.C. Constantinou, 12/1/08 (PB2009-115533).

MCEER-08-0028 "Experimental and Analytical Investigation of Blast Performance of Seismically Resistant Bridge Piers," by S.Fujikura and M. Bruneau, 12/8/08 (PB2009-115534).

MCEER-08-0029 "Evolutionary Methodology for Aseismic Decision Support," by Y. Hu and G. Dargush, 12/15/08.

MCEER-08-0030 "Development of a Steel Plate Shear Wall Bridge Pier System Conceived from a Multi-Hazard Perspective," by D. Keller and M. Bruneau, 12/19/08 (PB2010-102696).

MCEER-09-0001 "Modal Analysis of Arbitrarily Damped Three-Dimensional Linear Structures Subjected to Seismic Excitations," by Y.L. Chu, J. Song and G.C. Lee, 1/31/09 (PB2010-100922).

MCEER-09-0002 "Air-Blast Effects on Structural Shapes," by G. Ballantyne, A.S. Whittaker, A.J. Aref and G.F. Dargush, 2/2/09 (PB2010-102697).

MCEER-09-0003 "Water Supply Performance During Earthquakes and Extreme Events," by A.L. Bonneau and T.D. O'Rourke, 2/16/09 (PB2010-100923).

MCEER-09-0004 "Generalized Linear (Mixed) Models of Post-Earthquake Ignitions," by R.A. Davidson, 7/20/09 (PB2010-102698).

MCEER-09-0005 "Seismic Testing of a Full-Scale Two-Story Light-Frame Wood Building: NEESWood Benchmark Test," by I.P. Christovasilis, A. Filiatrault and A. Wanitkorkul, 7/22/09 (PB2012-102401).

MCEER-09-0006 "IDARC2D Version 7.0: A Program for the Inelastic Damage Analysis of Structures," by A.M. Reinhorn, H. Roh, M. Sivaselvan, S.K. Kunnath, R.E. Valles, A. Madan, C. Li, R. Lobo and Y.J. Park, 7/28/09 (PB2010-103199).

MCEER-09-0007 "Enhancements to Hospital Resiliency: Improving Emergency Planning for and Response to Hurricanes," by D.B. Hess and L.A. Arendt, 7/30/09 (PB2010-100924).

MCEER-09-0008 "Assessment of Base-Isolated Nuclear Structures for Design and Beyond-Design Basis Earthquake Shaking," by Y.N. Huang, A.S. Whittaker, R.P. Kennedy and R.L. Mayes, 8/20/09 (PB2010-102699).

MCEER-09-0009 "Quantification of Disaster Resilience of Health Care Facilities," by G.P. Cimellaro, C. Fumo, A.M Reinhorn and M. Bruneau, 9/14/09 (PB2010-105384).

MCEER-09-0010 "Performance-Based Assessment and Design of Squat Reinforced Concrete Shear Walls," by C.K. Gulec and A.S. Whittaker, 9/15/09 (PB2010-102700).

MCEER-09-0011 "Proceedings of the Fourth US-Taiwan Bridge Engineering Workshop," edited by W.P. Yen, J.J. Shen, T.M. Lee and R.B. Zheng, 10/27/09 (PB2010-500009).

MCEER-09-0012 "Proceedings of the Special International Workshop on Seismic Connection Details for Segmental Bridge Construction," edited by W. Phillip Yen and George C. Lee, 12/21/09 (PB2012-102402).

MCEER-10-0001 "Direct Displacement Procedure for Performance-Based Seismic Design of Multistory Woodframe Structures," by W. Pang and D. Rosowsky, 4/26/10 (PB2012-102403).

MCEER-10-0002 "Simplified Direct Displacement Design of Six-Story NEESWood Capstone Building and Pre-Test Seismic Performance Assessment," by W. Pang, D. Rosowsky, J. van de Lindt and S. Pei, 5/28/10 (PB2012-102404).

MCEER-10-0003 "Integration of Seismic Protection Systems in Performance-Based Seismic Design of Woodframed Structures," by J.K. Shinde and M.D. Symans, 6/18/10 (PB2012-102405).

MCEER-10-0004 "Modeling and Seismic Evaluation of Nonstructural Components: Testing Frame for Experimental Evaluation of Suspended Ceiling Systems," by A.M. Reinhorn, K.P. Ryu and G. Maddaloni, 6/30/10 (PB2012-102406).

MCEER-10-0005 "Analytical Development and Experimental Validation of a Structural-Fuse Bridge Pier Concept," by S. El-Bahey and M. Bruneau, 10/1/10 (PB2012-102407).

MCEER-10-0006 "A Framework for Defining and Measuring Resilience at the Community Scale: The PEOPLES Resilience Framework," by C.S. Renschler, A.E. Frazier, L.A. Arendt, G.P. Cimellaro, A.M. Reinhorn and M. Bruneau, 10/8/10 (PB2012-102408).

MCEER-10-0007 "Impact of Horizontal Boundary Elements Design on Seismic Behavior of Steel Plate Shear Walls," by R. Purba and M. Bruneau, 11/14/10 (PB2012-102409).

MCEER-10-0008 "Seismic Testing of a Full-Scale Mid-Rise Building: The NEESWood Capstone Test," by S. Pei, J.W. van de Lindt, S.E. Pryor, H. Shimizu, H. Isoda and D.R. Rammer, 12/1/10 (PB2012-102410).

MCEER-10-0009 "Modeling the Effects of Detonations of High Explosives to Inform Blast-Resistant Design," by P. Sherkar, A.S. Whittaker and A.J. Aref, 12/1/10 (PB2012-102411).

MCEER-10-0010 "L'Aquila Earthquake of April 6, 2009 in Italy: Rebuilding a Resilient City to Withstand Multiple Hazards," by G.P. Cimellaro, I.P. Christovasilis, A.M. Reinhorn, A. De Stefano and T. Kirova, 12/29/10.

MCEER-11-0001 "Numerical and Experimental Investigation of the Seismic Response of Light-Frame Wood Structures," by I.P. Christovasilis and A. Filiatrault, 8/8/11 (PB2012-102412).

MCEER-11-0002 "Seismic Design and Analysis of a Precast Segmental Concrete Bridge Model," by M. Anagnostopoulou, A. Filiatrault and A. Aref, 9/15/11.

MCEER-11-0003 'Proceedings of the Workshop on Improving Earthquake Response of Substation Equipment," Edited by A.M. Reinhorn, 9/19/11 (PB2012-102413).

MCEER-11-0004 "LRFD-Based Analysis and Design Procedures for Bridge Bearings and Seismic Isolators," by M.C. Constantinou, I. Kalpakidis, A. Filiatrault and R.A. Ecker Lay, 9/26/11.

MCEER-11-0005 "Experimental Seismic Evaluation, Model Parameterization, and Effects of Cold-Formed Steel-Framed Gypsum Partition Walls on the Seismic Performance of an Essential Facility," by R. Davies, R. Retamales, G. Mosqueda and A. Filiatrault, 10/12/11.

MCEER-11-0006 "Modeling and Seismic Performance Evaluation of High Voltage Transformers and Bushings," by A.M. Reinhorn, K. Oikonomou, H. Roh, A. Schiff and L. Kempner, Jr., 10/3/11.

MCEER-11-0007 "Extreme Load Combinations: A Survey of State Bridge Engineers," by G.C. Lee, Z. Liang, J.J. Shen and J.S. O'Connor, 10/14/11.

MCEER-12-0001 "Simplified Analysis Procedures in Support of Performance Based Seismic Design," by Y.N. Huang and A.S. Whittaker.

MCEER-12-0002 "Seismic Protection of Electrical Transformer Bushing Systems by Stiffening Techniques," by M. Koliou, A. Filiatrault, A.M. Reinhorn and N. Oliveto, 6/1/12.

MCEER-12-0003 "Post-Earthquake Bridge Inspection Guidelines," by J.S. O'Connor and S. Alampalli, 6/8/12.

MCEER-12-0004 "Integrated Design Methodology for Isolated Floor Systems in Single-Degree-of-Freedom Structural Fuse Systems," by S. Cui, M. Bruneau and M.C. Constantinou, 6/13/12.

MCEER-12-0005 "Characterizing the Rotational Components of Earthquake Ground Motion," by D. Basu, A.S. Whittaker and M.C. Constantinou, 6/15/12.

MCEER-12-0006 "Bayesian Fragility for Nonstructural Systems," by C.H. Lee and M.D. Grigoriu, 9/12/12.

MCEER-12-0007 "A Numerical Model for Capturing the In-Plane Seismic Response of Interior Metal Stud Partition Walls," by R.L. Wood and T.C. Hutchinson, 9/12/12.

MCEER-12-0008 "Assessment of Floor Accelerations in Yielding Buildings," by J.D. Wieser, G. Pekcan, A.E. Zaghi, A.M. Itani and E. Maragakis, 10/5/12.

MCEER-13-0001 "Experimental Seismic Study of Pressurized Fire Sprinkler Piping Systems," by Y. Tian, A. Filiatrault and G. Mosqueda, 4/8/13.

MCEER-13-0002 "Enhancing Resource Coordination for Multi-Modal Evacuation Planning," by D.B. Hess, B.W. Conley and C.M. Farrell, 2/8/13.

MCEER-13-0003 "Seismic Response of Base Isolated Buildings Considering Pounding to Moat Walls," by A. Masroor and G. Mosqueda, 2/26/13.

MCEER-13-0004 "Seismic Response Control of Structures Using a Novel Adaptive Passive Negative Stiffness Device," by D.T.R. Pasala, A.A. Sarlis, S. Nagarajaiah, A.M. Reinhorn, M.C. Constantinou and D.P. Taylor, 6/10/13.

MCEER-13-0005 "Negative Stiffness Device for Seismic Protection of Structures," by A.A. Sarlis, D.T.R. Pasala, M.C. Constantinou, A.M. Reinhorn, S. Nagarajaiah and D.P. Taylor, 6/12/13.

MCEER-13-0006 "Emilia Earthquake of May 20, 2012 in Northern Italy: Rebuilding a Resilient Community to Withstand Multiple Hazards," by G.P. Cimellaro, M. Chiriatti, A.M. Reinhorn and L. Tirca, June 30, 2013.

MCEER-13-0007 "Precast Concrete Segmental Components and Systems for Accelerated Bridge Construction in Seismic Regions," by A.J. Aref, G.C. Lee, Y.C. Ou and P. Sideris, with contributions from K.C. Chang, S. Chen, A. Filiatrault and Y. Zhou, June 13, 2013.

MCEER-13-0008 "A Study of U.S. Bridge Failures (1980-2012)," by G.C. Lee, S.B. Mohan, C. Huang and B.N. Fard, June 15, 2013.

MCEER-13-0009 "Development of a Database Framework for Modeling Damaged Bridges," by G.C. Lee, J.C. Qi and C. Huang, June 16, 2013.

MCEER-13-0010 "Model of Triple Friction Pendulum Bearing for General Geometric and Frictional Parameters and for Uplift Conditions," by A.A. Sarlis and M.C. Constantinou, July 1, 2013.

MCEER-13-0011 "Shake Table Testing of Triple Friction Pendulum Isolators under Extreme Conditions," by A.A. Sarlis, M.C. Constantinou and A.M. Reinhorn, July 2, 2013.

MCEER-13-0012 "Theoretical Framework for the Development of MH-LRFD," by G.C. Lee (coordinating author), H.A Capers, Jr., C. Huang, J.M. Kulicki, Z. Liang, T. Murphy, J.J.D. Shen, M. Shinozuka and P.W.H. Yen, July 31, 2013.

MCEER-13-0013 "Seismic Protection of Highway Bridges with Negative Stiffness Devices," by N.K.A. Attary, M.D. Symans, S. Nagarajaiah, A.M. Reinhorn, M.C. Constantinou, A.A. Sarlis, D.T.R. Pasala, and D.P. Taylor, September 3, 2014.

MCEER-14-0001 "Simplified Seismic Collapse Capacity-Based Evaluation and Design of Frame Buildings with and without Supplemental Damping Systems," by M. Hamidia, A. Filiatrault, and A. Aref, May 19, 2014.

MCEER-14-0002 "Comprehensive Analytical Seismic Fragility of Fire Sprinkler Piping Systems," by Siavash Soroushian, Emmanuel "Manos" Maragakis, Arash E. Zaghi, Alicia Echevarria, Yuan Tian and Andre Filiatrault, August 26, 2014.

MCEER-14-0003 "Hybrid Simulation of the Seismic Response of a Steel Moment Frame Building Structure through Collapse," by M. Del Carpio Ramos, G. Mosqueda and D.G. Lignos, October 30, 2014.

MCEER-14-0004 "Blast and Seismic Resistant Concrete-Filled Double Skin Tubes and Modified Steel Jacketed Bridge Columns," by P.P. Fouche and M. Bruneau, June 30, 2015.

MCEER-14-0005 "Seismic Performance of Steel Plate Shear Walls Considering Various Design Approaches," by R. Purba and M. Bruneau, October 31, 2014.

MCEER-14-0006 "Air-Blast Effects on Civil Structures," by Jinwon Shin, Andrew S. Whittaker, Amjad J. Aref and David Cormie, October 30, 2014.

MCEER-14-0007 "Seismic Performance Evaluation of Precast Girders with Field-Cast Ultra High Performance Concrete (UHPC) Connections," by G.C. Lee, C. Huang, J. Song, and J. S. O'Connor, July 31, 2014.

MCEER-14-0008 "Post-Earthquake Fire Resistance of Ductile Concrete-Filled Double-Skin Tube Columns," by Reza Imani, Gilberto Mosqueda and Michel Bruneau, December 1, 2014.

MCEER-14-0009 "Cyclic Inelastic Behavior of Concrete Filled Sandwich Panel Walls Subjected to In-Plane Flexure," by Y. Alzeni and M. Bruneau, December 19, 2014.

MCEER-14-0010 "Analytical and Experimental Investigation of Self-Centering Steel Plate Shear Walls," by D.M. Dowden and M. Bruneau, December 19, 2014.

MCEER-15-0001 "Seismic Analysis of Multi-story Unreinforced Masonry Buildings with Flexible Diaphragms," by J. Aleman, G. Mosqueda and A.S. Whittaker, June 12, 2015.

MCEER-15-0002 "Site Response, Soil-Structure Interaction and Structure-Soil-Structure Interaction for Performance Assessment of Buildings and Nuclear Structures," by C. Bolisetti and A.S. Whittaker, June 15, 2015.

MCEER-15-0003 "Stress Wave Attenuation in Solids for Mitigating Impulsive Loadings," by R. Rafiee-Dehkharghani, A.J. Aref and G. Dargush, August 15, 2015.

MCEER-15-0004 "Computational, Analytical, and Experimental Modeling of Masonry Structures," by K.M. Dolatshahi and A.J. Aref, November 16, 2015.

MCEER-15-0005 "Property Modification Factors for Seismic Isolators: Design Guidance for Buildings," by W.J. McVitty and M.C. Constantinou, June 30, 2015.

MCEER-15-0006 "Seismic Isolation of Nuclear Power Plants using Sliding Bearings," by Manish Kumar, Andrew S. Whittaker and Michael C. Constantinou, December 27, 2015.

MCEER-15-0007 "Quintuple Friction Pendulum Isolator Behavior, Modeling and Validation," by Donghun Lee and Michael C. Constantinou, December 28, 2015.

MCEER-15-0008 "Seismic Isolation of Nuclear Power Plants using Elastomeric Bearings," by Manish Kumar, Andrew S. Whittaker and Michael C. Constantinou, December 29, 2015.

MCEER-16-0001 "Experimental, Numerical and Analytical Studies on the Seismic Response of Steel-Plate Concrete (SC) Composite Shear Walls," by Siamak Epackachi and Andrew S. Whittaker, June 15, 2016.

MCEER-16-0002 "Seismic Demand in Columns of Steel Frames," by Lisa Shrestha and Michel Bruneau, June 17, 2016.

MCEER-16-0003 "Development and Evaluation of Procedures for Analysis and Design of Buildings with Fluidic Self-Centering Systems" by Shoma Kitayama and Michael C. Constantinou, July 21, 2016.

MCEER-16-0004 "Real Time Control of Shake Tables for Nonlinear Hysteretic Systems," by Ki Pung Ryu and Andrei M. Reinhorn, October 22, 2016.

MCEER-16-0006 "Seismic Isolation of High Voltage Electrical Power Transformers," by Kostis Oikonomou, Michael C. Constantinou, Andrei M. Reinhorn and Leon Kemper, Jr., November 2, 2016.

MCEER-16-0007 "Open Space Damping System Theory and Experimental Validation," by Erkan Polat and Michael C. Constantinou, December 13, 2016.

MCEER-16-0008 "Seismic Response of Low Aspect Ratio Reinforced Concrete Walls for Buildings and Safety-Related Nuclear Applications," by Bismarck N. Luna and Andrew S. Whittaker.

MCEER-16-0009 "Buckling Restrained Braces Applications for Superstructure and Substructure Protection in Bridges," by Xiaone Wei and Michel Bruneau, December 28, 2016.

MCEER-16-0010 "Procedures and Results of Assessment of Seismic Performance of Seismically Isolated Electrical Transformers with Due Consideration for Vertical Isolation and Vertical Ground Motion Effects," by Shoma Kitayama, Michael C. Constantinou and Donghun Lee, December 31, 2016.

MCEER-17-0001 "Diagonal Tension Field Inclination Angle in Steel Plate Shear Walls," by Yushan Fu, Fangbo Wang and Michel Bruneau, February 10, 2017.

MCEER-17-0002 "Behavior of Steel Plate Shear Walls Subjected to Long Duration Earthquakes," by Ramla Qureshi and Michel Bruneau, September 1, 2017.

MCEER
EARTHQUAKE ENGINEERING TO EXTREME EVENTS
University at Buffalo, The State University of New York
133A Ketter Hall ▪ Buffalo, New York 14260-4300
Phone: (716) 645-3391 ▪ Fax: (716) 645-3399
Email: *mceer@buffalo.edu* ▪ Web: *http://mceer.buffalo.edu*
University at Buffalo *The State University of New York*

ISSN 1520-295X